Class III Phosphoinositide 3-Kinase in Melanoma

Inauguraldissertation

zur
Erlangung der Würde eines Doktors der Philosophie
vorgelegt der
Philosophisch-Naturwissenschaftlichen Fakultät
der Universität Basel

von

Ann Christine Mertz Biro

aus Zürich, Schweiz

Basel, 2011

Index

Genehmigt von der Philosophisch-Naturwissenschaftlichen Fakultät
auf Antrag von

Prof. Dr. Matthias P. Wymann (Universität Basel)

Prof. Dr. Martin Spiess (Universität Basel)

Basel, 24. Mai 2011

Prof. Dr. Martin Spiess
Dekan

1 Index

Index

2 Abstract

The first isoform of phosphoinositide 3-kinases (PI3K) had been found in *Saccharomyces cerevisiae* when screening for mutants not exhibiting normal vacuolar protein sorting (Vps), Vps34. Class III PI3K/Vps34 has long been worked on in regards to its role in endosomal sorting and autophagy, a process allowing cells to survive nutrient-deprived conditions. Most research groups have investigated the functions of Vps34 in the yeast model system *Saccharomyces cerevisiae*. Newer publications now use mammalian cell lines, *Caenorhabditis elegans* or *Drosophila melanogaster*, deciphering interesting differences between the various species in regards to Vps34 characteristics. Our cancer model system, melanoma tumors, are known to be very aggressive and their treatment difficult, due to mutations leading to drug resistance. Autophagy and whether its induction would be beneficial or not for cancer patients, has been the topic of discussions in the field lately.

In this work, we investigated the role of class III PI3K by two different methods, a pharmacological and a genetic approach. We started with natural compound screenings on hVps34 in genetically modified yeast systems. The pure fraction of *Citrus medica* extracts giving best results turned out to be limettin. Limettin inhibited hVps34 in both our *in vivo* yeast system and in *in vitro* kinase assays using the immunoprecipitated enzyme from HEK293 cells. Our candidate inhibitor seemed very specific for the human isoform, but still required quite high concentrations in the assays performed. Further chemical designing and eventual fitting to the hVps34 ATP binding pocket would be necessary to render this molecule into one of the first specific class III PI3K inhibitors.

In addition to pharmacological approaches, class III PI3K state-of-the-art genetic knockdown experiments were done in melanoma cell lines in order to characterize this isoform's role in melanoma more specifically. Vps34 is not essential in yeast, but leads to serious temperature sensitivity phenotypes. In one melanoma cell line (A375) tested, knockdown had similar as but milder effects than known in other cancer types. Two others though (A2058 and 1205lu), did not tolerate the longterm loss of class III PI3K. We suppose that the importance of hVps34 depends on the genetic background of cell types. Further studies are required to define precisely which effectors determine the intolerance described i.e. which melanoma types could be targeted by inhibition of class III PI3K.

3 Introduction

3.1 *Early Publications on Phosphoinositide 3-kinases (PI3K)*

3.1.1 Yeast PI3K

In 1986, Rothman and Stevens published the discovery of a group of yeast mutants that failed to properly sort CPY (carboxypeptidase Y) to the vacuole, the yeast's lysosome. Their so called eight "vpl mutants" defined a new class of proteins required for sorting of vacuolar proteins during the secretory pathway (Rothman and Stevens 1986). Hence the first PI3K to be described in yeast was Vps34, which was one of the genes involved in vacuolar protein sorting, originally termed Vpt29 or Vpl7 (Robinson, Klionsky et al. 1988). At that time though, nothing was known about its kinase function yet. One of the first publications on PI3K activity in yeast was by Auger et al. in 1989. The authors claimed to have found PI3K lipid kinase activity in *Saccharomyces cerevisiae,* similarly to an enzymatic reaction phosphorylating D-3 position of the inositol ring which was at that time known in mammalian cells. Biochemical character of the PI3K enzyme seemed different in yeast. Yet not only PI-4P, as originally thought, but PI(3)P were found in liquid chromatography analysis of intact yeast cells labelled with (^{3}H)inositol. These results suggested an important and conserved functional role in cell cycle for PI3K in eukaryotes (Auger, Carpenter et al. 1989).

3.1.2 Mammalian PI3K isoforms

One of the first publications on a kinase phosphorylating D-3 instead of D-4 position of inositol in mammalian cells was a manuscript by Whitman M et al. in 1987 where they used platelet-derived growth factor (PDGF)-stimulated murine fibroblasts. Phosphoinositide kinase activity was found to associate with anti-phosphotyrosine immunoprecipitates from these cells. A new class of lipids, phosphorylated at the D3-hydroxy-group of the inositol headgroup of phosphoinositides was discovered (Whitman, Kaplan et al. 1987; Wymann and Pirola 1998).

Today, the members of the PI3K family are subdivided into three classes (Table 1), according to their *in vitro* substrate specificity, their structure and functional homologies. More details on the organization of PI3K were summarized later in a review by Marone et al. in 2008, from which publication the following scheme is adapted (Figure 1) (Marone, Cmiljanovic et al. 2008).

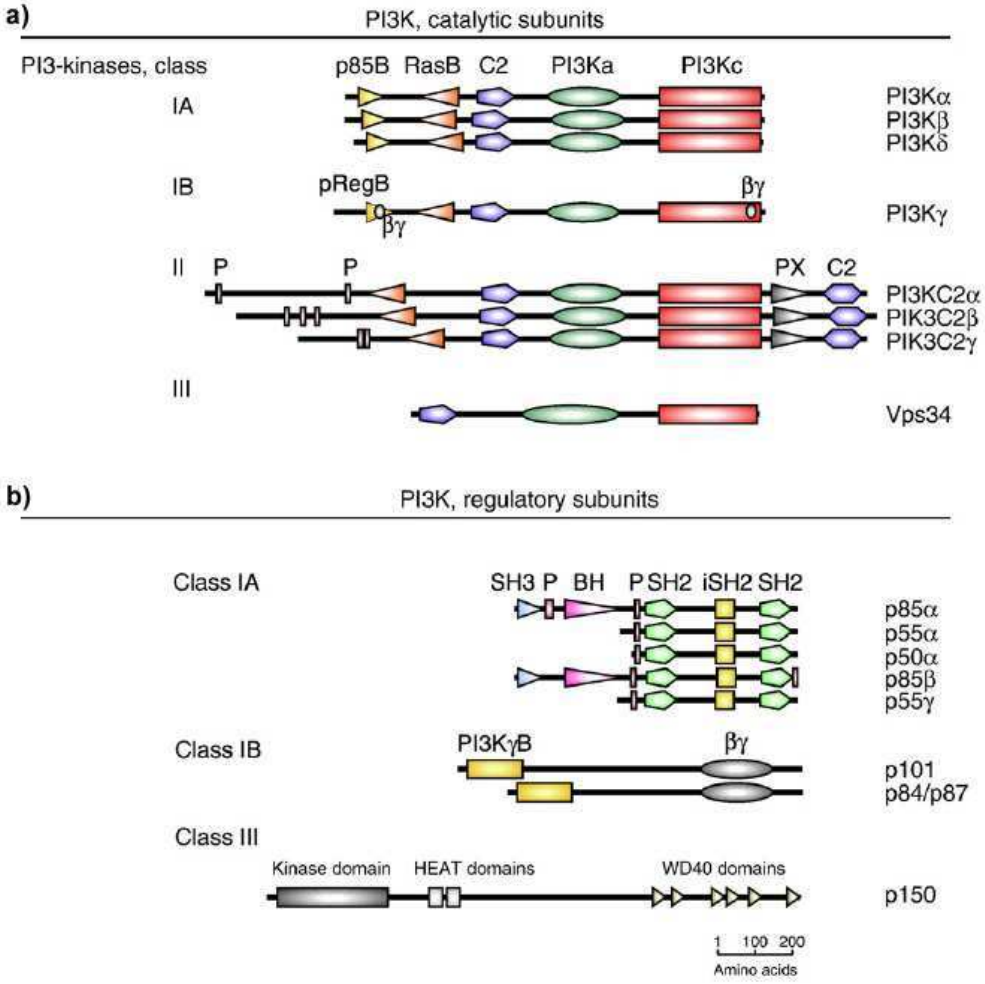

Figure 1: Domain Structures of Mammalian PI3K isoforms

The members of the phosphoinositide 3-kinase (PI3K) family are subdivided into three classes, according to their *in vitro* substrate specificity, their structure and functional homologies.
The upper panel (*a*) displays the catalytic subunits, the lower panel (*b*) shows their adaptors/regulatory subunits. *a*) The catalytic subunits contain a core catalytic domain (PI3Kc), including the ATP-binding site and a regulatory subunit binding domain at their N-terminus. Other known domains are a Ras-binding domain (RBD), a C2 domain (protein kinase C homology domain 2) and a PI3K accessory domain (helical, PI3Ka). Class II PI3K display several proline-rich (P) stretches, a PX (phox) and an additional C2 domain at their C-terminus. Class III PI3K, Vps34, only has a C2, PI3Ka and PI3Kc domain. *b*) The regulatory subunits/adaptors of class IA PI3K contain a proline-rich region and two SH2 (Src-homology 2) domains, an interSH2 region (iSH2) that binds to the catalytic subunit. SH3 (Src-homology 3) and BH (BCR homology) domains are found at the N-terminus of p85α and p85β. The structures of class IB adaptors are less well investigated. P150/hVps15, the adaptor of Vps34, contains a kinase domain, a HEAT (Huntingtin, Elongation Factor 3, protein phosphatase 2A and yeast TOR1) domain and several WD40 repeats. (Marone, Cmiljanovic et al. 2008)

3.1.3 PI3K in Other Model Organisms: Early to Recent Publications

The fruitfly *Drosophila melanogaster* possesses one isoform of each three classes of PI3K, namely Pi3k_92D (dp110) with its regulatory subunit Pi3k57 (p67), PI3K_68D and Pi3k_59F (DVps34p). DVps34p is usually localized to perinuclear structures, reflecting the early endosomal compartment. Class III PI3K has a role in autophagosome biogenesis, acting together with Ird1 (Vps15/p150 homologue) and DAtg6 (Beclin1 homologue). This association was observed under both fed and starved conditions, consistent with findings in mammalian cells (more about autophagy in a later chapter). Apparently the kinase activity of DVps34p is sufficient to drive early but not later steps of autophagy. There are differences between phenotypes in class III PI3K and ESCRT (endosomal sorting complex required for transport) machinery mutants, suggesting that DVps34p has a more severe kinetic effect on autophagosome formation than on the fusion to the lysosome later on. The normal ESCRT pathway is not disrupted in mutants of DVps34p. Endocytic recycling seems to be affected though, as accumulations of Notch was found in DVps34p mutant cells of the eye imaginal disc. In contrast to mutations in *Tor* (target of rapamycin) (Zhang, Stallock et al. 2000), fly cells proliferate at a similar rate to control cells upon mutations in class III PI3K. Expression of kinase-defective isoforms also had no effect on the cell size in starved or refed flies. The same mutants exhibited no effect on phosphorylation of S6K-Thr398 or Akt/PKB-Ser505, substrates of TORC1 and TORC2 (TOR complexes 1 and 2). Starvation induced a shift from perinuclear structures to a more widely distributed pattern of DVps34p, presumably nascent autophagosomes. Class III PI3K in *Drosophila* seems to function downstream of TOR-dependent nutrient signalling, in contrast to suggestions in mammalian cells (Byfield, Murray et al. 2005; Nobukuni, Joaquin et al. 2005; Juhasz, Hill et al. 2008).

One gene of each PI3K class I to III has been found in the nematode *Caenorhabditis elegans*, named AGE-1 (p110) with regulatory subunit AAP-1 (p55), F39B1.1 and Let-512. A loss of function mutation in PI3K class IA causes entry into *dauer* stage, a condition related to prolonged life span as seen in other organisms (Vanhaesebroeck, Leevers et al. 1997). Loss of function of Let-512 is lethal, hence the gene name. This finding is in contrast to viable deletion mutants in yeast (Wymann and Pirola 1998). CeVps34 is ubiquitously expressed during development (arrest in larvae stage 3 or 4 upon mutation) and accumulates at a perinuclear localization, maybe even at the nuclear envelope, unlike in other organisms where it is usually found in endosomal compartments. Defects in endocytic uptake are a consequence of reduction of class III PI3K in worm, as this isoform is involved in membrane transport. Roggo et al. have demonstrated that Let-512 in worm is essential for vesicle budding even prior to the *trans*-Golgi network (TGN) (Roggo, Bernard et al. 2002).

Class Type	***Saccharomyces cerevisiae***	***Caenorhabditis elegans***	***Drosophila melanogaster***	**Mammals**
Class I, catalytic	not present	AGE-1 (p110)	Pi3k_92D (dp110)	PIK3CA (p110α) PIK3CB (p110β) PIK3CD (p110δ) PIK3CG (p110γ)
Class I, regulatory	not present	AAP-1 (p55)	Pi3k57 (p67)	PIK3R1 (p85a/p55a/p50a) PIK3R2 (p85b) PIK3R3 (p55g) PIK3R5 (p101) PIK3R6 (p87/p84)
Class II	not present	F39B1.1	PI3K_68D	PIK3C2A (PI3K-C2α) PIK3C2B (PI3K-C2β) PIK3C2G (PI3K-C2γ)
Class III, catalytic	VPS34p	Let-512	Pi3k_59F (DVps34p)	PIK3C3 (hVps34 or Vps34)
Class III, regulatory	VPS15p	Vps15-like	Ird1	PIK3R4 (p150/vps15)

Table 1: The PI3K family members in different species

This table lists the homologs of PI3K isoforms in different species.
Table adapated from (Vanhaesebroeck, Guillermet-Guibert et al.)

3.2 *More Recent Knowledge of PI3K*

3.2.1 Class I PI3K

Class I PI3K are found in all cell types, p110δ and p110γ mainly in leukocytes (Kok, Geering et al. 2009). This class of PI3K can be divided into two subgroups (Table 1): class I A (p110α, β and δ) which bind to regulatory subunit p85 type and class I B (p110γ) which binds p87 (p84/p87PIKAP/PIK3R6) or p101 (PIK3R5) (Vanhaesebroeck, Leevers et al. 1997). The p85 subunits contain Src homology 2 (SH2) domains which bind phosphorylated tyrosine (Figure 1).

It was originally thought that class I A are activated by tyrosine kinases and class I B by G-protein coupled receptors only. Recent data though suggests that most class I PI3K might be activated by G-protein coupled receptors (GPCRs), either directly via Gβγ protein or indirectly via Ras for example (Figure 2). In general, p85 subunits provide at least three functions to p110 proteins: stabilization, inactivation of their kinase activity in the basal unstimulated state and recruitment to phospho-tyrosine residues in receptor and adaptor molecules. They bring the catalytic subunits in contact with their lipid substrates in the membrane. In addition to the SH2 domains do p85 isoforms contain a proline-rich region closer to their N-term (Vanhaesebroeck, Guillermet-Guibert et al.). Subunits p85 α and p85 β also contain an SH3 domain, a second proline-rich region and a BCR (breakpoint cluster region) homology (BH) domain (Chamberlain, Chan et al. 2008). There is evidence that p85 isoforms can interact with small GTPases such as Rac, Rho and Cdc42 (Vanhaesebroeck, Ali et al. 2005), but so far that was only checked in isolated p85, not when the subunit is in complex with p110. Mammals have five distinct p85 isoforms with distinct biological functions (Vanhaesebroeck, Guillermet-Guibert et al.). Loss of p85 subunit often leads to changes in p110 expression, hence the clear interpretation of redundancy of regulatory subunits is difficult (Vanhaesebroeck, Ali et al. 2005).

p101 and p84/p87 regulatory subunits of p110γ are important for the relay of signals by Gβγ and Ras (Kurig, Shymanets et al. 2009). These subunits have distinct tissue distribution, but both help generation of $PI(3,4,5)P_3$ at the plasma membrane. $PI(3,4,5)P_3$ produced by p110γ in complex with the regulatory subunit p101 is endocytosed to motile vesicles associated with microtubules, so called “speckles”. For the first time, the authors suggest two diverse PI3Kγ complexes, depending on the interacting adaptor of p110γ. The choice of adaptor is leading to distinct $PI(3,4,5)P_3$ pools at the plasma membrane, provoking specific cell responses e.g. only the regulatory subunit p84/p87 together with p110γ amplifies mast cell degranulation and allergic reactions (Bohnacker, Marone et al. 2009).

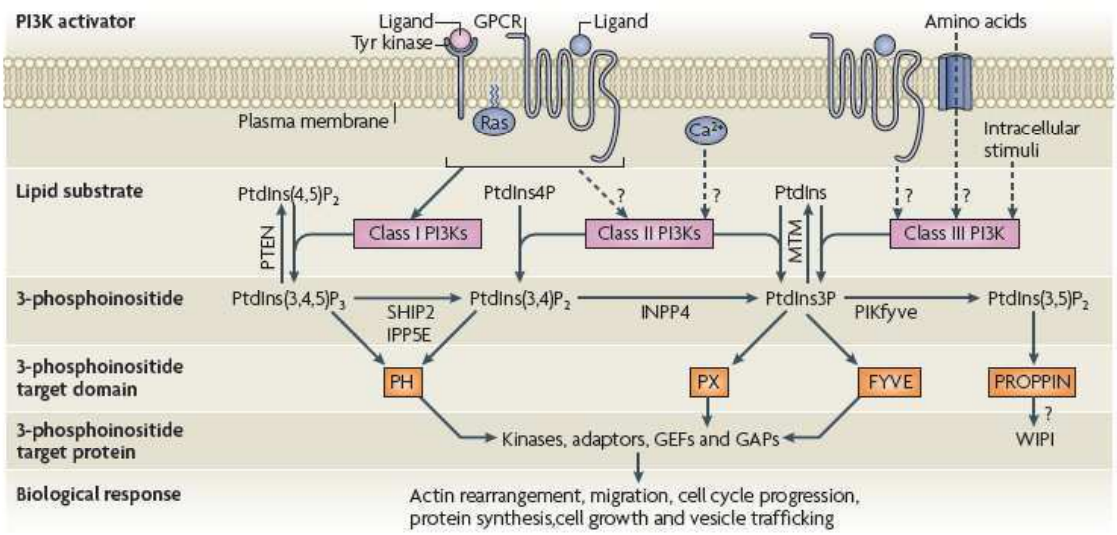

Figure 2: PI3K signalling pathways

In this scheme isoforms of the PI3K family are depicted in their signalling pathway environments, showing typical effectors (such as proteins containing the domains PH, e.g. Akt/PKB binding $PI(3,4,5P)_3$, PX or e.g. EEA1 or Hrs containing a FYVE domain binding PI(3)P) and in/outputs of the various kinases. Well-known downstream effects are rearrangement of the actin cytoskeleton, leading to polarity of a cell or migration of immune cells such as mast cells towards the site of inflammation, directed by class IB PI3K isoform (Collmann et al., unpublished data). Lipid production of PI3K isoforms is usually balanced by phosphatases such as PTEN or SHIP. Upon mutations that occur in cancer cells, this important balance can be ablated, leading to uncontrolled signalling inputs and hence drastic changes in cell growth or migration control. (Prasad, Tandon et al. 2008; Vanhaesebroeck, Guillermet-Guibert et al.)

All p110 subunits have a RBD (Ras binding domain). The contribution of Ras in PI3K activation is unclear in normal physiology and in diseases such as cancer where Ras can be constitutively activated. Ras is important for p87 bound to p110γ but not for p101 bound to p110γ activation (Bohnacker, Marone et al. 2009; Vanhaesebroeck, Guillermet-Guibert et al.). Ras is required for maximal signalling by the *Drosophila melanogaster* p110 class I PI3K (Orme, Alrubaie et al. 2006). Mice in which endogenous p110 α cannot interact with Ras (due to RBD mutations) are resistant to tumorigenesis induced by oncogenic Ras. This indicates that p110 α is an effector of oncogenic Ras in cancer development (Gupta, Ramjaun et al. 2007). p110β can be activated by binding to active RAB5 (Kurosu, Maehama et al. 1997). The RAB5-binding site on p110 β involves the RBD and the C-terminal part of the helical domain. RAB5 is present on early endosomes (Kurosu and Katada 2001). P110β has been found in clathrin-coated vesicles (Christoforidis, Miaczynska et al. 1999; Shin, Hayashi et al. 2005). There might be feedback loops between PI3K and GTPases, as PI3K are found both downstream and upstream of small GTPases (Vanhaesebroeck, Guillermet-Guibert et al.). GPCRs mainly transmit their signal through allosteric activation of heterotrimeric G proteins. It was tested *in vitro* that Gβγ subunits directly activate p110β and γ but not p110α and δ (Kurosu, Maehama et al. 1997). Active Gα-GTP can even inhibit p110α (Ballou, Chattopadhyay et al. 2006; Taboubi, Milanini et al. 2007).

$PI(3,4,5)P_3$ gets converted to $PI(4,5)P_2$ and $PI(3,5)P_2$ by PI-3- or PI-5-phosphatases. A major PI-3-phosphatase is PTEN (phosphatase and tensin homologue deleted on chromosome 10), which is frequently inactivated in cancer and hence leading to PI3K activation. PTEN can couple to p110β (Vanhaesebroeck, Guillermet-Guibert et al.). $PI(3,4,5)P_3$ and $PI(3,4)P_2$ coordinate the localization of multiple effector proteins which bind these lipids via their PH (pleckstrin homology) domain, e.g. Akt/PKB or Btk. These lipids are mainly generated at the plasma membrane (Vanhaesebroeck, Guillermet-Guibert et al.).

Class I PI3K do not have stable binding partners but can function as scaffolds, e.g. p110γ binding to PKC (protein kinase C) (Hirsch, Braccini et al. 2009; Lehmann, Muller et al. 2009). PI3K can regulate small GTPases from Rac, Ras and Arf families by regulating their GEFs (guanine nucleotide-exchange factors) and GAPs (GTPase activating proteins) (Vanhaesebroeck, Leevers et al. 2001). Rac is positively regulated by all PI3K isoforms while RhoA is negatively regulated by p110δ and p110α does not affect RhoA at all (Eickholt, Ahmed et al. 2007; Papakonstanti, Ridley et al. 2007; Papakonstanti, Zwaenepoel et al. 2008).

Tumour-specific somatic mutations were only found in p110α first (Samuels, Wang et al. 2004). Later there were some mutations found in p110δ correlated to leukemia (Cornillet-Lefebvre, Cuccuini et al. 2006). Most mutations in p110α are missense mutations that result in an amino acid substitution in so called “hot-spot regions” in the kinase domain or helical domain, while there are no mutations found so far in the RBD (Vogt, Kang et al. 2007; Zhao and Vogt 2008). “Hot-spot region” mutations examples are His1047Arg or Glu545Lys of p110α (Miled, Yan et al. 2007; Mandelker, Gabelli et al. 2009). Amplifications of the p110α gene are also reported and have been found for the other isoforms as well (Shayesteh, Lu et al. 1999; Kok, Geering et al. 2009).

3.2.2 Class II PI3K

Class II PI3Ks were discovered based on their sequence homology with class I and class III PI3K. Their functional context is still poorly understood. Yeast does not have any isoforms and only one isoform is found in both *D. melanogaster* and *C.elegans*. Mammals have three class II PI3K isoforms: PI3K-C2α, PI3K-C2β and PI3K-C2γ. They are molecules of 166-190kDa in size (Vanhaesebroeck, Guillermet-Guibert et al.). PI3K-C2α and PI3K-C2β are broadly distributed in tissue, but PI3K-C2γ is more restricted to liver, breast and prostate tissue (Elis, Triantafellow et al. 2008; Kok, Geering et al. 2009).

Pharmacological inhibitors have not been published so far. Sensitivity to pan-PI3K inhibitors are slightly different than for the other classes though. Usually these inhibitors are applied at high dosages that already affect class II PI3K, a possible side-effect that should be kept in mind for interpretations of PI3K isoform-specific functions (Virbasius, Guilherme et al. 1996; Domin, Pages et al. 1997; Knight, Gonzalez et al. 2006).

PX (phox) domain in the C-terminal end of PI3K-C2α can bind PI(4,5)P_2, but today it is not clear what function this represents (Song, Xu et al. 2001; Stahelin, Karathanassis et al. 2006). Class II PI3K do not have any regulatory subunits but contain extended N- and C-termini (Vanhaesebroeck, Guillermet-Guibert et al.) and Ras binding domains (RBD).

Activation of class II PI3K might require the relocalization of a cytosolic pool to the plasma membrane. Many stimuli have been discovered to activate PI3K-C2α and β, e.g. insulin, EGF and PDGF, TNF-α, leptin and LPA (Figure 2). The exact mechanisms are often still unclear though (Arcaro, Zvelebil et al. 2000; Elis, Triantafellow et al. 2008).

PI and PI(4)P are substrates of class II PI3K, whereas *in vitro* PI3K-C2α can produce PI(3,4,5)P_3 from PI(4,5)P_2 if activated by clathrin (Domin, Pages et al. 1997). PI(3)P are mainly localized in endosomes under unstimulated conditions and are bound by PX or FYVE domains. Examples of proteins containing such domains are PIKfyve (Fab1), EEA1, HRS (Vps27) or Alfy (Birkeland and Stenmark 2004; Di Paolo and De Camilli 2006; Hurley 2006; Lemmon 2008). It is still not known to what extent class II PI3K contribute to basal level PI(3)P.

Downregulation of PI3K-C2α by RNAi does not affect the steady state levels of total PI(3)P at the plasma membrane, as demonstrated in L6 muscle cell lines. Eventually do class II PI3K contribute to the acute production of PI(3)P, e.g. PI3K-C2α generates the lipids at the plasma membrane upon insulin stimulation while there is no increase in lipids at the endosomes (Falasca, Hughes et al. 2007). Downregulation of PI3K-C2α but not PI3K-C2β leads to a reduction in cell proliferation and viability by induced apoptosis in more than half of 23 cancer cell lines tested by Elis W. et al. (Elis, Triantafellow et al. 2008).

Genetic studies in fly (*D. melanogaster*, *PI3K68D*) and worm (*C.elegans*, *F39B1.1*) provide evidence for a possible link between class II PI3Ks and Tyr kinase signalling pathways but there is still investigation required for further details (Ashrafi, Chang et al. 2003; MacDougall, Gagou et al. 2004). Links between class II PI3K and EGFR have been proposed earlier in human carcinoma cell lines. (Arcaro, Zvelebil et al. 2000)

In summary, class II PI3Ks are involved in cell migration, glucose metabolism, exocytosis, smooth muscle cell contraction and apoptosis (Falasca and Maffucci 2007). Viable and fertile null-mice exist for PI3K-C2β but there are no obvious phenotypes in epidermal differentiation, the only study done on this mouse strain so far (Harada, Truong et al. 2005).

3.2.3 Class III PI3K

Class III PI3K or Vps34, was originally identified in a screen for genes involved in endosomal sorting to the yeast vacuole, the equivalent of the mammalian lysosome (Robinson, Klionsky et al. 1988; Herman and Emr 1990). Vps34 is conserved from yeast to plants and mammals. It fulfills multiple functions through association with distinct multiprotein complexes. Vps34 forms a constitutive heterodimer with Vps15 (p150 in mammals) which is myristoylated

and hence locates the complex to intracellular membranes (Vanhaesebroeck, Guillermet-Guibert et al.).

In yeast, three complexes including Vps34 have been reported so far: The Vps34-containing complex involved in autophagy consists of Vps34, Vps15, Atg14 and Vps30. The vacuole protein sorting complex contains Vps38 and Vps30 besides class III PI3K and its partner Vps15. In a third complex, Vps34 and Vps15 are interacting with Gprotein α subunit activated with GTP and lead to a pheromone response upon mating factor binding (Vanhaesebroeck, Guillermet-Guibert et al.).

In mammals, there is also an autophagy complex containing Vps34 and p150 (Vps15), ATG14L (also known as barkor), Beclin1, UVRAG, Ambra1, Rubicon and Bif1 (Figure 3). As for endosomal trafficking there are different complexes, some consisting of UVRAG with Vps34 and p150, others containing MTM1 in addition to the PI3K. Effectors are FYVE domain bearing proteins such as HRS or ESCRTII and III (Simonsen and Tooze 2009). Vps34-associated effector proteins might also regulate the catalytic activity of Vps34, e.g. Bif1 (Bax-interacting factor 1) which stimulates the kinase activity in the UVRAG-Beclin1 complex (Liang, Feng et al. 2006; Takahashi, Coppola et al. 2007).

Class III PI3K has a limited substrate specificity, generating PI(3)P from PI. It is not clear today, which effectors class III and II PI3K share and to what extent their functions overlap (Schu, Takegawa et al. 1993; Volinia, Dhand et al. 1995). Studies in *C.elegans* suggest that Vps34-independent sources of PI(3)P exist, as the phenotype of a Vps34-null mutant can be rescued by reducing PI(3)P-ase activity. Kinase dead versions could not rescue the deletion phenotype in yeast or worm though, hinting that the lipid kinase activity of Vps34 is important for its biological functions (Roggo, Bernard et al. 2002; Xue, Fares et al. 2003).

It is still controversary in the field, whether Vps34 is regulated by extracellular stimuli (Figure 2). There is evidence for regulation by nutrients such as amino acids and glucose or GPCRs (Byfield, Murray et al. 2005; Nobukuni, Joaquin et al. 2005) in human cell lines while similar processes could not be confirmed in other model organisms such as *Drosophila melanogaster* (Juhasz, Hill et al. 2008). GPCR stimulation was proposed to happen in yeast during the pheromone response to mating factors. Pheromones lead to the activation and dissociation of G protein α subunit from Gβγ at the plasma membrane. It then passes on to the endosome where it binds and activates Vps34-Vps15 which leads to increase of PI(3)P formation and hence recruitment of PI(3)P-binding effectors. Interestingly, here it is Gprotein α subunit that activates the PI3K while it is Gβ γ that binds class I PI3K isoforms (Slessareva, Routt et al. 2006). A closer look into this topic is given in the following chapter “Nutrient Regulation”.

Vps34 might also work as a scaffold protein. Homozygous deletions in yeast are viable but exhibit growth defects even under non-stressed conditions and, as mentioned before, defects in vacuolar protein sorting (Backer 2008). The global deletion of Vps34 in yeast and fly

is lethal and null-mice have not been reported so far (Vanhaesebroeck, Guillermet-Guibert et al.). All known biological functions of Vps34 in mammals are related to regulation of vesicular traffic, e.g. autophagy, endocytosis and phagocytosis. Some studies indicate that class III PI3K is controlling amino acid-dependent activation of S6 kinase 1 (Byfield, Murray et al. 2005; Nobukuni, Joaquin et al. 2005), this link is still under debate though.

Vps34's involvement in autophagy was first shown in yeast (Kihara, Noda et al. 2001). In flies, the role of class III PI3K in autophagy is strongly limited to the early formation steps of autophagosomes (Juhasz, Hill et al. 2008). In mammals, its role is still not well-defined. The origin of autophagosomes is still not clear, but there are links to the Golgi, plasma membrane and ER (endoplasmatic reticulum). Omegasomes are cup shaped vesicles formed from the ER membrane of amino acid starved mammalian cells, possibly representing nascent autophagosomes (Axe, Walker et al. 2008).

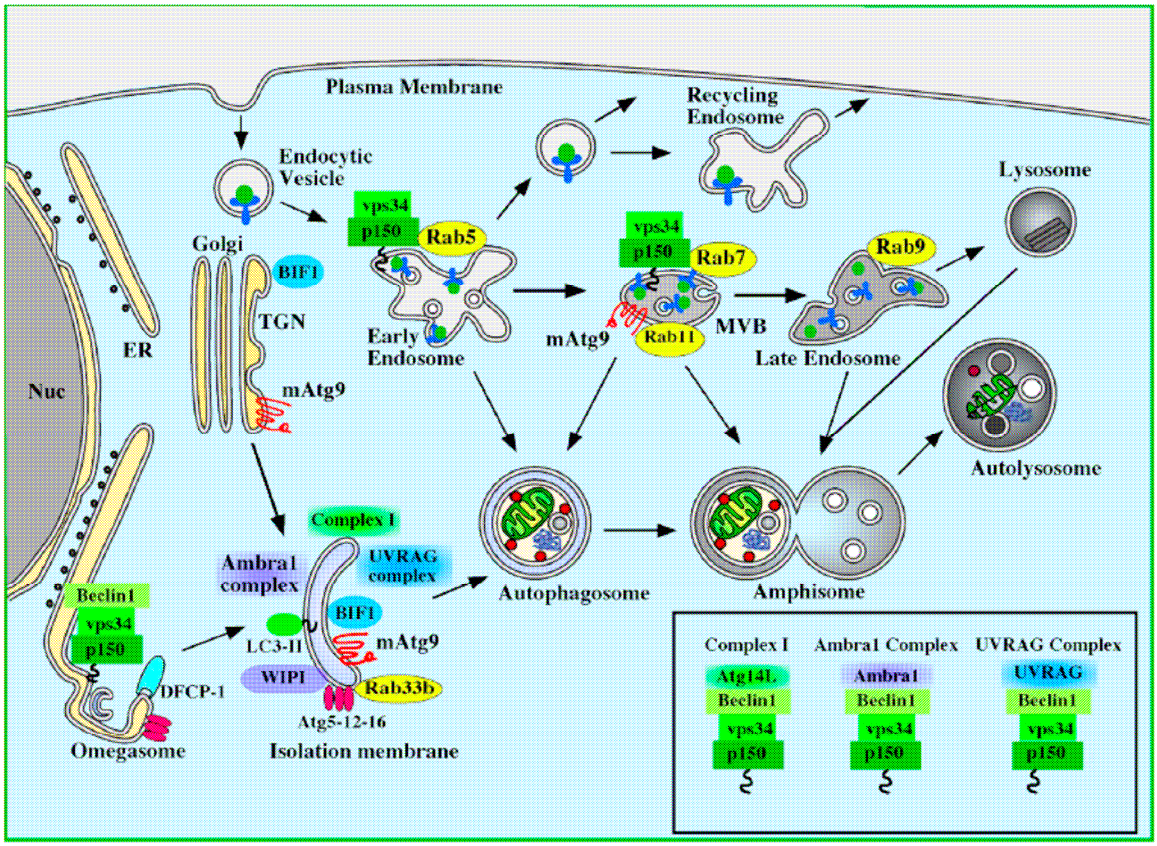

Figure 3: PI3K class III signalling pathway

PI3K class III interacts with different effectors than the other isoforms. Shown above is the current view of hVps34 in its signalling environment in mammalian cells. Vps34 exists in different complexes: Complex I consists of Vps34, p150, Beclin1 and Atg14L/Barkor and is localized at the isolation membrane (IM) thought to be at the endoplasmatic reticulum (ER). There are two others, the Ambra1 and the UVRAG complex, both are required for autophagy and their name-giving proteins associate directly with Beclin1. Ambra1 positively affects Vps34 kinase activity. UVRAG stimulates Rab7 and hence fusion of the autophagosome with late endosomes, eventually by recruitment of BIF-1 that could provide the machinery to undergo membrane curvature. Literature is still unclear on this.
Nuc= nucleus, ER= endoplasmatic reticulum, TGN= trans-Golgi network, MVB= multivesicular body (Simonsen and Tooze 2009)

As Vps34 was found in yeast mutants defective for vacuolar protein sorting, endocytosis was checked in other organisms. In *D. melanogaster*, deletion leads to severe defects in pinocytosis (Juhasz, Hill et al. 2008). In mammals, the detailed role class III PI3K in endocytosis has been difficult to interpret due to the complexity of the mammalian endosomal system. It consists of early and late endosomes, marked by Rab5 and Rab7 respectively. The degradation pathway contains an intermediate compartment called multivesicular body (Futter, Collinson et al. 2001). Rab5 loaded with GTP interacts with the WD-repeats of Vps15 (p150), inducing enhanced PI(3)P production at the endosomes. Effector proteins such as EEA1, HRS and ESCRT proteins then bind and maturation of late endosomes, marked by Rab7, takes place. In the end, these vesicles fuse with acidic lysosomes, marked by LAMP1. This

endosomal trafficking is also used for receptor sorting, e.g. for receptor Tyr kinase or transferring receptors. Upon Vps34 inhibition, recycling of transferring receptor or internalization of PDGF (platelet-derived growth factor) or EGF (epidermal growth factor) receptors are delayed (Siddhanta, McIlroy et al. 1998; Murray, Panaretou et al. 2002; Stein, Feng et al. 2003; Cao, Laporte et al. 2007; Cao, Backer et al. 2008). Various waves of PI(3)P accumulation happen during phagocytosis, probably through Vps34 (Ellson, Anderson et al. 2001). Contrary to the normal endocytic pathway, in phagocytosis class III PI3K seems to act upstream of Rab5 by interaction with dynamin. Dynamin controls clathrin-mediated endocytosis (Kinchen, Doukoumetzidis et al. 2008).

Many diseases are linked to mutations in enzymes that regulate the turnover of PI(3)P, such as members of the myotubularin family and PIKfyve. A specific role for class III PI3K is less clear, although processes like autophagy are certainly involved in infection and inflammation mechanisms (Levine and Kroemer 2008). A role for Vps34 in proliferation has been reported in cancer cell lines, but no deletions or inactivating mutations in the VPS34 gene have been observed so far. Vps34 might be involved in schizophrenia though (Siddhanta, McIlroy et al. 1998; Johnson, Overmeyer et al. 2006; Tang, Zhao et al. 2008).

3.3 *PI3K and Cancer*

Cancer cells evolve from a benign non-invasive state to metastatic tumors which proliferate aggressively out of their normal tissue context. Accumulation of genetic alterations lead to multiple inputs to signal transduction pathways, e.g. the PI3K pathway (Fig.4). Constitutive activation of PI3K promotes cell mass and cell cycle entry, inhibits apoptosis and enhances cell migration, all typical indicaters of cancer cells (Marone, Erhart et al. 2009). There are many reasons for increased PI3K activity resulting in abnormally high $PI(3,4,5)P_3$ levels e.g. oncogenic Ras, loss of PTEN, constitutively activated protein tyrosine kinase receptors such as EGFR or PDGFR or mutated PI3K (mostly class Iα PI3K). $PI(3,4,5)P_3$ are then bound by effector proteins containing a pleckstrin homology (PH) domain like Akt/PKB and GEFs signalling into growth and metastasis pathways (Wymann and Marone 2005) (Figure 4).

SHIP1 is a haematopoietic-specific inhibitory enzyme mostly studied for its regulatory role in B and T cells, macrophages and mast cells (Rohrschneider, Fuller et al. 2000; Leung, Tarasenko et al. 2009). Observations in mice suggest a mechanism in which SHIP1 negatively regulates the PI3K pathway by hydrolysis of $PI(3,4,5)P_3$ and might hence control cell proliferation in a cancer context (Bunney and Katan).

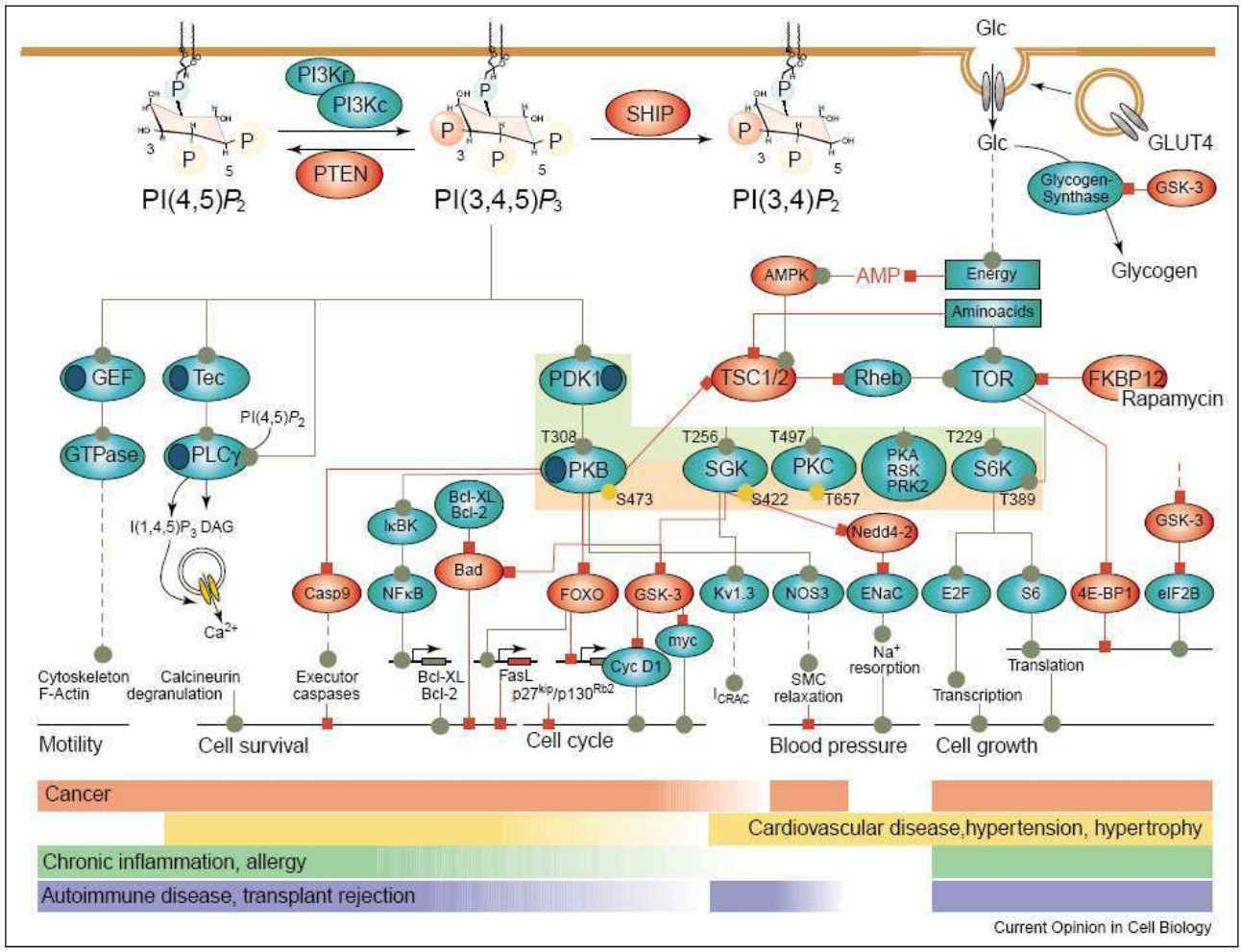

Figure 4: PI3K signalling complexity

The PI3K signalling network has become complex and it seems to be involved in many diseases. Shown above are positive (green dots) and negative (red squares) regulations among the effectors of this pathway. Figure from Wymann and Marone, 2005.
Constitutive activation of PI3K promotes cell mass and cell cycle entry, inhibits apoptosis and enhances cell migration, all typical indicaters of cancer cells (Marone, Erhart et al. 2009). There are many reasons for increased PI3K activity resulting in abnormally high $PI(3,4,5)P_3$ levels, their lipid product. Examples are oncogenic Ras, loss of PTEN, constitutively activated protein tyrosine kinase receptors such as EGFR, PDGFR) or mutated PI3K (mostly PI3K class I α). $PI(3,4,5)P_3$ are then bound by effector proteins containing a pleckstrin homology (PH) domain like Akt/PKB and GEFs signalling into growth and metastasis pathways (Wymann and Marone 2005). SHIP1 is a haematopoietic-specific inhibitory enzyme mostly studied for its regulatory role in B and T cells, macrophages and mast cells (Rohrschneider, Fuller et al. 2000; Leung, Tarasenko et al. 2009).

3.3.1 PI3K and Melanoma (Skin cancer)

Melanoma is a tumor with bad prognosis, especially once it has become metastatic. In a Swedish study on primary malignant melanoma, patients' survival rate within the first five years of follow up were as low as 10-15% in both males and females. (Ragnarsson-Olding, Nilsson et al. 2009) Melanoma often exhibit already at early stages mutated B-Raf or constitutively activated N-Ras. If loss of PTEN occurs, there is an increase in aggressiveness of the tumor,

similar to what is seen upon up-regulation of PKB. Mutations in PI3K class I α happen very rarely in cutaneous melanoma, it is more likely that the protein is upregulated (Curtin, Stark et al. 2006; Omholt, Krockel et al. 2006; Stark and Hayward 2007).

The PI3K pathway was originally targeted with the potent steroidal fungal metabolite wortmannin (Arcaro and Wymann 1993) or LY294002 (Vlahos, Matter et al. 1994), a pan-PI3K inhibitor with low potency, low specificity and high toxicity. These inhibitors also inhibit related proteins such as mTOR. More recent inhibitors like PI-103 and ZSTK474 led to improved specificity. Newer dual inhibitors affecting both mTOR and PI3K are in clinical trials now, treating patients with advanced malignancies. In a study by Marone et al. in 2009, we reported our results on NVP-BEZ235 tested in mice and *in vitro*. This compound blocked proliferation of melanoma cells by G1 cell cycle arrest and was well tolerated in mice. Both primary tumor (up to 60% reduction) and metastases were greatly reduced upon treatment while no adverse effects on the immune system was observed. Angiogenesis for the nutrient supply of the tumor was shown to be sensitive to the inhibitor tested, as we could see a clear reduction of neovascularization in mice treated with this compound. Most probably it was a combination of effects on the PI3K/mTOR pathway in addition to the VEGF receptor (vascular endothelial growth factor), as VEGFR inhibitors were not as efficient. NVP-BEZ235 not only reduced proliferation of tumor cells in mice but also augmented tumor necrosis (Marone, Erhart et al. 2009).

Tormo et al. described the therapeutic induction of autophagy in melanoma cells in a recent publication in Cancer Cell. The authors used three different mouse models: In the first mouse model, B16 melanoma cells were inoculated in immunocompetent mice. In their second model, they used GFP-labelled B16 or SK-Mel-103 cells in SCID-beige mice. Their third approach was a disease model using Tyr::NRAS^{Q61K}; INK4a/ARF$^{-/-}$ mice, that exhibit features similar to the human disease. These mouse models were used to show that melanoma cells retain an innate immune system response to recognize cytosolic double-stranded RNA (dsRNA) and start stress response programs to block tumor growth. The dsRNA was identified to be an inducer of autophagy, requiring Atg5 for the cell death process. Knockdown of Beclin1 led to cellular senescence or cell death in many melanoma cell lines tested. As Atg5 knockdown was lethal, too, they used Atg5-/- MEFs which showed a similar reaction to dsRNA as observed earlier in their melanoma cell lines. The authors conclude from their results that their artificial dsRNA induced an early but persistent autophagy and a late apoptotic program, hence killing the melanoma cells (Tormo, Checinska et al. 2009).

Another publication describing apoptosis and autophagy induction in melanoma cell lines was written by Liu et al. They conclude that in a A375 melanoma cell line, application of *polygonatum cyrtonema* (PC) lectin induces cell death by autophagy followed by apoptosis through mitochondria-mediated ROS-p38-p53 pathways. Beclin1 levels were increased after treatment with PC lectin and mature forms of LC-3 were observed, all representing symptoms

of autophagy. ROS (reactive oxygen species) were generated and p38 (MAPK) and p53 (tumor suppressor involved in cell cycle control) activated as well, evidence for increased apoptosis (Liu, Cheng et al. 2009).

3.4 *Nutrient regulation*

There are two mTOR complexes (Figure 8), of which mTORC1 (containing mTOR, raptor, PRAS40 and mLST8) is rapamycin-sensitive and controls cell growth, metabolism and autophagy through various signals, among them amino acids. A typical readout is phosphorylation of downstream substrate S6K1 and 4EBP1.

In the study of Byfield et al. in 2005, HEK293T cells overexpressing hVps34 exhibited a two-fold increase in S6K activity, similar to what can be observed upon stimulation with insulin. Blocking hVps34 function by overexpressing FYVE domain-construct did bind and hence block PI(3)P signalling indicated by ablation of EEA1 endosomal localization. Other attempts to block hVps34 by antibodies targeting the kinase or by application of siRNA gave similar results in HeLa cells. Overall, Byfield et al. suggested that both hVps34 and its product PI(3)P are required for both amino acid and insulin-stimulation of S6K1. They admit the possible differences in mammalian and yeast pathways, as observed for AMPK's role in autophagy (Wang, Wilson et al. 2001; Byfield, Murray et al. 2005).

Another group claimed to have found a link between mTORC1 and hVps34 in the same year, Nobukuni et al. working with siRNA technique in HEK293 and HeLa cells. Their results showed that effects of amino acids on S6K1 Thr398 phosphorylation are not mediated by TSC1/2. Wortmannin, a pan-PI3K inhibitor, did block the amino acid response though. It could be shown that this did not happen via class I PI3K. Under amino acid deprivation, little PI(3)P was detected in their cells. Upon knockdown of hVps34, they saw a coordinate reduction in amino acid-induced phosphorylation of S6K1. Hence they suggested hVps34 to be an upstream regulator of amino acid signal input towards mTORC1 (Nobukuni, Joaquin et al. 2005) (Figure 5). Amino acid activation of mTORC1 increases growth while it suppresses autophagy. Hormones and growth factors activate the Tor complex through canonical signalling via PI3K class I, in contrast, amino acids stimulate the complex via PI3K class III.

In a study by Gulati et al. in 2008, they claimed that amino acids induce an increase in intracellular calcium and in response enhanced binding of calmodulin (CaM) to hVps34 (Figure 5). This binding then leads to activation of the mTORC1 signalling. Agents that increase calcium levels within the cell have been reported to induce S6K1 phosphorylation without inducing PKB activation. HeLa cells were treated with BAPTA-AM, a calcium chelator. Treatment caused an attenuation of S6K1 activation under restimulation with amino acids. Similar effects were seen after application of EGTA, another calcium chelator. To check calcium levels within the cells, Gulati et al. used a calcium-sensitive indicator called Fluo-4.

Addition of amino acids led to a rapid increase in calcium levels. Leucine alone induced a similar reaction, influx of extracellular calcium. Thapsigargin (calcium-ATPase inhibitor) treatment gave supporting results. Removal of leucine form the medium inhibited hVps34 activity to the same extent as removal of total amino acids. Treatment with W7, a cell-permeable CaM antagonist, blocked the phosphorylation of S6K1 Thr398 by amino acid stimulation. Calmodulin was found to interact with hVps34 if calcium was present in vitro and no treatment with EGTA was applied. SiRNA knockdown of hVps34 abrogated the interaction of CaM-beads with mTOR, but hVps34 and mTOR seem to interact independently of calcium and amino acids. Analysis of the sequence of hVps34 revealed a potential CaM-binding motif in the PI3K accessory domain. In their experiments, calcium seemed to stabilize the interaction between CaM and hVps34. Moreover, treatment with calcium chelators even abolished the kinase activitiy *in vitro*. Overall, this study showed that the rise in intracellular calcium levels increases the direct binding of calcium/CaM to a conserved motif in hVps34 which is required for kinase activity and increased signalling towards mTORC1 upon amino acid stimulation, especially leucine availability (Byfield, Murray et al. 2005; Nobukuni, Joaquin et al. 2005; Wullschleger, Loewith et al. 2006; Gulati, Gaspers et al. 2008).

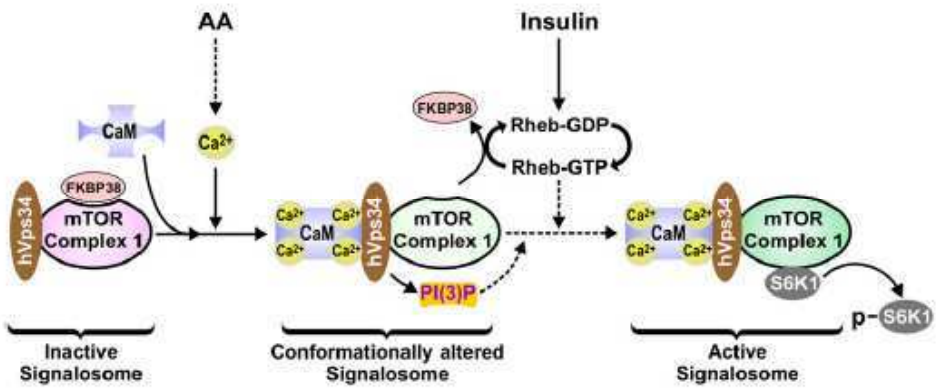

Figure 5: mTORC1 signal inputs

According to Gulati et al. amino acids signal towards mTORC1 via calcium which then binds to calmodulin and triggers a response from hVps34. Due to a conformational change in the signalosome, mTORC1 phosphorylates the ribosomal S6K1 upon this response by hVps34. (Gulati, Gaspers et al. 2008)

Juhasz et al. generated mutants of the *Drosophila melanogaster* orthologue of hVps34 which resulted in defects in autophagosome formation and endocytosis. In contrast to what has been described by other research groups (Byfield, Murray et al. 2005; Nobukuni, Joaquin et al. 2005; Gulati and Thomas 2007), Juhasz et al. did not find any effects on TOR signalling in these Vps34 mutants in the fly. Instead they observed regulation through TOR and Atg1 of starvation-induced recruitment of PI3P to nascent autophagosomes. Their results suggest that at least in the fly, Vps34 is regulated by TOR-dependent nutrient signals at the site of

autophagosome formation. TOR mutants show a decrease in cell size, while neither Vps34 mutants nor cells overexpressing kinase-dead Vps34 did. Proliferation was not affected either, indicating that in fly eye imaginal disc cells, TOR signalling is not compromised in Vps34 mutants. Readouts such as phosphorylated Thr398 of S6K1 were not affected in Vps34-deficient cells. According to their data, Vps34 seems to be acting downstream of TOR-dependent nutrient signalling in the fruit fly (Juhasz, Hill et al. 2008).

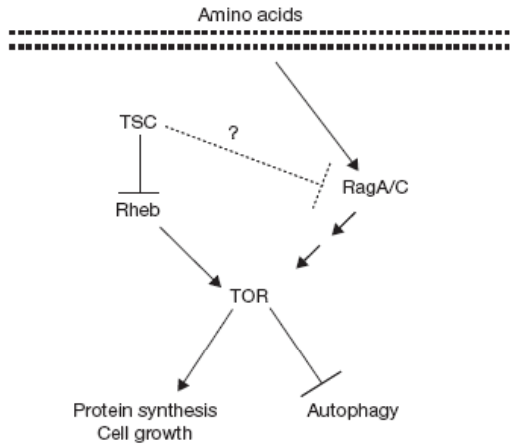

Figure 6: Schematic view of TOR's in- and outputs

According to Kim et al., amino acids signal towards Rags which then activate TOR to both block autophagy and trigger protein synthesis and cell growth. Unknown so far is if and how TSC1/2 complexes could block Rags. (Kim, Goraksha-Hicks et al. 2008)

A recent review by Avruch et al. focuses on the mechanisms by which mTORC1 is regulated by amino acids. They state that there are both pro and contra to the involvement of class III PI3K in amino acid regulation of TOR signalling. Extracellular amino acids are capable of regulating hVps34 lipid kinase activity (Byfield, Murray et al. 2005), possibly through a calcium-dependent mechanism (Gulati, Gaspers et al. 2008). Depletion of hVps34 or hVps15 (p150) inhibits S6K1 phosphorylation (Nobukuni, Joaquin et al. 2005). HVps34 can be co-precipitated with mTOR, hence hVps34 might activate mTORC1 via generation of its lipid products, PI(3)P (Gulati, Gaspers et al. 2008). On the other hand, in fly (Juhasz, Hill et al. 2008) and worm (Roggo, Bernard et al. 2002), no impact of Vps34 depletion was observed when TOR signalling was investigated.

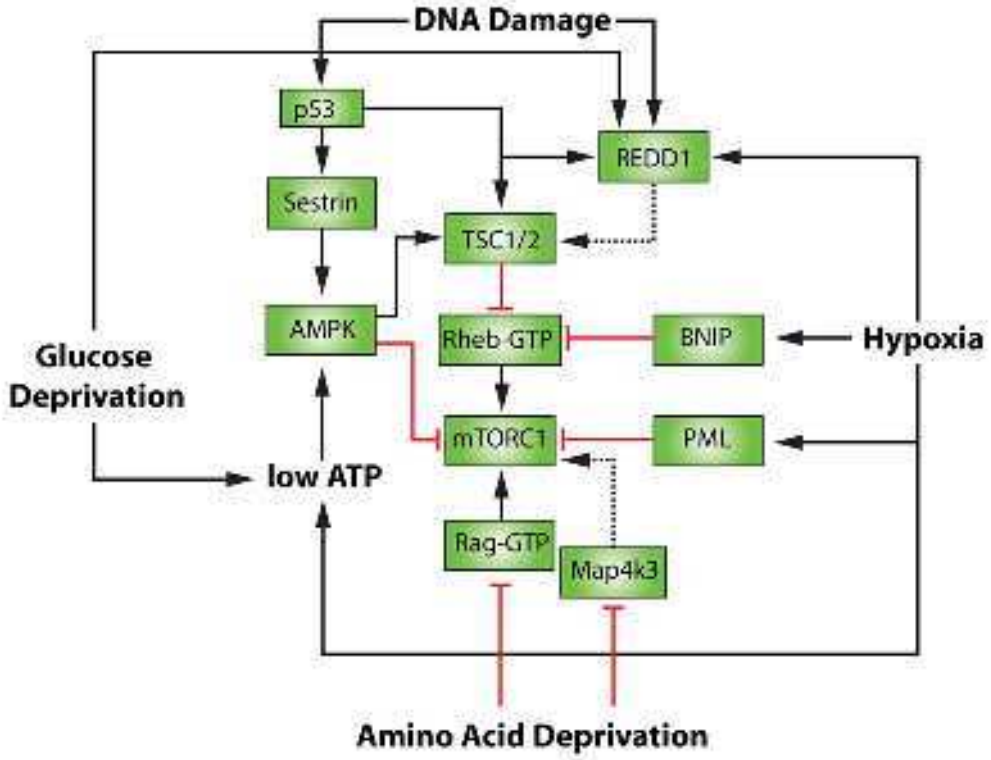

Figure 7: Nutrient signalling input towards mTORC1

Rag GTPases activate mTORC1 upon amino acid (AA) stimulation, mainly leucine and arginine. Whether MAP4K3 acts directly on Rags is content of discussions in the field today. (Sengupta, Peterson et al.; Zoncu, Efeyan et al.)

Yan et al. in their recent publication in 2009 state that according to their studies, hVps34 does require hVps15 (p150) for kinase activity also in nutrient regulation and does bind CaM *in vitro*, but they could not observe any effects after treatment with BAPTA-AM or W7. hVps34 seemed unaffected by calcium chelation *in vitro*. In representative mammalian cells (here Chinese-hamster ovary cell line), hVps34 seems to be clearly regulated through ist interaction with hVps15 (p150), but independent of calcium and calmodulin (CaM). Yan et al. discovered that residual EGTA (calcium chelator) can block hVps34 activity, hence the putative misinterpretation of Gulati et al. The suggested CaM-binding motif in hVps34, which they had found by mutations in the helical domain, could also be an artefact. Mutations of this area were all hydrophobic-to-charged alterations which might simply disrupt the folding and hence lead to loss of activity of hVps34 (Yan, Flinn et al. 2009).

In an attempt to find interacting partners of mTORC1 that have been hidden by technical issues so far, Sancak et al. discovered RagC, a small GTPase related to Ras (Figure 6 and 7). There are three other Rags, termed RagA, B and D. RagA and B are orthologues of yeast Gtr1p, while RagC and D are orthologues of yeast Gtr2p. As RagC copurifies with raptor and in yeast Gtr1p and 2 regulate microautophagy and vacuolar sorting, they checked for interaction of the mammalian proteins in HEK293T cells. Rags function as heterodimers, RagA/C or B/D (Figure 7 and 8). They do not directly stimulate kinase activity of mTORC1 in vitro, but regulate

the localization within the cell upon amino acid signalling. Sancak et al. propose that since both mTOR and Rheb are present in Rab7-positive endosomes after amino acid stimulation, amino acids might control the mTORC1 pathway via the Rag proteins in order for mTORC1 to meet its activator Rheb. This hypothesis would explain why activators of Rheb, e.g. insulin, do not stimulate the mTORC1 pathway when cells are in a nutrient deprived state (Sancak, Peterson et al. 2008; Sengupta, Peterson et al.; Zoncu, Efeyan et al.).

Many signals, including amino acids, are known to activate mTORC1. Kim et al. identified the small GTPases Rags as activators of TORC1 in response to amino acid signals (Figure 6). In *Drosophila melanogaster*, knockdown of Rags led to suppression of stimulation of TORC1 by amino acids, while expression of constitutively active Rags (GTP-loaded) activated TORC1 when phosphorylation of dS6K at Thr398 was taken as readout. Rags are apparently regulating cell size as expected of a TOR regulator, as well as autophagy and survival during starvation. Especially dRagA could be shown to be involved in a nutrient response to amino acids (Kim, Goraksha-Hicks et al. 2008).

Another player in the TOR nutrient sensing field has been discovered by Findlay et al. in *Drosophila melanogaster*. MAP4K3 (CG7097 in the fly), a *Ste20* family member, seems required for maximal S6K/4EBP1 phosphorylation and regulates cell growth. It is itself regulated by amino acids but not insulin and insensitive to rapamycin, suggesting that MAP4K3 is not downstream of TOR but upstream in this pathway. An almost complete knockdown of MAP4K3 was required to get efficient suppression of S6K1 phosphorylation at Thr398, while the effect seemed independent of TSC1/2 complexes. They picture MAP4K3 in a signalling branch parallel to TSC1/2, passing on signals from amino acid input towards mTORC1 (Findlay, Yan et al. 2007).

Nicklin et al. showed in 2009 that cellular uptake of L-glutamine and ist subsequent rapid efflux in the presence of essential amino acids (EEA) activates mTORC1. SLC1A5 (solute carrier family 1 member 5 or ASCT2), a high-affinity transporter for L-glutamine, regulates this uptake and loss of the sodium-dependent transporter results in reduction of cell growth and activation of autophagy. SLC7A5 (LAT1)/SLC3A2, a bidirectional transporter, regulates the simultaneous efflux of L-glutamine and transport of L-leucine/EEA into cells. The exchange of L-glutamine for L-leucine happens before S6K1 activation as they showed in HeLa cells. They claim that SLC1A5 and SLC7A5 may act upstream of TSC1/2 to mediate amino acid signals towards mTOR. The findings seemed independent of cell types, as similar results were obtained in MCF-7 breast cancer cells. SLC1A5 and L-glutamine suppressed autophagy in RT112 cells, a human urinary bladder carcinoma cell line. Overall, Nicklin et al. presented amino acid transporters upstream of mTORC1, which are involved in regulation of autophagy by bidirectional transport of AA (amino acids) (Nicklin, Bergman et al. 2009).

Wang and Proud summarized today's knowledge of nutrient control concerning TORC1 in a review in *Trends in Cell Biology* in 2009. In order to illustrate the above mentioned

publications on the composition of mTOR complexes, Rags, upstream control of mTORC1 by amino acids and putative links between mTORC1 and autophagy/hVps34, figures from this article are pasted below (Figure 8) (Wang and Proud 2009).

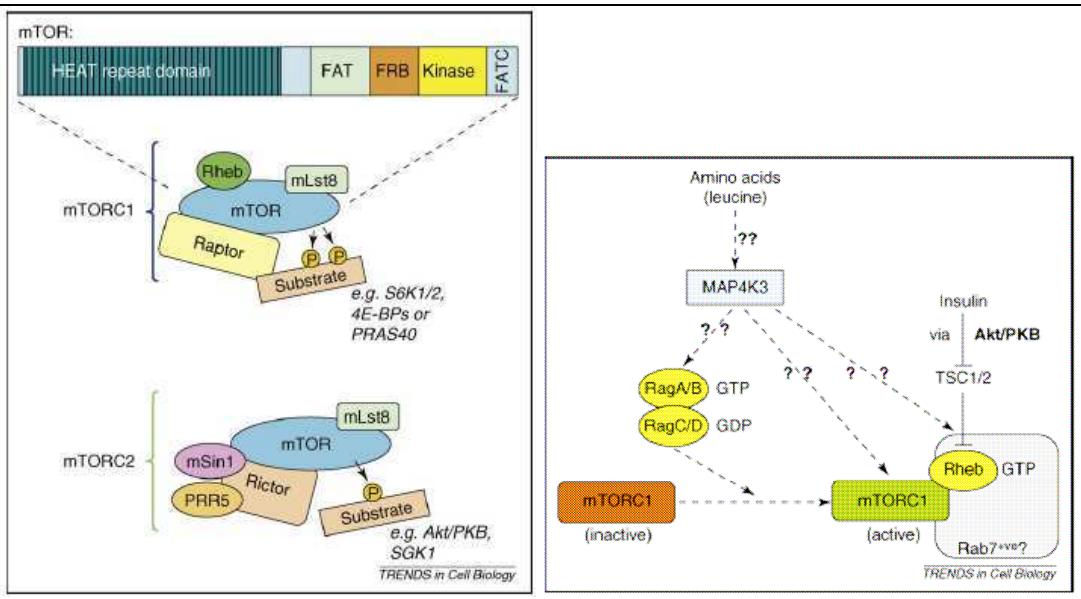

Figure 8: Nutrient control controlled by mTORC1

Schemes above illustrate today's knowledge of nutrient control involving mTORC1 (details on left panel) and Rag GTPases. (Wang and Proud 2009)
Left panel: mTOR consists of several domains; helical HEAT repeat domains found in many cytoplamic proteins, a FAT domain for stability (found in FRAP-ATM-TTRAP), a FRB domain which is bound by FKBP12-rapamycin upon inhibition of mTOR by rapamycin, a kinase domain and a C-terminal FAT domain (FATC).
Right panel: Putative ways of extracellular stimulation via Rags towards mTORC1 are depicted in this scheme. Amino acids, mainly leucine, are thought to signal to MAP4K3 (in parallel to insulin signals towards TSC1/2), which then either stimulates mTORC1 or Rheb directly or via heterodimeric Rags that first need to activate mTORC1 prior to further signalling.

3.5 *Autophagy*

3.5.1 Yeast Autophagy

Autophagic bodies in yeast were first described as such by Takeshige et al. in 1992. In their study they transferred mutants lacking different proteinases and carboxypeptidase Y (CPY) from a nutrient rich to a synthetic medium devoid of various nutrients and observed "spherical bodies" in the vacuoles that they called "autophagic bodies". The contents of these 400-900nm in diameter sized bodies were organelles usually found in the cytosol. Accumulation of autophagic bodies were not only induced by nitrogen starvation but also by depletion of nutrients such as carbon or single amino acids that in response caused cell cycle arrest. PMSF (phenylmethylsulfonyl fluoride) seemed to reversibly induce the same phenotype in wild type cells (Takeshige, Baba et al. 1992).

A year later, the same research group published a list of APG genes (later termed ATG genes). These were supposed to be involved in autophagy in yeast, i.e. APG1-15. Mutants defective for these genes did not accumulate autophagic bodies under nutrient-depleted conditions, were defective in protein degradation in the vacuoles induced by nitrogen starvation and lost viability much faster than wild type yeast if starved. Homozygous diploids of each APG mutant did not sporulate (Tsukada and Ohsumi 1993).

“Autophagosomes” were first described by Baba et al. as double membraned structures that apparently fused with vacuoles, hence they were thought to be precursors of autophagic bodies (Figure 10 and 11). Electron microscopy was applied to investigate the process. They often detected a cup-shaped structure next to clusters of autophagosomes which they interpreted as newly forming autophagosomes. As for the origin of the membranes involved they assumed it to be either smooth ER (Dunn 1990) or from post-Golgi (Baba, Takeshige et al. 1994).

In yeast there are various flavours of autophagy, two major forms are macroautophagy and microautophagy. In macroautophagy, the initial sequestration takes place away from the vacuole, resulting in cytoplasmic compartments called autophagosomes (Figure 10). Microautophagy on the other hand describes a process where the limiting membrane of the vacuole starts to invaginate, pinching off small vesicles that contain material from the cytosol. A variation thereof is micropexophagy, where peroxisomes are taken up into the vacuole. Micro- and macroautophagy are not mechanistically identical in *S. cerevisiae*. Yeast possess yet another pathway to the Cvt-pathway, “cytoplasm-to-vacuole-transport”, which takes place constitutively. Maturation of prApe1 (precursor of mApe1, mature Ape1) can be used as a marker of autophagy in yeast strains defective for Cvt trafficking but not autophagy. A majority of genes are shared by the two distinct pathways, e.g. Vps34 and Atg9 are involved in both processes. On the other hand, Cvt9 is only part of the Cvt machinery and Atg17 only found during autophagy. Proteasomes are another location for degrading proteins in yeast, but this machinery requires specific polyubiquination signals on the proteins to be degraded or unfolded proteins for the UPR, unfolded protein response. Mitochondria are recycled in a process called mitophagy (Abeliovich and Klionsky 2001).

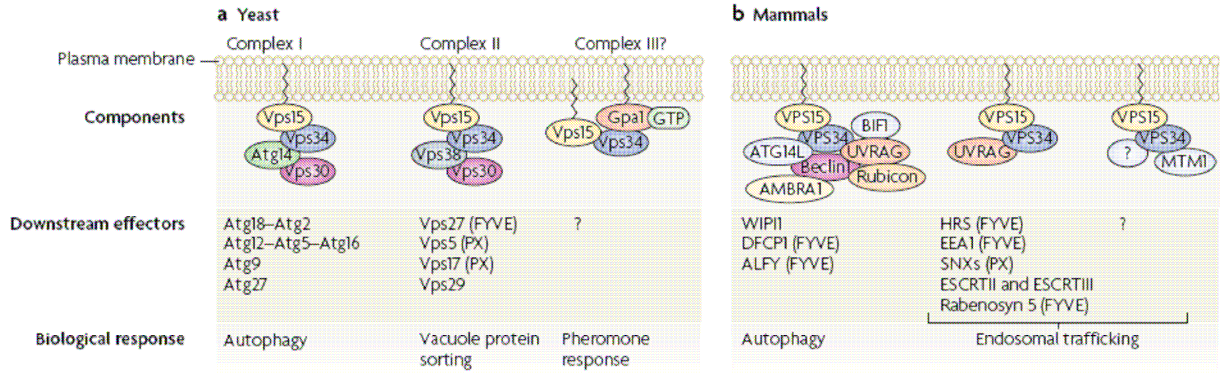

Figure 9: Autophagy and Endosomal trafficking complexes in yeast and mammals

Although the complexes for autophagy and endosomal trafficking differ slightly in yeast (panel a) and mammalian cells (panel b), many homologs have been found already. (Vanhaesebroeck, Guillermet-Guibert et al.)

3.5.2 Autophagy in Mammalian Cells and in other Organisms

In 1999, Liang et al. described Beclin1 (Figure 9), the human orthologue of yeast Atg6/Vps30, to be a tumor suppressor. Beclin1 is a Bcl-2-interacting, coiled-coil protein and is deleted in 40-75% of sporadic human breast cancers and ovarian cancers (Aita, Liang et al. 1999). It has structural similarity to the yeast protein Atg6p, so that Beclin1 expression can promote autophagy in *atg6* deletion mutants. The human cancer cell line MCF-7 does not express detectable endogenous Beclin1 levels. Upon stable conditional transfection with Beclin1, autophagic vacuoles marking nutrient deprivation-induced autophagy could be observed in these cells. No evidence of apoptosis was found, the nuclei appeared normal. Induced autophagy seemed to reduce proliferation rates and led to flatter appearance, larger size and increased contact inhibition of the cells. Clonigenicity *in vitro* was highly impaired and injection into nude mice gave rise to significantly less tumor formations. Out of eleven tested human breast carcinoma cell lines, only three expressed endogenous Beclin1 while all 32 samples of normal breast epithelial tissue stained for strong Beclin1 immunoreactivity. The authors suggest that Beclin1 is a key enzyme in inhibition of tumorigenesis through autophagy (Liang, Jackson et al. 1999).

Alfy, was discovered by Simonsen et al. in 2004. It represents a 400kD protein that contains a FYVE-domain and WD-40 repeats. Results in HeLa cells suggest that Alfy is indeed binding PI(3)P and colocalizes with protein granules and autophagic membranes. Alfy-positive structures accumulate in the cytoplasm after serum and amino acid starvation. These structure at least partially costain with autophagy markers such as LC-3 and hAtg5. The authors imply a scaffold role for Alfy in the autophagic machinery as it recognizes protein aggregates and localizes close to ubiquitin-loaded structures (Simonsen, Birkeland et al. 2004).

Zeng et al. described a new role for Beclin1 in 2006. In U-251 glioblastoma cells immunoprecipitates contained not Bcl-2 but hVps34. Knockdown of Beclin1 blocked autophagy induced by nutrient deprivation or C_2-ceramide. Endocytosis on the other hand was not impaired, as EGFR sorting or internalization of fluid phase markers such as HRP were not affected. Their results suggested that Beclin1 was not a simple chaperone or adaptor of the hVps34 complex in normal vesicular trafficking but mainly a positive regulator of the autophagic pathway (Zeng, Overmeyer et al. 2006). These findings were in agreement with results in *Caenorhabditis elegans* published earlier by another group (Melendez, Talloczy et al. 2003).

The group of Vojo Deretic showed in 2006 that autophagy can be used as a mechanism to reduce bacterial load i.e. as defense against intracellular pathogens (Figure 13). In their study, they had a closer look at murine Irgm1 of the family of immunity related GTPases (IRG). IFN-γ (interferon γ) induces autophagy in macrophages, but expression of Irgm1 by itself already leads to onset of autophagy in macrophages. Cells exhibited a MDC (monodansylcadaverine)-positive profile, a preliminary marker for autophagic organelles. Classical inhibitors of autophagy e.g. wortmannin and 3-MA (3-methyladenine) inhibited this reaction. The autophagosome-like structures detected in their experiments showed double-membrane character, known as phagophores i.e. nascent autophagosomes. Irgm1 seemed important in early stages of autophagosome formation, in detail in LC-3 (human Atg8) maturation. Further steps of such autophagic processes seemed to depend on Beclin1 and the usual autophagy complex subunits. Similar results were obtained in human cell lines, U937, HEK293T and HeLa. Human macrophages behaved the same way, IRGM (human orthologue of murine Irgm1) inducing autophagy as seen earlier in murine cells. Unlike the IRG family in mice, the human IRGM is not activated by IFN-γ. Nonetheless did IRGM participate in IFN-γ or starvation induced autophagy in human macrophages, indicating a more general role for IRGM in autophagy. More details on the role of IRGM in defense against intracellular pathogens require further investigations (Singh, Davis et al. 2006).

In 2006, Liang et al. identified a novel coiled-coil UV irradiation resistance-associated gene (UVRAG) that positively regulated the Beclin1-hVps34 complex. UVRAG is monoallelically mutated at a high frequency in human colon cancers, hence it is a candidate to be a tumor suppressor. UVRAG and Beclin1 interdependently induce autophagy. The new player promotes autophagy and suppresses proliferation and tumorigenicity of human colon cancer cells tested in their study (Liang, Feng et al. 2006). In a later publication, the same author claimed that UVRAG binds Beclin1 and interacts with the endosomal fusion machinery. Rab7 gets stimulated and autophagosomes then fuse with late endosomes, enhancing delivery of autophagic cargo to the lysosome. UVRAG-endosomal sorting is genetically separate from UVRAG-Beclin1-mediated autophagosome formation. UVRAG therefore functions as a multivalent trafficking effector (Liang, Lee et al. 2008).

Another positive regulator of autophagy directed by Beclin1 is Ambra1, discovered by Fimia et al. in 2007. Ambra1 (Activating molecole in Beclin1-regulated autophagy) bears a WD40-domain at its N-terminus and has a crucial role in embryogenesis. Ambra1 downregulation led to reduced capability of Beclin1 to interact with hVps34 and also kinase activity of Vps34 was impaired in these cells. Upon functional deficiency, severe neural tube defects were observed in mouse embryos as autophagy was impaired, ubiquitinated proteins aggregated and cell proliferation became unbalanced while apoptosis was strongly increased (Fimia, Stoykova et al. 2007).

To date it is not clear where the membranes of autophagosomes originate from. In 2008, Takahashi et al. published a study in which they describe Bif-1 (Endophilin B1), a member of the endophilin family. Bif-1 possesses membrane binding and liposome tubulation activities. Under nutrient deprivation conditions, Bif-1 accumulates in punctate structures that colocalize with LC-3, Atg5 and Atg9, markers of autophagosomes. Bif-1 positive vesicles were shown to fuse with Atg9-positive small membranes to form autophagosomes in both HeLa and COS7 cells. As the N-BAR domain of Bif-1 interacts with Beclin1 through UVRAG and promotes activation of hVps34, they suggest Bif-1 to be a potential regulator of autophagosome formation (Takahashi, Coppola et al. 2007; Takahashi, Meyerkord et al. 2008).

Axe et al. described autophagosome formation from membrane compartments connected to the endoplasmatic reticulum (ER) (Figure 10 and 11). They applied a novel protein termed DFCP1 (double-FYVE domain-containing protein 1) and observed PI(3)P lipids translocating from unusual localizations on ER and Golgi membranes to autophagosomes upon amino acid starvation. Translocation was dependent on hVps34 and Beclin1 in the HEK293 cells tested (Axe, Walker et al. 2008).

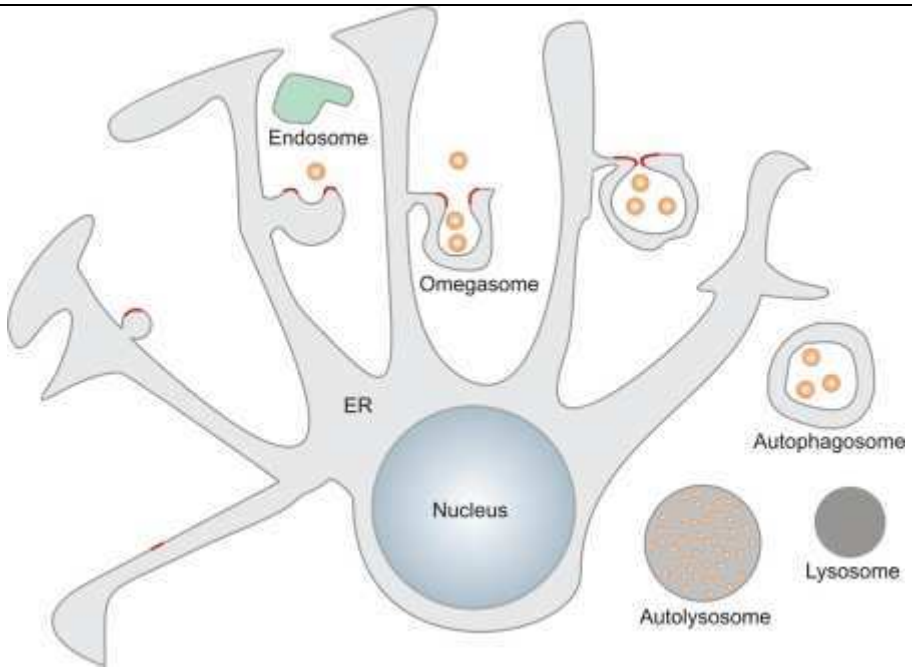

Figure 10: From omegasomes and autophagosomes

According to Simonsen et al., omegasomes are precursors of autophagosomes. Omegasomes obtained their name from their "omega"-shape, originating from endoplasmatic reticulum (ER). (Simonsen and Stenmark 2008)

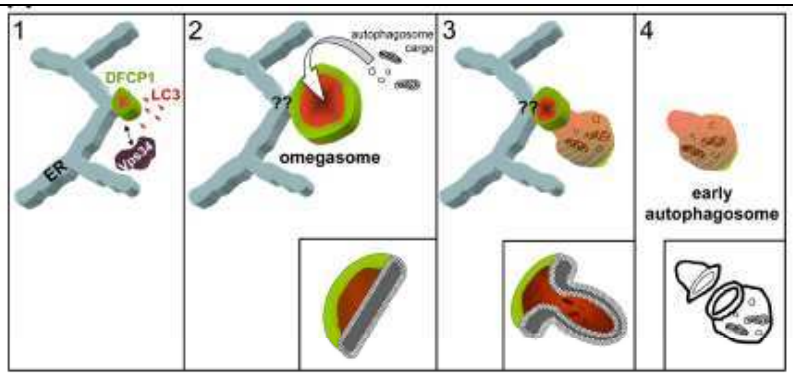

Figure 11: Autophagosome formation- three dimensional

Three-dimensional scheme of autophagosome formation from ER. Early formation is controlled by Vps34, amongst other proteins. DFCP1 is a newly proposed marker for early autophagosomes, colocalizing with PI(3)P and LC3. (Axe, Walker et al. 2008)

ESCRT complexes are involved in endosomal protein sorting, among many functions they are required for membrane fission during viral budding. Alix, binding members of ESCRT complex I and III, was hypothesized to control autophagy alike ESCRT proteins. Petiot et al. could show that Alix is not influencing the degradation of the EGFR and does not influence autophagy. Hence, autophagy requires the function of ESCRT proteins, but Alix is only required for viral budding and cytokinesis (Petiot, Strappazzon et al. 2008). More details on the ESCRT

machinery were described in an article by Wollert et al. in 2009, summarizing all the proteins involved. Structural information was nicely presented by Im et al. in Developmental Cell in the same year, see figure 11 below (Im, Wollert et al. 2009; Wollert, Yang et al. 2009).

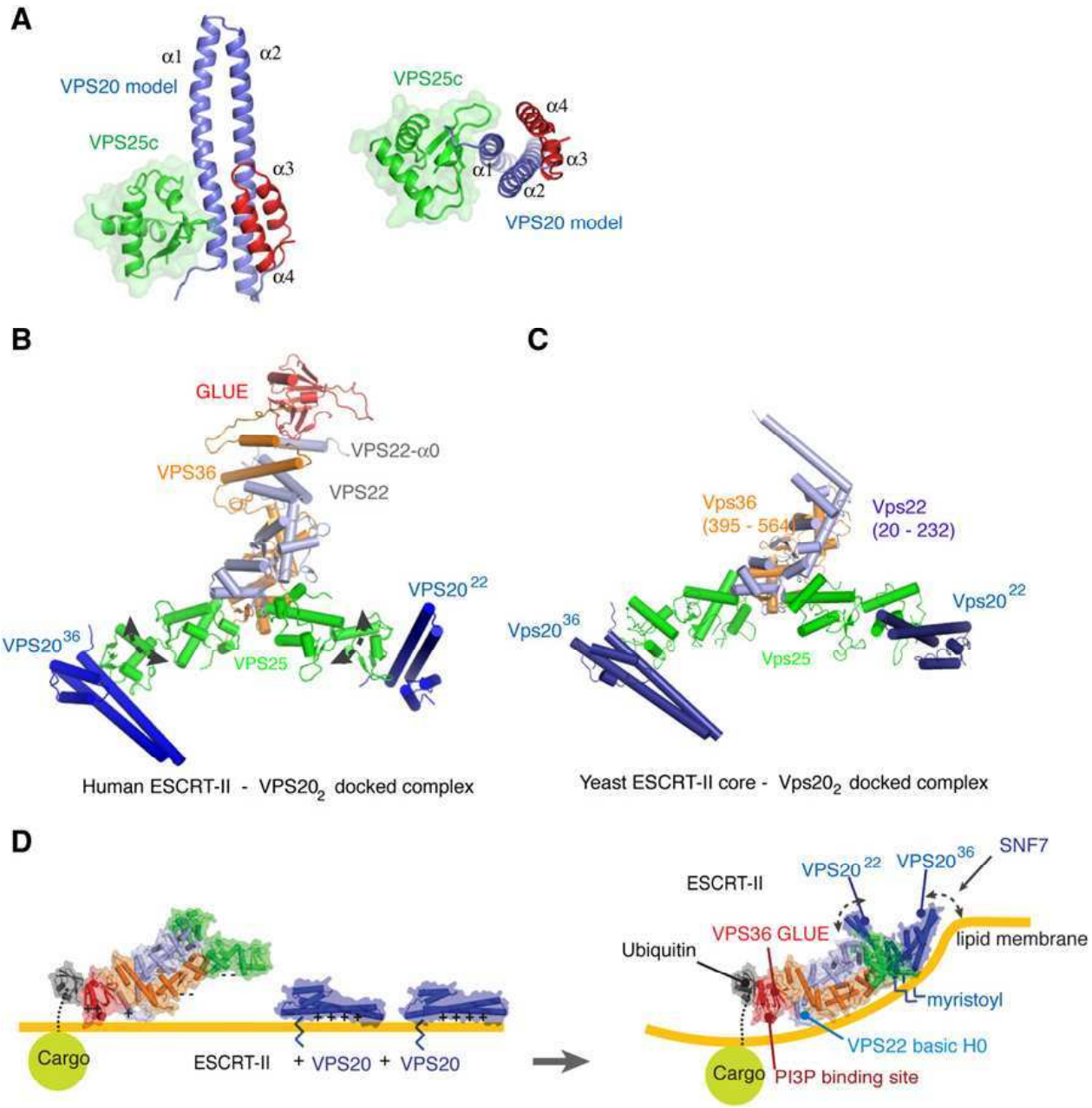

Figure 12: Structures of human versus yeast ESCRT-II

Depicted are structures of alpha-helices of Vps20-ESCRT-II supercomplex, showing how the curvature of membranes during endosomal sorting might take place. (Im, Wollert et al. 2009) A) Digital modeling of Vps20 according to crystal structure of Vps24. B) Model of human ESCRT-II-Vps20 supercomplex. C) Yeast ESCRT-II-Vps20 supercomplex model. D) Proposed mechanism for negative curvature during membrane docking of human ESCRT-II-Vps20 supercomplex.

The most recently discovered players in autophagic processes were described by Mauvezin et al. and Dikic et al., nicely reviewed by Spowart and Lum in 2010. DOR, a nuclear protein, is involved in stress-induced autophagy. It exits the nucleus and relocates to punctate

cytoplasmic structures, presumably autophagosomes upon stress. DOR does not remain associated with the autophagic machinery, hence it might be a cofactor to target material to the autophagosomes in a recycling manner. DOR has as well been found in *Drosophila melanogaster*, not to be mixed up with Dor, the homologue of Vps18. Nix is a selective autophagy receptor that mediates mitochondrial clearance and is found during maturation of reticulocytes (Mauvezin, Orpinell et al.; Novak, Kirkin et al.; Spowart and Lum).

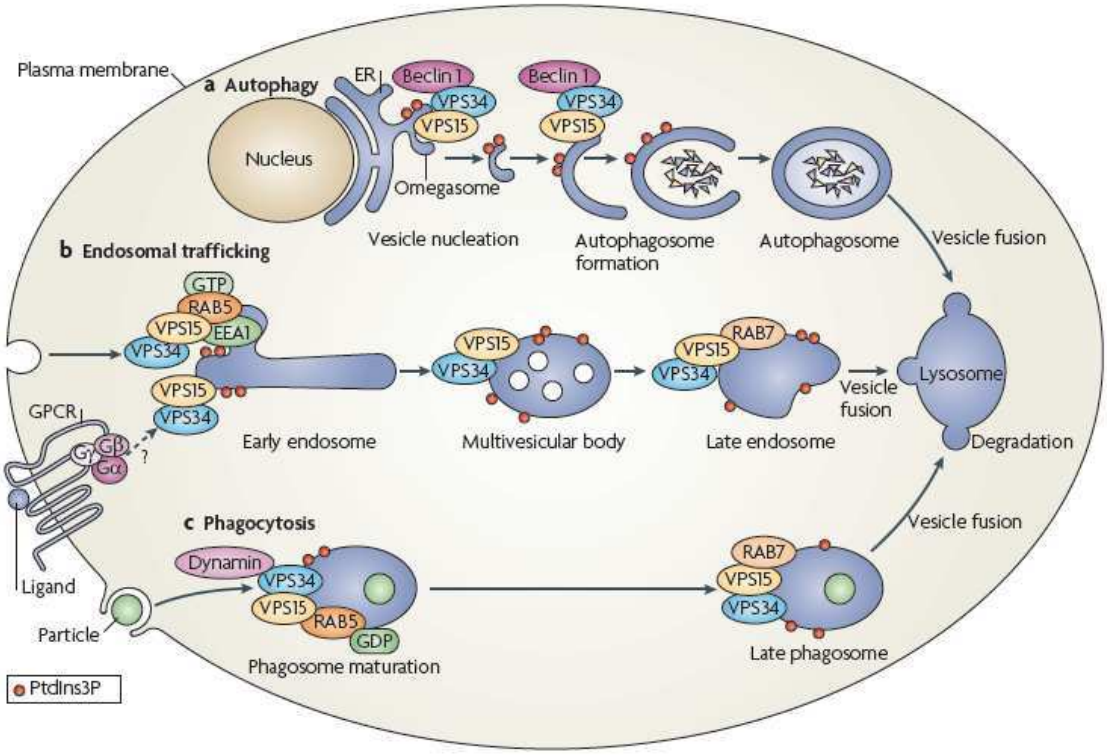

Figure 13: Autophagy- Endosomal sorting- Phagocytosis

Vps34 is involved in all three processes, changing interactors but always binding to its adaptor p150/Vps15. The cell responds to a variety of stimulations, be it nutrient deprivation or GPCR-bound ligands. In the end cargo is transported to the lysosome in all cases, autophagy, endosomal trafficking or phagocytosis. (Vanhaesebroeck, Guillermet-Guibert et al. 2010)

3.5.3 PI3K and Autophagy

Inactivation of Atg orthologues in higher eukaryotes has shown that the autophagic machinery is highly conserved throughout evolution. 31 Atg genes have been described in yeast, of which 18 are involved in starvation-induced autophagosome formation. These core Atg proteins are divided into four subgroups: 1. Atg1/ULK1 and their regulators, 2. Vps34 complex I (Vps34, Vps15/p150, Atg14/Atg14L and Vps30/Atg6/Beclin1 or their mammalian orthologues, together with Rab5) (Vps34 complex II contains Vps38/UVRAG instead of Atg14/L

and plays a role in endosomal sorting), 3. Atg9 cycling complex, 4. ubiquitin-like proteins Atg12 and Atg8/LC-3 and their conjugation systems.

Other complexes seem important for autophagy function, such as COP I (coat protein complex I) which maintains ER-Golgi transport and hence endosomal/lysosomal function and also ESCRT complexes 0-III (endosomal sorting complex required for transport) which are required for MVB (multivesicular body) formation and sorting of ubiquitinated integral membrane receptors towards the MVB. Many ESCRT proteins are essential for autophagy, as deletion of Vps27/HRS or Vps4 (AAA-ATPase) results in accumulation of nondegradative autophagosomes. There are contradictory results though in yeast, challenging this hypothesis in favor of endosome-fusion-defect hypothesis.

Another complex is the socalled HOPS (homotypic vacuole fusion and protein sorting) complex, containing Vps11, 16, 18, 33, 39/Vam6 and Vps41 in yeast. The HOPS complex regulates tethering and fusion of endosomes to the vacuole in yeast and lysosomal delivery and autophagosome maturation in the fly. If the same complex and function is conserved in mammalian cells still needs to be investigated, as mammalian UVRAG does not cover all functions of yeast Vps38 for example.

The CORVET (class C core vacuole/endosome tethering) complex consisting of Vps3 and 8 in addition to core proteins exists in yeast and interacts with Vps21, the orthologue of mammalian Rab5. CORVET and HOPS function overlap in certain cases, hence the eventual difference from yeast to human context.

Another Vps34 complex contains Rubicon (RUN domain and cysteine-rich domain containing, Beclin1-interacting protein), which in contrast to Atg14L reduces hVps34 activity. (Figure 14) Rubicon is found both on early and late endosomes, possibly regulating autophagy at multiple steps (Simonsen and Tooze 2009).

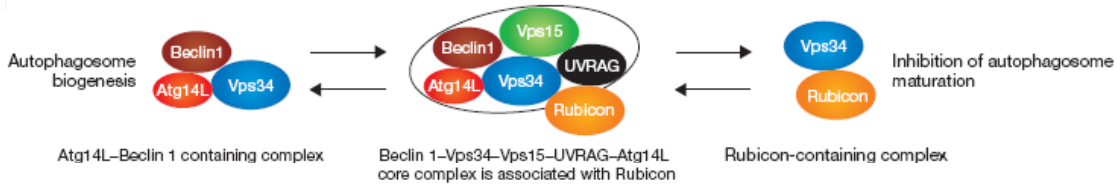

Figure 14: Autophagy players

Rubicon and Atg14L both bind to Vps34-containing complexes regulating autophagy, they have distinct functions though. Rubicon reduces hVps34 activity, in contrast to Atg14L. (Zhong, Wang et al. 2009)

Vergne et al. found Jumpy (MTMR14) , a PI(3)P phosphatase, to be associated with early autophagosomes. Jumpy controls the recruitment of Atg18 (WIPI-1) and affects the

distribution of Atg9 and LC-3. For the first time, the initiation of autophagy is controlled not only by PI(3)P producing kinase but also by a specific PI(3)P phosphatase which apparently is even linked to disease, e.g. congenital centronuclear myopathy (Vergne, Roberts et al. 2009).

3.5.4 Cancer Therapy- Pro or Contra Autophagy?

Beth Levine published a collection of questions and answers on autophagy and its role in cancer in Nature Cell Biology in 2007. An important evolutionary conserved function of autophagy is to help maintain the synthesis of essential proteins when nutrients are limited. Through protein recycling, activated autophagy can ensure cell's survival even if general protein translation is shut down. In contrast to apoptosis that invariably leads to cell death, autophagy usually contributes to cell survival. It can induce a cell death program if the apoptotic machinery is impaired or when autophagy is strongly increased that the cells literally "eat themselves to death". Cancer cells often confer resistance to apoptosis and many chemotherapeutic reagents induce autophagy. DNA damage is prevented by autophagy, probably by removing sources of oxidative stress, e.g. defective mitochondria or endoplasmatic reticulum. For these reasons, autophagic mechanisms can be considered beneficial for cancer therapy. On the contrary, some autophagy-specific genes might promote survival of cancer cells by allowing growth during poor nutrient conditions. When a tumor reaches 0.2-2mm in diameter , nutrients, growth factors and oxygen cannot diffuse efficiently to the cells at the center of the tumor mass due to inadequate vascularization. Hence autophagy might actually facilitate a tumor's survival in some cases (Folkman 2006). So far, there are contradictory experimental results in the literature as for whether "autophagy is cancer's friend or foe". Most probably it depends on the individual circumstances (such as vascularization in tumor environment, stage of tumor development etc.) and genetic background of the cancer cells if autophagy should be turned on or off by chemical compounds and which proteins are best to target (Levine 2007).

In a review in 2008, Jin and White state that due to its protective role in maintaining energy homeostasis and protein/organelle quality control, autophagy might be a tumor suppressing mechanism managing metabolic stress. Cellular damage manifests in activation of DNA damage response and may promote tumor initiation or drive cell-autonomous tumor progression. Autophagic processes usually localize to regions in solid tumors that are metabolically stressed. Defects in autophagy can then cause increased cell death and inflammation. These cytokine reactions lead to even more accelerated tumor progression. Hence, autophagy might be a tumor suppressor and future investigations should identify human tumors with deficient autophagy and develop more rational cancer therapies making use of the autophagy mechanisms (Jin and White 2008).

Dalby et al. published a recent review focusing on autophagy as a novel therapeutic strategy in cancer treatment. Autophagy has been described as programmed cell death type II (PCD-type II), a non-apoptotic form which is caspase-independent. Proapoptotic Bcl-2 family members such as Bak and Bax cause mitochondrial out membrane permeabilization and cytochrome c release. In knockout fibroblasts, resistance to apoptosis and induction of autophagic cell death was observed after starvation (Moretti, Attia et al. 2007). Several compounds have also been found to stimulate PCD-type II, e.g. rottlerin (Akar, Ozpolat et al. 2007). Autophagy might therefore function as an alternative cell death program in cells which are apoptosis defective or in which it is hard to induce. Examples of cancer types where autophagy might be beneficial for treatment are pancreatic cancer and breast cancer. PKCδ positively regulates the expression of TG 2 (tissue transglutaminase 2), which suppresses autophagic cell death. Knockdown or inhibition of either PKCδ or TG2 induces autophagic cell death with induction of apoptosis. TG2 is overexpressed in over 80% of pancreatic cancer cell lines and increased levels have been implicated in drug resistance. Targetting PKCδ or TG2 to induce autophagic cell death seems a promising therapeutic strategy for the treatment of pancreatic cancer. This hypothesis was already tested in nude mice bearing xenografts of TG2-expressing human pancreatic cancer cells. Knockdown of TG2 in these cells inhibited cancer cell proliferation while no signs of apoptosis were observed.

Another example was found in breast cancer cell line MCF-7 which do not express caspase 3. Hence they provide a higher threshold for the induction of apoptosis. 45-75% of all breast cancer tissue samples tested in that study had no detectable levels of caspase-3. When Bcl-2 was silenced in MCF-7 cells, autophagic but not apoptotic cell death was happening (Devarajan, Chen et al. 2002; Devarajan, Sahin et al. 2002) (Dalby, Tekedereli et al.).

3.6 *Drug Discovery and Inhibitors of PI3K*

During the last few years, various small molecule inhibitors of PI3K have been described. Most are not isoform-specific, as they target the catalytic site which exhibits a high homology between the different isoforms of PI3K, at least for the ATP-binding pocket. The x-ray coordinates of p110γ revealed that many inhibitors such as wortmannin, LY294002 etc. bind to these conserved residues in a similar manner (Walker, Pacold et al. 2000). Studies on the structure of each isoform would be required in order to find better optimized compounds that selectively inhibit a specific isoform.

A site mutagenesis study was done by Frazzetto et al. in 2008, replacing residues found in class I p110α by residues from p110β and vice versa. They claimed that certain inhibitors show a preference for p110α because of blocked interaction with non-conserved regions of p110β. The opposite was not observed though, challenging their hypothesis on the influence of this non-conserved regions adjacent to the catalytic site on the potency of an inhibitor. Other

groups support this view, suggesting that the non-conserved region of p110α (residues 852-59) remains a potential target for future compounds exhibiting greater selectivity for a PI3K isoform (Frazzetto, Suphioglu et al. 2008).

Earlier on, Knight et al. published a pharmacological map of the PI3K family defining p110α's role in insulin signalling. In order to investigate the unique roles of PI3K isoforms, the authors synthesized a diverse panel of PI3K inhibitors and checked for their target selectivity. Using crystal structures of three inhibitors (quinazolinone purine PIK-39, imidazoquinazoline PIK-90 and phenylthiazole PIK-93) bound to p110γ, they identified a conformationally mobile region that is uniquely exploited by selective inhibitors. Highly selective inhibitors projected out of the plane occupied by ATP, the most potent ones targeted deeper into a binding pocket that is not accessed by ATP (Ile 879, a residue structurally analogous to the gatekeeper residue in protein kinasese). When they applied these compounds, they found p110α to be the primary insulin-responsive PI3K isoform. P110β inhibitors had no effect on the other hand (Knight, Gonzalez et al. 2006).

Apsel et al. published an article on the discovery of dual inhibitors of both tyrosine and phopshoinositide kinases in 2008. In certain cases it might be beneficial to target different kinases simultaneously. PP121 blocked proliferation of tumor cells by inhibition of oncogenic tyrosine kinases and PI3K through a hydrophobic pocket conserved in both enzyme classes. Related compounds had strong effects on mTOR and other kinases, such as PP242 blocking mTOR quite efficiently (Apsel, Blair et al. 2008).

Another dual inhibitor was discovered by Maira et al., NVP-BEZ235. This imidazo(4,5-c)quinoline derivative was shown to inhibit both PI3K and mTOR. Hence it exhibited *in vivo* antitumor activity in various tumor cell lines and prostate tumor (PC3M, highly metastatic human prostate tumor cell line) xenografts in mice respectively. BEZ235 possesses strong antiproliferative capacity by G1-arrest, but showed no effects on cell viability. Application of the compound was well tolerated in mice as body weight gain was still normal during/ 10 days after treatment. When tested in increasing ATP concentrations, the compound's IC50 values increased in a linear manner. Results suggest that the compound binds to the ATP-binding pocket that is present in both PI3K and mTOR, competing with ATP. The specificity of the compound was tested in cell-based and by *in vitro* assays. The authors conclude that BEZ235 is a dual pan-PI3K/mTOR inhibitor, applicable for both cellular and *in vivo* settings. Phase I clinical trials in cancer patients have started in 2008 (Maira, Stauffer et al. 2008).

Dual targeting of both PI3K and mTOR was first applied as therapy in various melanoma cell lines and in xenografts in mice by Marone et al. in 2009 (see Publications), using the same compound NVP-BEZ235 presented by Maira et al. (Maira, Stauffer et al. 2008) and similar compounds. Exposure of the cells to these inhibitors resulted in complete G1-arrest shown by flow cytometry, other markers of cell cycle arrest proven by western blotting, but only negligible apoptosis levels. When the same cells were treated with pan-class I PI3K inhibitor ZSTK474

(Yaguchi, Fukui et al. 2006) or mTORC1 inhibitor rapamycin, only minor effects on cell proliferation were observed. A B16 mouse melanoma tumor model was used to test efficacy of tumor growth attenuation in both primary and lymph node metastatic sites. No obvious toxicity could be found, moreover, the mice displayed reduced numbers and significantly smaller tumor cells. The authors claim that neovascularization was blocked and necrosis of the tumor increased, suggesting that compounds targeting both PI3K and mTOR simultaneously could be beneficial in melanoma therapy (Marone, Erhart et al. 2009).

A recent paper on the structure variation of class III PI3K was published by Miller et al. The crystal structure of Vps34 (Figure 15) revealed an ATP-binding pocket distinct from class I PI3K isoforms, explaining potency differences for many inhibitors. Vps34 seems to alternate between a closed form of the phosphoinositide-binding loop and C-terminal helix in the cytosol and an open form on the endo-membranes. 3-methyladenine (3-MA) is preferentially binding class III PI3K (via the hinge) over the the other classes, even if the IC50 is very high at 10mM in order to block autophagy. The ATP-binding pocket of Vps34 is more constricted than the corresponding pocket of class I isoforms, e.g. p110γ. The P-loop curls inward and the hinge between N-and C-lobes is shorter, too. Propeller-like inhibitors such as PIK-39 bind the other isoforms much better due to the increased rigidity of class III PI3K. The authors came up with PT210, a derivative of PIK93, with reversed kinase specificity. PT210 showed much higher IC50 for p110γ (4uM) than for Vps34 (450nM). This way of designing small molecule inhibitors according to their putative binding possibilities will be more and more applied in future drug design, not only for PI3K but also for other enzymes (Miller, Tavshanjian et al.).

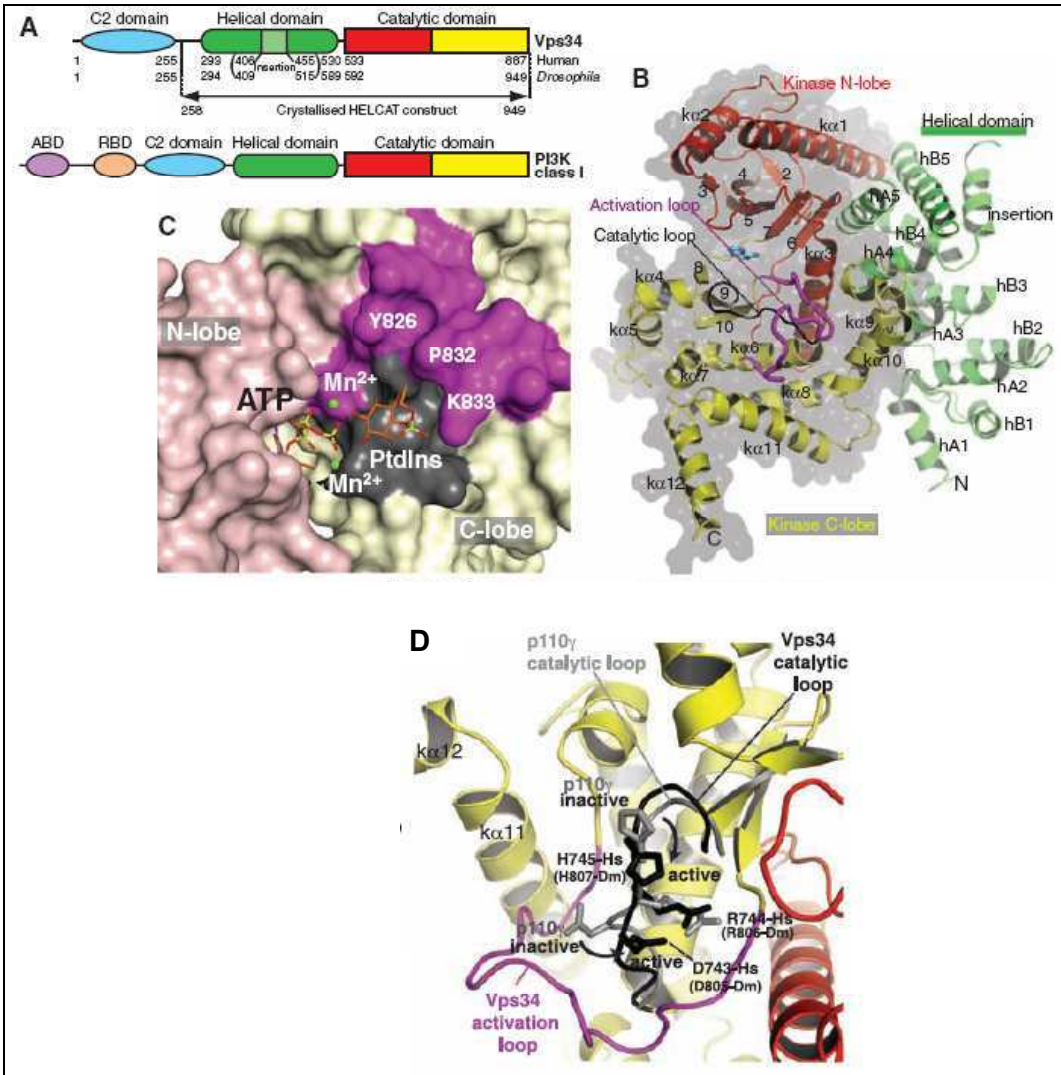

Figure 15: Structural differences Vps34 versus p110gamma

Panel A shows the major domains of Vps34 and PI3K class I, B depicts the structural folds of DmVps34' helical and catalytic domains. Panel C is a model of how the lipid PI is bound by Vps34. Panel D is a close-up of the conformation changes (active/non-active) in p110gamma (grey) or DmVps34 (black). The ATP-binding pocket of Vps34 is more constricted than the pocket of p110gamma. The authors could prove a change in specificity of inhibitors for any of the isoforms depending on the accessibility of the ATP-binding pocket by the small molecule inhibitors newly designed. (Miller, Tavshanjian et al.)

Abeliovich, H. and D. J. Klionsky (2001). "Autophagy in yeast: mechanistic insights and physiological function." Microbiol Mol Biol Rev **65**(3): 463-79, table of contents.

Aita, V. M., X. H. Liang, et al. (1999). "Cloning and genomic organization of beclin 1, a candidate tumor suppressor gene on chromosome 17q21." Genomics **59**(1): 59-65.

Akar, U., B. Ozpolat, et al. (2007). "Tissue transglutaminase inhibits autophagy in pancreatic cancer cells." Mol Cancer Res **5**(3): 241-9.

Apsel, B., J. A. Blair, et al. (2008). "Targeted polypharmacology: discovery of dual inhibitors of tyrosine and phosphoinositide kinases." Nat Chem Biol **4**(11): 691-9.

Arcaro, A., M. J. Zvelebil, et al. (2000). "Class II phosphoinositide 3-kinases are downstream targets of activated polypeptide growth factor receptors." Mol Cell Biol **20**(11): 3817-30.

Ashrafi, K., F. Y. Chang, et al. (2003). "Genome-wide RNAi analysis of Caenorhabditis elegans fat regulatory genes." Nature **421**(6920): 268-72.

Auger, K. R., C. L. Carpenter, et al. (1989). "Phosphatidylinositol 3-kinase and its novel product, phosphatidylinositol 3-phosphate, are present in Saccharomyces cerevisiae." J Biol Chem **264**(34): 20181-4.

Avruch, J., X. Long, et al. (2008). "Amino Acid Regulation of TOR Complex 1." Am J Physiol Endocrinol Metab.

Avruch, J., X. Long, et al. (2009). "Amino acid regulation of TOR complex 1." Am J Physiol Endocrinol Metab **296**(4): E592-602.

Axe, E. L., S. A. Walker, et al. (2008). "Autophagosome formation from membrane compartments enriched in phosphatidylinositol 3-phosphate and dynamically connected to the endoplasmic reticulum." J Cell Biol **182**(4): 685-701.

Baba, M., K. Takeshige, et al. (1994). "Ultrastructural analysis of the autophagic process in yeast: detection of autophagosomes and their characterization." J Cell Biol **124**(6): 903-13.

Backer, J. M. (2008). "The regulation and function of Class III PI3Ks: novel roles for Vps34." Biochem J **410**(1): 1-17.

Ballou, L. M., M. Chattopadhyay, et al. (2006). "Galphaq binds to p110alpha/p85alpha phosphoinositide 3-kinase and displaces Ras." Biochem J **394**(Pt 3): 557-62.

Birkeland, H. C. and H. Stenmark (2004). "Protein targeting to endosomes and phagosomes via FYVE and PX domains." Curr Top Microbiol Immunol **282**: 89-115.

Bohnacker, T., R. Marone, et al. (2009). "PI3Kgamma adaptor subunits define coupling to degranulation and cell motility by distinct PtdIns(3,4,5)P3 pools in mast cells." Sci Signal **2**(74): ra27.

Bunney, T. D. and M. Katan "Phosphoinositide signalling in cancer: beyond PI3K and PTEN." Nat Rev Cancer **10**(5): 342-52.

Byfield, M. P., J. T. Murray, et al. (2005). "hVps34 is a nutrient-regulated lipid kinase required for activation of p70 S6 kinase." J Biol Chem **280**(38): 33076-82.

Cao, C., J. M. Backer, et al. (2008). "Sequential Actions of Myotubularin Lipid Phosphatases Regulate Endosomal PI(3)P and Growth Factor Receptor Trafficking." Mol Biol Cell **19**(8): 3334-3346.

Cao, C., J. Laporte, et al. (2007). "Myotubularin lipid phosphatase binds the hVPS15/hVPS34 lipid kinase complex on endosomes." Traffic **8**(8): 1052-67.

Chamberlain, M. D., T. Chan, et al. (2008). "Disrupted RabGAP function of the p85 subunit of phosphatidylinositol 3-kinase results in cell transformation." J Biol Chem **283**(23): 15861-8.

Christoforidis, S., M. Miaczynska, et al. (1999). "Phosphatidylinositol-3-OH kinases are Rab5 effectors." Nat Cell Biol **1**(4): 249-52.

Cornillet-Lefebvre, P., W. Cuccuini, et al. (2006). "Constitutive phosphoinositide 3-kinase activation in acute myeloid leukemia is not due to p110delta mutations." Leukemia **20**(2): 374-6.

Curtin, J. A., M. S. Stark, et al. (2006). "PI3-kinase subunits are infrequent somatic targets in melanoma." J Invest Dermatol **126**(7): 1660-3.

Dalby, K. N., I. Tekedereli, et al. "Targeting the prodeath and prosurvival functions of autophagy as novel therapeutic strategies in cancer." Autophagy **6**(3): 322-9.

Devarajan, E., J. Chen, et al. (2002). "Human breast cancer MCF-7 cell line contains inherently drug-resistant subclones with distinct genotypic and phenotypic features." Int J Oncol **20**(5): 913-20.

Devarajan, E., A. A. Sahin, et al. (2002). "Down-regulation of caspase 3 in breast cancer: a possible mechanism for chemoresistance." Oncogene **21**(57): 8843-51.

Di Paolo, G. and P. De Camilli (2006). "Phosphoinositides in cell regulation and membrane dynamics." Nature **443**(7112): 651-7.

Domin, J., F. Pages, et al. (1997). "Cloning of a human phosphoinositide 3-kinase with a C2 domain that displays reduced sensitivity to the inhibitor wortmannin." Biochem J **326 (Pt 1)**: 139-47.

Dunn, W. A., Jr. (1990). "Studies on the mechanisms of autophagy: formation of the autophagic vacuole." J Cell Biol **110**(6): 1923-33.

Eickholt, B. J., A. I. Ahmed, et al. (2007). "Control of axonal growth and regeneration of sensory neurons by the p110delta PI 3-kinase." PLoS One **2**(9): e869.

Elis, W., E. Triantafellow, et al. (2008). "Down-regulation of class II phosphoinositide 3-kinase alpha expression below a critical threshold induces apoptotic cell death." Mol Cancer Res **6**(4): 614-23.

Ellson, C. D., K. E. Anderson, et al. (2001). "Phosphatidylinositol 3-phosphate is generated in phagosomal membranes." Curr Biol **11**(20): 1631-5.

Falasca, M., W. E. Hughes, et al. (2007). "The role of phosphoinositide 3-kinase C2alpha in insulin signaling." J Biol Chem **282**(38): 28226-36.
Falasca, M. and T. Maffucci (2007). "Role of class II phosphoinositide 3-kinase in cell signalling." Biochem Soc Trans **35**(Pt 2): 211-4.
Fimia, G. M., A. Stoykova, et al. (2007). "Ambra1 regulates autophagy and development of the nervous system." Nature **447**(7148): 1121-5.
Findlay, G. M., L. Yan, et al. (2007). "A MAP4 kinase related to Ste20 is a nutrient-sensitive regulator of mTOR signalling." Biochem J **403**(1): 13-20.
Folkman, J. (2006). "Angiogenesis." Annu Rev Med **57**: 1-18.
Frazzetto, M., C. Suphioglu, et al. (2008). "Dissecting isoform selectivity of PI3K inhibitors: the role of non-conserved residues in the catalytic pocket." Biochem J **414**(3): 383-90.
Futter, C. E., L. M. Collinson, et al. (2001). "Human VPS34 is required for internal vesicle formation within multivesicular endosomes." J Cell Biol **155**(7): 1251-64.
Gulati, P., L. D. Gaspers, et al. (2008). "Amino acids activate mTOR complex 1 via Ca2+/CaM signaling to hVps34." Cell Metab **7**(5): 456-65.
Gulati, P. and G. Thomas (2007). "Nutrient sensing in the mTOR/S6K1 signalling pathway." Biochem Soc Trans **35**(Pt 2): 236-8.
Gupta, S., A. R. Ramjaun, et al. (2007). "Binding of ras to phosphoinositide 3-kinase p110alpha is required for ras-driven tumorigenesis in mice." Cell **129**(5): 957-68.
Harada, K., A. B. Truong, et al. (2005). "The class II phosphoinositide 3-kinase C2beta is not essential for epidermal differentiation." Mol Cell Biol **25**(24): 11122-30.
Herman, P. K. and S. D. Emr (1990). "Characterization of VPS34, a gene required for vacuolar protein sorting and vacuole segregation in Saccharomyces cerevisiae." Mol Cell Biol **10**(12): 6742-54.
Hirsch, E., L. Braccini, et al. (2009). "Twice upon a time: PI3K's secret double life exposed." Trends Biochem Sci **34**(5): 244-8.
Hurley, J. H. (2006). "Membrane binding domains." Biochim Biophys Acta **1761**(8): 805-11.
Im, Y. J., T. Wollert, et al. (2009). "Structure and function of the ESCRT-II-III interface in multivesicular body biogenesis." Dev Cell **17**(2): 234-43.
Itakura, E. and N. Mizushima (2009). "Atg14 and UVRAG: mutually exclusive subunits of mammalian Beclin 1-PI3K complexes." Autophagy **5**(4): 534-6.
Jin, S. and E. White (2008). "Tumor suppression by autophagy through the management of metabolic stress." Autophagy **4**(5): 563-6.
Johnson, E. E., J. H. Overmeyer, et al. (2006). "Gene silencing reveals a specific function of hVps34 phosphatidylinositol 3-kinase in late versus early endosomes." J Cell Sci **119**(Pt 7): 1219-32.
Juhasz, G., J. H. Hill, et al. (2008). "The class III PI(3)K Vps34 promotes autophagy and endocytosis but not TOR signaling in Drosophila." J Cell Biol **181**(4): 655-66.
Kihara, A., T. Noda, et al. (2001). "Two distinct Vps34 phosphatidylinositol 3-kinase complexes function in autophagy and carboxypeptidase Y sorting in Saccharomyces cerevisiae." J Cell Biol **152**(3): 519-30.
Kim, E., P. Goraksha-Hicks, et al. (2008). "Regulation of TORC1 by Rag GTPases in nutrient response." Nat Cell Biol **10**(8): 935-45.
Kinchen, J. M., K. Doukoumetzidis, et al. (2008). "A pathway for phagosome maturation during engulfment of apoptotic cells." Nat Cell Biol **10**(5): 556-66.
Knight, Z. A., B. Gonzalez, et al. (2006). "A pharmacological map of the PI3-K family defines a role for p110alpha in insulin signaling." Cell **125**(4): 733-47.
Kok, K., B. Geering, et al. (2009). "Regulation of phosphoinositide 3-kinase expression in health and disease." Trends Biochem Sci **34**(3): 115-27.
Kurig, B., A. Shymanets, et al. (2009). "Ras is an indispensable coregulator of the class IB phosphoinositide 3-kinase p87/p110gamma." Proc Natl Acad Sci U S A **106**(48): 20312-7.
Kurosu, H. and T. Katada (2001). "Association of phosphatidylinositol 3-kinase composed of p110beta-catalytic and p85-regulatory subunits with the small GTPase Rab5." J Biochem **130**(1): 73-8.
Kurosu, H., T. Maehama, et al. (1997). "Heterodimeric phosphoinositide 3-kinase consisting of p85 and p110beta is synergistically activated by the betagamma subunits of G proteins and phosphotyrosyl peptide." J Biol Chem **272**(39): 24252-6.
Lehmann, K., J. P. Muller, et al. (2009). "PI3Kgamma controls oxidative bursts in neutrophils via interactions with PKCalpha and p47phox." Biochem J **419**(3): 603-10.
Lemmon, M. A. (2008). "Membrane recognition by phospholipid-binding domains." Nat Rev Mol Cell Biol **9**(2): 99-111.

Leung, W. H., T. Tarasenko, et al. (2009). "Differential roles for the inositol phosphatase SHIP in the regulation of macrophages and lymphocytes." Immunol Res **43**(1-3): 243-51.
Levine, B. (2007). "Cell biology: autophagy and cancer." Nature **446**(7137): 745-7.
Levine, B. and G. Kroemer (2008). "Autophagy in the pathogenesis of disease." Cell **132**(1): 27-42.
Liang, C., P. Feng, et al. (2006). "Autophagic and tumour suppressor activity of a novel Beclin1-binding protein UVRAG." Nat Cell Biol **8**(7): 688-99.
Liang, C., J. S. Lee, et al. (2008). "Beclin1-binding UVRAG targets the class C Vps complex to coordinate autophagosome maturation and endocytic trafficking." Nat Cell Biol **10**(7): 776-87.
Liang, X. H., S. Jackson, et al. (1999). "Induction of autophagy and inhibition of tumorigenesis by beclin 1." Nature **402**(6762): 672-6.
Liu, B., Y. Cheng, et al. (2009). "Polygonatum cyrtonema lectin induces apoptosis and autophagy in human melanoma A375 cells through a mitochondria-mediated ROS-p38-p53 pathway." Cancer Lett **275**(1): 54-60.
MacDougall, L. K., M. E. Gagou, et al. (2004). "Targeted expression of the class II phosphoinositide 3-kinase in Drosophila melanogaster reveals lipid kinase-dependent effects on patterning and interactions with receptor signaling pathways." Mol Cell Biol **24**(2): 796-808.
Maira, S. M., F. Stauffer, et al. (2008). "Identification and characterization of NVP-BEZ235, a new orally available dual phosphatidylinositol 3-kinase/mammalian target of rapamycin inhibitor with potent in vivo antitumor activity." Mol Cancer Ther **7**(7): 1851-63.
Mandelker, D., S. B. Gabelli, et al. (2009). "A frequent kinase domain mutation that changes the interaction between PI3Kalpha and the membrane." Proc Natl Acad Sci U S A **106**(40): 16996-7001.
Marone, R., D. Erhart, et al. (2009). "Targeting melanoma with dual phosphoinositide 3-kinase/mammalian target of rapamycin inhibitors." Mol Cancer Res **7**(4): 601-13.
Mathew, R., V. Karantza-Wadsworth, et al. (2007). "Role of autophagy in cancer." Nat Rev Cancer **7**(12): 961-7.
Mauvezin, C., M. Orpinell, et al. "The nuclear cofactor DOR regulates autophagy in mammalian and Drosophila cells." EMBO Rep **11**(1): 37-44.
Melendez, A., Z. Talloczy, et al. (2003). "Autophagy genes are essential for dauer development and life-span extension in C. elegans." Science **301**(5638): 1387-91.
Miled, N., Y. Yan, et al. (2007). "Mechanism of two classes of cancer mutations in the phosphoinositide 3-kinase catalytic subunit." Science **317**(5835): 239-42.
Miller, S., B. Tavshanjian, et al. "Shaping development of autophagy inhibitors with the structure of the lipid kinase Vps34." Science **327**(5973): 1638-42.
Moretti, L., A. Attia, et al. (2007). "Crosstalk between Bak/Bax and mTOR signaling regulates radiation-induced autophagy." Autophagy **3**(2): 142-4.
Murray, J. T., C. Panaretou, et al. (2002). "Role of Rab5 in the recruitment of hVps34/p150 to the early endosome." Traffic **3**(6): 416-27.
Nicklin, P., P. Bergman, et al. (2009). "Bidirectional transport of amino acids regulates mTOR and autophagy." Cell **136**(3): 521-34.
Nobukuni, T., M. Joaquin, et al. (2005). "Amino acids mediate mTOR/raptor signaling through activation of class 3 phosphatidylinositol 3OH-kinase." Proc Natl Acad Sci U S A **102**(40): 14238-43.
Novak, I., V. Kirkin, et al. "Nix is a selective autophagy receptor for mitochondrial clearance." EMBO Rep **11**(1): 45-51.
Omholt, K., D. Krockel, et al. (2006). "Mutations of PIK3CA are rare in cutaneous melanoma." Melanoma Res **16**(2): 197-200.
Orme, M. H., S. Alrubaie, et al. (2006). "Input from Ras is required for maximal PI(3)K signalling in Drosophila." Nat Cell Biol **8**(11): 1298-302.
Papakonstanti, E. A., A. J. Ridley, et al. (2007). "The p110delta isoform of PI 3-kinase negatively controls RhoA and PTEN." Embo J **26**(13): 3050-61.
Papakonstanti, E. A., O. Zwaenepoel, et al. (2008). "Distinct roles of class IA PI3K isoforms in primary and immortalised macrophages." J Cell Sci **121**(Pt 24): 4124-33.
Petiot, A., F. Strappazzon, et al. (2008). "Alix differs from ESCRT proteins in the control of autophagy." Biochem Biophys Res Commun **375**(1): 63-8.
Prasad, N. K., M. Tandon, et al. (2008). "Phosphoinositol phosphatase SHIP2 promotes cancer development and metastasis coupled with alterations in EGF receptor turnover." Carcinogenesis **29**(1): 25-34.

Robinson, J. S., D. J. Klionsky, et al. (1988). "Protein sorting in Saccharomyces cerevisiae: isolation of mutants defective in the delivery and processing of multiple vacuolar hydrolases." Mol Cell Biol **8**(11): 4936-48.

Roggo, L., V. Bernard, et al. (2002). "Membrane transport in Caenorhabditis elegans: an essential role for VPS34 at the nuclear membrane." Embo J **21**(7): 1673-83.

Rohrschneider, L. R., J. F. Fuller, et al. (2000). "Structure, function, and biology of SHIP proteins." Genes Dev **14**(5): 505-20.

Rothman, J. H. and T. H. Stevens (1986). "Protein sorting in yeast: mutants defective in vacuole biogenesis mislocalize vacuolar proteins into the late secretory pathway." Cell **47**(6): 1041-51.

Samuels, Y., Z. Wang, et al. (2004). "High frequency of mutations of the PIK3CA gene in human cancers." Science **304**(5670): 554.

Sancak, Y., T. R. Peterson, et al. (2008). "The Rag GTPases bind raptor and mediate amino acid signaling to mTORC1." Science **320**(5882): 1496-501.

Schu, P. V., K. Takegawa, et al. (1993). "Phosphatidylinositol 3-kinase encoded by yeast VPS34 gene essential for protein sorting." Science **260**(5104): 88-91.

Shayesteh, L., Y. Lu, et al. (1999). "PIK3CA is implicated as an oncogene in ovarian cancer." Nat Genet **21**(1): 99-102.

Shin, H. W., M. Hayashi, et al. (2005). "An enzymatic cascade of Rab5 effectors regulates phosphoinositide turnover in the endocytic pathway." J Cell Biol **170**(4): 607-18.

Siddhanta, U., J. McIlroy, et al. (1998). "Distinct roles for the p110alpha and hVPS34 phosphatidylinositol 3'-kinases in vesicular trafficking, regulation of the actin cytoskeleton, and mitogenesis." J Cell Biol **143**(6): 1647-59.

Simonsen, A., H. C. Birkeland, et al. (2004). "Alfy, a novel FYVE-domain-containing protein associated with protein granules and autophagic membranes." J Cell Sci **117**(Pt 18): 4239-51.

Simonsen, A. and H. Stenmark (2008). "Self-eating from an ER-associated cup." J Cell Biol **182**(4): 621-2.

Simonsen, A. and S. A. Tooze (2009). "Coordination of membrane events during autophagy by multiple class III PI3-kinase complexes." J Cell Biol **186**(6): 773-82.

Singh, S. B., A. S. Davis, et al. (2006). "Human IRGM induces autophagy to eliminate intracellular mycobacteria." Science **313**(5792): 1438-41.

Slessareva, J. E., S. M. Routt, et al. (2006). "Activation of the phosphatidylinositol 3-kinase Vps34 by a G protein alpha subunit at the endosome." Cell **126**(1): 191-203.

Song, X., W. Xu, et al. (2001). "Phox homology domains specifically bind phosphatidylinositol phosphates." Biochemistry **40**(30): 8940-4.

Spowart, J. and J. J. Lum "Opening a new DOR to autophagy." EMBO Rep **11**(1): 4-5.

Stahelin, R. V., D. Karathanassis, et al. (2006). "Structural and membrane binding analysis of the Phox homology domain of phosphoinositide 3-kinase-C2alpha." J Biol Chem **281**(51): 39396-406.

Stark, M. and N. Hayward (2007). "Genome-wide loss of heterozygosity and copy number analysis in melanoma using high-density single-nucleotide polymorphism arrays." Cancer Res **67**(6): 2632-42.

Stein, M. P., Y. Feng, et al. (2003). "Human VPS34 and p150 are Rab7 interacting partners." Traffic **4**(11): 754-71.

Taboubi, S., J. Milanini, et al. (2007). "G alpha(q/11)-coupled P2Y2 nucleotide receptor inhibits human keratinocyte spreading and migration." Faseb J **21**(14): 4047-58.

Takahashi, Y., D. Coppola, et al. (2007). "Bif-1 interacts with Beclin 1 through UVRAG and regulates autophagy and tumorigenesis." Nat Cell Biol **9**(10): 1142-51.

Takahashi, Y., D. Coppola, et al. (2007). "Bif-1 interacts with Beclin 1 through UVRAG and regulates autophagy and tumorigenesis." Nat Cell Biol **9**(10): 1142-51.

Takahashi, Y., C. L. Meyerkord, et al. (2008). "BARgaining membranes for autophagosome formation: Regulation of autophagy and tumorigenesis by Bif-1/Endophilin B1." Autophagy **4**(1): 121-4.

Takeshige, K., M. Baba, et al. (1992). "Autophagy in yeast demonstrated with proteinase-deficient mutants and conditions for its induction." J Cell Biol **119**(2): 301-11.

Tang, R., X. Zhao, et al. (2008). "Investigation of variants in the promoter region of PIK3C3 in schizophrenia." Neurosci Lett **437**(1): 42-4.

Tormo, D., A. Checinska, et al. (2009). "Targeted activation of innate immunity for therapeutic induction of autophagy and apoptosis in melanoma cells." Cancer Cell **16**(2): 103-14.

Tsukada, M. and Y. Ohsumi (1993). "Isolation and characterization of autophagy-defective mutants of Saccharomyces cerevisiae." FEBS Lett **333**(1-2): 169-74.

Vanhaesebroeck, B., K. Ali, et al. (2005). "Signalling by PI3K isoforms: insights from gene-targeted mice." Trends Biochem Sci **30**(4): 194-204.
Vanhaesebroeck, B., J. Guillermet-Guibert, et al. (2010). "The emerging mechanisms of isoform-specific PI3K signalling." Nat Rev Mol Cell Biol **11**(5): 329-41.
Vanhaesebroeck, B., S. J. Leevers, et al. (2001). "Synthesis and function of 3-phosphorylated inositol lipids." Annu Rev Biochem **70**: 535-602.
Vanhaesebroeck, B., S. J. Leevers, et al. (1997). "Phosphoinositide 3-kinases: a conserved family of signal transducers." Trends Biochem Sci **22**(7): 267-72.
Vergne, I., E. Roberts, et al. (2009). "Control of autophagy initiation by phosphoinositide 3-phosphatase Jumpy." Embo J **28**(15): 2244-58.
Virbasius, J. V., A. Guilherme, et al. (1996). "Mouse p170 is a novel phosphatidylinositol 3-kinase containing a C2 domain." J Biol Chem **271**(23): 13304-7.
Vogt, P. K., S. Kang, et al. (2007). "Cancer-specific mutations in phosphatidylinositol 3-kinase." Trends Biochem Sci **32**(7): 342-9.
Volinia, S., R. Dhand, et al. (1995). "A human phosphatidylinositol 3-kinase complex related to the yeast Vps34p-Vps15p protein sorting system." Embo J **14**(14): 3339-48.
Walker, E. H., M. E. Pacold, et al. (2000). "Structural determinants of phosphoinositide 3-kinase inhibition by wortmannin, LY294002, quercetin, myricetin, and staurosporine." Mol Cell **6**(4): 909-19.
Wang, X. and C. G. Proud (2009). "Nutrient control of TORC1, a cell-cycle regulator." Trends Cell Biol **19**(6): 260-7.
Wang, Z., W. A. Wilson, et al. (2001). "Antagonistic controls of autophagy and glycogen accumulation by Snf1p, the yeast homolog of AMP-activated protein kinase, and the cyclin-dependent kinase Pho85p." Mol Cell Biol **21**(17): 5742-52.
Whitman, M., D. Kaplan, et al. (1987). "Evidence for two distinct phosphatidylinositol kinases in fibroblasts. Implications for cellular regulation." Biochem J **247**(1): 165-74.
Wollert, T., D. Yang, et al. (2009). "The ESCRT machinery at a glance." J Cell Sci **122**(Pt 13): 2163-6.
Wullschleger, S., R. Loewith, et al. (2006). "TOR signaling in growth and metabolism." Cell **124**(3): 471-84.
Wymann, M. P. and R. Marone (2005). "Phosphoinositide 3-kinase in disease: timing, location, and scaffolding." Curr Opin Cell Biol **17**(2): 141-9.
Wymann, M. P. and L. Pirola (1998). "Structure and function of phosphoinositide 3-kinases." Biochim Biophys Acta **1436**(1-2): 127-50.
Xue, Y., H. Fares, et al. (2003). "Genetic analysis of the myotubularin family of phosphatases in Caenorhabditis elegans." J Biol Chem **278**(36): 34380-6.
Yaguchi, S., Y. Fukui, et al. (2006). "Antitumor activity of ZSTK474, a new phosphatidylinositol 3-kinase inhibitor." J Natl Cancer Inst **98**(8): 545-56.
Yan, Y., R. J. Flinn, et al. (2009). "hVps15, but not Ca2+/CaM, is required for the activity and regulation of hVps34 in mammalian cells." Biochem J **417**(3): 747-55.
Zeng, X., J. H. Overmeyer, et al. (2006). "Functional specificity of the mammalian Beclin-Vps34 PI 3-kinase complex in macroautophagy versus endocytosis and lysosomal enzyme trafficking." J Cell Sci **119**(Pt 2): 259-70.
Zhang, H., J. P. Stallock, et al. (2000). "Regulation of cellular growth by the Drosophila target of rapamycin dTOR." Genes Dev **14**(21): 2712-24.
Zhao, L. and P. K. Vogt (2008). "Helical domain and kinase domain mutations in p110alpha of phosphatidylinositol 3-kinase induce gain of function by different mechanisms." Proc Natl Acad Sci U S A **105**(7): 2652-7.
Zhong, Y., Q. J. Wang, et al. (2009). "Distinct regulation of autophagic activity by Atg14L and Rubicon associated with Beclin 1-phosphatidylinositol-3-kinase complex." Nat Cell Biol **11**(4): 468-76.

4 Aim of Studies

Class III PI3K is involved in many cellular processes, among them autophagy (Kihara, Noda et al. 2001). Autophagy helps the cell to survive nutrient-deprived conditions by "self-eating" and recycling of organelles and metabolic waste. Especially cancer cells are confronted with lack of nutrients before angiogenesis is increased in their cellular surroundings. Whether autophagy is beneficial or not for cell survival in a cancer context and at what stage or for which cancer cells this might apply, is content of current discussions in the field (Folkman 2006; Levine 2007).

To answer our main question on the importance of Vps34 and its involvement in cancer cell survival, we started both a genetic and a pharmacological approach:

"What substance of natural origin will inhibit human Vps34? How specific? At what concentrations?"

Our first approach was to screen a library of natural compounds for specific human Vps34 inhibitors in a genetically modified yeast model system. We made use of the temperature sensitive phenotype of Vps34 deletion mutants. Yeast PI3K deletion mutants were complemented with a hybrid human/yeast Vps34 construct which allowed us to screen for substances that abrogated growth at higher temperature. The crude plant extracts that showed hits in this first round screen were then fractionated and retested on yeast mutants. To avoid misleading side effects, we then tested the putative inhibitors on yeast Vps34 and rechecked for human PI3K class III specificity in mammalian cell lines. In vitro kinase assays were applied in the end to define the effective inhibitor concentration.

"How important is hVps34 for melanoma cell survival? What effects are observed upon temporary or longterm reduction or loss of the kinase? In which cell lines is it essential or is its loss tolerated? Could hVps34 be used as a drug target in patients?"

The second approach, this time genetic, was done in human melanoma cell lines. We made use of knockdown methods by state-of-the-art siRNA or stable shRNA techniques in melanoma cell lines. Our aim was to characterize different melanoma cell lines upon hVps34 loss, comparing our results to published data on other cell types. We asked whether targeting hVps34 might affect melanoma survival and hence the kinase might serve as a putative drug target in these cancer model systems.

5 Results

5.1 *Genetic Approach: Class III in Melanoma*

5.1.1 Varying endogenous levels of hVps34 and Beclin1 were found in melanoma cell lines

To get a first hint of the importance of hVps34 (class III PI3K) in a melanoma cancer model system, we selected a variety of human melanoma cell lines with different genetic backgrounds (Table 2). The selection of melanoma cell lines expressing either all or only some PI3K class I isoforms were tested for protein levels of hVps34 and its interactor Beclin1 (hVps30 or hAtg6). In order to compare the levels of these proteins, lysates of two melanocyte cell types and HEK293 as a standard lab cell line were checked as well. A2058, 1205lu and WM115 were selected as the only melanoma cell lines in this batch expressing all four PI3K class I isoforms. A375 are the only ones that express wild type PTEN (phosphatase and tensin homolog), a tumor suppressor protein counteracting production of $PI(3,4,5)P_3$ by PI3K class I isoforms. All of the other melanoma cell lines in our selection have abnormally high levels of these lipids, leading to increased signalling inputs to downstream targets.

Metastatic A375 from the selection were chosen for further analysis as they exhibited low levels of both endogenous Beclin1 and hVps34 (Fig. 16). In contrast, A2058 and 1205lu were picked as examples for melanoma cell lines expressing high endogenous levels of these proteins.

	PG-02	***SchM-99***	***A2058***	***A375***	***1205lu***	***WM115***	***SKMel23***	***SKMel28***	***HEK293***
PI3K class I isoforms	α, β, δ	α, β, δ	α, β,γ, δ	α, β, δ	α, β,γ, δ	α, β,γ, δ	α, β, δ	α, β, δ	α, β, δ
PTEN status	WT	WT	mut	WT	mut	mut	mut	mut	WT
Metastasis?	none	none	low	yes	yes	RGP/VGP	unknown	unknown	none
Melanoma origin	none	none	lymph node	malignant tumor	lung	early melanoma	unknown	malignant tumor	none

Table 2: Characteristics of Melanoma cell line Selection

RGP/VGP= radial growth phase/ vertical growth phase; WT= wild type; mut= mutated, antibodies against PTEN could not detect PTEN in Western blots

PG-02 and SchM-99 are melanocytes, HEK293 are human embryonic kidney cells, the others are all melanoma cell lines.

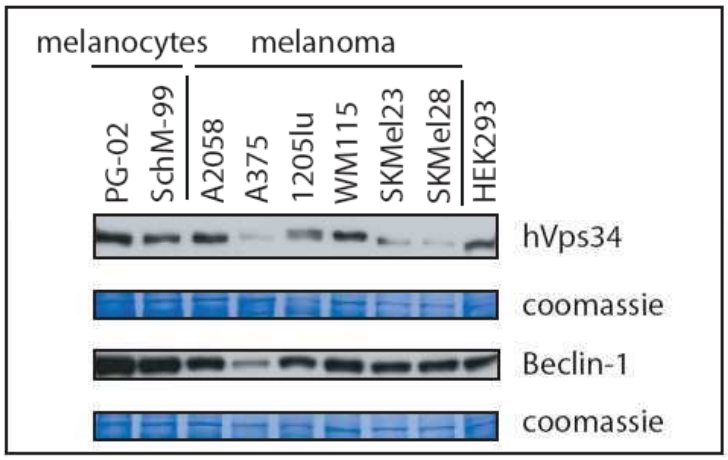

Figure 16: Varying endogenous levels of hVps34 and Beclin1 in melanoma cell line selection

Endogenous protein levels of hVps34 and Beclin1 were compared in melanoma cell lines and melanocytes. HEK293 were added as well in order to show the expressions in a standard cell line.
Coomassie staining of the membranes was used as reference.
Antibodies: see Materials and Methods

5.1.2 Lentiviral stable hVps34 knockdown in HEK293 and A375 cell lines is tolerated

For further studies on the effect upon loss or reduction of hVps34 in a cellular context, melanoma A375 and standard epithelial lab cell line HEK293 were infected with shRNA-bearing lentiviruses to generate stable hVps34 knockdown cell lines. Mock shRNA transfections (lacking targeting sequence) and two constructs of shRNA bearing diverse targeting sequences were used for both cell lines. The two constructs termed pLKa and pLKb rendered different efficacy in knocking down of hVps34. We could observe a considerable reduction of hVps34 protein levels for pLKa- infected cells and almost endogenous levels of the protein if infected with pLKb (Figure 17C and D). If we compared untreated cells (later named control) with mock-infected cells, we saw an increase in Beclin1 protein levels, possibly originating from Beclin1-involved processes induced by the infection with lentivirus.

Upon knockdown of hVps34, protein levels of its complex partner Beclin1 were always affected (Figure 17). Similar results were obtained in earlier experiments applying siRNA against hVps34, independent of the cell lines tested (Figure 17B).

For later experiments with stable knockdowns, melanoma cell lines A2058 and 1205lu had to be dropped though, as transfections with shRNA-bearing viruses in these two cell lines were successful but none of the constructs resulted in viable stable knockdowns. Short term knockdown of hVps34 by siRNA in our preliminary experiments in A2058 and 1205lu already induced a decrease in proliferation (Figure 17A). A possible explanation for this phenomenon is based on the endogenously high protein levels of hVps34 in these melanoma samples, proposing that a threshold protein level of hVps34 is more essential in these cell lines.

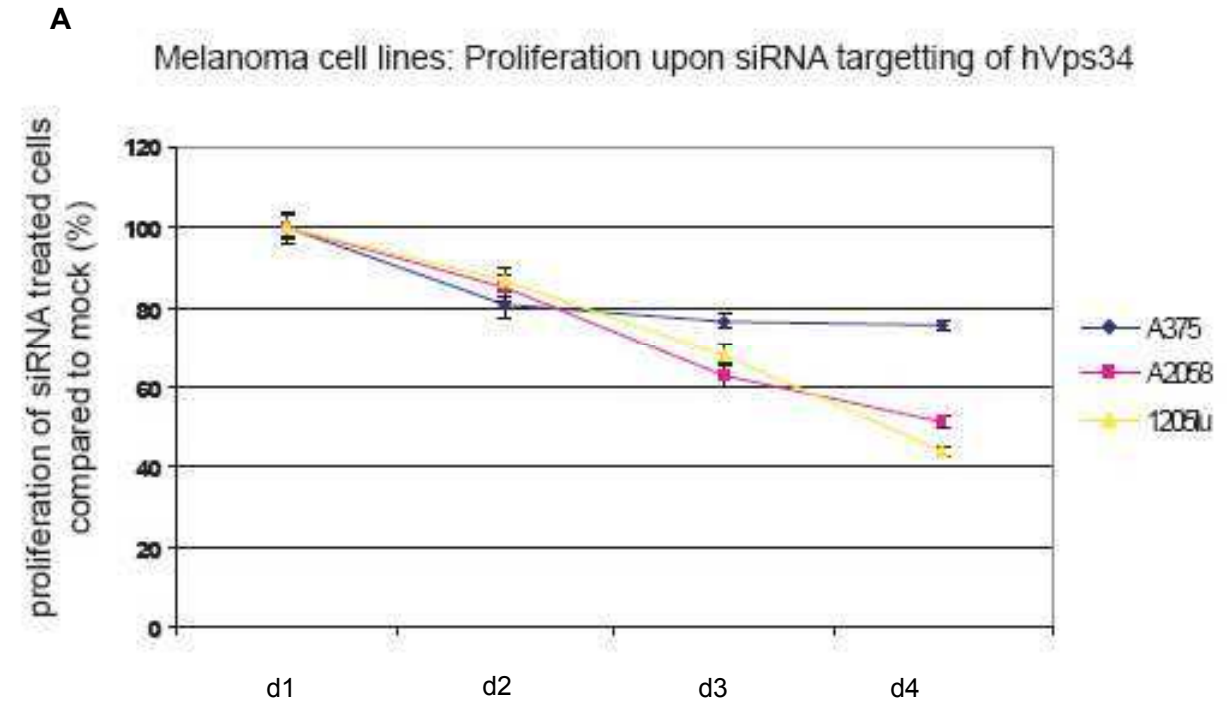

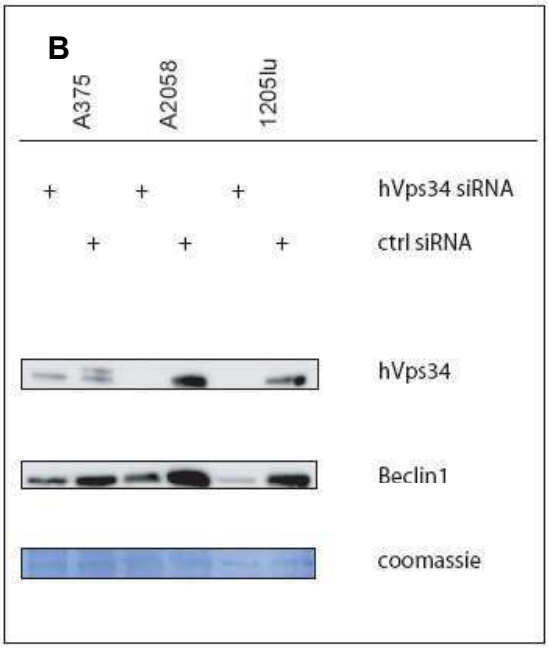

Figure17: hVps34 knockdown cell lines

Panel A: Three different melanoma cell lines were transiently transfected with siRNA targeting hVps34. Proliferation is mainly affected in A2058 and 1205lu cell lines, four days after transfection. n= 3

Panel B: Beclin1 protein levels seem to be reduced upon hVps34 targetting by siRNA, independent of the cell line.

Panel C and D: HEK293 or melanoma A375 cell lines with stable knockdown of hVps34 via lentiviral transfections of shRNA.

Loading control is tubulin. pLKa (*p*lasmid *L*entiviral *K*nockdown a) and pLKb are two shRNA constructs targeting different sites on the mRNA of hVps34. Stably transfected in the according cell lines, they give rise to different reduction of hVps34 protein levels, enabling us to test for hVps34 threshold levels for various effects.

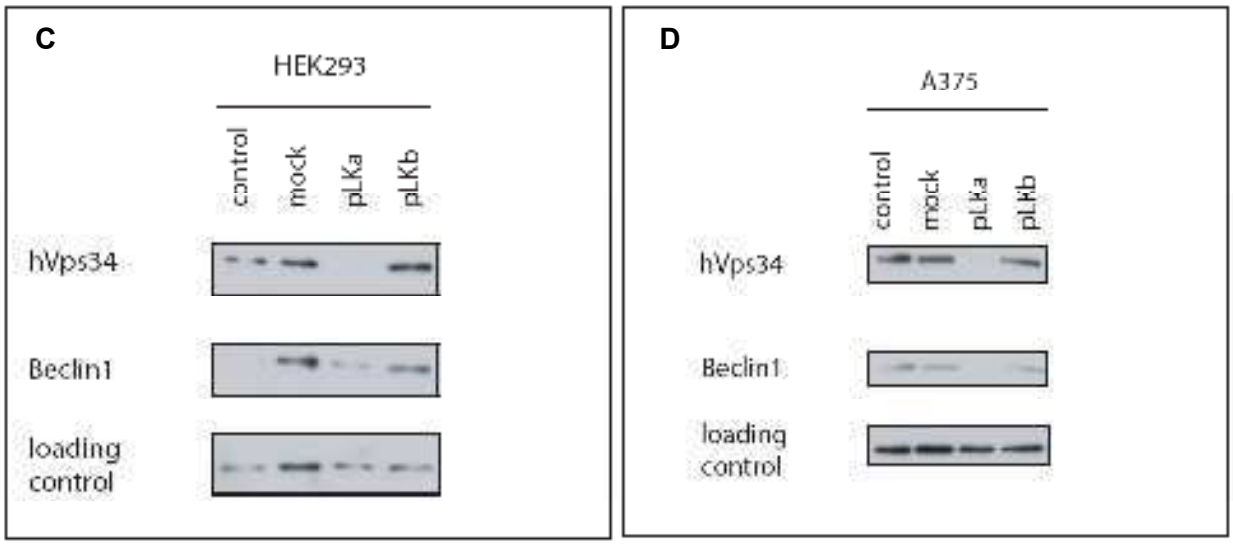

5.1.3 Loss of hVps34 leads to vacuolarization in A375 melanoma but not in HEK293

Similar to published data on hVps34 knockdown in glioblastoma U251 (Johnson, Overmeyer et al. 2006), A375 bearing stable shRNA constructs knocking down hVps34 (pLKa) showed a so-called vacuolarization phenotype (Fig.18 upper panel). The lysosomes/late endosomes seemed to significantly increase in size and number. A375 with reduced hVps34 protein levels (pLKa) showed ten times more vacuolarizations than mock-transfected cells. This effect was dose-dependent, as cells expressing the less-efficient shRNA construct (pLKb), exhibited lysosomes/late endosomes resembling mock-transfected or control cells (Fig.18).

To our surprise, the HEK293 stable knockdowns did not show the same phenotype, no matter how strong hVps34 protein levels were reduced (Fig. 18 lower panel and Fig. 17C for Western Blot). We suppose that the observed vacuolarization phenotype might have to do with the cancer-related changes in cell types, as previous publications on this phenotype were also done in cancer cells (Johnson, Overmeyer et al. 2006). Unfortunately we did not succeed in finding other melanoma cell lines with endogenous low levels of hVps34 (and its interactor Beclin1) that we could have stably knocked down. Further experiments on a bigger selection of melanoma cell lines would need to be done to test this hypothesis.

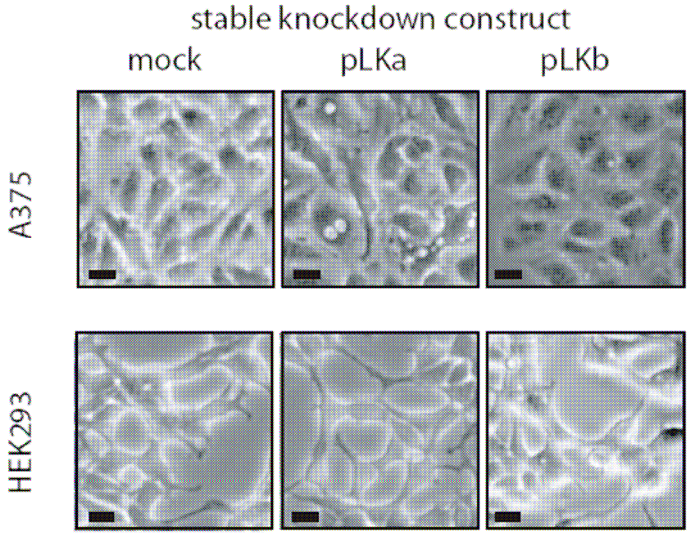

Figure 18: Loss of hVps34 leads to vacuolarization phenotype in A375 melanoma but not in HEK293

As observed earlier (Johnson, Overmeyer et al. 2006), melanoma A375 stably transfected with shRNA against hVps34 show vacuolarization in a dose-dependent manner (pLKa vs. pLKb). HEK293 did not exhibit this phenotype.
Bars of equal size in all pictures, phenotype visible at original magnification 20x

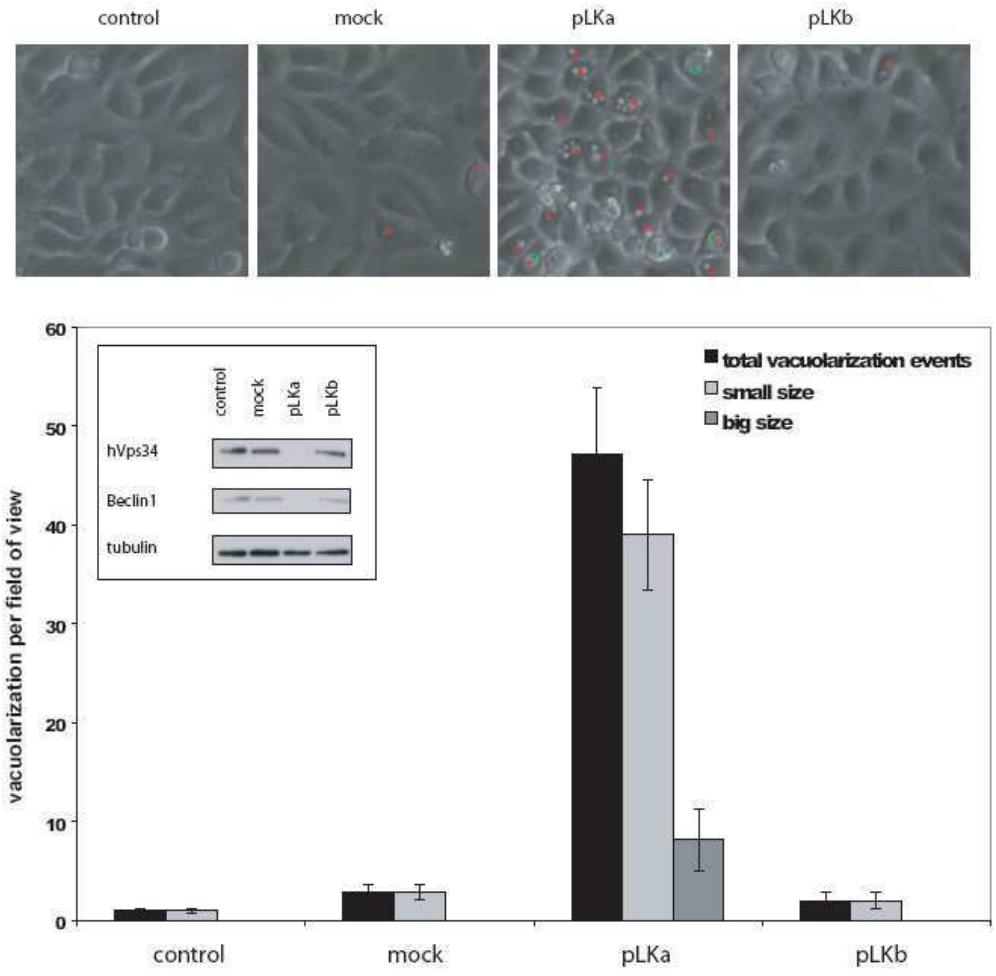

Figure 19: Quantification

Vacuolarization phenotype was quantified in A375 with reduced hVps34 protein levels, done in at least three independent experiments. We distinguished between big and small size of vacuolarization (grey bars). Solid black bars show total vacuolarization events. Blot from Figure 17D is added for information on knockdown.

5.1.4 Proliferation upon hVps34 reduction is affected in both A375 and HEK293

a)

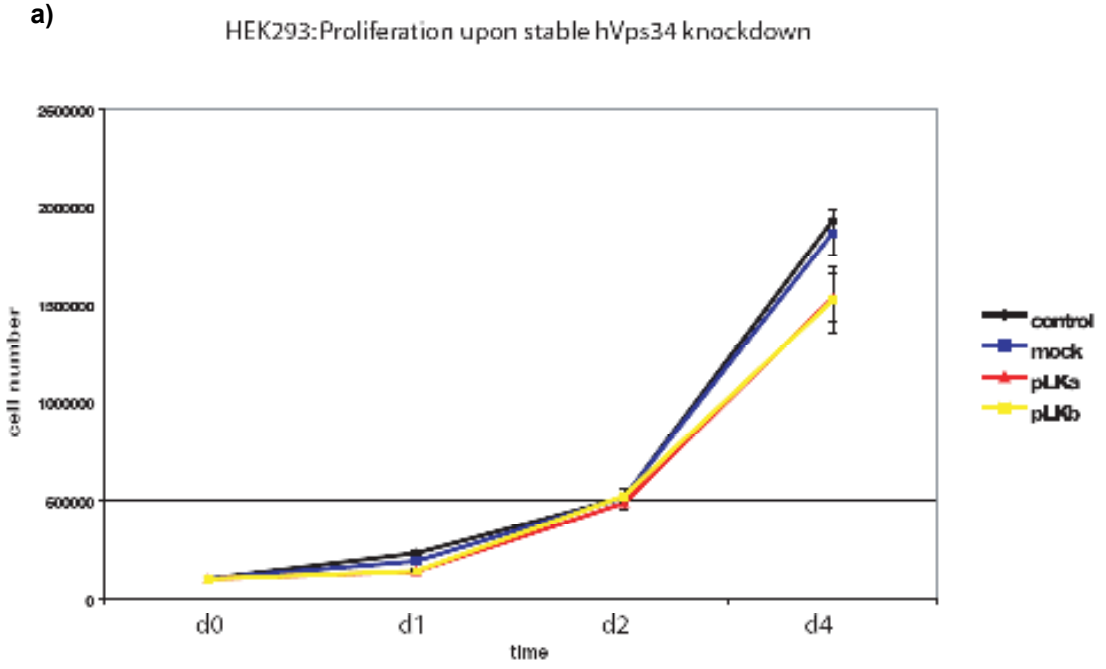

b)

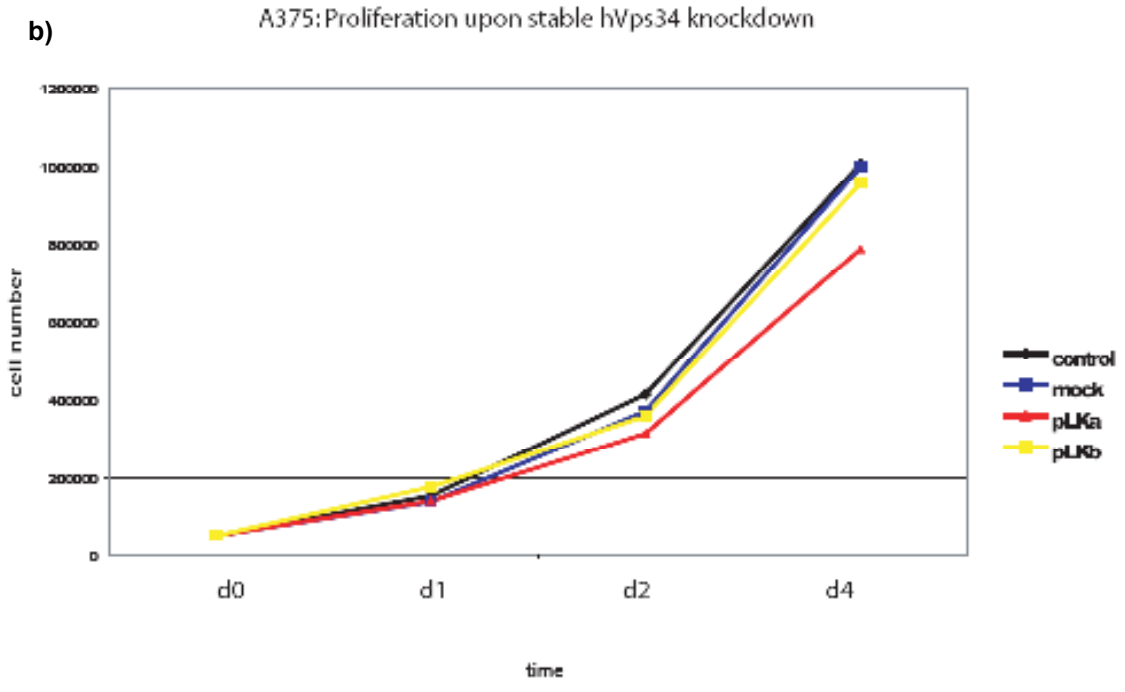

Figure 20: a+b Proliferation slightly affected in both A375 and HEK293 upon stable knockdown of hVps34

Untreated cells are shown as control cells, mock and stable knockdowns were grown in medium containing puromycin prior to the proliferation experiments. During the experiment, no selective antibiotic was applied and media were the same in all four samples per cell line shown. Data was obtained from at least three different experiments done in triplicates.

As our stable knockdown cell lines seemed to grow slower in culture, proliferation was measured in both HEK293 and A375 cell lines by counting cell numbers over four days after plating. We compared untreated control cells, mock-infected or two different stable knockdown construct (pLKa and pLKb) bearing cell lines. Mock and control cell lines grew at similar rates while both knockdowns showed a slight but significant decrease of 20% in speed in HEK293 (Figure 20a) after four days.

In A375, cells transfected with mock and control cells grew at similar speed, along with the non-efficient knockdown construct (pLKb) bearing cells. Upon efficient knockdown of hVps34 (pLKa), proliferation was again reduced by significant 20% (Figure 20b). Overall, these results show that hVps34 is certainly not essential in A375 which already have very low hVps34 basal protein levels endogenously. Loss of class III PI3K is still affecting proliferation though, even if not as much as seen in other melanoma cell lines (A2058 and 1205lu in our hands) which were not viable with reduced levels of hVps34.

5.1.5 Cell size is only slightly increased in A375 and HEK293 upon hVps34 loss

As we had found similarities in the vacuolarization phenotype (Figure 18 and 19) between our knockdown cell lines and others in the literature, we wondered whether our A375 stables would exhibit another published phenotype. hVps34 loss in U251 cell line apparently increased cell size very strongly, resulting in cells double the original size or more (Johnson, Overmeyer et al. 2006). We could not observe such a big change in cell size by binocular microscope. To not miss any smaller increases in size, we used our cell counter, measuring either cell volume or total cell size over nucleus size. Our experiments in A375 (Figure 21b) and HEK293 (Figure 21a) showed significant but only minor increases in cell size of about 10 to 15 % when measuring cell volume (in femto liters) or cell diameter (over nucleus size). The surprising difference might be cell type-dependent for the glioblastoma cell line as we could not observe such a big change neither in our stable knockdowns in HEK293 or A375 (Figure 21) nor in our preliminary siRNA experiments with more melanoma cell lines (not shown).

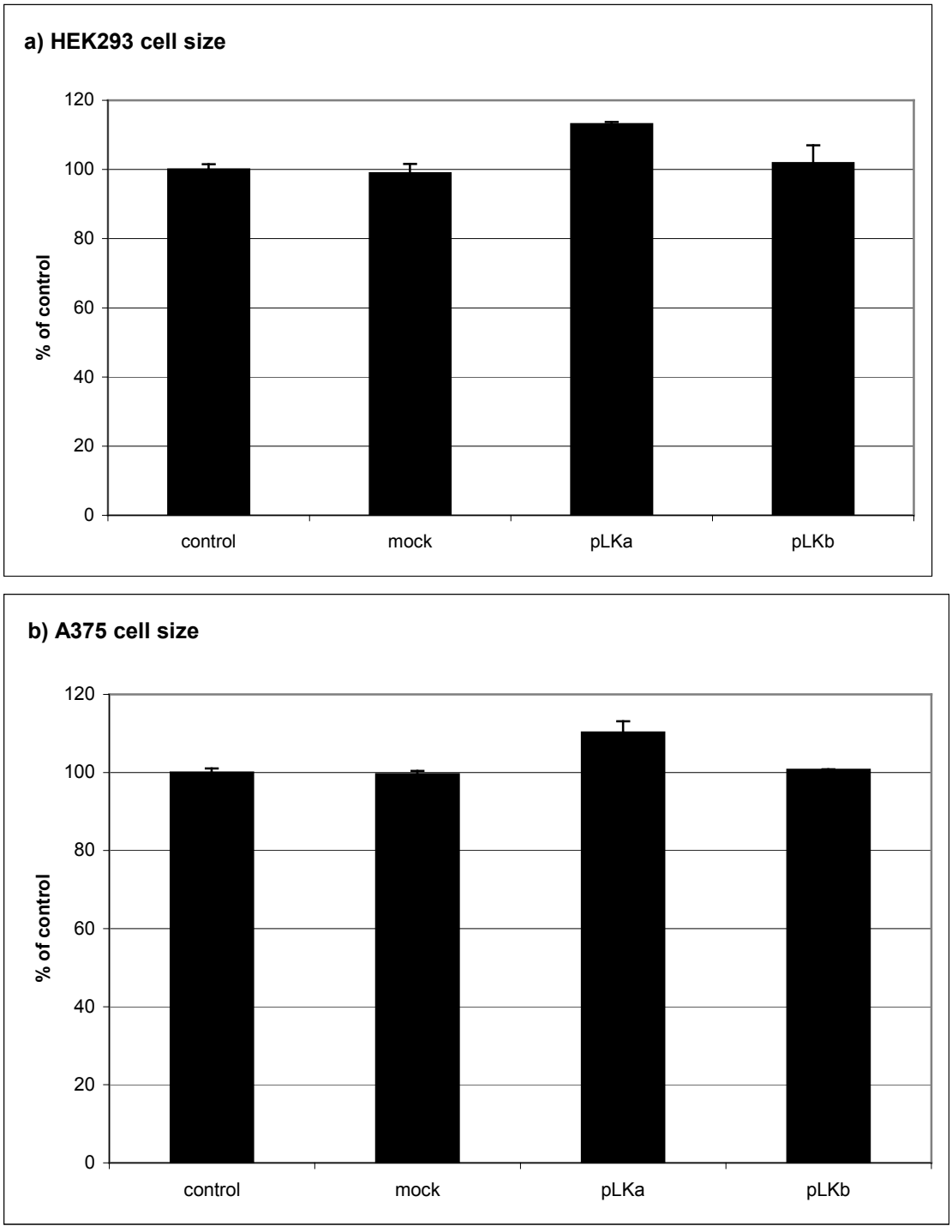

Figure 21: Mild effects on cell size upon hVps34 loss

Untreated cells were taken as control, all stably transfected cell lines were treated with puromycin prior to the experiments. Cell size is shown as percentage of control cells for each cell line, measurements of cell volume were done in six experiments in triplicates.

5.1.6 PI(3)P production is maintained in A375 depleted for hVps34 but abolished upon treatment with pan-PI3K inhibitor wortmannin

hVps34 produces most of the PI(3)P lipids in a cell, along with PI3K class II isoforms. We wondered whether there was a compensation by class II isoforms upon loss of hVps34 in our stable knockdown cells. Stable knockdowns of PI3K class III in A375 still maintained PI(3)P levels (Fig. 22 left panel). Tests with high levels of wortmannin, that also inhibit PI3K class II isoforms, abolished the lipid pools detected by transiently transfected marker eGFP-2xFYVEhrs (Fig. 22 right panel). We therefore suggest that the origin of these remaining lipid pools comes from PI3K class II isoforms. Knockdown of PI3K class II alpha is according to publications on this isoform and melanoma cell line (Elis, Triantafellow et al. 2008) affecting cell viability in A375, so it will be technically difficult to approach the question of PI(3)P origin. The same authors do not find class II beta to be essential in A375. Class II gamma is only found in liver, breast and prostate tissue, not skin, therefore we could exclude its contribution to the PI(3)P pools in hVps34 depleted cells.

Further experiments would need to be done to check the PI(3)P compensation hypothesis and elaborate which isoform of PI3K class II is required for homeostasis of PI(3)P pools in cells lacking hVps34. Eventually this applies for more cell lines than just A375 and was the reason for the other melanoma cell lines in our selection not to tolerate loss of hVps34.

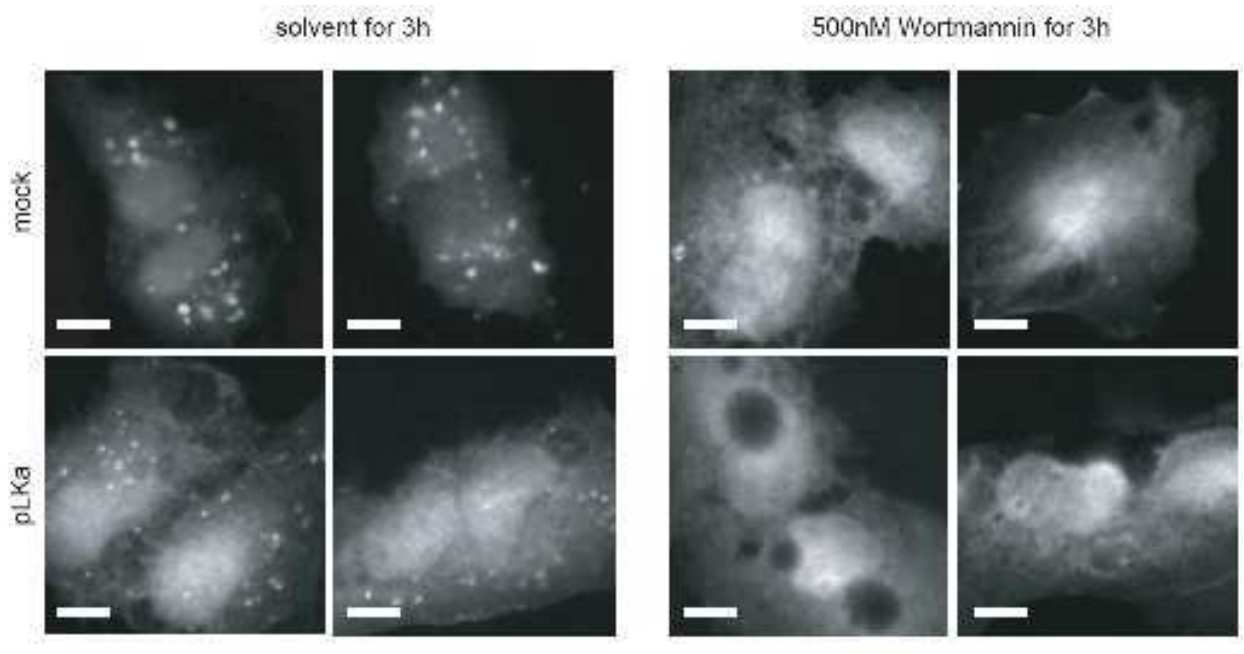

Figure 22: PI(3)P pool still present in A375 if hVps34 lost

Bars of equal size in all pictures, two pictures are shown per condition. Vacuolarization phenotype is visible in stable A375 hVps34 knockdown cell line as seen before.PI(3)P are detected by marker eGFP-2xFYVEhrs which was transiently transfected a day prior to microscopy experiments.

5.2 *Pharmacological Approach: Yeast Screening*

USE OF TRANSGENIC YEAST TO DISCOVER MAMMALIAN PI-3-KINASE ISOFORM INHIBITORS OF NATURAL ORIGIN

(manuscript in preparation)

***Ann C. Mertz*[1]**, *Anna Melone*[1], *Peter Küenzi*[2], *Michael Adams*[2], *Sabine Kiefer*[2], *Matthias Hamburger*[2], *Matthias P. Wymann*[1]

[1]Institute of Biochemistry and Genetics, Center for Biomedicine, University of Basel, Mattenstrasse 28, CH-4058 Basel, Switzerland; [2]Institute of Pharmaceutical Biology, University of Basel, Switzerland

5.2.1 Abstract

Phosphoinositide 3-kinase (PI3K) activity is found in all eukaryotic cells. These lipid kinases are linked to a diverse set of key cellular functions, including proliferation and motility, thus contributing to chronic inflammation and metastasis. Different PI3K isoforms seem to be involved in distinct cellular processes, but it is currently difficult to assess these functions due to the lack of PI3K isoform-specific inhibitors. We are therefore using *Saccharomyces cerevisiae* (Baker's yeast) to screen PI3K/inhibitor interactions as exploratory genetic tools. Yeast strains are transformed with plasmids coding for hybrid yeast/mammalian PI3K class III (Vps34). By nature, *Saccharomyces cerevisiae* exclusively expresses a single PI3K isoform, Vps34p, a class III PI3K producing PtdIns 3-*P*. Here, a hybrid *Saccharomyces cerevisiae/Homo sapiens* Vps34p (Sc/Hs_Vps34p) was engineered to complement deletion of *vps34* and allow growth at 37°C. When this hybrid protein is inactivated, rescue is lost. Compounds which reduce growth rates of *vps34* yeast expressing Sc/Hs_Vps34p can thus be identified as inhibitors of Vps34p. As this lipid kinase is involved in autophagy and phago/lysosome fusion processes, it is a putative drug target in cancer and inflammation.

In our studies we screened various libraries of natural compounds for inhibitory effects on Vps34. The compounds were mixed extracts of different origins. Upon selection, these extracts were further fractionated and the fractions retested. In order to confirm the isoform-specificity, the positive fractions were checked for inhibition of the other PI3K isoforms by applying them to mammalian cells.

Our data suggests that a fraction of *Citrus medica* extract had inhibitory effects on the human but not the yeast Vps34p and did not affect the mammalian PI3K class I isoforms.

Structurally related chemicals applied at the same concentrations did not lead to an inhibition of hVps34 activity in the cell lines tested. Further chemical engineering will show how this new hVps34 inhibitor candidate could be used for future drug designing of more potent but still specific hVps34 inhibitors.

5.2.2 Materials and Methods

Yeast media: YPD (peptone (Life Technology), yeast extract (Becton Dickinson) , glucose (Sigma)) and SD-ura (Yeast Nitrogen Base without amino acids (Becton Dickinson), amino acid mix (AppliChem)). Agar for plates from DIFCO/Becton Dickinson. Plasmid transformation into yeast was performed by the LiCl method according to Gietz and Woods as published (Gietz, Schiestl et al. 1995). Plasmids used in this study:

Plasmids used	**Gene**	**Vector**	**Origin**
Yeast			
Yeast Vps34	*S.c.* Vps34	YE195 (Gietz)	This study
Hybrid Vps34	Hybrid *S.c./H.s.* Vps34	YE195 (Gietz)	This study
KD of hybrid Vps34	Kinase-dead of 244	YE195 (Gietz)	This study
Mammalian			
PI(3)P detector	EGFP-2xFYVEhrs	pEGFP-C2 (Clontech)	gift (Harald Stenmark)

Cloning of active and of kinase dead versions of hybrid *S.c./H.s.* Vps34. Induction of yeast plasmid expression by 50uM $CuSO_4$ in appropriate media. Culture densities were measured at OD_{595nm} on a BioPhotometer from Eppendorf. Localization of PI(3)P detector eGFP-2xFYVE$_{hrs}$ was monitored in HeLa grown in DMEMc from Sigma. Transfection into mammalian cells was performed with JetPEI from PolyPlus/Chemie Brunschwig. Coumarin and wortmannin were obtained from P.Küenzi and applied at specified concentrations from stock in DMSO. Hoechst dye was from Sigma. Antibodies for Western blots were as following: hVps34 (1:2000 in 5% milk in TBST, Zymed Laboratories, cat. 38-2100), phospho-MAPK (1:10'000 in 5% BSA in TBST, Sigma, cat. M8159), phospho-PKB Serine 473 (1:2000 in 5% BSA in TBST, Cell Signalling, cat. 4051S), phospho-PKB Threonine 389 (1:2000 in 5% BSA in TBST, Cell Signalling, cat. 9206) and alpha-actin (1:10'000 in 5% milk in TBST, Sigma, cat. A5044). *In vitro* kinase assays were performed using hot ATP (P^{32}) from Perkin Elmer and TLC plates from Merck were exposed to x-ray film from Fuji Film.

5.2.3 Results

5.2.3.1 Temperature Sensitivity and Compound Screen Idea

Yeast *vps34* deletion mutants display temperature sensitivity. When grown at normal room temperature they exhibit enlarged vacuoles, but are still viable (Emr 1994). Upon

temperature increase to 37°C, the deletion mutants cannot grow anymore (Fig. 1a). In order to make use of this phenomenon, we constructed various hybrid human/yeast Vps34-bearing plasmids (Fig. 1c) (later called “hybrid Vps34p”) that contained the human kinase domain. The necessary flanking nucleotides of yeast *VPS34* to allow human *VPS34* to rescue growth at higher temperature in a *vps34* deletion mutant had to be determined (Fig. 1b and c, red box). We then checked for constructs that allowed growth at high temperature (Fig. 1a). After we had achieved this step, we planned to apply the system for primary screening of chemical compounds. Our screening idea was to screen for chemical compounds that inhibit the rescue phenotype by targeting the human kinase domain part of our hybrid construct. A kinase-dead version of this construct was used to ensure inhibitor specificity for the kinase function of Vps34p and served as a control (Fig. 1b and c). Another control used was the normal yeast Vps34p expressed from plasmid (Fig. 1a and c).

Our chemical library contained crude plant extracts at first. Putative hVps34 kinase activity inhibiting plant extracts were thereafter fractionated by HPLC and purified fractions tested again at various concentrations dissolved in DMSO. The practical work flow is depicted schematically in figure 2a. Validation of the extracts/compounds was done according to figure 2b, always considering results in triplicates.

5.2.3.2 Growth of yeast *vps34* deletion mutants are rescued by hybrid Vps34p

Plasmid borne hybrid Vps34p led to rescue of growth at high temperature when expressed in *vps34* mutants grown on YPD containing 50uM copper-sulfate ($CuSO_4$) to induce expression. Yeast cultures bearing the hybrid Vps34p were growing to the same extent as cells expressing the normal yeast kinase. Only *vps34* deletion mutants were clearly distinct in their growth behaviour at 37°C when compared to wild type (Fig. 1a). To make the yeast cells even more sensitive to the compounds in our library, we had planned to use *erg6*Δ mutants that render multidrug resistant (MDR) efflux pumps unfunctional, but these strains in combination with the deletion of *VPS34* were too sick for screening.

5.2.3.3 Extracts and pure fraction from *Citrus medica* inhibit growth of transformed mutant yeast at high temperature

From all the crude plant extracts that were tested, we obtained the best results with ethanol extracts from *Citrus medica.* Yeast cells expressing hybrid Vps34 repeatedly showed defects in growth when treated with these extracts. The pure fractions were also tested, this time in varying concentrations diluted in DMSO. The effect was dose-dependent, giving up to

60% reduction in growth compared to vehicle-treated cells when in liquid culture (Fig.3a). Best results were obtained with fraction “MACMS2”, that turned out to be limettin (Fig. 3b). Limettin (5,7-dimethoxycoumarin) is part of the coumarin-related compounds and has a molecular weight of 206.19 g/mol. Structurally-related compounds (Fig. 3c) that are commercially available were checked for similar effects, but none of them showed comparable effects, even at high concentrations (Fig.3a).

5.2.3.4 Pure fraction of *Citrus medica* compound does not influence class I PI3K isoforms

In order to check for specificity of our most promising pure fraction of *Citrus medica* extracts (MACMS2/limettin), we treated HEK293 cells with different concentrations of the compound (Fig.4). Lower concentrations than those applied in yeast tests were checked. In general yeast requires higher dosages of kinase inhibitors than mammalian cells due to their efflux pumps which often cause multidrug resistance (MDR) in yeast (Prasad, Gaur et al. 2006). We chose HEK293 since all class I PI3K isoforms are expressed and endogenous hVps34 levels are high when compared to other cell lines available in our lab. Wortmannin is a well-known pan-PI3K inhibitor (Arcaro and Wymann 1993) and blocks phosphorylation of PKB/Akt at Serine 473 and phosphorylation of S6K1 at Threonine 389 at the concentration applied, hence we used it as a positive control. As a negative control we treated the cells with 10uM coumarin, a compound which is structurally related (Fig. 3c) to our putative hVps34 inhibitor and since it had not exhibited strong effects in yeast. Wortmannin led to the expected decreases of phosphorylation, but none of the other compounds had any effects as can be seen in Fig.4. pMAPK was checked to interpret any further downstream effects, but none were observed.

5.2.3.5 Less PI(3)P detected by microscopy in HeLa treated with pure fraction

A way to confirm the efficiency of our candidate hVps34 inhibitor MACMS2 in mammalian cells was via microscopy. We checked whether a GFP-labelled 2xFYVE domain originating from Hrs was still detecting PI(3)P lipids, the product of hVps34 kinase activity. PI(3)P usually localize at the endosomes in punctuate structures (Raiborg, Bremnes et al. 2001). We used HeLa cells as a model system, as these cells are bigger than HEK293 and hence more suitable for microscopy. In cells treated with 200uM of putative inhibitor, we observed less GFP-dots per cell, which we interpreted as equal to less PI(3)P produced due to inhibition of the kinase. Cells observed by binocular microscope seemed to be healthy after the treatment, so no cytotoxicity assay was performed.

Wortmannin was once more used as positive control and led to total depletion of any PI(3)P, leaving only cytosolic GFP-signal. 100uM coumarin did not have any obvious effect on the GFP-signal when compared to vehicle-treatment (Fig.5).

5.2.3.6 *In vitro* kinase assay confirms reduction of hVps34 activity upon short incubation with pure fraction

As a last confirmation of the inhibitory effect of our compound MACMS2 on hVps34, we performed *in vitro* kinase assays with hVps34 immunoprecipitated from HEK293. Immunoprecipitated kinase was treated with a titration of MACMS2 ranging from 2uM to 200uM for 10 minutes prior to kinase reactions. As controls, treatment with 1uM wortmannin and overexpression of kinase-dead hVps34 was used to demonstrate clear inhibition of PI(3)P production (Fig. 6a). Comparing the quantified PI(3)P production of inhibitor treated hVp34, we observed a reduction of about 40% versus vehicle-treated kinase (Fig.6b). As seen in the growth studies in yeast at 37°C (Fig. 3a), we again documented a dose-dependence of the inhibitor. This recurrent dose-dependence of our putative hVps34 inhibitor suggests a real specificity for the human Vps34 kinase domain, even if working concentrations are high.

5.2.4 Discussion

hVps34 is involved in many cellular processes such as endocytosis, protein sorting to the lysosome (Wurmser and Emr 1998) and autophagy (Zeng, Overmeyer et al. 2006), and is therefore a rapidly expanding field nowadays. Further characterization of the presented compound-kinase interaction might be able to lead to more potent hVps34 inhibitors, a challenging task, as there are no specific class III PI3K inhibitors on the market to date. A recent publication (Miller, Tavshanjian et al.) opens up new possibilities to design class III-specific PI3K inhibitors. S. Miller et al. discovered differences in the ATP-binding pockets of class III versus class I PI3K isoforms. Wortmannin, the most popular pan-PI3K inhibitor (Arcaro and Wymann 1993), clearly exhibits a difference in concentration required for inhibition (IC-50), even if it shows no stronger specificity for one class over the other.

We suggest that MACMS2/limettin be used as a scaffold structure for more optimized specific hVps34 kinase activity inhibitors of the future. Now that the structure of hVps34's ATP-binding pocket is known in this field of research, drug designing can be implemented subsequently. Specific class III PI3K inhibitors promise to be interesting tools in future medical

treatment of various diseases such as neurodegenerative pathologies like Alzheimers Disease and many others (Chu, Zhu et al. 2007).

5.2.5 Figures and Figure legends

Figure 1a.

Yeast cultures were grown overnight in appropriate media and spotted onto YPD plates containing 50uM $CuSO_4$ the day after. Three days later growth at 24°C was compared to 37°C i.e. increased temperature. Shown is a representative experiment which was repeated several times.

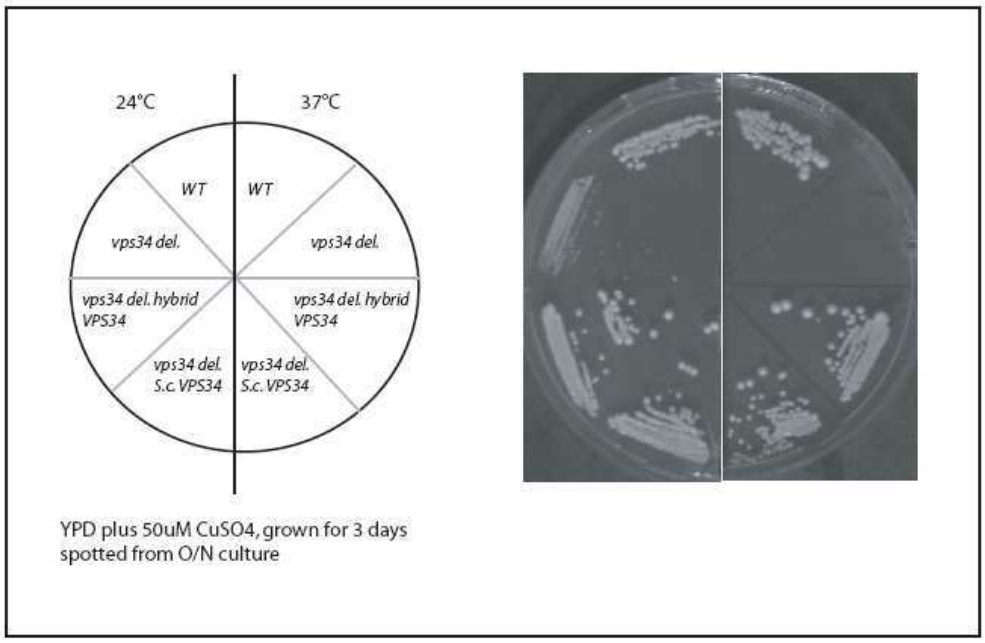

Figure 1b Summary table- Rescue phenotypes

	vps34 deletion		Wildtype	
Plasmid expression	24°C	37°C	24°C	37°C
No plasmid	+	-	+	+
Yeast Vps34p	+	+	+	+
Hybrid *S.c./H.s.* Vps34p	+	+	+	+

+ growth observed
- no growth observed

Figure 1c.

The schematic drawing of cloning of the hybrid *S.c./H.s.* VPS34 plasmid, which includes the human kinase domain, flanked by yeast VPS34 nucleotides in order to allow for complementation of a *vps34* deletion mutant (red box). All plasmids are based on a well-known Gietz vector, YE195, with copper-induction promotor.

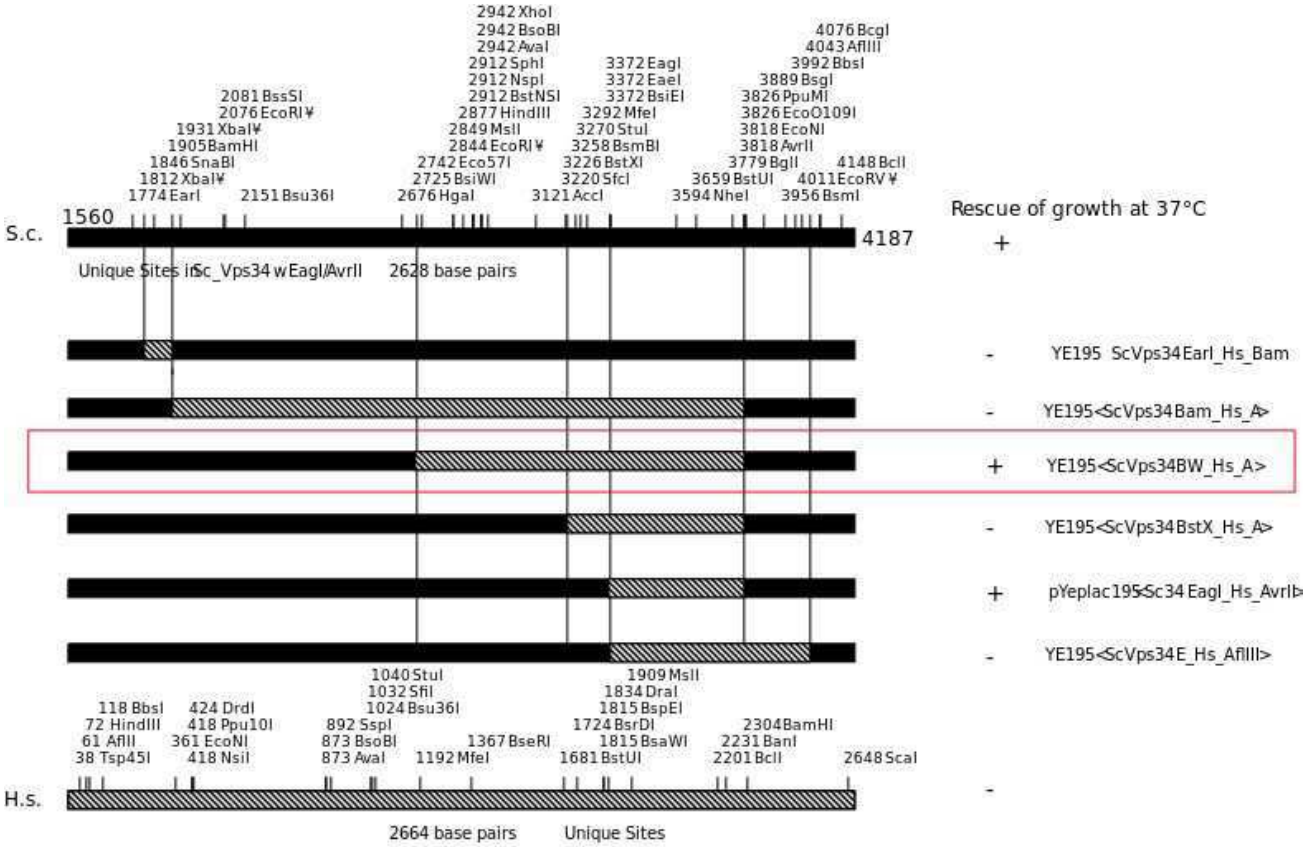

Figure 2a.

Schematic drawing of how the primary screen of crude plant extracts was achieved. Growth was supervised via OD_{600} measurements, tests done in triplicates. Drop-out medium SD-ura-trp was used in order to ensure expression of the appropriate plasmids. Copper at this concentration and over this period of time did not affect the growth of our yeast strains (tested prior to screen).

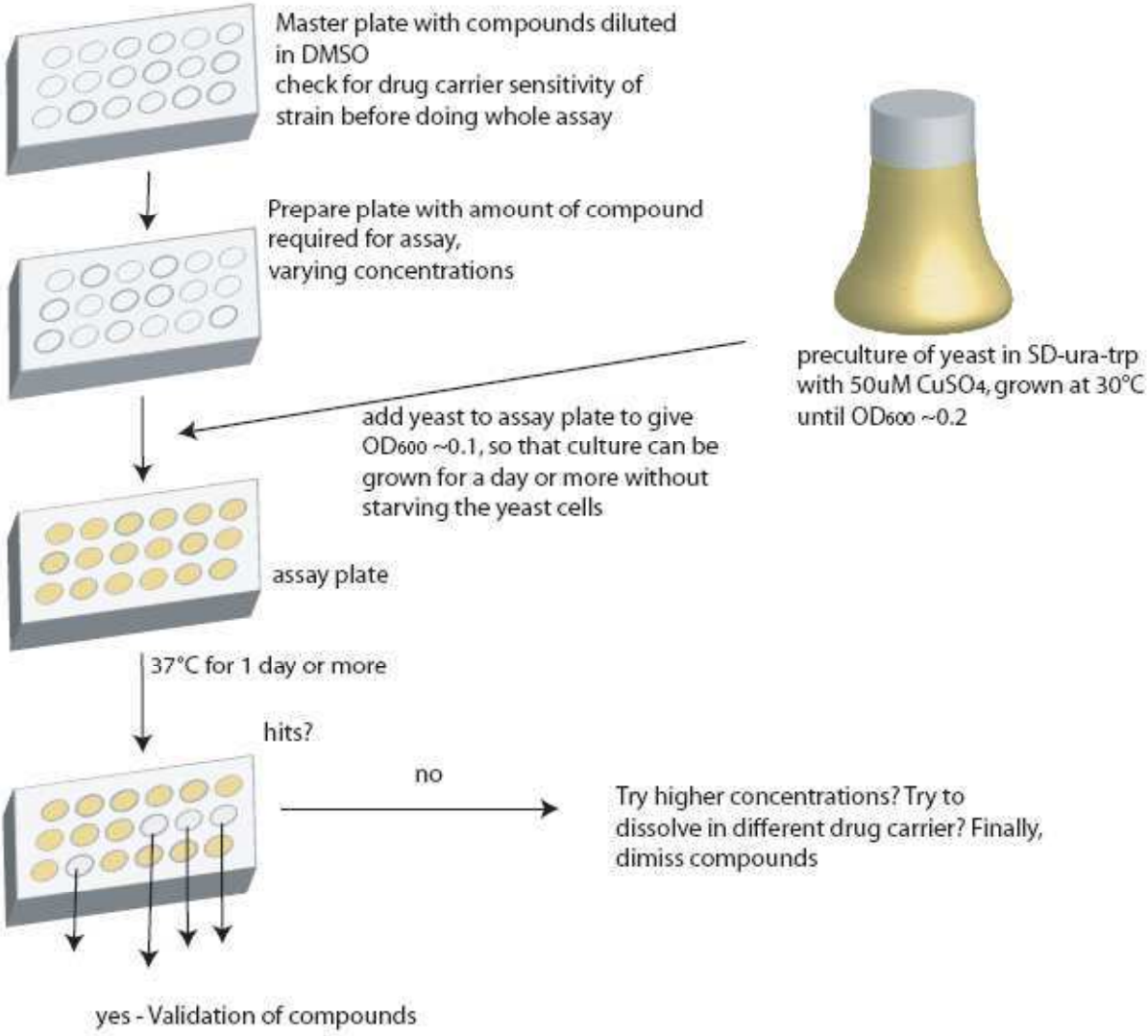

Figure 2b and c.

One representative crude extract 96 well plate and its results from the primary screen is shown in Fig. 2b. Results were validated as described in the text box (lower panel, Fig. 2c). If plant extracts or pure fractions succeeded repeatedly in this validation (Fig. 2c), they were further examined for efficacy and specificity in mammalian cell lines.

b)

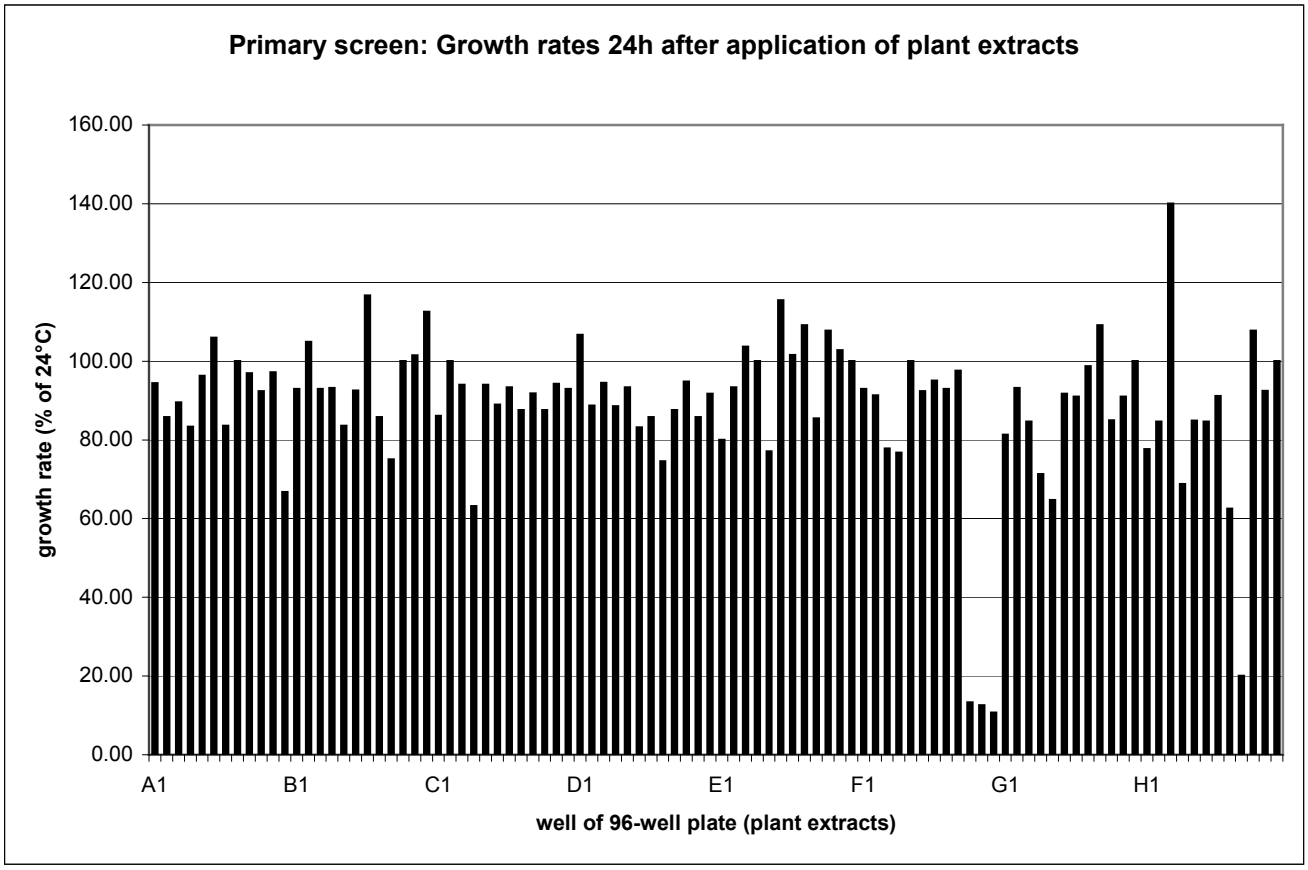

c)

Validation of compounds

Check OD_{600} in all wells after 1 day or longer. Low OD_{600} values correlate with growth inhibition by the compound i.e. inhibition of the hybrid Vps34p at 37°C, a temperature at which yeast requires to have the hybrid protein expressed.

Hybrid at 37°C grows: hybrid Vps34p not affected

Hybrid at 37°C doesn't grow: probably the hybrid protein is inhibited!

control temperature (no Vps34p required, wt and hybrid should both grow) and control wild type strain

Hybrid at 24°C grows: compound does not affect other proteins

Hybrid at 24°C doesn't grow: something other than Vps34p affected

Wild type at 37°C grows: S.c. Vps34p not affected

Wild type at 37°C doesn't grow: either S.c. Vps34p or some other protein affected

Wild type at 24°C grows:compound does not affect other proteins

Wild type at 24°C doesn't grow: something other than Vps34p affected

Once some hits are found, control strains should be used to make sure that the effects on growth are dependent on the hybrid Vps34p (*wt* and *vps34* deletion plus *S.c. VPS34* should be unaffected, both only have *S.c. VPS34* not the hybrid Vps34p.)

Figure 3a-c.

The most promising candidate hVps34 inhibitor “MACMS2” (3b) was tested further in varying concentrations to check for dose-dependence (3a). Certain effects on growth could already be observed at room temperature, but increased strongly upon culturing at 37°C. Structurally-related compounds (3c) which are commercially available were tested in parallel, shown only at their highest concentration here.

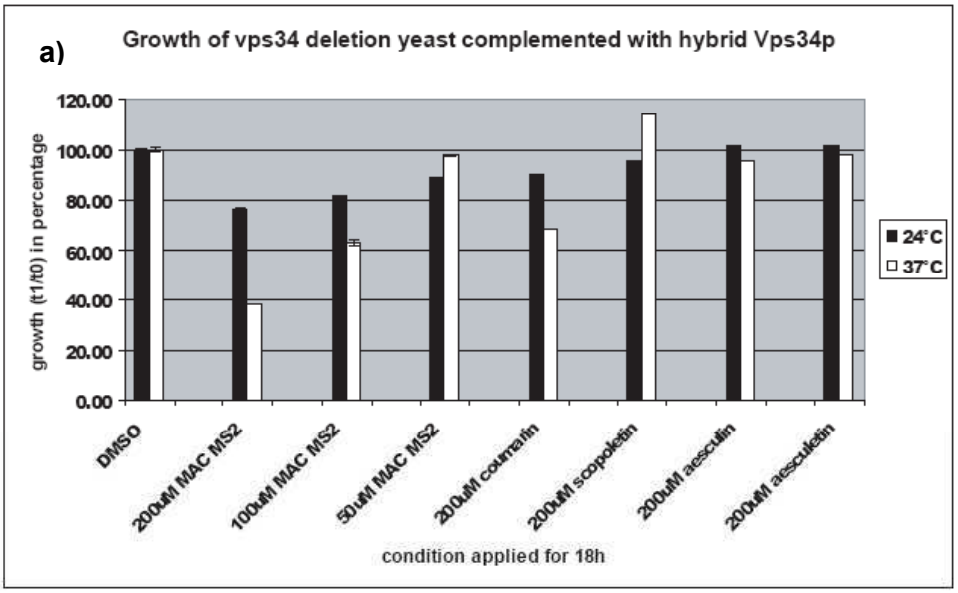

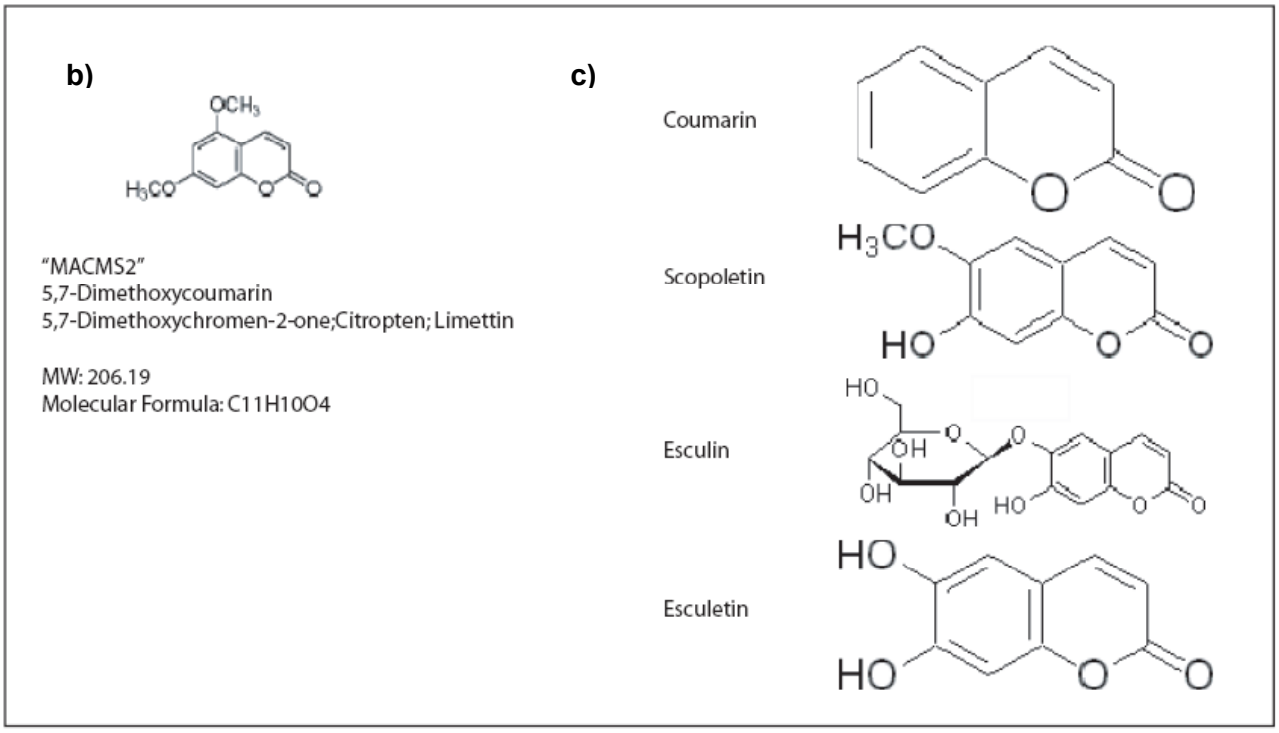

Figure 4.

Effects of our most promising candidate hVps34 inhibitor on class I PI3K were not found when checking signalling pathways usually involved in PI3K related pathways. We here applied increasing concentrations on HEK293 cells, a cell line expressing all class I isoforms and high levels of class III PI3K i.e. hVps34.

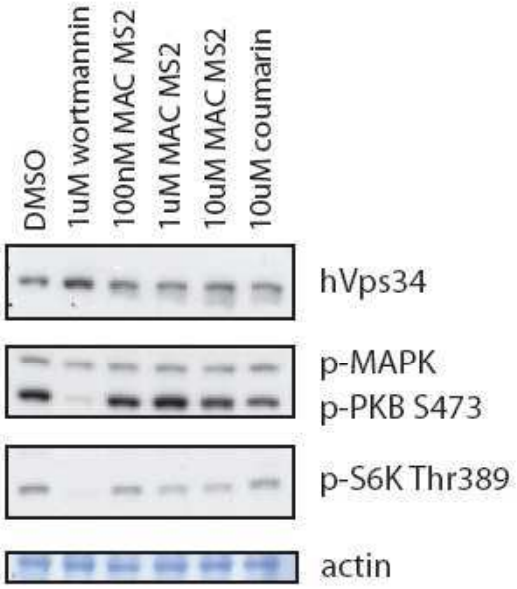

Figure 5.

Indirect confirmation of inhibitory effect of our most promising candidate compound on hVps34 kinase activity. hVps34 product PI(3)P was detected by GFP-labelled FYVE-domains originating from Hrs, a well-known PI(3)P bindig protein. Hoechst staining is shown for orientation reasons. Treatment of the HeLa cells was for 1.5h prior to fixation of the cells.

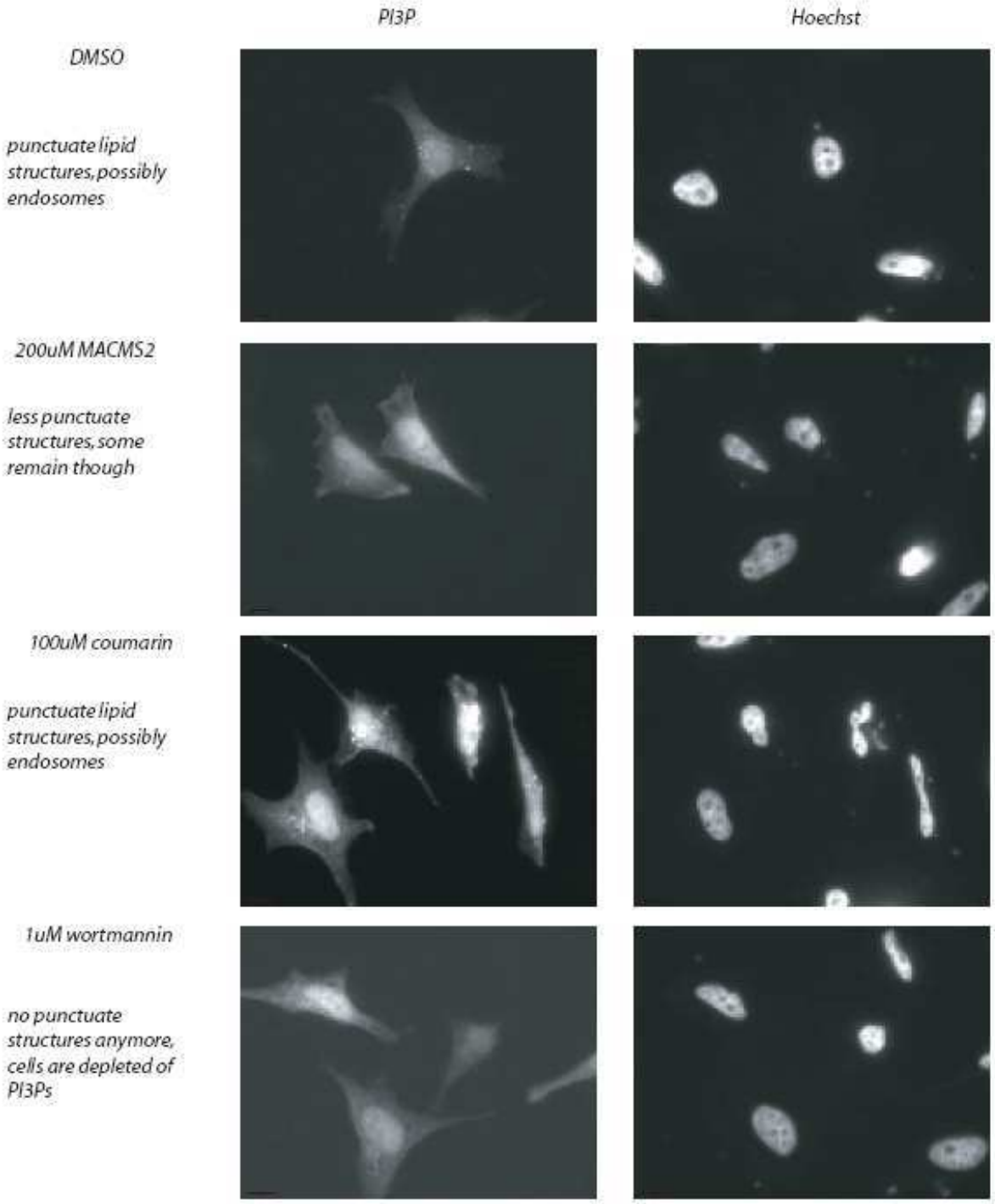

Figure 6a.

In vitro lipid kinase assay confirming inhibitory effect of our most promising candidate compound on hVps34 kinase activity. Recombinant hVps34 from HEK293 cells were treated for 10 minutes with candidate compound at varying concentrations. Wortmannin (WM) was used as positive control inhibitor and kinase-inactive (KR) recombinant hVps34 as negative control. TLC plates were exposed to x-ray film for 3h. Standard dilutions of lipids were spotted on the same plate to allow for approximate quantification of lipid produced.

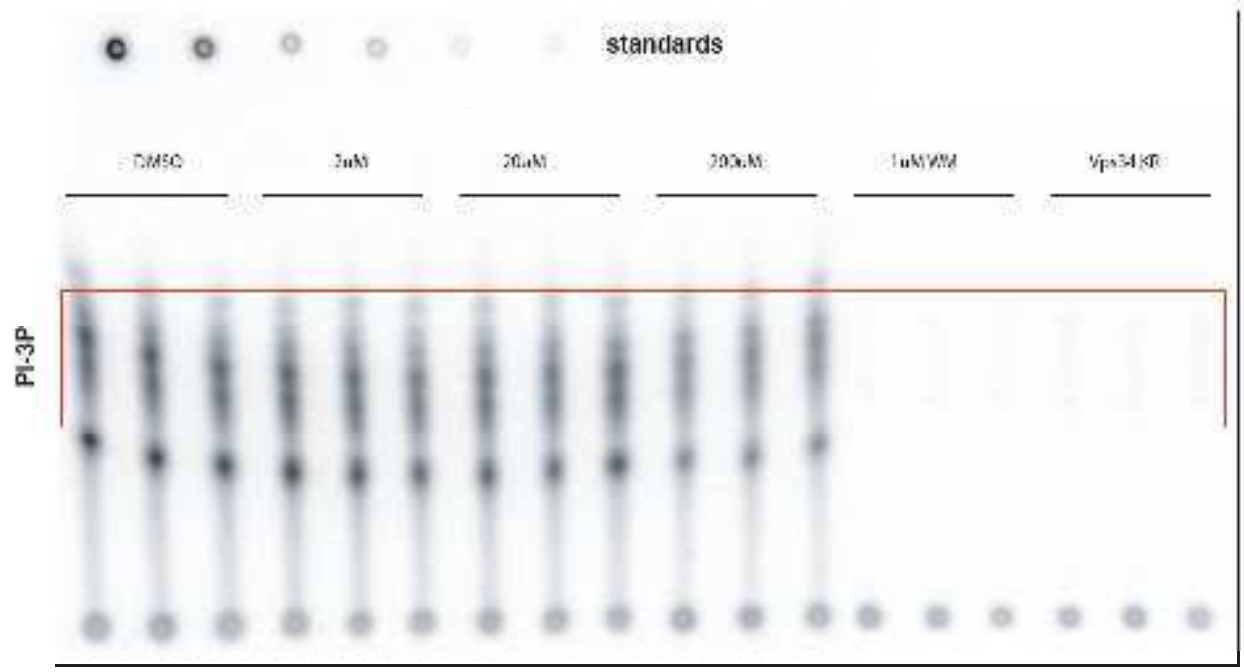

Figure 6b.

Inhibitory effect of candidate hVps34 inhibitor on kinase activity. Shown is a quantification of the lipid kinase assay results. Lipid production with vehicle-treated kinase was taken for normalization, percentage of kinase activity is depicted in the graph. IP was treated with candidate inhibitor for 10minutes prior to kinase assay.

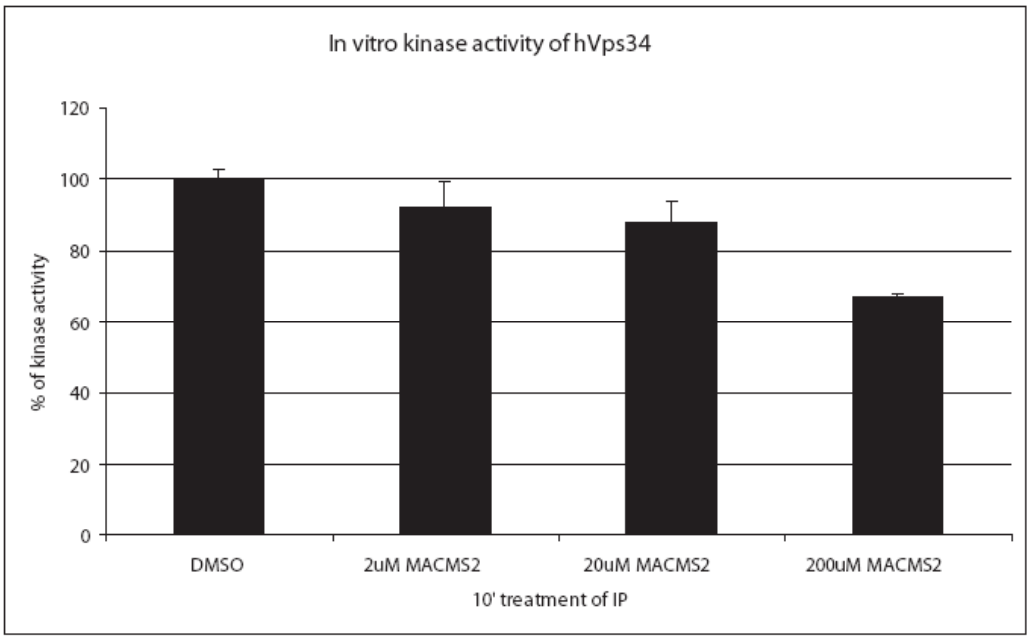

Figure 6c.

Western blot of recombinant hVps34 expressed in HEK293. Both wild type (WT) and kinase-inactive (KR, for control) form of hVps34 were expressed and immunoprecipitation via GST-tag was successful.

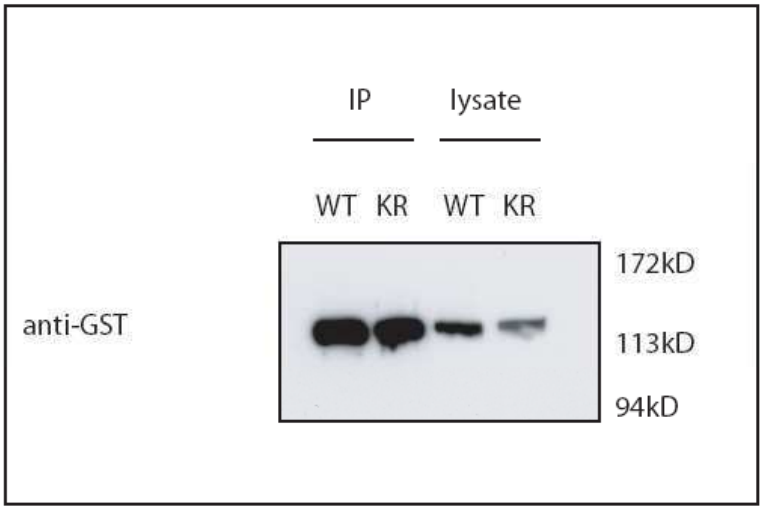

Abeliovich, H. and D. J. Klionsky (2001). "Autophagy in yeast: mechanistic insights and physiological function." Microbiol Mol Biol Rev **65**(3): 463-79, table of contents.
Aita, V. M., X. H. Liang, et al. (1999). "Cloning and genomic organization of beclin 1, a candidate tumor suppressor gene on chromosome 17q21." Genomics **59**(1): 59-65.
Akar, U., B. Ozpolat, et al. (2007). "Tissue transglutaminase inhibits autophagy in pancreatic cancer cells." Mol Cancer Res **5**(3): 241-9.
Apsel, B., J. A. Blair, et al. (2008). "Targeted polypharmacology: discovery of dual inhibitors of tyrosine and phosphoinositide kinases." Nat Chem Biol **4**(11): 691-9.
Arcaro, A. and M. P. Wymann (1993). "Wortmannin is a potent phosphatidylinositol 3-kinase inhibitor: the role of phosphatidylinositol 3,4,5-trisphosphate in neutrophil responses." Biochem J **296 (Pt 2)**: 297-301.
Arcaro, A., M. J. Zvelebil, et al. (2000). "Class II phosphoinositide 3-kinases are downstream targets of activated polypeptide growth factor receptors." Mol Cell Biol **20**(11): 3817-30.
Ashrafi, K., F. Y. Chang, et al. (2003). "Genome-wide RNAi analysis of Caenorhabditis elegans fat regulatory genes." Nature **421**(6920): 268-72.
Auger, K. R., C. L. Carpenter, et al. (1989). "Phosphatidylinositol 3-kinase and its novel product, phosphatidylinositol 3-phosphate, are present in Saccharomyces cerevisiae." J Biol Chem **264**(34): 20181-4.
Axe, E. L., S. A. Walker, et al. (2008). "Autophagosome formation from membrane compartments enriched in phosphatidylinositol 3-phosphate and dynamically connected to the endoplasmic reticulum." J Cell Biol **182**(4): 685-701.
Baba, M., K. Takeshige, et al. (1994). "Ultrastructural analysis of the autophagic process in yeast: detection of autophagosomes and their characterization." J Cell Biol **124**(6): 903-13.
Backer, J. M. (2008). "The regulation and function of Class III PI3Ks: novel roles for Vps34." Biochem J **410**(1): 1-17.
Ballou, L. M., M. Chattopadhyay, et al. (2006). "Galphaq binds to p110alpha/p85alpha phosphoinositide 3-kinase and displaces Ras." Biochem J **394**(Pt 3): 557-62.
Birkeland, H. C. and H. Stenmark (2004). "Protein targeting to endosomes and phagosomes via FYVE and PX domains." Curr Top Microbiol Immunol **282**: 89-115.
Bohnacker, T., R. Marone, et al. (2009). "PI3Kgamma adaptor subunits define coupling to degranulation and cell motility by distinct PtdIns(3,4,5)P3 pools in mast cells." Sci Signal **2**(74): ra27.
Bunney, T. D. and M. Katan "Phosphoinositide signalling in cancer: beyond PI3K and PTEN." Nat Rev Cancer **10**(5): 342-52.
Byfield, M. P., J. T. Murray, et al. (2005). "hVps34 is a nutrient-regulated lipid kinase required for activation of p70 S6 kinase." J Biol Chem **280**(38): 33076-82.
Cao, C., J. M. Backer, et al. (2008). "Sequential Actions of Myotubularin Lipid Phosphatases Regulate Endosomal PI(3)P and Growth Factor Receptor Trafficking." Mol Biol Cell **19**(8): 3334-3346.
Cao, C., J. Laporte, et al. (2007). "Myotubularin lipid phosphatase binds the hVPS15/hVPS34 lipid kinase complex on endosomes." Traffic **8**(8): 1052-67.
Chamberlain, M. D., T. Chan, et al. (2008). "Disrupted RabGAP function of the p85 subunit of phosphatidylinositol 3-kinase results in cell transformation." J Biol Chem **283**(23): 15861-8.
Chang, Y. Y., G. Juhasz, et al. (2009). "Nutrient-dependent regulation of autophagy through the target of rapamycin pathway." Biochem Soc Trans **37**(Pt 1): 232-6.
Christoforidis, S., M. Miaczynska, et al. (1999). "Phosphatidylinositol-3-OH kinases are Rab5 effectors." Nat Cell Biol **1**(4): 249-52.
Chu, C. T., J. Zhu, et al. (2007). "Beclin 1-independent pathway of damage-induced mitophagy and autophagic stress: implications for neurodegeneration and cell death." Autophagy **3**(6): 663-6.
Cornillet-Lefebvre, P., W. Cuccuini, et al. (2006). "Constitutive phosphoinositide 3-kinase activation in acute myeloid leukemia is not due to p110delta mutations." Leukemia **20**(2): 374-6.
Curtin, J. A., M. S. Stark, et al. (2006). "PI3-kinase subunits are infrequent somatic targets in melanoma." J Invest Dermatol **126**(7): 1660-3.
Dalby, K. N., I. Tekedereli, et al. "Targeting the prodeath and prosurvival functions of autophagy as novel therapeutic strategies in cancer." Autophagy **6**(3): 322-9.

Devarajan, E., J. Chen, et al. (2002). "Human breast cancer MCF-7 cell line contains inherently drug-resistant subclones with distinct genotypic and phenotypic features." Int J Oncol **20**(5): 913-20.

Devarajan, E., A. A. Sahin, et al. (2002). "Down-regulation of caspase 3 in breast cancer: a possible mechanism for chemoresistance." Oncogene **21**(57): 8843-51.

Di Paolo, G. and P. De Camilli (2006). "Phosphoinositides in cell regulation and membrane dynamics." Nature **443**(7112): 651-7.

Domin, J., F. Pages, et al. (1997). "Cloning of a human phosphoinositide 3-kinase with a C2 domain that displays reduced sensitivity to the inhibitor wortmannin." Biochem J **326 (Pt 1)**: 139-47.

Dunn, W. A., Jr. (1990). "Studies on the mechanisms of autophagy: formation of the autophagic vacuole." J Cell Biol **110**(6): 1923-33.

Eickholt, B. J., A. I. Ahmed, et al. (2007). "Control of axonal growth and regeneration of sensory neurons by the p110delta PI 3-kinase." PLoS One **2**(9): e869.

Elis, W., E. Triantafellow, et al. (2008). "Down-regulation of class II phosphoinositide 3-kinase alpha expression below a critical threshold induces apoptotic cell death." Mol Cancer Res **6**(4): 614-23.

Ellson, C. D., K. E. Anderson, et al. (2001). "Phosphatidylinositol 3-phosphate is generated in phagosomal membranes." Curr Biol **11**(20): 1631-5.

Emr, S. a. (1994). "Vps34p required for yeast vacuolar protein sorting is a multiple specificity kinase that exhibits both protein kinase and phophatidylinositol-specific PI 3-kinase activities." The Journal of Biological Chemistry **269**(Dec 16): 31552-31562.

Falasca, M., W. E. Hughes, et al. (2007). "The role of phosphoinositide 3-kinase C2alpha in insulin signaling." J Biol Chem **282**(38): 28226-36.

Falasca, M. and T. Maffucci (2007). "Role of class II phosphoinositide 3-kinase in cell signalling." Biochem Soc Trans **35**(Pt 2): 211-4.

Fimia, G. M., A. Stoykova, et al. (2007). "Ambra1 regulates autophagy and development of the nervous system." Nature **447**(7148): 1121-5.

Findlay, G. M., L. Yan, et al. (2007). "A MAP4 kinase related to Ste20 is a nutrient-sensitive regulator of mTOR signalling." Biochem J **403**(1): 13-20.

Folkman, J. (2006). "Angiogenesis." Annu Rev Med **57**: 1-18.

Frazzetto, M., C. Suphioglu, et al. (2008). "Dissecting isoform selectivity of PI3K inhibitors: the role of non-conserved residues in the catalytic pocket." Biochem J **414**(3): 383-90.

Furuya, N., J. Yu, et al. (2005). "The evolutionarily conserved domain of Beclin 1 is required for Vps34 binding, autophagy and tumor suppressor function." Autophagy **1**(1): 46-52.

Futter, C. E., L. M. Collinson, et al. (2001). "Human VPS34 is required for internal vesicle formation within multivesicular endosomes." J Cell Biol **155**(7): 1251-64.

Gietz, R. D., R. H. Schiestl, et al. (1995). "Studies on the transformation of intact yeast cells by the LiAc/SS-DNA/PEG procedure." Yeast **11**(4): 355-60.

Gulati, P., L. D. Gaspers, et al. (2008). "Amino acids activate mTOR complex 1 via Ca2+/CaM signaling to hVps34." Cell Metab **7**(5): 456-65.

Gulati, P. and G. Thomas (2007). "Nutrient sensing in the mTOR/S6K1 signalling pathway." Biochem Soc Trans **35**(Pt 2): 236-8.

Gupta, S., A. R. Ramjaun, et al. (2007). "Binding of ras to phosphoinositide 3-kinase p110alpha is required for ras-driven tumorigenesis in mice." Cell **129**(5): 957-68.

Harada, K., A. B. Truong, et al. (2005). "The class II phosphoinositide 3-kinase C2beta is not essential for epidermal differentiation." Mol Cell Biol **25**(24): 11122-30.

Herman, P. K. and S. D. Emr (1990). "Characterization of VPS34, a gene required for vacuolar protein sorting and vacuole segregation in Saccharomyces cerevisiae." Mol Cell Biol **10**(12): 6742-54.

Hirsch, E., L. Braccini, et al. (2009). "Twice upon a time: PI3K's secret double life exposed." Trends Biochem Sci **34**(5): 244-8.

Hurley, J. H. (2006). "Membrane binding domains." Biochim Biophys Acta **1761**(8): 805-11.

Im, Y. J., T. Wollert, et al. (2009). "Structure and function of the ESCRT-II-III interface in multivesicular body biogenesis." Dev Cell **17**(2): 234-43.

Jin, S. and E. White (2008). "Tumor suppression by autophagy through the management of metabolic stress." Autophagy **4**(5): 563-6.

Johnson, E. E., J. H. Overmeyer, et al. (2006). "Gene silencing reveals a specific function of hVps34 phosphatidylinositol 3-kinase in late versus early endosomes." J Cell Sci **119**(Pt 7): 1219-32.
Juhasz, G., J. H. Hill, et al. (2008). "The class III PI(3)K Vps34 promotes autophagy and endocytosis but not TOR signaling in Drosophila." J Cell Biol **181**(4): 655-66.
Kihara, A., T. Noda, et al. (2001). "Two distinct Vps34 phosphatidylinositol 3-kinase complexes function in autophagy and carboxypeptidase Y sorting in Saccharomyces cerevisiae." J Cell Biol **152**(3): 519-30.
Kim, E., P. Goraksha-Hicks, et al. (2008). "Regulation of TORC1 by Rag GTPases in nutrient response." Nat Cell Biol **10**(8): 935-45.
Kinchen, J. M., K. Doukoumetzidis, et al. (2008). "A pathway for phagosome maturation during engulfment of apoptotic cells." Nat Cell Biol **10**(5): 556-66.
Knight, Z. A., B. Gonzalez, et al. (2006). "A pharmacological map of the PI3-K family defines a role for p110alpha in insulin signaling." Cell **125**(4): 733-47.
Kok, K., B. Geering, et al. (2009). "Regulation of phosphoinositide 3-kinase expression in health and disease." Trends Biochem Sci **34**(3): 115-27.
Kurig, B., A. Shymanets, et al. (2009). "Ras is an indispensable coregulator of the class IB phosphoinositide 3-kinase p87/p110gamma." Proc Natl Acad Sci U S A **106**(48): 20312-7.
Kurosu, H. and T. Katada (2001). "Association of phosphatidylinositol 3-kinase composed of p110beta-catalytic and p85-regulatory subunits with the small GTPase Rab5." J Biochem **130**(1): 73-8.
Kurosu, H., T. Maehama, et al. (1997). "Heterodimeric phosphoinositide 3-kinase consisting of p85 and p110beta is synergistically activated by the betagamma subunits of G proteins and phosphotyrosyl peptide." J Biol Chem **272**(39): 24252-6.
Lahtz, C., R. Stranzenbach, et al. (2010). "Methylation of PTEN as a prognostic factor in malignant melanoma of the skin." J Invest Dermatol **130**(2): 620-2.
Lehmann, K., J. P. Muller, et al. (2009). "PI3Kgamma controls oxidative bursts in neutrophils via interactions with PKCalpha and p47phox." Biochem J **419**(3): 603-10.
Lemmon, M. A. (2008). "Membrane recognition by phospholipid-binding domains." Nat Rev Mol Cell Biol **9**(2): 99-111.
Leung, W. H., T. Tarasenko, et al. (2009). "Differential roles for the inositol phosphatase SHIP in the regulation of macrophages and lymphocytes." Immunol Res **43**(1-3): 243-51.
Levine, B. (2007). "Cell biology: autophagy and cancer." Nature **446**(7137): 745-7.
Levine, B. and G. Kroemer (2008). "Autophagy in the pathogenesis of disease." Cell **132**(1): 27-42.
Liang, C., P. Feng, et al. (2006). "Autophagic and tumour suppressor activity of a novel Beclin1-binding protein UVRAG." Nat Cell Biol **8**(7): 688-99.
Liang, C., J. S. Lee, et al. (2008). "Beclin1-binding UVRAG targets the class C Vps complex to coordinate autophagosome maturation and endocytic trafficking." Nat Cell Biol **10**(7): 776-87.
Liang, X. H., S. Jackson, et al. (1999). "Induction of autophagy and inhibition of tumorigenesis by beclin 1." Nature **402**(6762): 672-6.
Liu, B., Y. Cheng, et al. (2009). "Polygonatum cyrtonema lectin induces apoptosis and autophagy in human melanoma A375 cells through a mitochondria-mediated ROS-p38-p53 pathway." Cancer Lett **275**(1): 54-60.
MacDougall, L. K., M. E. Gagou, et al. (2004). "Targeted expression of the class II phosphoinositide 3-kinase in Drosophila melanogaster reveals lipid kinase-dependent effects on patterning and interactions with receptor signaling pathways." Mol Cell Biol **24**(2): 796-808.
Maira, S. M., F. Stauffer, et al. (2008). "Identification and characterization of NVP-BEZ235, a new orally available dual phosphatidylinositol 3-kinase/mammalian target of rapamycin inhibitor with potent in vivo antitumor activity." Mol Cancer Ther **7**(7): 1851-63.
Mandelker, D., S. B. Gabelli, et al. (2009). "A frequent kinase domain mutation that changes the interaction between PI3Kalpha and the membrane." Proc Natl Acad Sci U S A **106**(40): 16996-7001.
Marone, R., V. Cmiljanovic, et al. (2008). "Targeting phosphoinositide 3-kinase: moving towards therapy." Biochim Biophys Acta **1784**(1): 159-85.
Marone, R., D. Erhart, et al. (2009). "Targeting melanoma with dual phosphoinositide 3-kinase/mammalian target of rapamycin inhibitors." Mol Cancer Res **7**(4): 601-13.

Mauvezin, C., M. Orpinell, et al. "The nuclear cofactor DOR regulates autophagy in mammalian and Drosophila cells." EMBO Rep **11**(1): 37-44.
Melendez, A., Z. Talloczy, et al. (2003). "Autophagy genes are essential for dauer development and life-span extension in C. elegans." Science **301**(5638): 1387-91.
Miled, N., Y. Yan, et al. (2007). "Mechanism of two classes of cancer mutations in the phosphoinositide 3-kinase catalytic subunit." Science **317**(5835): 239-42.
Miller, S., B. Tavshanjian, et al. (2010). "Shaping development of autophagy inhibitors with the structure of the lipid kinase Vps34." Science **327**(5973): 1638-42.
Moretti, L., A. Attia, et al. (2007). "Crosstalk between Bak/Bax and mTOR signaling regulates radiation-induced autophagy." Autophagy **3**(2): 142-4.
Murray, J. T., C. Panaretou, et al. (2002). "Role of Rab5 in the recruitment of hVps34/p150 to the early endosome." Traffic **3**(6): 416-27.
Nicklin, P., P. Bergman, et al. (2009). "Bidirectional transport of amino acids regulates mTOR and autophagy." Cell **136**(3): 521-34.
Nobukuni, T., M. Joaquin, et al. (2005). "Amino acids mediate mTOR/raptor signaling through activation of class 3 phosphatidylinositol 3OH-kinase." Proc Natl Acad Sci U S A **102**(40): 14238-43.
Novak, I., V. Kirkin, et al. "Nix is a selective autophagy receptor for mitochondrial clearance." EMBO Rep **11**(1): 45-51.
Omholt, K., D. Krockel, et al. (2006). "Mutations of PIK3CA are rare in cutaneous melanoma." Melanoma Res **16**(2): 197-200.
Orme, M. H., S. Alrubaie, et al. (2006). "Input from Ras is required for maximal PI(3)K signalling in Drosophila." Nat Cell Biol **8**(11): 1298-302.
Papakonstanti, E. A., A. J. Ridley, et al. (2007). "The p110delta isoform of PI 3-kinase negatively controls RhoA and PTEN." Embo J **26**(13): 3050-61.
Papakonstanti, E. A., O. Zwaenepoel, et al. (2008). "Distinct roles of class IA PI3K isoforms in primary and immortalised macrophages." J Cell Sci **121**(Pt 24): 4124-33.
Petiot, A., F. Strappazzon, et al. (2008). "Alix differs from ESCRT proteins in the control of autophagy." Biochem Biophys Res Commun **375**(1): 63-8.
Prasad, N. K., M. Tandon, et al. (2008). "Phosphoinositol phosphatase SHIP2 promotes cancer development and metastasis coupled with alterations in EGF receptor turnover." Carcinogenesis **29**(1): 25-34.
Prasad, R., N. A. Gaur, et al. (2006). "Efflux pumps in drug resistance of Candida." Infect Disord Drug Targets **6**(2): 69-83.
Ragnarsson-Olding, B. K., P. J. Nilsson, et al. (2009). "Primary ano-rectal malignant melanomas within a population-based national patient series in Sweden during 40 years." Acta Oncol **48**(1): 125-31.
Raiborg, C., B. Bremnes, et al. (2001). "FYVE and coiled-coil domains determine the specific localisation of Hrs to early endosomes." J Cell Sci **114**(Pt 12): 2255-63.
Robinson, J. S., D. J. Klionsky, et al. (1988). "Protein sorting in Saccharomyces cerevisiae: isolation of mutants defective in the delivery and processing of multiple vacuolar hydrolases." Mol Cell Biol **8**(11): 4936-48.
Roggo, L., V. Bernard, et al. (2002). "Membrane transport in Caenorhabditis elegans: an essential role for VPS34 at the nuclear membrane." Embo J **21**(7): 1673-83.
Rohrschneider, L. R., J. F. Fuller, et al. (2000). "Structure, function, and biology of SHIP proteins." Genes Dev **14**(5): 505-20.
Rothman, J. H. and T. H. Stevens (1986). "Protein sorting in yeast: mutants defective in vacuole biogenesis mislocalize vacuolar proteins into the late secretory pathway." Cell **47**(6): 1041-51.
Samuels, Y., Z. Wang, et al. (2004). "High frequency of mutations of the PIK3CA gene in human cancers." Science **304**(5670): 554.
Sancak, Y., T. R. Peterson, et al. (2008). "The Rag GTPases bind raptor and mediate amino acid signaling to mTORC1." Science **320**(5882): 1496-501.
Schu, P. V., K. Takegawa, et al. (1993). "Phosphatidylinositol 3-kinase encoded by yeast VPS34 gene essential for protein sorting." Science **260**(5104): 88-91.
Sengupta, S., T. R. Peterson, et al. (2010). "Regulation of the mTOR complex 1 pathway by nutrients, growth factors, and stress." Mol Cell **40**(2): 310-22.

Shayesteh, L., Y. Lu, et al. (1999). "PIK3CA is implicated as an oncogene in ovarian cancer." Nat Genet **21**(1): 99-102.
Shin, H. W., M. Hayashi, et al. (2005). "An enzymatic cascade of Rab5 effectors regulates phosphoinositide turnover in the endocytic pathway." J Cell Biol **170**(4): 607-18.
Siddhanta, U., J. McIlroy, et al. (1998). "Distinct roles for the p110alpha and hVPS34 phosphatidylinositol 3'-kinases in vesicular trafficking, regulation of the actin cytoskeleton, and mitogenesis." J Cell Biol **143**(6): 1647-59.
Simonsen, A., H. C. Birkeland, et al. (2004). "Alfy, a novel FYVE-domain-containing protein associated with protein granules and autophagic membranes." J Cell Sci **117**(Pt 18): 4239-51.
Simonsen, A. and H. Stenmark (2008). "Self-eating from an ER-associated cup." J Cell Biol **182**(4): 621-2.
Simonsen, A. and S. A. Tooze (2009). "Coordination of membrane events during autophagy by multiple class III PI3-kinase complexes." J Cell Biol **186**(6): 773-82.
Singh, S. B., A. S. Davis, et al. (2006). "Human IRGM induces autophagy to eliminate intracellular mycobacteria." Science **313**(5792): 1438-41.
Slessareva, J. E., S. M. Routt, et al. (2006). "Activation of the phosphatidylinositol 3-kinase Vps34 by a G protein alpha subunit at the endosome." Cell **126**(1): 191-203.
Song, X., W. Xu, et al. (2001). "Phox homology domains specifically bind phosphatidylinositol phosphates." Biochemistry **40**(30): 8940-4.
Spowart, J. and J. J. Lum "Opening a new DOR to autophagy." EMBO Rep **11**(1): 4-5.
Stahelin, R. V., D. Karathanassis, et al. (2006). "Structural and membrane binding analysis of the Phox homology domain of phosphoinositide 3-kinase-C2alpha." J Biol Chem **281**(51): 39396-406.
Stark, M. and N. Hayward (2007). "Genome-wide loss of heterozygosity and copy number analysis in melanoma using high-density single-nucleotide polymorphism arrays." Cancer Res **67**(6): 2632-42.
Stein, M. P., Y. Feng, et al. (2003). "Human VPS34 and p150 are Rab7 interacting partners." Traffic **4**(11): 754-71.
Taboubi, S., J. Milanini, et al. (2007). "G alpha(q/11)-coupled P2Y2 nucleotide receptor inhibits human keratinocyte spreading and migration." Faseb J **21**(14): 4047-58.
Takahashi, Y., D. Coppola, et al. (2007). "Bif-1 interacts with Beclin 1 through UVRAG and regulates autophagy and tumorigenesis." Nat Cell Biol **9**(10): 1142-51.
Takahashi, Y., D. Coppola, et al. (2007). "Bif-1 interacts with Beclin 1 through UVRAG and regulates autophagy and tumorigenesis." Nat Cell Biol **9**(10): 1142-51.
Takahashi, Y., C. L. Meyerkord, et al. (2008). "BARgaining membranes for autophagosome formation: Regulation of autophagy and tumorigenesis by Bif-1/Endophilin B1." Autophagy **4**(1): 121-4.
Takeshige, K., M. Baba, et al. (1992). "Autophagy in yeast demonstrated with proteinase-deficient mutants and conditions for its induction." J Cell Biol **119**(2): 301-11.
Tang, R., X. Zhao, et al. (2008). "Investigation of variants in the promoter region of PIK3C3 in schizophrenia." Neurosci Lett **437**(1): 42-4.
Tormo, D., A. Checinska, et al. (2009). "Targeted activation of innate immunity for therapeutic induction of autophagy and apoptosis in melanoma cells." Cancer Cell **16**(2): 103-14.
Tsukada, M. and Y. Ohsumi (1993). "Isolation and characterization of autophagy-defective mutants of Saccharomyces cerevisiae." FEBS Lett **333**(1-2): 169-74.
Vanhaesebroeck, B., K. Ali, et al. (2005). "Signalling by PI3K isoforms: insights from gene-targeted mice." Trends Biochem Sci **30**(4): 194-204.
Vanhaesebroeck, B., J. Guillermet-Guibert, et al. (2010). "The emerging mechanisms of isoform-specific PI3K signalling." Nat Rev Mol Cell Biol **11**(5): 329-41.
Vanhaesebroeck, B., S. J. Leevers, et al. (2001). "Synthesis and function of 3-phosphorylated inositol lipids." Annu Rev Biochem **70**: 535-602.
Vanhaesebroeck, B., S. J. Leevers, et al. (1997). "Phosphoinositide 3-kinases: a conserved family of signal transducers." Trends Biochem Sci **22**(7): 267-72.
Vergne, I., E. Roberts, et al. (2009). "Control of autophagy initiation by phosphoinositide 3-phosphatase Jumpy." Embo J **28**(15): 2244-58.

Virbasius, J. V., A. Guilherme, et al. (1996). "Mouse p170 is a novel phosphatidylinositol 3-kinase containing a C2 domain." J Biol Chem **271**(23): 13304-7.
Vlahos, C. J., W. F. Matter, et al. (1994). "A specific inhibitor of phosphatidylinositol 3-kinase, 2-(4-morpholinyl)-8-phenyl-4H-1-benzopyran-4-one (LY294002)." J Biol Chem **269**(7): 5241-8.
Vogt, P. K., S. Kang, et al. (2007). "Cancer-specific mutations in phosphatidylinositol 3-kinase." Trends Biochem Sci **32**(7): 342-9.
Volinia, S., R. Dhand, et al. (1995). "A human phosphatidylinositol 3-kinase complex related to the yeast Vps34p-Vps15p protein sorting system." Embo J **14**(14): 3339-48.
Walker, E. H., M. E. Pacold, et al. (2000). "Structural determinants of phosphoinositide 3-kinase inhibition by wortmannin, LY294002, quercetin, myricetin, and staurosporine." Mol Cell **6**(4): 909-19.
Wang, X. and C. G. Proud (2009). "Nutrient control of TORC1, a cell-cycle regulator." Trends Cell Biol **19**(6): 260-7.
Wang, Z., W. A. Wilson, et al. (2001). "Antagonistic controls of autophagy and glycogen accumulation by Snf1p, the yeast homolog of AMP-activated protein kinase, and the cyclin-dependent kinase Pho85p." Mol Cell Biol **21**(17): 5742-52.
Whitman, M., D. Kaplan, et al. (1987). "Evidence for two distinct phosphatidylinositol kinases in fibroblasts. Implications for cellular regulation." Biochem J **247**(1): 165-74.
Wollert, T., D. Yang, et al. (2009). "The ESCRT machinery at a glance." J Cell Sci **122**(Pt 13): 2163-6.
Wu, H., V. Goel, et al. (2003). "PTEN signaling pathways in melanoma." Oncogene **22**(20): 3113-22.
Wullschleger, S., R. Loewith, et al. (2006). "TOR signaling in growth and metabolism." Cell **124**(3): 471-84.
Wurmser, A. E. and S. D. Emr (1998). "Phosphoinositide signaling and turnover: PtdIns(3)P, a regulator of membrane traffic, is transported to the vacuole and degraded by a process that requires lumenal vacuolar hydrolase activities." Embo J **17**(17): 4930-42.
Wymann, M. P. and R. Marone (2005). "Phosphoinositide 3-kinase in disease: timing, location, and scaffolding." Curr Opin Cell Biol **17**(2): 141-9.
Wymann, M. P. and L. Pirola (1998). "Structure and function of phosphoinositide 3-kinases." Biochim Biophys Acta **1436**(1-2): 127-50.
Xue, Y., H. Fares, et al. (2003). "Genetic analysis of the myotubularin family of phosphatases in Caenorhabditis elegans." J Biol Chem **278**(36): 34380-6.
Yaguchi, S., Y. Fukui, et al. (2006). "Antitumor activity of ZSTK474, a new phosphatidylinositol 3-kinase inhibitor." J Natl Cancer Inst **98**(8): 545-56.
Yan, Y., R. J. Flinn, et al. (2009). "hVps15, but not Ca2+/CaM, is required for the activity and regulation of hVps34 in mammalian cells." Biochem J **417**(3): 747-55.
Zeng, X., J. H. Overmeyer, et al. (2006). "Functional specificity of the mammalian Beclin-Vps34 PI 3-kinase complex in macroautophagy versus endocytosis and lysosomal enzyme trafficking." J Cell Sci **119**(Pt 2): 259-70.
Zhang, H., J. P. Stallock, et al. (2000). "Regulation of cellular growth by the Drosophila target of rapamycin dTOR." Genes Dev **14**(21): 2712-24.
Zhao, L. and P. K. Vogt (2008). "Helical domain and kinase domain mutations in p110alpha of phosphatidylinositol 3-kinase induce gain of function by different mechanisms." Proc Natl Acad Sci U S A **105**(7): 2652-7.
Zhong, Y., Q. J. Wang, et al. (2009). "Distinct regulation of autophagic activity by Atg14L and Rubicon associated with Beclin 1-phosphatidylinositol-3-kinase complex." Nat Cell Biol **11**(4): 468-76.
Zoncu, R., A. Efeyan, et al. (2010). "mTOR: from growth signal integration to cancer, diabetes and ageing." Nat Rev Mol Cell Biol **12**(1): 21-35.

6 Peer-reviewed publications

6.1 *"Targeting Melanoma with Dual PI3K/mTOR Inhibitors"*

Romina Marone, Dominik Erhart, **Ann C Mertz**, Thomas Bohnacker, Christian Schnell, Vladimir Cmiljanovic, Frédéric Stauffer, Carlos Garcia-Echeverria, Bernd Giese, Sauveur-Michel Maira, Matthias P. Wymann. "Targeting Melanoma with Dual PI3K/mTOR Inhibitors", *published in Molecular Cancer Research, 2009*

6.2 *"(E,Z)-3-(3',5'-dimethoxy-4'-hydroxy-benzylidene)-2-indolinone (Indolinone) blocks mast cell degranulation"*

Sabine Kiefer, **Ann C Mertz**, A. Koryakina, M. Hamburger, P. Küenzi. „(E,Z)-3-(3',5'-dimethoxy-4'-hydroxy-benzylidene)-2-indolinone (Indolinone) blocks mast cell degranulation", *published in European Journal of Pharmaceutical Sciences, 2010*

6.3 *"Separation and detection of all phosphoinositide isomers by ESI-MS"*

Sabine Kiefer, J. Rogger, Anna Melone, **Ann C Mertz**, A. Koryakina, P. Küenzi. "Separation and detection of all phosphoinositide isomers by ESI-MS", *published in Journal of Pharmaceutical and Biomedical Analysis, 2010*

Fulltext of each publication at end of thesis

7 Discussion

7.1 Vps34 in disease model systems

There are not many publications on hVps34 in a disease context yet, most researchers focus on its role in endosomal transport or autophagy. How class III PI3K is indirectly involved in various diseases, even if it has never been found to be the cause thereof, starts to get the attention of the field. A recent article on hVps34 in an Alzheimer's Disease (AD) model system links regulation of hVps34 kinase activity with cell-cycle control and prognosis of AD. During mitosis, Vps34 is phosphorylated at Thr159 of the C2 domain by Cdk1, negatively regulating its interaction with Beclin1 and hence inhibiting autophagy. This happens simultaneously to an increase in cyclin B levels during mitosis. Furuya et al. claim to have discovered the key mechanism by which autophagy is downregulated during mitosis, resulting from a decrease of PI(3)P production originally coming from inhibition of Vps34 kinase activity through Cdk1 phosphorylation. Cdk5/p25, which is known to act on certain substrates of Cdk1, can phosphorylate the same position in the class III PI3K isoform. The authors suggest that phosphorylation of Thr159 in Vps34 is a key regulatory mechanism by which class III PI3K activity in cell-cycle control, development and human diseases such as Alzheimer's Disease is controlled. (Furuya, Yu et al.)

In our mammalian cell study, we used a cancer model system, i.e. a selection of melanoma cell lines with genetically different backgrounds. Our main focus was on the importance of hVps34 in these cells: Could the cells survive without hVps34 on short or long term? Is hVps34 a putative target for drugs in melanoma therapy? Can we find a specific inhibitor for this isoform which is not affecting the other PI3K classes? Which function of hVps34 is essential, is its depletion balanced through production of PI(3)P by class II isoforms?

7.1.1 Vps34 in melanoma

hVps34, as an early regulator of autophagy, has been linked to a protective role in cellular and animal models of Alzheimer's Disease (AD) and other neuropathies. (Furuya, Yu et al.) (Cao, Backer et al. 2008; Tang, Zhao et al. 2008) According to our knowledge, no articles have so far been published on functions of the class III PI3K isoform in the melanoma subset described in our study. The aim of our study was to describe the effects of genetic downregulation or pharmacological inhibition of hVps34 in a melanoma model system. Overall we found similarities between the characteristics of our subset of melanoma cell lines and published data on neuronal cell lines upon reduction or loss of hVps34. (Johnson, Overmeyer et

al. 2006) To our surprise, tolerance to loss of hVps34 was very diverse between individual melanoma cell lines tested. Short term and slow reduction of the kinase by siRNA technique was mildly affecting proliferation in many melanoma cell lines. On the other hand, stable knockdown via lentiviral expression of shRNA targeting hVps34 led to cell death in several melanoma cell lines (e.g. A2058 and 1205lu repeatedly in our hands) and was only tolerated in A375 melanoma cell line in our studies. The same genetic modulations did not abrogate viability in other cell types such as the standard lab cell line HEK293 and other cancer cell lines, e.g. breast cancer cell line MCF-7. Up to now we cannot explain which characteristics allowed loss of hVps34 in A375 while other melanoma cell lines would not tolerate a longterm reduction.

Our results suggest that targeting class III PI3K isoform in certain melanoma types might be beneficial for patients by slowing down or even abolishing growth of the cancer cells while in other genetic contexts it would require additional inhibition of other effectors of the same pathway. Among the selection of melanoma we analyzed, only A375 with wildtype PTEN survived longterm knockdown of hVps34. We hypothesize that the PTEN status of the melanoma cell lines and hence its normal or upregulated $PI(3,4,5)P_3$ signalling levels led to tolerance or loss of viability in the cell lines tested. This hypothesis requires more investigations on a wider selection of cell lines similar to A375 but with varying PTEN stati.

7.2 Autophagy in melanoma

Tormo et al. described the therapeutic induction of autophagy in melanoma cells in a recent publication in Cancer Cell (Tormo, Checinska et al. 2009). They used mouse models to show that melanoma cells retain an innate immune system response to recognize cytosolic double-stranded RNA (dsRNA) and start stress response programs to block tumor growth. The dsRNA was identified to be an inducer of autophagy, requiring Atg5 for the cell death process. Knockdown of Beclin1 led to cellular senescence or cell death in many melanoma cell lines tested. As Atg5 knockdown was lethal, too, they used Atg5-/- MEFs which showed a similar reaction to dsRNA as observed earlier in their melanoma cell lines. The authors conclude from their results that their artificial dsRNA induced an early but persistent autophagy and a late apoptotic program, hence killing the melanoma cells (Tormo, Checinska et al. 2009).

Another publication describing apoptosis and autophagy induction in melanoma cell lines was written by Liu et al. They conclude that in A375 melanoma cell line, application of *polygonatum cyrtonema* lectin induces cell death by autophagy followed by apoptosis through mitochondria-mediated ROS-p38-p53 pathways. Beclin1 levels were increased after treatment with PC lectin and mature forms of LC-3 were observed. ROS (reactive oxygen species) were generated and p38 (MAPK) and p53 (tumor suppressor involved in cell cycle control) activated as well (Liu, Cheng et al. 2009).

In our studies we did not focus on autophagy in melanoma. It would be interesting to see though how increased or reduced autophagy levels influence the prognosis of melanoma patients. Genetic targeting of hVps34 turned out to be lethal for at least some melanoma cell types we had tested, but not for non-cancer cell line HEK293. As for the cell lines (melanoma A375 and standard HEK293) we could use for our long term knockdown study, we can predict milder effects on their proliferation and very little change in cell size, as no drastic changes were observed. Up to now we do not know enough about the possible side effects of loss of class III PI3K in *in vivo* systems i.e. whole organisms. So far there is no mouse model for hVps34 that we are aware of, which could give clues about systemic effects of this enzyme's inhibition. From our mammalian cell line studies, we can suggest that at least in some melanoma types, chemical targeting of hVps34 as a regulator of autophagy would probably be beneficial for the patients.

7.3 Phospholipids in melanoma

Wu et al. published a review on the role of PTEN in melanoma. Loss of the tumor suppressor PTEN results in both aberrant cell growth and cell spreading/migration. So far, its role in melanoma has always been seen as a late event. (Wu, Goel et al. 2003) A more recent article by Lahtz et al. described the methylation status of PTEN as determining prognosis factor. Patients with methylated PTEN showed a decreased survival rate. (Lahtz, Stranzenbach et al. 2010)

In a so far unpublished study (collaboration with Anna Melone, University of Basel, Switzerland; data not shown) we investigated the role of phospholipids, i.e. especially the PI(3)P production, in a melanoma cell line and HEK293. Upon stable knockdown of hVps34, production of PI(3)P did not seem to be abrogated but somehow thought to be balanced by class II PI3K isoforms. PI(3)P levels were therefore assumed to be crucial for cell survival. They might locate mTOR and its complexes properly within the cell, be it under normal or nutrient deprived conditions. Or they serve as absolutely essential substrates for further phospho-modifications by class I PI3K isoforms and reduction of PI(3)P would hence lead to fatal effects in this signalling context. Today we know that an overload of $PI(3,4,5)P_3$ (upon PTEN loss as found in many tumors) is causing increased signalling and generation of tumor cell characteristics. How a cell would react to the absolute loss of PI(3)P is not known. As these lipids are involved in endosomal sorting and autophagosome formation, we guess that transport from the endosomes would be severely affected which might be lethal for the cell. If not under nutrient rich conditions, a change in nutrient availability might certainly do so. We could assume that the melanoma cell lines we had stably transfected with knockdown constructs against hVps34, had diverse PI(3)P levels from the beginning and hence relied more or less strongly on these lipids. Reduction of

the lipids upon knockdown might therefore have been too critical for the cell lines that usually produce high levels of PI(3)P, as they had high hVps34 levels. A375 on the other hand, which exhibit low levels of hVps34 endogenously, might have had an advantage in turning on class II PI3K to compensate for the reduction. We would need to measure and compare between cell lines the lipid levels in all the melanoma cell lines in our selection and in addition test HEK293 and melanocytes as well.

Detailed mechanisms underlying the importance of balanced phospholipid levels (here, PI(3)P) are content of current investigations.

8 Materials and Methods

8.1 *Protocols*

8.1.1 Yeast Cell Culture

Yeast strains were grown in standard yeast extract-peptone-dextrose (YPD) medium (1% yeast extract, 2% bacto peptone, 2% glucose, yeast extract from Gibco BRL or DIFCO laboratories, bacto peptone from Becton Dickinson), or in SD (synthetic growth medium with 2% glucose, lacking essential amino acids, yeast nitrogen base from Becton Dickinson) minimal medium with ammonium sulfate or without, supplemented with essential amino acids as required for maintenance of plasmids.

Transformation of yeast was performed according to Gietz et al., 1995. Yeast cells were harvested at an OD_{600} 0.1-0.8 and washed once in 1ml sterile water. About 10^9 yeast cells were incubated in 100 µl Li Acetate (pH 7.5) for 30 minutes at 25°C. 10 µl single stranded salmon sperm carrier DNA (20mg/ml) and 0.1-10µg of plasmid DNA were added and cells were incubated for 30 minutes at 25°C. Sterile 40% PEG 4000 solution was added to a final concentration of 35% and cells were incubated for 30 minutes at 25°C. Heat shock was performed at 42°C in a waterbath for 15 minutes and cells were incubated on ice for two minutes afterwards. 500µl TE (10mM Tris-HCl, 1mM EDTA, pH 7.5) were added and cells were collected by centrifugation. The pellet was resuspended in TE and plated onto appropriate medium.

8.1.2 Mammalian Cell Culture

Cell lines were grown at 37°C in 5% CO_2 incubators. Cell media for A375, 1205lu and WM115: RPMI complete. Cell media for HEK293, HEK293T, A2058, SKMel23, SKMel28 and PG-02 and SchM99: DMEM complete. Supplementation for complete media: 10% heat-inactivated FCS, 1% glutamine and 1% penicillin-streptomycin (all Sigma-Aldrich).

8.1.3 Molecular Biology

RNA isolation

Materials:

- Various cells
- Trizol (Invitrogen, 15596-026) or Tri-Reagent (Sigma, T9424)
- Chloroform (Fluka, 25690)
- Isopropanol
- 75% (v/v) Ethanol
- RNAse free water
- Filter tips

Procedure:

- Clean bench and pipettes carefully, wear gloves and lab coat to avoid contamination with RNAse.
- RNA isolation was performed according to the manufacturer's instruction, details see: http://tools.invitrogen.com/content/sfs/manuals/15596018%20pps%20Trizol%20Reagent%20061207.pdf
- Measure RNA concentration in a spectrophotometer.
- Use 2 μg total RNA for cDNA synthesis

cDNA synthesis:

Materials:

- RNA
- Oligo-$(dT)_{15}$ primer (0.5 μg/μl; Microsynth)
- DTT (supplied with M-MLV RTase)
- 5x RT buffer (supplied with M-MLV RTase)
- 10 mM dNTPs (Invitrogen, 10297-018)
- RNAsin (Promega, N2111)
- M-MLV RTase (Invitrogen, 28025-013)

Procedure (one reaction):

- For primer annealing mix 2 μg RNA and 8 μl oligo$(dT)_{15}$
- Fill up to 23μl final volume
- Incubate for 10 min. at 70°C
- In the meanwhile mix 4 μl 0.1M DTT, 8 μl 5xRT buffer, 2 μl 10 mM dNTPs, 1 μl RNAsin and 2 μl M-MLV RTase.
- Place annealing reaction on ice (2 min.)
- Add 4 μl 0.1M DTT, 8 μl 5xRT buffer, 2 μl 10 mM dNTPs, 1 μl RNAsin and 2 μl M- MLV RTase to the annealing reaction.
- Incubate at 37°C, 90 min.
- Heat to 95°C for 10 min.
- store at -20°C until used for PCR.

Plasmid DNA amplification and isolation:

Materials:

- LB-media (5 g NaCl (LB Miller = 10 g NaCl), 5 g yeast extract; 10 g bacto-tryptone, 5 ml of NaOH 1M, add 1 liter with H_2O (autoclave)
- LB-agar (LB media + 12.5 g Agar [DIFCO, 281230]), autoclave.
- For antibiotic selection add 100 μg/ml Ampicilline or 25μg/ml Kanamycin to the LB media or LB-agar
- Chemically competent bacteria (usually *E.coli* XL-1 Blue strain)
- Template plasmid DNA or ligation reaction
- TE- buffer (10 mM Tris-HCl, pH 7,6; 1mM EDTA, pH 8.0)

1. Preparation of chemically competent cells ($CaCl_2$ method)

Procedure:

- Take bacteria from -80°C stock by scratching the frozen tube content with a sterile tip and plate on LB agar solid media overnight at 37°C.
- Pick single colony and inoculate a 100 ml LB-Miller, grow overnight (shaking in 37°C, 300 rpm)
- Inoculate 1 liter LB-Miller with the overnight culture, inoculation 1:100.
- Grow in shaker (37°C, ca. 300 rpm) until OD_{600}= 0.6. Then put the flask on ice. Wait 20 min until culture is really cold. Pre-cool $CaCl_2$ solutions on ice!
- **From now keep at 4°C (coldroom)**
- Transfer bacteria to the centrifuge bottles and spin in the pre-cooled centrifuge about 20 min. 3000 rpm at 4°C.
- Discard the supernatant, resuspend the pellet in 500 ml ice-cold $CaCl_2$ ($^1/_2$ of initial volume). Mix strongly initially, then gently.
- Leave the bacteria for few hours at 4°C, mix gently occasionally. Cool down solution of $CaCl_2$/10-15% glycerol on ice.
- Spin 15 min at 4°C, 3000 rpm, discard the supernatant and resuspend very gently in 100 ml of pre-cooled $CaCl_2$/10-15% glycerol.
- Immediately aliquot the bacteria in 500 μl portions to Eppendorf tubes and freeze in liquid N_2 immediately.
- Store tubes at -80°C.

2. Transformation of competent bacteria

Procedure

- Thaw tube with bacterial suspension on ice.
- Aliquot bacterial suspension to 100 µl portions in pre-cooled tubes. Add DNA (plasmid [100 ng] or ligation [up to15 µl]).
- Mix and incubate for 30 min. on ice
- Heat shock for 45- 90s at 42°C. Place tube on ice.
- Add 900 μl of SOC media and shake for (1 hour, 37°C)
- Collect cells by centrifugation (1 min. 3000g)
- Remove 800 μl supernatant, resuspend cells in the remaining 200 μl.
- Plate suspension on LB agar plate with the respective antibiotic (for plasmid selection). When the fluid is absorbed, incubate plate up side down overnight at 37°C.

3. Plasmid amplification and purification:

Material:

- Transformed *E. coli*
- LB media, LB agar, supplemented with antibiotics
- Endofree plasmid maxi kit (Qiagen, 12362) or Genelute high performance endotoxin-free (Sigma, NA 0410) or Genelute Plasmid Miniprep kit (Sigma, PLN-350)
- TE-buffer

- Isopropanol
- 70% Ethanol

Procedure:

- Pick colonies form the transformed *E.coli* plates, streak backup on LB agar and inoculate LB media, both supplemented with the selective antibiotic.
- Growth conditions and plasmid isolation were performed according to the manufacturer's instructions.
- Plasmid DNA was eluted with 1xTE buffer
- The concentration and purity of the plasmid was measured in a spectrophotometer
- (Optional: ethanol precipitation, according to the manufacturer's instructions, to increase plasmid concentration and purity)
- Adjust plasmid DNA to 0.5 or 1.0 μg/μl in 1x TE

Agarose gel-electrophoresis

Material:

- Agarose, standard (Eurobio, 018054)
- 1x TAE buffer (40 mM Tris-acetate pH 8.0, 1mM EDTA)
- ethidium bromide
- Loading buffer (0.4% bromphenol, 0.4% xylene cyanol FF, 50% glycerol)
- Lambda marker, l HindIII/EcoRI (Labforce, 1695/1),
- pBR322 DNA/AluI Marker (Fermentas, SM0121)
- GenElute Gel Extraction Kit (Sigma, NA1111)

Procedure:

- Prepare 1-2% agarose gels.
- Melt agarose in TAE (40 mM Tris-acetate pH 8.0, 1mM EDTA)
- Add 0.3 μg/ml ethidium bromide.
- Pour liquid agarose on glass plates
- Place the combs and wait until agarose has solidified.
- Mix DNA samples (PCR reactions, restriction digests) with 0.1 volume loading buffer and load on the gel together with a DNA marker
- Separate DNA by electrophoresis (constant current 70 V)
- Visualize DNA under UV-light.
- For preparative electrophoresis excise DNA fragments of interest and purify with GenElute Gel Extraction Kit according to the instructions
- Run another gel for purified fragments to approximate the DNA amount, if used for ligation

Restriction endonuclease digests

Materials:

- PCR product or plasmid DNA 1-5μl
- Reaction buffers (2μl, NEB, type depends on restriction enzymes)

- NEB restriction enzymes (0.5µl)
- (Optional add 1:100 BSA, supplied with NEB enzymes)
- ddH_2O, up to 20µl final volume.

Procedure:

- Mix all required components (see material)
- Incubate 1h at 37°C, if required incubate additionally at 65°C afterwards
- Analyse and isolate digest products by agarose gel electrophoresis.

Ligation:

Material:

- Purified restriction endonuclease digest products (approx. equimolar concentrations, with compatible ends, 0.5- 2µl)
- 10x T4 Ligase buffer (1.5µl, NEB)
- T4 DNA Ligase (0.5µl, NEB, 102378)
- ddH_2O, fill up to 15µl final volume

Procedure:

- Thaw T4 Ligase buffer on ice.
- Mix all required components (see material)
- Incubate for 5 min. on ice, then for 16 h at 16°C or for 1h at room temperature
- Transform competent *E. coli* with ligation products.

Polymerase Chain Reaction (PCR)

Material:

- Template DNA (plasmid DNA [10-100 ng/ml, 1 µl], cDNA [1µl])
- 10x PCR reaction buffer (5 µl)
- 50 mM $MgCl_2$ stock solution (1.5 µl)
- Taq-DNA Polymerase (NEB, 102373) or Pwo-DNA Polymerase (Roche, 1164495500; 0.5 µl)
- 10 mM dNTPs (form dNTP set PCR grade, Invitrogen, 10297-018 [2.5 mM of dATP, dCTP, dTTP, dGTP; 1µl])
- Forward primer (10µM, 1µl)
- Reverse primer (10µM, 1µl)
- ddH_2O (fill up to final volume of 50 µl)
- 0.5 ml PCR tubes (Molecular BioProducts, 3430)
- T3 Thermocycler (Biometra, Göppingen)

Procedure:

- Thaw all frozen components on ice, except for DNA-Polymerase
- Combine all components on ice, except for the DNA Polymerase in 0.5 ml PCR tubes, volumes are given in material for one PCR reaction)
- Example of a PCR protocol:
  - Heated lid (105°C)
  - 95°C for 5 min, add DNA-Polymerase after 4 min (hot start)

a) Denaturing: 95°C, 45 s

b) Annealing: 62-65°C, 40 s

c) Elongation: 72°C, time dependent on size of the PCR product

d) Repeat step a)-c) 30 times

e) 72°C, 10 min.

f) 4°C

- Prepare PCR samples for agarose gel electrophoresis.

8.1.4 Protein Methods

SDS-PAGE Electrophoresis

Solutions

- Ultra pure Accu Gel 29:1 (40%), National Diagnostic, EC852
- Tris-HCl, pH8.8 (1.875 M)
- Tris-HCl, pH 6.8 (1.25M)
- 10% SDS (Sodium Dodecyl Sulfate solution):
- 10% Ammonium Persulfate solution
- 10x Electrode Buffer (Tris-Glycine):
  Glycine (144.2 g), Tris (30.3 g), SDS (10 g). Dissolve in 800 ml H_2O.
  1x: Dilute 100 ml of 10xElectrode Buffer with 900 ml distilled water.
- Cell lysis buffer (20 mM Tris/HCl, pH 8.0, 138 mM NaCl, 2.7 mM KCl, 5% glycerol), store at -20°C, **prior usage finish lysis buffer by addition of (final conc.):**
- 1% NP 40; Protease and phosphatase inhibitors (20 μM Leupeptin,18 μM Pepstatin, 20mmol/L NaF, 1 mM PMSF, 20 mM Sodiumfluoride, 1 mM Sodium-ortho-vanadate)
- 5x Loading Buffer: 1.25 M Tris-HCl pH 6.8 (2.5 ml), SDS (1g), 2-Mercaptoethanol (2.5 ml) Glycerol 87% (5.8 ml), Bromophenol blue (5 mg), H_2O distilled (35 ml)
- Staining solution: Coomassie Brillant Blue G250 (0,1%), 50%Methanol, 7%Acetic acid, 43% ddH_2O -
- Destaining solution: Methanol (20%), Acetic acid (5%), Distilled water (75%)
- PBS
- Cell lifter (Corning, F21222F)

Sample preparation:

For adherent cells: place cell culture dishes on ice

- Aspirate medium, wash 2x with cold PBS
- Add 100-200 μl cell lysis buffer and incubate on ice
- Scrape cells from the dishes and transfer cell lysates to eppendorf tubes
- Incubate 15 min. on ice
- Spin (16000g, 10 min., 4°C)
- Transfer supernatant to new eppendorf tubes, measure protein concentration with BioRad Protein Assay (BioRad, 500-0006), store at -20°C or -80°C, or proceed by addition 1/5th of 5x loading buffer. Heat to 95°C for 7 min.
- Store at -20°C until usage for SDS-PAGE

Gel preparation:

- Clean alumina and glass plates (Hoefer, SE202N-10 and SE202P-10), the spacers and the combs
- Assemble 10 gel units in the multicasting cassette with a plastic plate in between the single units (do not place the combs at this time)
- Prepare the resolving gel mixture (see table next page) and fill the multicasting cassette
- Overlay each gel unit with 1ml isopropanol. Polymerization takes about 30 min.
- Discard the isopropanol, wash gel surface with water and remove residual water with whatman paper
- Prepare the stacking gel solution and overlay the resolving gel with the stacking gel solution. Insert combs.
- After polymerization disassemble the cassette and store each gel in a plastic bag with 1 ml 1xTris, pH 8.8 at 4°C until usage.

For ten 0.75 mm gels in multicasting cassette

	Resolving gel (75 ml)					Stacking (30 ml)
	7.5 %	10 %	12%	15 %	20 %	5 %
Acrylamide Stock - ml	14.1	18.8	22.5	28.1	37.5	4.8
Distilled water - ml	44.9	40.2	36.5	30.9	21.5	21.6
TRIS-HCl pH 8.8 - ml	15	15	15	15	15	---
TRIS-HCl pH 6.8 - ml	---	---	---	---	---	3
Degas solution, then add						
10%-SDS -µl	750	750	750	750	750	300
TEMED -µl	37.5	37.5	37.5	37.5	37.5	30
10% Amm.Persulfate - µl	250	250	250	250	250	102
Mix carefully and cast gel						

Parameter settings for one 0.75 mm gel

- Constant current: 20-25 mA
- Set voltage: 250 V
- Time: approx. 60 min.

Electrophoretic Transfer / Semi-dry blotting

Material and solution:

- Transfer buffer (25 mM Tris, 192 mM Glycine, 20% methanol, pH 8.3)
- Immobilon FL (Millipore, IPFL00010), Immobilon P PVDF (Millipore, IPVH00010) cutted to gel size (9x6.5 cm)
- For one gel 6x whatman paper (9x6.5 cm)
- Semidry blotting device
- Methanol

Procedure:

- Label and activate membrane in methanol for 1 min.
- Equilibrate in Transfer buffer.
- Mount SDS-PAGE/membrane sandwich.
- Blot proteins to the membrane with constant current of approx. 10 mA per cm^2 for 75 min (0.75mm gel) or 120 min. (1.5 mm gel).
- Disassemble sandwich, incubate in blocking buffer for 30 min.
- Add 1^{st} antidbody (see antibody table below for their dilution, blocking buffer, time).
- Wash 3x 5 min. with TBS, 0.1%Tween
- Add 2^{nd} antibody (HRP) for 1 hour
- Wash 3x 5 min. with TBS, 0.1%Tween
- Detection: either enhanced chemoluminiscence (ECL)

8.1.5 Microscopy

Preparation of mounting solution:

Material:

- 50 mM Tris-HCl, pH7.5-8.0
- Mowiol (Plüss-Staufer, Oftringen, Hoechst 4-88/cmB339161)
- Glycerol (Fluka, 49770)
- n-Propylgallat (Sigma, P3130)

Procedure:

- Stir 5 g Mowiol in 20 ml Tris-HCl buffer (0.05M, pH7.5-8.0) on a magnet stirrer (30-40°C, 16h).
- Add 10 ml 100% Glycerol and stir 16 h.
- Spin 10 min. at 1500 rpm at room temperature.
- Add 10 mg/ ml n-propylgallat as anti-fading agent.
- Aliquot the Mowiol solution
- Spin aliquots to remove air bubbles, store at -20°C.
- Thaw the aliquot at least 30 min. before usage at 37°C

Preparation of 10% *para*-formaldehyde in PBS (10% PFA/PBS):

Material:

- Weigh 100 g PFA to 400 ml water.
- Boil in a waterbath under the extractor hood
- Shake from time to time.
- Add cautiously drops of 5N NaOH to completely dissolve the PFA (PFA is not soluble at that pH without NaOH).
- After complete solution of the PFA add 100 ml 10x PBS.
- Fill up to 1 liter with water.
- Solution can be further diluted to 4% PFA/PBS. Store at 4°C

Preparation of adherent cells:

Material

- PBS
- 4% *para*-formaldehyde in PBS pH = 8.0
- Mounting solution, Mowiol, see above
- Hoechst 33342 (Molecular Probes, H-1399), cell permeable
- 12- well, or 24- well plate
- 18 mm or 12 mm diameter coverslips
- Microscopy slides
- ddH_2O

Procedure:

- Grow cells on sterile coverslips in a 12 well or 24-well plate
- Transfect according to experiment
- Perform your experiment of interest
- Wash cells twice with PBS, aspirate PBS, add ice cold 4% PFA in PBS.
- Incubate on ice for 30 min.
- Wash with PBS.
- Optional nuclear staining: add PBS with 1:1000 Hoechst 33342 (stock solution 1 mM in ddH_2O), incubate (15 min., 4°C, in the dark).

Preparation of the microscopy slides:

- Put one drop of mounting solution onto a microscopy slide
- Take the coverslip with fine forceps and wash with H_2O, quickly.
- Soak residual liquid from the edge of the coverslip with a fine paper towel.
- Place coverslip upside down onto the drop of mounting solution on the microscopy slide.
- Dry for min. 30 min. at room temperature in the dark.
- Then store at 4°C in the dark.

8.1.6 Generating Stable Knockdown Cell lines

Lentivirus production and infection of target cells

8.1.6.1.1.1 Material

- Cells: Target cells and carrier cells HEK293T
- Helper Plasmids: HDM-pVSV/G; HDM-Hpgm2; HDM-Tat1b and pRC-CMV-RaII
- Plasmids: GFP control plasmid; shRNA constructs
- OPTIMEM
- Fugene transfection reagent
- Polybrene 3mg/mL stock
- 0.45um filters and 5-10mL syringes with luer lock
- Cell media DMEMc
- Selective antibiotic, e.g. puromycin
- PBS
- Trypsin
- New 6 well dishes
- Parafilm
- Box for transport
- BL2 working bench and incubator
- Lab material for BL2
- Lab gloves for BL2
- Lab coat for BL2

Procedure

- Seed carrier cells HEK293T at 600'000cells/well in 2mL in 6well dish
- Transfect carrier cells HEK293T the day after (80% confluent)
- mix helper plasmids and construct plasmid or control GFP plasmid
    - helper plasmids at 0.08- 0.16ug per well
    - construct plasmid at 1.6ug per well
- incubate at 70°C for 10 min.
- add OPTIMEM to give 100uL/well
- add 8uL Fugene per well
- incubate at RT for 15min.
- add mix to HEK293T cells
- transfer cells to BL2 incubator

- Seed target cells at about 100’000 cells/well (might vary with cell line) in 2mL in 6well dish
- Collect media from carrier cells into syringe with filter to remove cell debris
- Add polybrene to virus-loaded media at 3uL/mL
- Infect target cells (30-50% confluent) by adding filtered media containing virus particles
- Perform collection and infection twice a day for 2-3 days
- Check for infection rate by detection of GFP signal in control cells
- Discard carrier cells
- Wash target cells with PBS and split them
- Add selective antibiotic e.g. puromycin at according concentration tested earlier in this cell line
- Split several times to remove virus particles, perform for about ten days
- If desired a p21 ELISA can be performed to check lentivirus titer before transferring cells to BL1 cell culture room again
- Check for knockdown of target gene by Western blot (see Protein Methods) or Northern blot (see RNA isolation etc.)
- Freeze stable knockdown cell lines in several tubes in liquid nitrogen as backup! Do not use cells for experiments anymore after 10-15 passages as secondary mutations due to selective pressure might arise.

BL2: Transport cell culture plates always sealed with parafilm in closed box labelled BL2! Desinfect work place with bleach! Wear two pairs of gloves at all times! Discard waste according to BL2 safety rules!

8.1.7 Proliferation Assays

Material

- Cell line
- Medium
- Trypsin
- PBS
- Casy Counter and Analyzer (cell counter) (Innovatis AG)
- Casyton cell counter solution

Procedure

- Seed cells at 50’000-100’000 cells/2mL in 3cm petri dishes without selective antibiotics
- Trypsinize cells with 100uL and resuspend in 900uL medium to obtain 1mL cell suspension
- Measure 50uL cell suspension in 10mL casyton cell counter solution with cell counter using program for certain cell line specifics

- Do measurements in triplicates, repeat experiment several times
- Check confluency and health of cell cultures with binocular microscope, take pictures daily
- Measure cell number daily over 3-7 days

8.1.8 Cell Size Assays

- perform similar to proliferation assays
- measure cell size, eventually normalize to nuclear volume
- normalization to nuclear volume:
    - To a second batch, resuspend cells in casyton solution containing 0.5% triton X-100 to obtain nuclear volume for normalization if necessary
- measure cell size/volume daily over 3 days

8.2 *Consumables*

Restriction enzymes were purchased from New England Biolabs. Chemicals were from Sigma-Aldrich if not stated differently.

Product	Supplier	Cat. No.
2- Mercaptoethanol	Sigma	M 7522
AccuGel 40%	National Diagnostics	EC-852
Agar Technical	DIFCO/BD	281230
Agarose, standard	Eurobio	018054
Ammonium persulfate (APS)	Bio-RAD	161-0700
Ampicillin trihydrate	Sigma	10045
Chloroform	Fluka	25690
Dimethyl sulfoxide	Sigma	154938
dNTP set PCR grade	Invitrogen	10297-018
Dulbecco's MEM medium	Bioconcept	1-26F01
ECL Western Blotting Detection	Amersham	RPN2106
Endofree plasmid maxi kit	Qiagen	12362
GenElute Gel Extraction Kit	Sigma	NA1111
Genelute high performance endotoxin-free	Sigma	NA 0410
GenElute Plasmid Miniprep	Sigma	PLN-350
Glucose D(+) Monohydrate	Sigma	49159
HEPES	Sigma	H3375
HOECHST 33342	Juro supply	H-1399
Hyperfilm ECL	Amersham	RPN3103
Immobilon Western substrate reagents	Millipore	WBKLS0500
Immobilon-P PVDF membrane	Millipore	IPVH00010
Jet PEI transfection reagent	Polyplus Transfection	101-40
Lambda marker, l HindIII/EcoRI	Labforce	1695/1
Leupeptin	Alexis	260-009-M025
L-Glutamine (200mM)	Sigma	G7513
Luria Broth Base	life technologies	127-95-027
Magnesium chloride	Fluka	63068
M-MLV RTase	Invitrogen	28025-013
N,N,N,N'-Tetramethyl-ethylenediamine, TEMED	Bio-Rad	161-0800
Oligo$(dT)_{15}$ primer	Microsynth	non commercial
Penicillin-Streptomycin 100x	Sigma	P0781
Pepstatin A	Fluka	77170
Potassium chloride	Fluka	60128
Pwo DNA Polymerase	Roche	11644955001
RNasin	Promega	N2111
RPMI 1640 medium	Gibco/Invitrogen	31870-025
Sodium chloride	Fluka	71376
Sodium dodecyl sulfate	Fluka	71729
Sodium orthovanadate	Sigma	S6508
Super RX film	Fuji	F57164052
T4 DNA ligase	NEB	102378
Taq DNA Polymerase	NEB	102373

8.3 *Antibodies*

Epitop	Species	Origin/Supplier	8.3.1.1.1.1 Cat. no.
HVps34	Rabbit, polyclonal	Zymed/Invitrogen labs	38-2100
Beclin-1	Rabbit, polyclonal	Cell Signalling	3738
PKB/Akt	mouse	Non commercial	Gift from E.Hirsch, Italy
Alpha-tubulin	Mouse, monoclonal	Sigma	T9026

8.4 *Plasmids*

ShRNA: Mission shRNA from Sigma-Aldrich

- mock: TRCN0000037798 or SHC001, pLKO.1-puro without targeting sequence
- pLKa: TRCN0000037794, pLKO.1-puro with targetting sequence CGAGAGATCAGTTAAATACTC
- pLKb: TRCN0000037797 (in A375), pLKO.1-puro with targeting sequence TGATGAATCATCTCCAATCTC or TRCN0000037795 (in HEK293), pLKO.1-puro with targeting sequence AGTGAGAATGGGCCAAATCTC

Plasmids:

- pGEM-eGFP-FYVEhrs, gift from Harald Stenmark
- HDM-pCMV-VSV-G envelope vector: encodes envelope protein
- HDM-Hpgm2: encodes codon optimized HIV gag-pol
- HDM-Tat1b: encodes transactivator of transcription
- pRC-CMV-RaII

9 Abbreviations

3-MA	3-methyladenine
AA	amino acids
AD	Alzheimer's Disease
Akt/PKB	protein kinase B
Arg	arginine
BCR homology domain	breakpoint cluster region homology domain
Ca	calcium
CaM	calmodulin
COP 1	coat protein complex 1
CORVET	class C core vacuole/endosome tethering
CPY	carboxypeptidase Y
C-term	carboxy-terminus
Cvt	cytoplasm-to-vacuole-transport
DsRNA	double-stranded RNA
EEA	essential amino acids
EGF	epidermal growth factor
EGTA	calcium chelator
ER	endoplasmatic reticulum
ESCRT	endosomal sorting complex required for transport
FYVE domain	PI(3)P binding domain
GAP	GTPase activating protein
GDP	guanosine diphosphate
GEF	guanine nucleotide exchange factor
GFP	green fluorescent protein
Glu	glutamine
GPCR	G-protein coupled receptor
GTP	guanosine triphosphate
GTPase	molecular switch either bound by GDP or GTP
HEK293	human embryonic kidney cell line
His	histidine
HOPS	homotypic vacuole fusion and protein sorting complex
IFN-gamma	interferon gamma
IRG	immunity related GTPase
KD	kinase dead
kDa	kilo Dalden
Leu	leucine
LiAc	lithium acetate
LPA	lysophosphatidic acid
Lys	lysine
MDC	mono-dansyl cadaverine

MEF	mouse embryonic fibroblasts
mL	milliliters
mM	millimolar
mut	mutated
MVB	multivesicular body
nM	nanomolar
N-term	amino terminus
PDGF	platelet-derived growth factor
PH domain	pleckstrin homology domain
PI	phosphoinositides
PI(3,4,5)P3	" " with three phosphate groups added
PI3K	phosphoinositide-3 kinases
PI(3)P	PI with one phosphate group added
PI-4,5P_2	PI with two phosphate groups added
PI-4P	PI with one phosphate group added
PKC	protein kinase C
PM	plasma membrane
PTEN	phosphatase and tensin homolog
PX domain	phox domain
RBD	Ras binding domain
RGP	radial growth phase
Rheb	Ras homolog enriched in brain
ROS	reactive oxygen species
RT	room temperature
S6K	RPS-6 kinase
SD	synthetic yeast medium, selective
Ser	serine
SH2 domain	src homology domain 2
SH3 domain	src homology domain 3
ShRNA	short hairpin RNA
SiRNA	small interfering RNA
Tg	Thapsigargine
TGN	trans-Golgi network
Thr	threonine
TNF-alpha	tumor-necrosis factor alpha
Tor	target of rapamycin
TORC1	" " complex 1
TORC2	" " complex 2
TSC1/2	tuberous sclerosis complex 1/2
uL	microliters
uM	micromolars
UPR	unfolded protein response
VEGF	vascular endothelial growth factor

VGP	vertical growth phase
Vps	vacuolar protein sorting
WD repeats	beta-transducin repeats, usually WD 40
Wm	wortmannin
WT	wild type
YPD	yeast full medium

10 Acknowledgments

First I would like to thank…

… Matthias for giving me the chance to perform my PhD studies in his lab. When I had to abruptly stop the bench work, you still gave me the opportunity to write up my thesis at home and have the defense a bit later than originally planned. Merci for your understanding!

Many thanks go to…

… the present and former members of the institute who helped me along my way. Lab work was tough and frustrating at times, but your scientific advice and collegiality always brought me back my motivation and smiles!

… my parents who always believe in me. Moral support is most important for graduate students!

My deepest gratitude…

… I would like to express towards my husband, Akos. Your love and support is priceless!

Last but not least…

… I would like to thank my little daughter, Eva. Your strength and will to live amazed me from the start, you are the biggest source of motivation. I can no longer imagine my world without your smiles!

“Scio me nihil scire.”

Ich weiss, dass ich nichts weiss.

(Socrate, 469-399 BC)

Acknowledgments

11 Curriculum Vitae

Ann Christine Mertz Biro

Date of Birth: 07.10.1982
Place of Birth: Basel, Switzerland
Marital Status: married, 1 child, born 23.07.2010
Nationality: Swiss

Address:
Waldenburgerstrasse 16
CH-4052 Basel
Tel. +41 61 312 99 81 (Private)
E-Mail: ann.mertz@unibas.ch

Education

06/2006 - today	PhD studies in the laboratory of Prof. Matthias P. Wymann at Center for Biomedicine, Department of Biomedicine, University of Basel, Switzerland *"Class III PI3K in Melanoma"*
09/2004 – 11/2005	University of Basel (Biozentrum) Masters degree of Science (MSc) in Molecular Biology, Major in Biochemistry (Lab of Prof. Michael N. Hall) Degree: *cum laude* *"Pib2p, a novel vacuolar membrane and endosome localized FYVE protein, mediates exocytosis of the general amino acid permease in yeast, Gap1p"* under supervision of Dr. Stephen B. Helliwell, Biochemistry Department, Biozentrum
10/2001 – 09/2004	University of Basel (Biozentrum) Bachelor degree of Science (BSc) in Molecular Biology Disciplines: Biochemistry, Biophysics and Structural Biology, Microbiology, Immunology, Cell Biology, Neurobiology and Medical Biology
12/2000-12/2005	Student job at the English Bookstore "Bider and Tanner", Basel
08/1996 – 06/2000	Gymnasium BZB to obtain Latin-Matura (Eidg. Matura)

Scholarships

08/1996 – 06/2000	Scholarship for highly gifted children of the Kanton Baselland

Research Experience

06/2006 to present	Research Associate in the laboratory of Prof. Matthias P. Wymann at Center for Biomedicine, Department of Biomedicine, University of Basel, Switzerland
2008 to present	Assist. Clinical Study Reports Evaluation (Pharmacology and Toxicology) SDPS Pharma Solutions, Victoria, Canada
01/2006 - 05/2006	Scientific Associate, Internship, Molecular Biology and Microbiology techniques, Novartis Institutes of Biomedical Research (NIBR), Basel
07/2001- 10/2001	Validation and introduction of new database (Reference Manager V.10) at Novartis Ophthalmics, Basel

Teaching Experience

2006 to present	Tutor in "Basic Biology" for students at the University of Basel Assistant in "Enzyme kinetics course" for Medical students at University of Basel
1/2009 – 6/2009	Supervisor of Master student in Pharmacology at the University of Basel
2005	Tutor in „Applied Ethics" course for Biology students at the University of Basel

Methodological Training

2/2007	Practical and Theoretical Laboratory animal course (LTK1), Roche, Switzerland
2002	Practical course in Medical Biology, University of Basel

Methodological Skills

Yeast and bacteria:

- microscopy (fluorescence, light, indirect immunofluorescence)
- yeast genetics (incl. practical work such as mating and dissecting of yeast)
- Tandem-Affinity-Purification
- GST-fusion-protein purification
- liquid LacZ assays
- Yeast-Two-Hybrid screening
- synthetic lethality screening (in yeast)
- standard molecular biology techniques (PCR (polymerase chain reaction), Westernblotting, Co-immunoprecipitations, Cloning etc.)
- radioactively (C^{14}) labelled amino acids uptakes in yeast

Mammalian cell lines and mice:

- mammalian cell transfections
- siRNA and shRNA (generation of stable cell lines) application in various cell lines
- lab work at BL2 level (lentiviral shRNA)
- in vitro lipid kinase assays (P^{32})
- various in vitro recombinant kinase assay (KinaseGlo, Adapta etc.)
- inhibitor screening of natural compounds in mammalian and yeast cell systems, assay design
- TR-FRET (Time-resolved Fluorescence-Fluorescence Resonance Energy Transfer)
- genotyping of mice strains (by PCR)

IT Skills

MS Windows, MS Office (Word, Excel, Power Point), basic MacOS, Reference Manager V.10 or EndNotes, Adobe Photoshop/Illustrator, PubMed

Language Skills

German	mother tongue
English	Proficient user, understanding, reading, oral and written production C2 Level within the European Framework of Reference 2006: TOEFL score within top 4 % (653 of 677 points) Travelling through Canada, USA, New Zealand

	1996: English Course in Cambridge, UK 1985-1986: Preschool in New Jersey, USA
French	Independent user, understanding and reading at B2 Level within the European Framework of Reference, oral and written production B1 Level
Latin	Latin-Matura

Memberships

Schweizerische Gesellschaft für Zellbiologie, Molekularbiologie und Genetik (ZMG, Swiss Society for Cell Biology, Molecular Biology and Genetics, member of USGEB)

References

Supervisor during PhD studies:
Matthias P. Wymann PhD
Institute of Biochemistry and Genetics
Department of Biomedicine
University of Basel
Mattenstrasse 28
CH-4058 Basel
Switzerland
phone +41 61 695 30 46
matthias.wymann@unibas.ch

Supervisor during Masters studies:
Stephen B. Helliwell PhD
Novartis Institutes for BioMedical Research
CH-4057 Basel
Switzerland
phone +41 61 696 31 67
fax +41 61 696 31 70
stephen.helliwell@novartis.com

Supervisor during Internship at Novartis:
Dominic Hoepfner PhD
Novartis Institutes for BioMedical Research
CH-4057 Basel
Switzerland
phone +41 61 696 31 65
fax +41 61 696 31 70
dominic.hoepfner@novartis.com

Supervisor at SDPS Pharma Solutions
Beat P. Mertz PhD
89 Howe St
V8V 4K2 Victoria BC
Canada
phone +1 250 384 51 40

beat@sdps.ca

Peer-Reviewed Articles

Sabine Kiefer, **Ann C Mertz**, A. Koryakina, M. Hamburger, P. Küenzi. „(E,Z)-3-(3',5'-dimethoxy-4'-hydroxy-benzylidene)-2-indolinone (Indolinone) blocks mast cell degranulation", *published in European Journal of Pharmaceutical Sciences, 2010*

Sabine Kiefer, J. Rogger, Anna Melone, **Ann C Mertz**, A. Koryakina, P. Küenzi. "Separation and detection of all phosphoinositide isomers by ESI-MS", *published in Journal of Pharmaceutical and Biomedical Analysis, 2010*

Romina Marone, Dominik Erhart, **Ann C Mertz**, Thomas Bohnacker, Christian Schnell, Vladimir Cmiljanovic, Frédéric Stauffer, Carlos Garcia-Echeverria, Bernd Giese, Sauveur-Michel Maira, Matthias P. Wymann. "Targeting Melanoma with Dual PI3K/mTOR Inhibitors", *published in Molecular Cancer Research, 2009*

Articles in Preparation

Anna Melone, **Ann C Mertz**, Matthias P. Wymann. "Regulation of nutrient sensing by cellular PI(3)P and endomembrane localization of mTORC1", *in preparation*

Ann C Mertz, Anna Melone, Peter Küenzi, Sabine Kiefer, Michael Adams, M. Hamburger, Matthias P. Wymann. "Use of transgenic yeast to discover mammalian PI-3-kinase isoform inhibitors of natural origin", *in preparation*

Ann C Mertz, Danilo Ritz, Matthias Peter, Mike Tyers, Stephen B. Helliwell. „Pib2p, a novel endosome and vacuolar membrane localized FYVE protein, mediates exocytosis of the general amino acid permease, Gap1p" *submitted Dec 2010*

Presentation

Ann C Mertz, Peter Küenzi, Sabine Kiefer, Matthias P. Wymann. „Using transgenic yeast to uncover functions of mammalian PI-3-kinase isoforms", at MAIN students' meeting, 5/2007

Targeting Melanoma with Dual Phosphoinositide 3-Kinase/ Mammalian Target of Rapamycin Inhibitors

Romina Marone,[1] Dominik Erhart,[1] Ann C. Mertz,[1] Thomas Bohnacker,[1] Christian Schnell,[3] Vladimir Cmiljanovic,[2] Frédéric Stauffer,[3] Carlos Garcia-Echeverria,[3] Bernd Giese,[2] Sauveur-Michel Maira,[3] and Matthias P. Wymann[1]

[1]Institute of Biochemistry and Genetics, Department of Biomedicine and [2]Department of Chemistry, University of Basel, and [3]Oncology Disease Area, Novartis Institutes for Biomedical Research, Basel, Switzerland

Abstract

Phosphoinositide 3-kinase (PI3K)/protein kinase B/Akt and Ras/mitogen-activated protein kinase pathways are often constitutively activated in melanoma and have thus been considered as promising drug targets. Exposure of melanoma cells to NVP-BAG956, NVP-BBD130, and NVP-BEZ235, a series of novel, potent, and stable dual PI3K/ mammalian target of rapamycin (mTOR) inhibitors, resulted in complete G1 growth arrest, reduction of cyclin D1, and increased levels of $p27^{KIP1}$, but negligible apoptosis. In contrast, treatment of melanoma with the pan-class I PI3K inhibitor ZSTK474 or the mTORC1 inhibitor rapamycin resulted only in minor reduction of cell proliferation. In a syngeneic B16 mouse melanoma tumor model, orally administered NVP-BBD130 and NVP-BEZ235 efficiently attenuated tumor growth at primary and lymph node metastatic sites with no obvious toxicity. Metastatic melanoma in inhibitor-treated mice displayed reduced numbers of proliferating and significantly smaller tumor cells. In addition, neovascularization was blocked and tumoral necrosis increased when compared with vehicle-treated mice. In conclusion, compounds targeting PI3K and mTOR simultaneously were advantageous to attenuate melanoma growth and they develop their potential by targeting tumor growth directly, and indirectly via their interference with angiogenesis. Based on the above results, NVP-BEZ235, which has entered phase I/II clinical trials in patients with advanced solid tumors, has a potential in metastatic melanoma therapy.
(Mol Cancer Res 2009;7(4):601–13)

Introduction

Cancer cells evolve from a benign, noninvasive state to metastatic tumors, which grow and proliferate aggressively and display diminished cell death out of their normal tissue context. This process is driven by the accumulation of genetic and epigenetic alterations (1), which leads to sustained inputs into multiple signal transduction pathways. Activation of phosphoinositide 3-kinase (PI3K) is a prominent relay to tumor growth as it promotes increase in cell mass and cell cycle entry, counteracts apoptosis, modulates cytoskeletal rearrangements, and enhances cell migration (2-4).

Excess growth factor expression, constitutively activated protein tyrosine kinase receptors (e.g., epidermal growth factor receptor, c-kit, platelet-derived growth factor receptor, Met), oncogenic Ras, loss of phosphatase and tensin homologue deleted in chromosome 10 (PTEN), and mutated PI3K can lead to an increase in the levels of the PI3K product PtdIns(3,4,5)P_3. The latter serves as a docking site for pleckstrin homology domain-containing proteins such as protein kinase B (PKB/ Akt) and guanine nucleotide exchange factors feeding into growth and metastasis (3, 5). A major output of PKB/Akt activation is the phosphorylation of tuberin in the tuberous sclerosis complex (TSC1/2), which releases the TSC1/ 2→Rheb→mammalian target of rapamycin (mTOR) pathway and leads to increased translation and transcription (6).

Metastatic melanoma is a tumor with an exceptionally bad prognosis. Melanoma display already at early stages often mutated B-Raf (V600E; 66%) or constitutively activated N-Ras (mutation Q61K/L/R, 20%). An increase in tumor aggressiveness is observed in metastatic melanoma, which often correlates with the loss of PTEN (up to 60%) or up-regulation of PKBγ/ Akt3 (43-67%). Mutations of PI3K itself, as observed in other tumors for PI3Kα (PIK3CA; ref. 7), are rare in cutaneous melanoma (8, 9); however, the PI3Kα protein was found to be up-regulated (10). Occasional mutations found in STK11/LKB1 (11) could also contribute to the activation of mTOR independent from PI3K in melanoma. Therefore, the Ras/mitogen-activated protein kinase (MAPK) and PI3K/mTOR signaling pathways were proposed as promising drug targets for the treatment of advanced melanoma (12).

Clinical trials targeting the MAPK pathway (single therapy with the B-Raf inhibitor sorafenib/Nexavar/BAY 43-9006; ref. 13) did not yield significant success in melanoma despite beneficial effects of sorafenib in the treatment of renal cell carcinoma (14). Now sorafenib is in clinical trials in combination with bevacizumab (Avastin), and other Raf inhibitors also entered clinical trials (PLX4032, Plexxikon; Raf265, Novartis). Trials with rapamycin derivatives targeting mTOR (CCI-779/temsirolimus, Wyeth) in melanoma had to be concluded too due to inefficacy (15). New clinical

Received 8/4/08; revised 11/7/08; accepted 12/14/08; published online 4/16/09.
Grant support: Swiss Cancer League (01924-08-2006), Swiss National Science Foundation (3100A0-109718), and EU FP6 programme EU LSHG-CT-2003-502935/BBW 03.0441-3 (M.P. Wymann).
The costs of publication of this article were defrayed in part by the payment of page charges. This article must therefore be hereby marked *advertisement* in accordance with 18 U.S.C. Section 1734 solely to indicate this fact.
Note: Supplementary data for this article are available at Molecular Cancer Research Online (http://mcr.aacrjournals.org/).
Matthias P. Wymann, Institute of Biochemistry and Genetics, Department of Biomedicine, University of Basel, Mattenstrasse 28, CH-4058 Basel, Switzerland. Phone: 41-61-695-3046; Fax: 41-61-267-3566. E-mail: Matthias.Wymann@UniBas.CH

doi:10.1158/1541-7786.MCR-08-0366

trials targeting Raf and mTOR simultaneously have been initiated recently.[4]

In preclinical models, the PI3K pathway was initially targeted with LY294002, a PI3K inhibitor with low potency, low specificity, and high toxicity (16). LY294002 and wortmannin inhibit the whole PI3K family and related proteins, including mTOR, PI4K, DNA-PK (17), and Polo-like kinases (18). Improvements in PI3K inhibitor potency and selectivity were made with the pyridofuropyrimidine PI103 (19-21), and, recently, the first orally administered pan-PI3K inhibitor ZSTK474 was presented (22, 23).

Here, we report for the first time in melanoma the action of PI3K/mTOR inhibitors with drug-like properties, including NVP-BEZ235, which has entered phase I/II clinical studies for patients with advanced solid malignancies. Our results reported herein provide a basis for the evaluation and rational of action of PI3K pathway targeting in solid tumors and document a significant efficiency and insignificant adverse effects of the compounds used.

Results

Dual PI3K/mTOR Inhibitors Block Proliferation of Melanoma Cells

Melanoma cells often show constitutive activation of the PI3K pathway due to mutations and attenuation of the phosphatase PTEN or changes in PKBγ expression. Here, a collection of human melanoma cell lines generated from different tumor stages and three mouse melanoma lines of the B16 family were used to investigate the susceptibility of melanoma to PI3K pathway inhibition. Currently, the effect of PI3K inhibition on cell proliferation is controversial (12, 22, 24-27); therefore, we first reevaluated the effect of the classic PI3K inhibitors wortmannin and LY294002. When cells were exposed to a single dose of inhibitor for 3 days, wortmannin was ineffective due to its limited stability (Fig. 1A and B). A set of newly identified, ATP-competitive PI3K/mTOR inhibitors, NVP-BAG956, NVP-BBD130, and NVP-BEZ235 (see Table 1; Supplementary Fig. S1; refs. 28, 29), showed a long-term effect on melanoma cell proliferation, superior to even much elevated concentrations of LY294002 (Fig. 1A and B). NVP compounds prevented growth (<20% of normal growth) in >85% of the tested melanoma lines, independent of the status of PTEN and BRaf (Supplementary Table S1) or the tumor stage the cells were derived from. The arrest in proliferation correlated with a reduction in cellular and nuclear size (data not shown). Interestingly, inhibitor-treated cells were able to reenter proliferation at a reduced rate and to gain normal cell volume when NVP-BAG956 and NVP-BEZ235 were removed, whereas cells exposed to NVP-BBD130 were arrested for up to 10 days and remained small (7 days in the absence of inhibitor; see Supplementary Fig. S2). Although in prolonged stasis, no significant cell death was observed.

To understand the mode of action of these novel compounds, we performed time course– and concentration-dependent experiments using malignant, aggressively growing cell lines, such as A2058, which have constitutively activated PI3K/PKB/Akt (Fig. 1C) and MAPK pathways (see Supplementary Fig. S3). All used PI3K inhibitors decreased phosphorylation of PKB/Akt, whereas the phosphorylation status of MAPK was not affected. The effect of wortmannin was short lived; levels of phosphorylated PKB/Akt were back to normal 2 to 4 hours after treatment. In the case of LY294002, the PKB/Akt phosphorylation was restored after 1 day. In contrast, a single addition of NVP compounds caused very prominent and prolonged dephosphorylation of PKB/Akt, even in melanoma showing PI3K inhibitor-resistant proliferation (e.g., C32; see Fig. 1A and C). The potency of the three novel inhibitors to block phosphorylation of PKB/Akt in A2058 cells was in the nmol/L range (IC_{50} value for NVP-BBD130 was 11 ± 4.6 nmol/L, for NVP-BEZ235 18 ± 6.4 nmol/L, and for NVP-BAG956 67 ± 25 nmol/L; Fig. 1D). In addition, inhibition of PKB/Akt phosphorylation correlated with loss of A2058 cell proliferation for NVP-BBD130 and NVP-BEZ235 (IC_{50} for NVP-BBD130 was 34 ± 2.6 nmol/L and for NVP-BEZ235 was 26 ± 2.5 nmol/L), whereas more of NVP-BAG956 was required to hinder proliferation (IC_{50} was 290 ± 20 nmol/L; see Fig. 1E). Altogether, when compared with the established compounds, the novel inhibitors exert prolonged action with superior stability in complex medium.

G1 Cell Cycle Arrest of Melanoma Cells Upon Treatment with PI3K/mTOR Inhibitors

The effect of PI3K inhibitors on the cell cycle is shown here in detail for A2058 melanoma cells (Fig. 2; more melanoma lines in Supplementary Table S2): Melanoma treated with wortmannin and LY294002 showed no significant shifts in cell cycle profiles compared with nontreated cells, whereas PC3M cells, which are very sensitive to PI3K inhibitors (Supplementary Fig. S4A; refs. 30-32), displayed a prominent cell cycle arrest in G1 with LY294002. NVP-BAG956, NVP-BBD130, and NVP-BEZ235 resulted in a complete arrest of most tumor cells in G1, which correlated with a lack of proliferation and DNA replication (as measured by [^{3}H]thymidine incorporation; Fig. 2B). PI3K inhibitor–resistant proliferation was observed in C32 melanomas, which consequently also showed no G1 arrest (Fig. 1A; Supplementary Table S2). Moreover, PI3K inhibition did not induce evident signs of apoptosis as monitored by the absence of sub-G1 peaks (Fig. 2A and data not shown) and Annexin V–positive cells (Supplementary Fig. S4B; Supplementary Table S2). PI3K/mTOR inhibitors thus have cytostatic, but no cytotoxic, effects on melanoma cells.

Cell cycle progression is regulated by the oscillating expression of cyclins and the inhibition of specific cyclin/cyclin-dependent kinase (Cdk) complexes by Cdk inhibitors. Expression of cyclin D1 is down-regulated in A2058 cells treated with NVP compounds and is somewhat reduced by treatment with LY294002 (Fig. 2C). A minor decrease in cyclin D1 was observed in control and wortmannin-treated cells, as they reached confluence at later stages. In inhibitor-resistant C32 cells, PI3K/mTOR inhibition caused compound-dependent elevations in cyclin D1 levels (Fig. 2C). Similarly, $p27^{Kip1}$ expression was clearly induced by NVP-BAG956, NVP-BBD130, and NVP-BEZ235 in A2058 cells but not in C32 cells.

To investigate stringency and rapidity of the cell cycle arrest in G1 induced by PI3K pathway inhibition, A2058 cells were synchronized with the microtubule disruptor nocodazole in G2-M and released subsequently in the presence of vehicle

[4] http://www.clinicaltrials.gov

or PI3K inhibitors: (*a*) the initial treatment with nocodazole arrested cells in G2-M (from 30% to 60% of cells in G2-M; Fig. 2D); (*b*) after nocodazole removal, control and wortmannin-treated cells showed a profile typical of proliferating cells after 24 h, whereas cells exposed to LY294002 required 48 h to restart proliferation. In the presence of NVP-BAG956, NVP-BBD130, or NVP-BEZ235, A2058 cells were only able to exit G2-M and then remained in G1 (Fig. 2D).

Primary and Metastatic Tumors Require the PI3K Pathway for Growth In vivo

To evaluate the efficacy of different PI3K/mTOR inhibitors *in vivo*, we used a syngeneic B16BL6 mouse melanoma model, in which cells, injected intradermally in both ears, rapidly progress to primary tumors and cervical lymph node metastasis. Treatment with vehicle control, PI3K/mTOR inhibitors, and a vascular endothelial growth factor receptor (VEGFR) protein tyrosine kinase inhibitor (PTK787) were started 7 days following tumor inoculation. A ~60% reduction in the primary tumor size was achieved with different doses and regimens of NVP-BBD130, NVP-BEZ235 and PI103 (Fig. 3A), and PTK787 (data not shown). Moreover, mice treated with NVP-BBD130, NVP-BEZ235, or PTK787 showed a significant reduction in the size of the cervical lymph node metastasis (Fig. 3B; PTK787: data not shown). For NVP-BBD130, tumor and metastasis size reduction correlated with a stringent reduction in the amount of phosphorylated PKB/Akt and $p70^{S6K}$ 2 hours after the last treatment (Fig. 4A). A partial recovery to basal level was seen after 16 hours. In addition, reduced expression of cyclin D1 and increased levels of $p27^{Kip1}$ were detected in metastatic tissue 2 hours after dosing (Fig. 4B). Intriguingly, treatment with PI103 at the concentration used here did not significantly reduce the mass of lymph node metastasis (Fig. 3B), which was in agreement with overshooting signals for phosphorylated PKB/Akt and $p70^{S6K}$ in primary and metastatic tumor tissue (Fig. 4A). As PI103 is cleared rapidly from the tumor (half life <2 hours; see ref. 20), these elevated and dose-dependent signals could represent a release of feedback loops in the PI3K/mTOR signaling system.

A closer analysis of metastatic sections revealed that cell size was decreased in tumor tissue from inhibitor-treated animals (Fig. 5A), but not in hepatocytes of the same mice. This is encouraging, as liver cell size dynamically responds to starvation and the current PI3K/mTOR treatment regimen seems not to fully mimic nutrient deprivation. Plasma levels of liver marker enzymes and proteins were also not significantly affected by the treatment with PI3K/mTOR inhibitors (except alanine aminotransferase; see Supplementary Table S3). Interestingly, PI3K inhibitor–mediated reduction in cell size went along with a decreased mitotic index (Fig. 5B). The few remaining mitotic cells were usually located around preexisting, large blood vessels. In addition to reduced cell proliferation, metastatic tissue from mice treated with NVP-BEZ235 displayed significantly increased necrosis levels compared with tumors from vehicle control–treated mice (Fig. 5C).

To survive and grow, tumors with a diameter larger than 1 mm require blood vessels to be fully supplied with nutrients and oxygen. Staining of metastatic sections for the endothelial cell marker CD31 revealed that NVP-BBD130 and NVP-BEZ235 completely abrogated neoangiogenesis in metastatic tissue, whereas vehicle control–, PI103-, or PTK787-treated tumors displayed a well-developed microvasculature (Fig. 6A; quantification in Fig. 6B). Large and preexisting blood vessels at the tumor border remained unaffected by all treatments (data not shown). Altogether, the above results show that the novel NVP compounds have a direct effect on tumor cell growth and proliferation, and exert, in addition, antiangiogenic effects supporting tumor necrosis.

PI3K/mTOR Inhibitors Are Well Tolerated

Tumor-bearing mice showed a disease-related drop in body weight by 5% to 10% and had >2-fold enlarged spleens when compared with healthy controls (Table 2). PI3K inhibitor–treated animals showed a less dramatic increase in spleen size and an overall tendency to regain body weight, reaching significance for PTK787 and NVP-BEZ235 (data not shown). The collected data illustrate that the tumor per se causes dramatic systemic changes, which were partially reversed by PI3K/mTOR inhibition. Interference with insulin-mediated glucose uptake also seemed negligible, as blood glucose levels did not significantly increase over concentrations determined in healthy and vehicle control–treated animals (Table 2).

PI3K and mTOR have been reported to play important roles in the immune system. Spleen and bone marrow of NVP-BBD130– and PI103-treated mice were therefore analyzed for adverse effects on immune cells. Tumor-bearing, vehicle control–treated mice displayed a reduction in the number of $CD3^+$ T cells, B cells, and natural killer cells, compared with healthy animals (Supplementary Table S4), and NVP-BBD130 treatment decreased lymphocyte counts in a statistically insignificant manner. Interestingly, treatment with PI103 resulted in an increase in the number of T cells, B cells, and natural killer cells back to levels similar to healthy control animals. Granulocytes, macrophages, and erythroid cell numbers were normal in the bone marrow of all tumor-bearing mice, and there was no indication that the applied PI3K/mTOR inhibitors interfered with hematopoiesis.

Cooperation of PI3K and mTOR in Melanoma Cell Proliferation

To discriminate between the importance of PI3K and mTOR, we ectopically expressed a constitutively active PKB/Akt (myristoylated PKB, Myr-PKB; ref. 33) to partially bypass the inhibitor-mediated block in PI3K signaling. To monitor PKB/Akt action, we used the mTOR-independent nuclear to cytoplasmic translocation of forkhead transcription factors (FOXO), which feed negatively into cell cycle progression and antiapoptotic events (34, 35). Nonphosphorylated FOXOs are localized to the nucleus but are retained in the cytoplasm when phosphorylated by PKB/Akt. In A2058 cells, PKB/Akt is maintained activated in a PI3K-dependent manner even in serum-free conditions, mainly due to the lack of the lipid phosphatase PTEN. As a consequence, ectopically expressed FOXO1 is quantitatively localized in the cytoplasm. Treatment of A2058 cells with NVP compounds caused a rapid inactivation of PKB/Akt and a subsequent translocation of FOXO1 to the nucleus (Fig. 7A). Stable expression of Myr-PKB in A2058

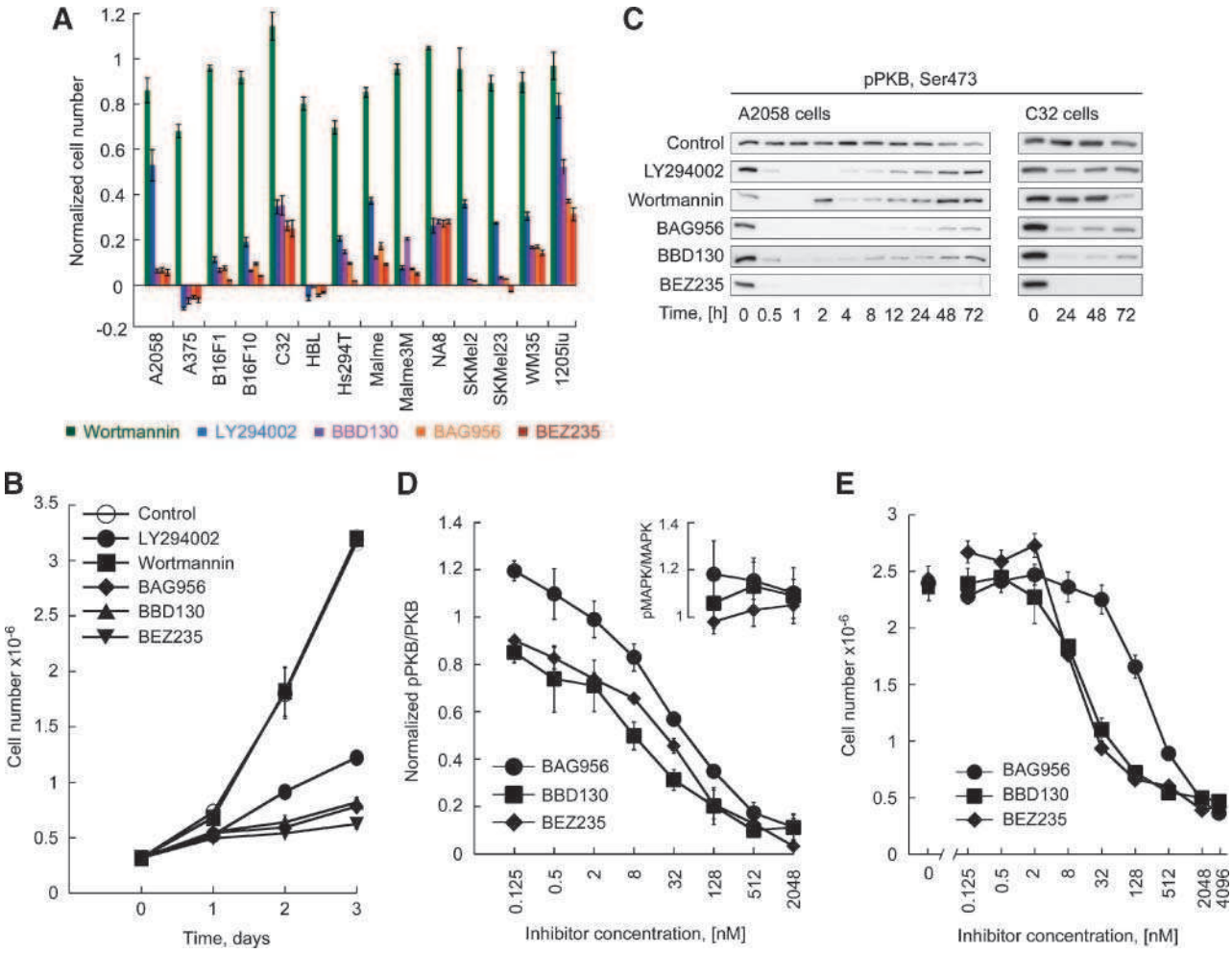

FIGURE 1. PI3K inhibitors affect proliferation and downstream signaling in melanoma cells. **A.** Antiproliferative effect of PI3K inhibitors. Melanoma cells were exposed to the indicated inhibitors (LY294002 at 25 μmol/L; wortmannin at 500 nmol/L; NVP-BAG956, NVP-BBD130, and NVP-BEZ235 at 1 μmol/L) for 3 d before cell numbers were determined. Cell numbers are depicted after the subtraction of initially seeded cells in relation to nontreated controls (ratio of treated over nontreated cultures). Columns, mean of triplicates; bars, SE. **B.** Time-dependent A2058 proliferation in the presence of PI3K inhibitors. A2058 cells were exposed to PI3K inhibitors at day 0 before cells were counted at the indicated time intervals. Points, mean of triplicates; bars, SE. **C.** Prolonged changes in phosphorylation of PKB/Akt upon PI3K inhibition. Phosphorylated PKB as detected in total cell lysates of A2058 and C32 cells treated with PI3K inhibitors for the indicated intervals are shown. An extended version of the figure is presented in Supplementary Fig. S3. **D.** Concentration-dependent inhibition of PKB phosphorylation. A2058 cells were exposed for 3 h to increasing concentrations of NVP-BAG956, NVP-BBD130, and NVP-BEZ235. Total cell lysates were subjected to immunoblotting for total and phosphorylated PKB or MAPK. Emerging signals were quantified using fluorescent secondary antibodies, and ratios of phosphosphorylated over nonphosphorylated kinases are displayed. Points, mean ($n > 3$); bars, SE. **E.** Inhibitory activity of PI3K inhibitors against melanoma cell proliferation. A2058 cells were treated at day 0 with increasing concentrations of NVP-BAG956, NVP-BBD130, and NVP-BEZ235. Cell proliferation was evaluated 3 d later. Points, mean of triplicates; bars, SE.

was sufficient to prevent nuclear translocation of exogenous FOXO1 in the presence of PI3K inhibitors, but did not rescue proliferation in the presence of, e.g., NVP-BEZ235 (Fig. 7B).

In serum-deprived HEK293 cells, Myr-PKB reconstituted phosphorylation of FOXO and GSK3β and also fed into mTOR signaling with phosphorylated $p70^{S6K}$, S6, and 4E-BP1 as readouts (Supplementary Fig. S5). Whereas FOXO and GSK-3β phosphorylation was to a large extent PI3K inhibitor resistant, signals downstream of mTOR were completely abrogated by NVP-BAG956, NVP-BBD130, NVP-BEZ235, and PI103, as well as by the mTORC1 inhibitor rapamycin. This corroborates mTOR inhibition by NVP compounds observed in TSC1 knockout mouse embryonic fibroblasts (Table 1; see ref. 28).

Recently, a selective pan-PI3K inhibitor without activity against mTOR (ZSTK474) was shown to block tumor cell growth with an overall 50% sensitivity rate (22, 23). To evaluate the requirement of a dual PI3K and mTOR inhibition to target melanoma, cells were comparatively exposed to NVP-BEZ235, ZSTK474, and/or rapamycin. The obtained results clearly illustrate that targeting either PI3K or mTOR in isolation can attenuate growth and proliferation of particularly sensitive cells (e.g., A375), whereas more resistant melanoma are only affected by the simultaneous targeting of PI3K and mTOR (Fig. 8A). Treatment of melanoma cells with a combination of ZSTK474 and rapamycin results in a more pronounced proliferation arrest compared with single compounds. The

differential modulation of the phosphorylation status of PKB and $p70^{S6K}$ by the various inhibitors in sensitive and more resistant cell lines shows that the degree of the coupling of PI3K to mTOR varies, and a retained activation of mTOR in the presence of PI3K inhibitor (as, e.g., in 1205lu cells; Fig. 8B) requires an efficient PI3K/mTOR dual-mode inhibitor to attenuate growth.

Discussion

The recognition that the PI3K pathway has gained as a putative target in cancer therapy (2-4) is reflected by a recent increase in patent literature covering novel PI3K inhibitors (36, 37) and documents the need for compounds with improved stability, efficacy, and potency. The newly developed series of ATP-competitive PI3K/mTOR inhibitors (28, 29), NVP-BAG956, NVP-BBD130, and NVP-BEZ235, fit these criteria, and NVP-BEZ235 has recently entered clinical trials. NVP-BEZ235 (28) and NVP-BBD130 (Supplementary Fig. S6) have advantageous pharmacologic profiles and show a high and sustained exposure in tumor tissue *in vivo*. Neither their effects in aggressive, metastatic tumors in syngeneic models nor the requirement of a dual inhibition of PI3K and mTOR was studied thus far.

Table 1. *In vitro* Inhibitory Activities of NVP Compounds and ZSTK474

A

Kinase type	Enzyme	NVP-BAG956 IC_{50} (μmol/L)	NVP-BBD130 IC_{50} (μmol/L)	NVP-BEZ235* IC_{50} (μmol/L)
Receptor TK	VEGFR1	2.56 ± 0.56	>10	>10
	Flt3	>10	>10	>10
	EGFR (HER1)	>10	>10	>10
	IGF1-R	>10	>10	>10
	EphB4	>10	>10	>10
	Ret	>10	>10	>10
	Tie-2 (Tek)	>10	>10	>10
	c-Met	>10	>10	>10
	FGFR-K650E	>10	>10	>10
Cytosolic TK	Fak	>10	>10	>10
	Jak2	>10	>10	>10
	c-Abl	>10	>10	>10
	c-Src	>10	>10	>10
Cytosolic S/TK	PKA	>10	>10	>10
	Akt (PKB)	>10	>10	>10
	PDK1†	0.24/0.26	>10	>10
	B-Raf–V600E	>10	>10	>10

B

	NVP-BAG956 IC_{50} (nmol/L)	NVP-BBD130 IC_{50} (nmol/L)	NVP-BEZ235* IC_{50} (nmol/L)	ZSTK474‡ IC_{50} (nmol/L)	PI103§ IC_{50} (nmol/L)
PI3Kα	56/56	72/71	4 ± 2	16	2/8
PI3Kβ	444/446	2,340/2,336	75 ± 45	44	3/88
PI3Kδ	34/35	201/201	7 ± 6	4.6	3/48
PI3Kγ	117/112	382/350	5 ± 4	49	15/150
mTOR	n.d.	n.d. [7.7]‖	20.7 [6.5]‖	>100,000	20-83

NOTE: *In vitro* activities of BAG956, BBD130, BEZ235, and ZSTK474. *In vitro* kinase assays were done with the indicated recombinant purified kinases in the presence of increasing concentration of the inhibitors (53).
Abbreviation: n.d., not determined.
*See Maira et al. (28).
†See Stauffer et al. (29).
‡See Kong and Yamori (23).
§See Fan et al. (19), Knight et al. (54), and Raynaud et al. (20).
‖Values in square brackets correspond to IC_{50} values obtained in TSC1 null mouse embryonic fibroblasts using phospho-S6 as output.

Incubation of asynchronously growing melanoma cells with NVP compounds resulted in a complete loss of PKB/Akt phosphorylation and induced growth arrest, but not apoptosis, which is in agreement with earlier reports for PI3K pathway inhibitors (12, 22, 26). The observed growth arrest was dose dependent and correlated with the loss of phosphorylation of PKB/Akt. Cells accumulated in the G1 cell cycle phase showing upregulation of the cell cycle inhibitor $p27^{Kip1}$, reduction in cyclin D1 levels, and a complete block of DNA synthesis. In all cell lines tested here, the effect of NVP compounds on cell proliferation was superior and prolonged when compared with the action of LY294002 and wortmannin. A small fraction of the cells tested responded only partially to PI3K/mTOR inhibition and consequently did not show a G1 arrest or changes in $p27^{Kip1}$. Increased cellular cyclin D1 has been previously associated with poor prognosis in many cancers and has also been reported to correlate with B-Raf inhibitor resistance in melanoma (38). Further studies will be required to determine if the inhibitor-induced increase in cyclin D1 levels depicted in C32 cells confers resistance to PI3K/mTOR inhibition in a general sense. Similarly, the low expression or mutation of the lipid phosphatase PTEN, a constitutive activation of the PI3K pathway, the presence of mutated Ras or Raf, or the p53 status cannot be currently translated into a reliable pattern to predict sensitivity of melanoma to PI3K/mTOR inhibition.

To assess the *in vivo* activity of NVP-BBD130 and NVP-BEZ235, a B16 melanoma model was used: This syngeneic mouse model allows the evaluation of pharmacologic effects on the progress of an aggressive primary tumor and the precise quantification of a secondary metastatic lymph node tumor. Moreover, other than in xenograft models, mice have here an intact immune system and the effects of drugs on immune cell counts can be monitored. This is important as melanoma patients mount spontaneous T cell–dependent responses against their tumor, which correlate with patient survival (39). One might thus anticipate that optimal treatment should not interfere with antitumoral immune responses.

NVP-BBD130 and NVP-BEZ235 could be administered orally and have excellent pharmacologic properties, whereas PI103 required i.p. application. Treatment of mice with different doses and regimens of inhibitors resulted in a ~60% reduction of the primary tumors independently of the inhibitor used. Size of lymph node metastasis was also greatly reduced in mice treated with NVP-BBD130 and NVP-BEZ235, whereas treatment with PI103 (10 mg/kg/d) had insignificant effects on the mass of metastasis. In a first report, Fan et al. (19) obtained an antitumoral activity of PI103 in glioma xenografts with doses as low as 5 mg/kg/d. In contrast, Raynaud et al. (20) used the same glioma tumor model and achieved comparable results only at 100 mg/kg/d and recently Chen et al. (21) showed that PI103 at 10 mg/kg/d was not efficacious as a single agent in a different glioblastoma model. In the melanoma model used

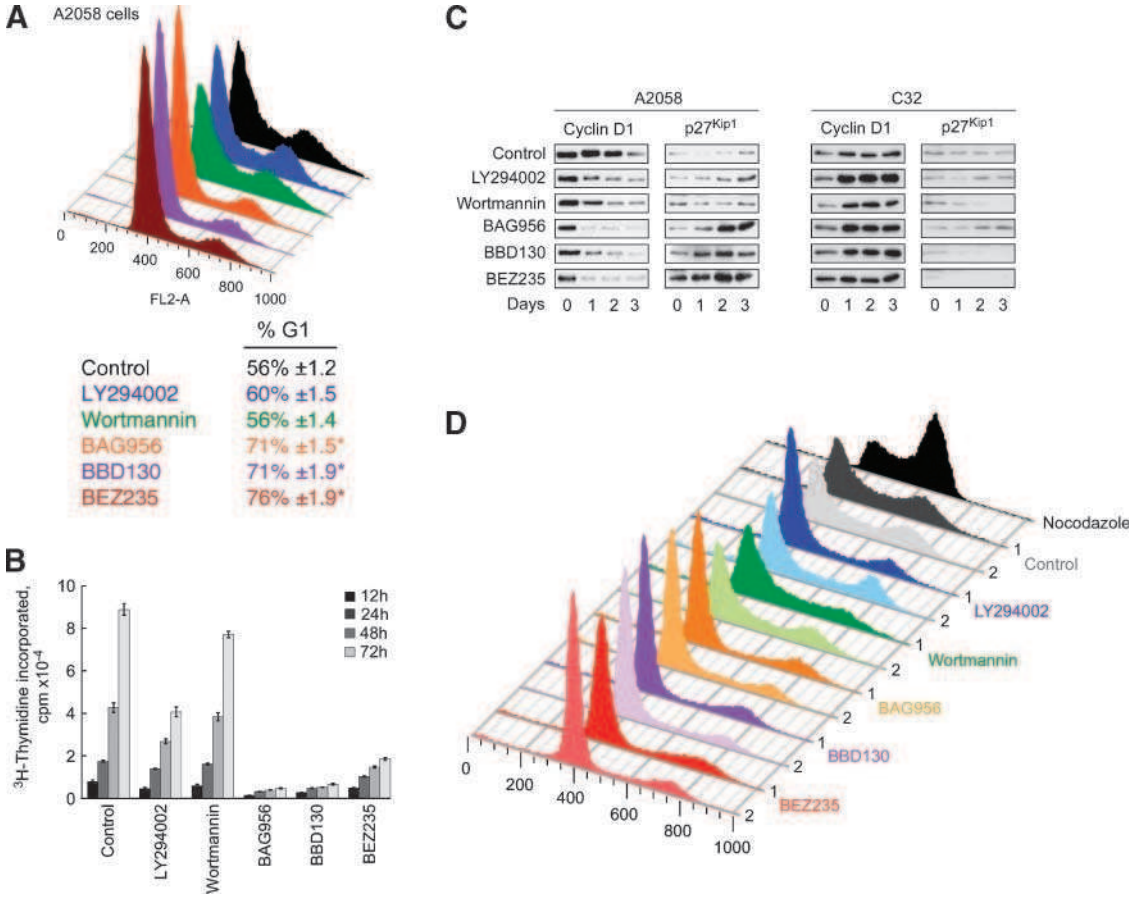

FIGURE 2. PI3K pathway inhibition causes growth arrest in G1 in melanoma. **A.** Determination of cell cycle profile changes by PI3K inhibitor treatment. A2058 melanoma cells were exposed to PI3K inhibitors for 3 d. Subsequently, the cell cycle profile was evaluated by fluorescence-activated cell sorting using propidium iodide staining. For more cell lines, see Supplementary Table S2. *, $P < 0.002$. **B.** PI3K and DNA replication. [^{3}H]thymidine incorporation into DNA was assessed in A2058 treated as above. Columns, mean ($n = 6$); bars, SE. **C.** Attenuation of PI3K activity affected cyclin D1 and cell cycle inhibitor p27^{Kip1} levels. A2058 and C32 cells, cultured with or without PI3K inhibitors, were lysed at the indicated times and assessed for cyclin D1 and p27^{Kip1} expression levels by immunoblotting. **D.** Evaluation of the role of PI3K in cell cycle transitions in melanoma cells. A2058 cells were synchronized in the G2-M phase by nocodazole treatment (*black curve*). Subsequently, cells were released from the nocodazole block and simultaneously exposed to the indicated PI3K inhibitors (*colored curves*). The cell cycle profile was then analyzed 1 and 2 d later as in **A**.

here, a dose of 10 mg/kg/d of PI103 was sufficient to attenuate primary tumor growth as observed for NVP-BEZ235, whereas a significant reduction in lymph node metastasis could not be detected. It is tempting to explain the lack of action on the lymph node metastasis by a restricted access of PI103 to metastatic tumor tissue. This is, however, challenged by the observation that increasing doses of PI103 caused a dose-dependent, paradoxical increase in phosphorylated PKB/Akt and p70^{S6K} in both the primary tumor and the metastasis in cervical lymph nodes. As Ser473 on PKB/Akt is mainly phosphorylated by TORC2 (40) in the absence of DNA damage (41, 42), and Thr389 phosphorylation on p70^{S6K} is mediated by TORC1, these phosphorylation patterns suggest that both mTOR complexes are in an overactivated state 2 hours after the last PI103 administration in a prolonged treatment scheme. As PI103 was used here at low doses and has a short half life (<2 hours; ref. 20), these results indicate that PI3K/mTOR signaling overshoots after a transient inhibition. BBD130, maintaining exposure to the tumor for a prolonged time (16 h/nmol/g), shows a clear reduction of Ser473 phosphorylation on PKB/Akt and Thr389 on p70^{S6K} until 16 hours after administration. The above result suggests that inhibitor half-life, exposure, and dosage frequency might affect the success of PI3K/mTOR modulation, and that phospho-PKB/Akt and phospho-p70^{S6K} need validation as biomarkers in conjunction with given compounds.

A close examination of melanoma tissue from mice treated with NVP-BBD130 and NVP-BEZ235 revealed that the mitotic index of metastatic cells in the cervical lymph nodes were reduced to more than half of untreated controls. This went along with a reduction in tumor cell mass, whereas cell size in other organs like the liver remained unaffected. The liver adapts to starvation by a reduction in cell size (43). As current PI3K/mTOR inhibitor treatments did not affect normal liver morphology, one may assume that nutrient uptake was functional. NVP-BBD130 at high single dose (40 mg/kg) showed a significant increase of the liver alanine aminotransferase in the plasma, which correlates with the increased liver retention of BBD130 compared with BEZ235 (Supplementary Fig. S6; ref. 28). Splitting the daily dose of NVP-BBD130 (2 × 20 mg/kg) reduced the

release of alanine aminotransferase. Moreover, we could not detect significant differences in blood glucose levels between inhibitor-treated and vehicle control mice, showing that the inhibition of the PI3Ks is not impairing the glucose homeostasis.

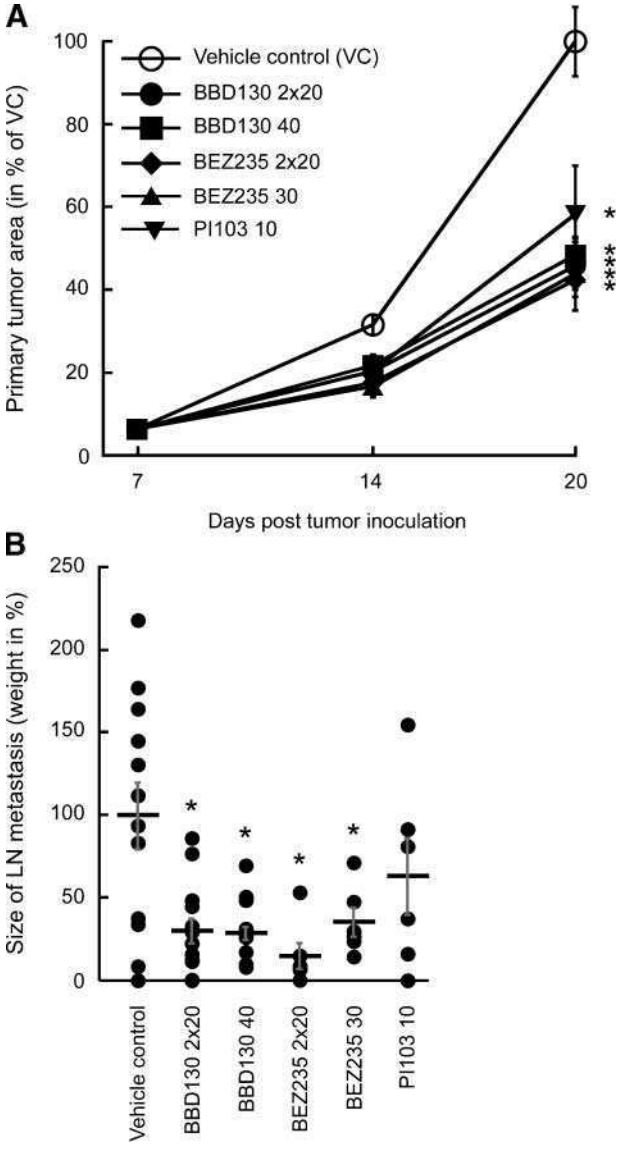

FIGURE 3. Antitumoral and antiangiogenic effect of PI3K inhibitors in the B16 mouse melanoma model. B16BL6 mouse melanoma cells were injected intradermally into ears of C57BL6 mice. One week later, tumors were established and treatment with vehicle and PI3K inhibitors (NVP-BBD130 at 40 mg/kg daily and 20 mg/kg twice daily, orally; NVP-BEZ235 at 40 mg/kg daily and 20 mg/kg twice daily, orally; PI103 at 10 mg/kg daily, i.p.) was started. Size of primary tumors was determined when indicated, whereas the mass of cervical lymph node metastasis was determined as the mice were sacrificed (*, $P < 0.05$ versus vehicle control group). **A.** Primary tumor size is depicted in percentage of the tumor size obtained in vehicle-treated (*VC*) animals 20 d after melanoma inoculation (for calculations, see Materials and Methods). Points, mean ($n > 6$); bars, SE. **B.** Formation of cervical lymph node metastasis. Mice were sacrificed 20 d after tumor inoculation and 2 wk of treatment with the indicated compounds. Cervical lymph node metastatic tissue was excised and weighted. Changes in metastatic mass are plotted in percentage of the mean end point of vehicle-treated animals. Points, mean ($n > 6$); bars, SE.

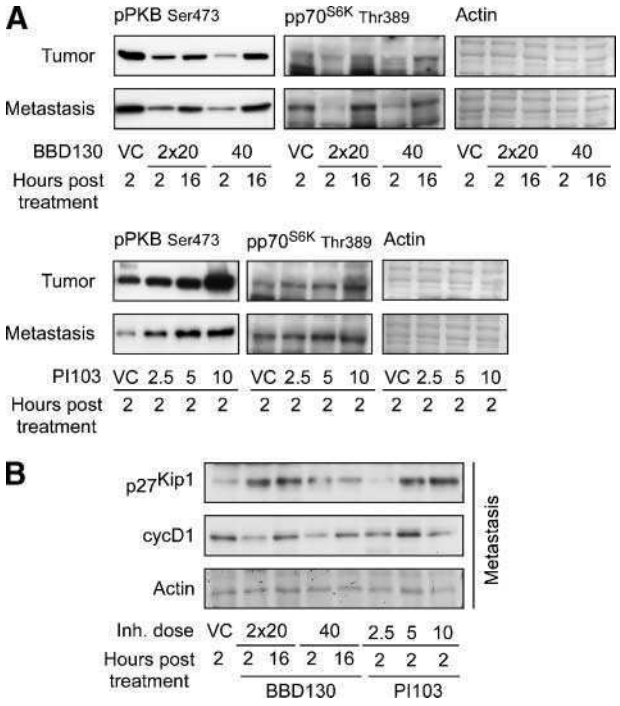

FIGURE 4. **A** and **B.** PI3K downstream signaling and cell cycle markers in tumor tissue. Tumor samples were collected at the indicated times after the last treatment with compound (posttreatment). Subsequently, total lysates of primary and metastatic tumors were resolved on SDS-PAGE and probed for phosphorylated PKB and $p70^{S6K}$, or $p27^{Kip1}$ and cyclin D1. Actin stained with Coomassie blue is shown as a loading control.

Angiogenesis is required for nutrient supply and growth of tumors beyond 1 mm (44) and has been shown to be sensitive to mTOR inhibition by rapamycin and its derivatives (45, 46). Supporting this notion, tumors excised from NVP-BBD130– and NVP-BEZ235–treated mice displayed a significant reduction in neovascularization, whereas large, preexisting blood vessels were not affected by targeting PI3K and mTOR. Intriguingly, mice treated with PI103 or the VEGFR inhibitor PTK787 showed no significant reduction in the amount of new blood vessels compared with vehicle control mice. Whereas NVP-BEZ235 and NVP-BBD130 are very potent PI3K and mTOR inhibitors, their effect on the VEGF receptor tyrosine kinase activity is negligible (IC_{50} for VEGFR1 >10 μmol/L). Despite this fact, they blocked the formation of new blood vessels more efficiently than PTK787. The PI3K/mTOR signaling pathway has been reported to control the expression of HIF-1 via activation of $p70^{S6K}$ and HDM2/MDM2. HIF-1 is the major regulator of VEGF transcriptional activity (47). Feedback loops from mTOR to PKB/Akt and PI3K activation have been reported (48), and also hypoxia-induced angiogenesis might require mTORC1 and mTORC2 (49). Therefore, NVP-BBD130 and NVP-BEZ235 interfere with VEGFR ligand production and VEGFR downstream signaling to block blood vessel formation and exert at the same time cytostatic effects on tumor cells. This dual action could explain the higher efficiency of NVP-BBD130 and NVP-BEZ235 compared with PTK787, an inhibitor more selectively targeting endothelial cells through VEGFR inhibition. The effect of

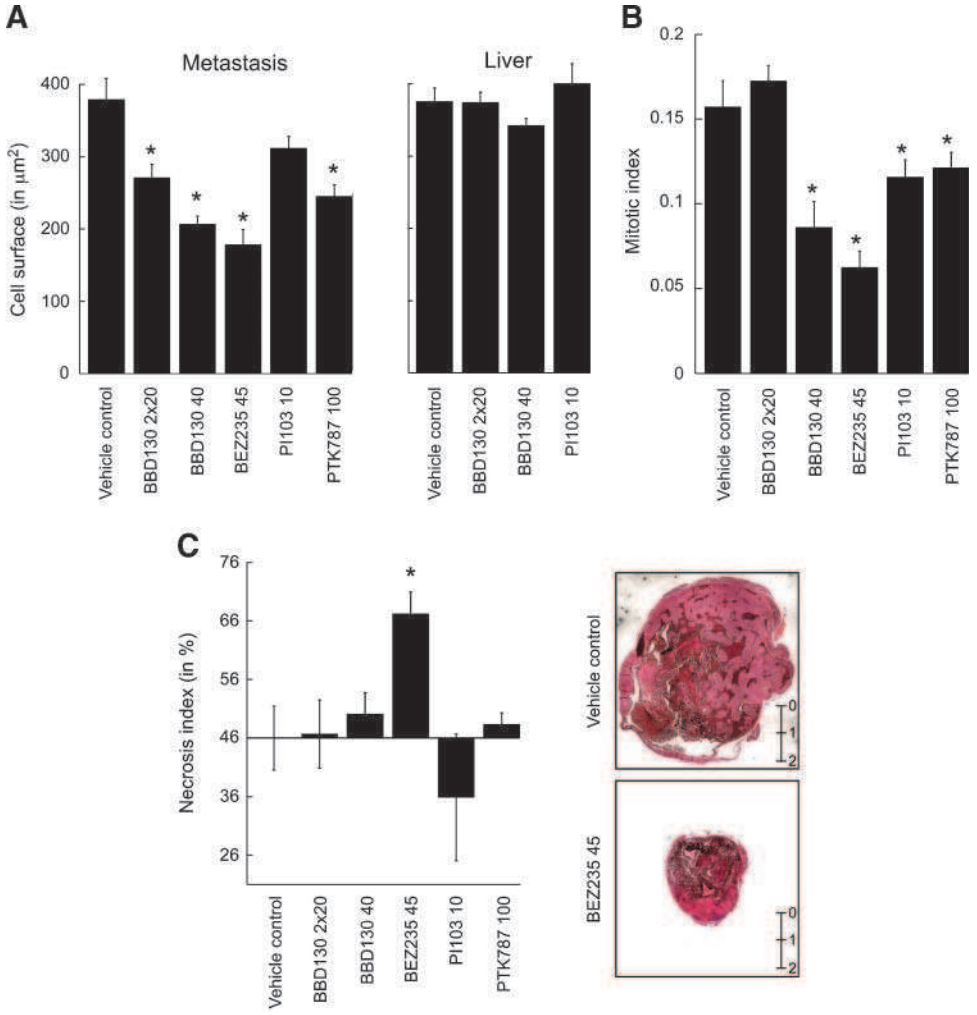

FIGURE 5. **A.** Tumor and hepatocyte cell size. Paraffin sections of metastatic melanoma and of liver tissue were stained with H&E, and cell size was measured as cross-section areas with ImageJ software. Columns, mean ($n > 300$); bars, SE. **B.** Mitotic index in metastatic tissue. Mitotic nuclei in lymph node metastasis were quantified in H&E-stained paraffin sections. Columns, mean ($n > 200$ cells); bars, SE. **C.** Necrosis in cervical lymph node metastasis. H&E-stained paraffin sections were analyzed for the presence of necrotic tissue and the percentage of necrotic cells was evaluated with the help of ImageJ. Columns, mean ($n > 4$); bars, SE. Scale in mm.

NVP-BBD130 and NVP-BEZ235 on neovascularization seemed to be crucial, as we noticed that tumor cells located in the vicinity of preexisting, large blood vessels still had some capacity to enter mitosis and displayed a nearly normal cell size (data not shown). It is therefore likely that the increased amount of necrotic tumor tissue observed in NVP-BEZ235–treated animals is caused by the very stringent targeting of neovascularization.

Our results indicate that the novel series of PI3K/TOR inhibitors attacks tumor progression by several molecular and physiologic mechanisms. To explore if the inhibition of mTOR in addition to PI3K is essential for blockage of tumor cell growth, we reintroduced constitutive PKB/Akt signaling in inhibitor-treated cells. When activated, PKB/Akt modulates directly and indirectly a range of transcription factors, among them the FOXOs. Here, NVP compounds abolished phosphorylation of FOXO1 by PKB/Akt, thus abrogating its binding to 14.3.3 proteins, which resulted in a translocation to the nucleus. Ectopic expression of constitutively active PKB/Akt (myr-PKB) yielded a PI3K inhibitor–resistant, cytosolic retention of FOXO1, but was unable to bypass the cell cycle arrest imposed by NVP compounds. This could be due to the fact that signals downstream of mTOR ($p70^{S6K}$, S6, and 4E-BP1 phosphorylation) remained inhibitor sensitive in the presence of constitutively active PKB/Akt.

Melanoma cells displayed a <50% drop in the rate of proliferation after high doses of rapamycin (mTOR inhibitor, 100 nmol/L) or <25% after ZSTK474 (pan-PI3K inhibitor, 1 µmol/L) treatment. NVP-BEZ235 is a pan-PI3K inhibitor but also blocks mTOR, targeting the ATP-binding site of TORC1 and TORC2 (28). Only the treatment of melanoma cells with dual inhibitors resulted in an efficient cytostatic, and in some rare cases cytotoxic, effect. The combination of rapamycin and ZSTK474 was more effective than either compound alone (<60%), but less effective than BEZ235. Whereas ZSTK474 inhibits class I PI3Ks, but not mTOR, rapamycin targets exclusively TORC1. Therefore, mTORC1 and simultaneously mTORC2 inhibition seems to be an important feature of NVP-BBD130 and NVP-BEZ235 action, which in combination with PI3K inhibition efficiently interferes with tumor growth *in vivo*.

In conclusion, inhibition of the PI3K/mTOR pathway via the nmol/L dual PI3K/mTOR inhibitors NVP-BBD130 and NVP-BEZ235 efficiently attenuates growth and proliferation of melanoma primary tumors and metastasis. Moreover, these

compounds efficiently target neovascularization, and NVP-BEZ235 augmented tumor necrosis. In all, the above results encourage clinical development of this compound series and the inclusion of patients with melanoma in ongoing phase I/II studies involving NVP-BEZ235.

Materials and Methods

Cell Culture

Melanoma cells were grown at 37°C in a 5% CO_2 atmosphere in DMEM (A2058, B16F1, B16F10, C32, HBL, Malme, Malme3M, NA8, SKMel2, and SKMel23 cells) or RPMI (A375, Hs294T, WM35, and 1205lu cells) supplemented with 10% heat-inactivated FCS, 1% L-glutamine, and 1% penicillin-streptomycin (all from Sigma). B16BL6 melanoma (from Dr. J. Fidler, Cancer Biology, The University of Texas M. D. Anderson Cancer Center, Houston, TX) were cultivated in MEM EBS (AMIMED) supplemented with 5% heat-inactivated FCS, 1% of each L-glutamine, penicillin-streptomycin, sodium pyruvate, nonessential amino acids, and 2% vitamins (stock solutions from AMIMED).

Proliferation and Cell Volume

One day after plating (7×10^3 cells/cm^2), melanoma cells were exposed to LY294002 (25 μmol/L); wortmannin (500 nmol/L); NVP-BAG956, NVP-BBD130, NVP-BEZ235, and ZSTK474 (1 μmol/L); and rapamycin (100 nmol/L). Compound concentrations were set 2 log units above the IC_{50} *in vitro* to ensure full PI3K inhibition, except for the μmol/L inhibitor LY294002. Cells were trypsinized and counted, and the volume was quantified using a Casy Counter and Analyser (Innovatis AG). To determine the nuclear volume, cells were resuspended in CASYton containing 0.5% Triton X-100, followed by repetitive pipetting (8×), before volume measurements.

Immunoblotting

Total cell lysates were prepared in NP40-based lysis buffer (pH 8.0, 20 mmol/L Tris-HCl, 138 mmol/L NaCl, 2.7 mmol/L KCl, 5% glycerol, 1 mmol/L $CaCl_2$, 1 mmol/L $MgCl_2$, 1% NP40, 20 μmol/L leupeptin, 18 μmol/L pepstatin, 1 mmol/L Na-O-vanadate, 20 mmol/L NaF, and 100 μmol/L phenylmethylsulfonyl fluoride). Proteins were separated on SDS-PAGE and transferred to Immobilon FL membranes (Millipore). Primary antibodies to PTEN, $pSer^{473}$-PKB/Akt, pThr308-PKB/Akt, $pThr389\text{-}p70^{S6K}$, pSer235/236-S6, pThr32-FOXO1, pSer9-GSK3β, 4E-BP1, and pThr37/46-4E-BP1 were from Cell Signaling Technology; primary antibodies to pMAPK and MAPK were from Sigma; the primary antibody to PKB was a kind gift of E. Hirsch (Turin, Italy); and primary antibodies to cyclin D1 and $p27^{Kip1}$ were from Santa Cruz Biotechnology. Secondary antibodies (e.g., horseradish peroxidase–conjugated rabbit anti-mouse IgG and goat anti-rabbit IgG; Sigma) were visualized using enhanced chemiluminescence (Millipore), and fluorescent secondary antibodies (Alexa Fluor 680 or IRDye 800) were detected using the Odyssey IR reader (LICOR).

Cell Cycle and Apoptosis

Melanoma cells were plated (7×10^3/cm^2), and PI3K inhibitors (LY294002 at 25 μmol/L; wortmannin at 500 nmol/L; NVP-BAG956, NVP-BBD130, and NVP-BEZ235 at 1 μmol/L) were added 24 h later. After 3 d of exposure to inhibitors, cells were trypsinized and prepared for cell cycle and apoptosis analysis (50). For cell cycle evaluation, cells were fixed and permeabilized in PBS supplemented with 4% paraformaldehyde/1% bovine serum albumin/0.1% saponin for 30 min at 4°C, and subsequently washed with 1% bovine serum albumin/0.1% saponin in PBS. The pellet was resuspended in 0.1% Triton X-100/0.1% sodium citrate solution (pH 7.4) containing 50 μg/mL propidium iodide and 10 μg/mL DNase-free RNase and incubated for 8 h at 4°C

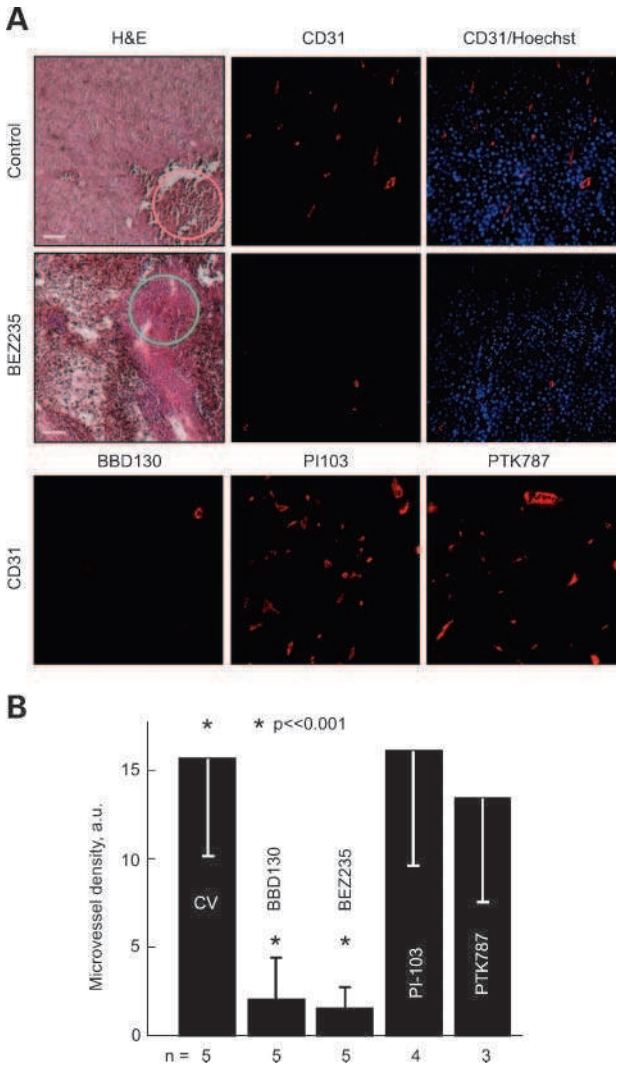

FIGURE 6. **A.** Effect of inhibitor treatment on neovascularization. Paraffin sections of metastatic tissue were stained with H&E (*left*), anti-CD31 anti-body to visualize the tumor vasculature (*red*), or Hoechst 33342 to stain nuclear DNA (*blue*). Nuclei are depicted in a picture merged with CD31 staining. **B.** Microvascular density was quantified in anti-CD31–stained slides as shown in **A**, using Hoechst staining to select regions with viable tissue (*green circle* in **A**). Necrotic tumor tissue was excluded from the evaluation (*red circle* in **A**). The number of metastases evaluated is indicated at the bottom of the graph (*n*; fields evaluated per tumor ≥4; *scale bar,* 0.1 mm).

Table 2. Effects of PI3K Inhibitors on Body, Spleen, and Liver Weights, and Glucose Levels in the B16 Mouse Melanoma Model

	Body weight (% change)	Spleen weight (mg)	Liver weight (mg)	Glucose* (mmol/L)
Healthy control	(19.3 ± 0.1 g)	73 ± 3	896 ± 34	10-15
Vehicle control	−4.5 ± 3.0	181 ± 29	869 ± 32	13.3 ± 0.7
BBD130 40 mg/kg/d	−6.6 ± 3.1	155 ± 23	821 ± 30	17.8 ± 2.4
BBD130 2 × 20 mg/kg/d	−3.7 ± 2.8	126 ± 10†	854 ± 34	12.6 ± 0.6
PI103 10 mg/kg/d	5.0 ± 2.8	219 ± 33	1,101 ± 25†	14.5 ± 1.3

NOTE: Effects of PI3K pathway inhibitors on body, spleen, and liver weights, and on glucose levels in the B16 melanoma mouse model. Mice were weighted weekly and sacrificed 13 days after initiation of treatment with the respective inhibitors for autopsy. Whole blood glucose was measured in samples drawn from the vena cava. During the experiment, the mice received water and food *ad libitum*. Data are presented as mean ± SE, $n > 6$.
*Healthy mice display normal blood glucose of 10 to 15 mmol/L, depending on their feeding status.
†$P < 0.05$ versus vehicle control group.

before fluorescence-activated cell sorting data acquisition (FACSCalibur, Becton Dickinson). Annexin V staining was done following the manufacturer's protocol (Becton Dickinson). In brief, cells were resuspended in 200 μL Annexin buffer [10 mmol/L HEPES (pH 7.4), 0.14 mol/L NaCl, 2.5 mmol/L $CaCl_2$] containing 2 μL of Cy5-labeled Annexin V (Becton Dickinson) and subsequently incubated 15 min at room temperature in the dark. Before cytometry, 2.5 μg of propidium iodide were added to the cells. Data were analyzed with FlowJo (Tree Star, Oregon Corporation).

DNA Synthesis and Thymidine Incorporation

A2058 cells were seeded in 96-well microtiter plates (2,000 per well) and 24 h later PI3K inhibitors (LY294002 at 25 μmol/L; wortmannin at 500 nmol/L; NVP-BAG956, NVP-BBD130, and NVP-BEZ235 at 1 μmol/L) were added for the indicated times. During the last 24 h of exposure to the inhibitors, 1 μCi of [^{3}H]thymidine was added per well. Subsequently, cells were harvested onto glass fiber filters using a cell harvester (FilterMate Harvester, Perkin-Elmer) and incorporated radioactivity was measured using a Perkin-Elmer MicroBeta TriLux.

Cell Cycle Synchronization

Melanoma cells were synchronized by incubation for 14 h with 1 μg/mL nocodazole in the medium described above. Subsequently, the cells were trypsinized, washed with PBS, and plated in the presence or absence of PI3K inhibitors (LY294002 at 25 μmol/L; wortmannin at 500 nmol/L; NVP-BAG956, NVP-BBD130, and NVP-BEZ235 at 1 μmol/L). The cell cycle profile was analyzed as described above.

In vivo *Mouse Melanoma Model*

B16BL6 mouse melanoma cells were grown until confluent, trypsinized, pelleted, and resuspended (50×10^6/mL) in Hanks buffer supplemented with 10% heat-inactivated FCS. Female C57BL/6 mice (Charles River) were anesthetized

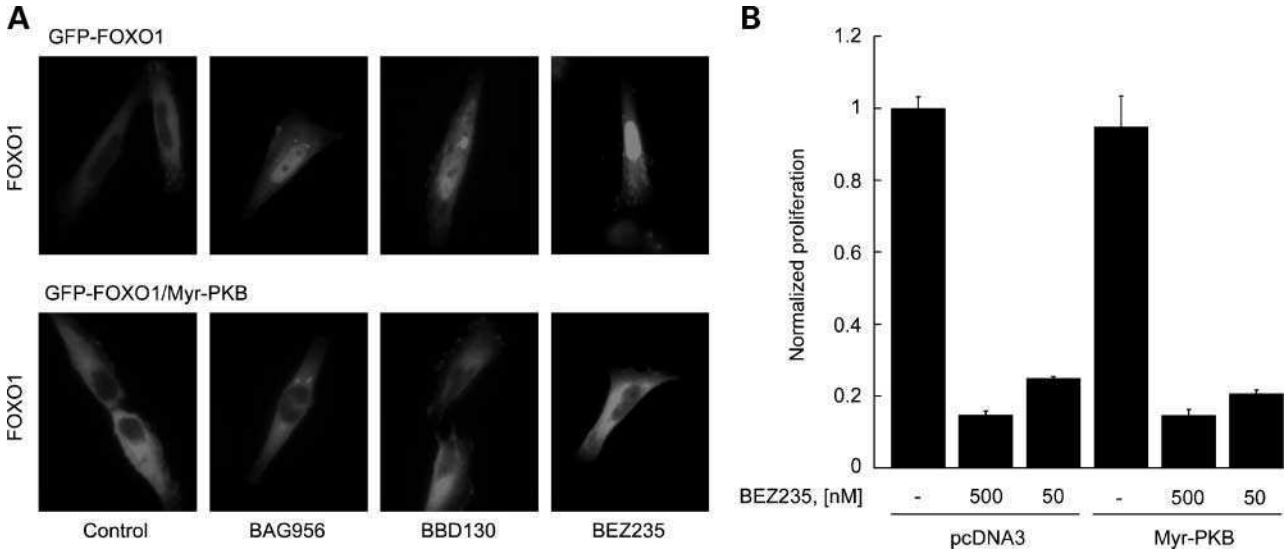

FIGURE 7. Requirement of PI3K and mTOR downstream signaling in melanoma proliferation. **A.** PI3K/PKB–dependent FOXO1 translocation to the nucleus. The localization of a GFP-FOXO1 (*red*) fusion protein was monitored in A2058 cells or A2058 cells stably expressing a myristoylated form of PKB after vehicle or the indicated PI3K inhibitors were added for 3 h. **B.** Constitutively active PKB does not rescue growth in the presence of PI3K/mTOR inhibitors. A2058 cells and A2058 cells stably expressing myristoylated PKB were ex-posed to NVP-BEZ235 for 3 d before cell numbers were determined (shown as percent of nontreated cells harboring a control plasmid). Columns, mean of triplicates; bars, SE.

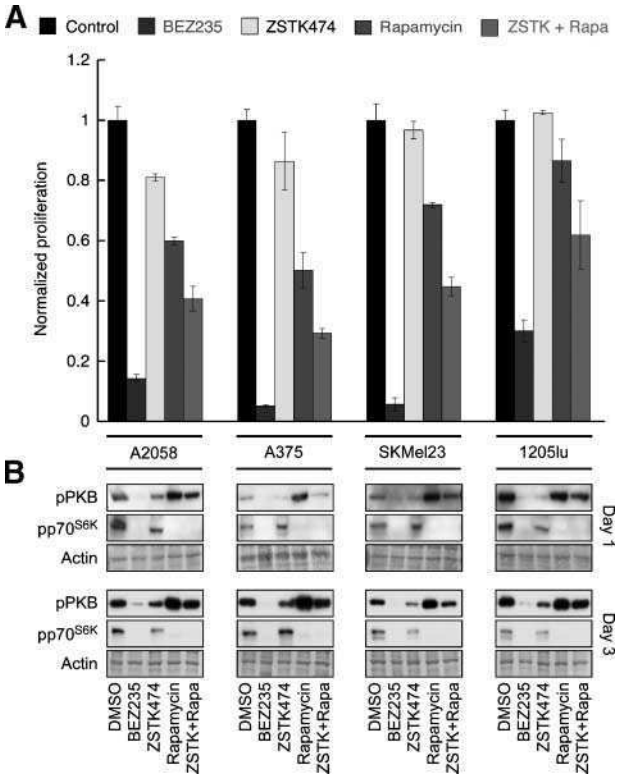

FIGURE 8. **A.** Antiproliferative effect of pan-PI3K, PI3K/mTOR, and mTOR inhibitors on melanoma cells. Melanoma cells were exposed to NVP-BEZ235 (1 μmol/L), ZSTK474 (1 μmol/L), and/or rapamycin (100 nmol/L). Proliferation was measured as above and is shown normalized to proliferation of vehicle-treated control cells. Columns, mean of triplicates; bars, SE. **B.** Changes in the phosphorylation of PKB and $p70^{S6K}$ upon PI3K and/or mTOR inhibition. Melanoma cells were exposed to inhibitors as indicated in **A** and total cell lysates were prepared 1 and 3 d later for detection of phosphorylated (Ser473) PKB and $p70^{S6K}$. Actin stained with Coomassie blue is shown as loading control.

with 3% isofluorane in O_2 (v/v) and placed on an operation table maintained at 37°C. Mouse ears were fixed with a double-sided tape over a steel cone and 1 μL of the cell suspension was injected intradermally using a microliter syringe with a 30-G needle. Primary tumor size was recorded every 7 d in mice anesthetized with isofluorane. One week after cell injection, oral treatment with vehicle control [10% NMP/PEG 300 (1-methyl-2-pyrrolidone/polyethylene glycol 300); 10:90, v/v], NVP-BBD130 (40 mg/kg daily and twice daily 20 mg/kg), NVP-BEZ235 (30 mg/kg daily and twice daily 20 mg/kg), PTK787 (100 mg/kg/d) and i.p. treatment with PI103 (2.5, 5, and 10 mg/kg/d) was started. NVP-BBD130, NVP-BEZ235, and PTK787 were dissolved by sonication in NMP and then the corresponding volume of PEG 300 was added. PI103 was instead dissolved in KZI (Cremophor EL/ethanol absolute 65:35, v/v) and the remaining volume (1:3, v/v) of 5% glucose (Braun Medical AG) was added. The inhibitors were given for the indicated period, before animals were sacrificed, and primary tumor, cervical lymph node metastases, spleen, liver, femurs, and blood (from the vena cava) were collected for further analysis.

The size of primary tumors at a given time point (=$area_t$) was determined by digital imaging as described in refs. (51, 52), and tumor progression was related to the tumor area at day 7 (=$area_{7days}$), and then expressed as percentage of the overall mean tumor size in untreated [vehicle control (VC)] animals (=mean_area_VC_{20days}). The depicted values were therefore calculated as follows:

$$\text{Primary tumor area } (\%) = [100 \times \text{area}_t/\text{area}_{7\text{d}}]/\text{mean\_area\_VC}_{20\text{d}}$$

A fraction of the primary tumors, metastases and liver samples were snap frozen in liquid nitrogen, the rest was fixed in 4% paraformaldehyde for paraffin embedding. Experiments were terminated (here at day 20) for ethical reasons.

Immunohistochemistry

Primary tumors, metastases, and liver tissues were embedded in paraffin using a Spin Tissue Processor (Microm International). Paraffin blocks were cut to 6-μm sections using the Microtome cool-cut HM355S (Microm International). For CD31 (antibody from Bachem AG) staining, tissue slides were deparaffinized using roticlean, and the antigen was unmasked by proteinase K treatment. The staining with the primary antibody was done overnight (antibody dilution 1:50). Subsequently, slides were incubated with a fluorescently labeled secondary antibody and Hoechst 33342 and mounted with crystal solution (Medite). For H&E staining, deparaffinized slides were incubated with hematoxylin solution followed by eosin and mounted with Cytoseal XYL (Medite).

Immune Cell Detection

Cell suspensions of spleen and bone marrow were generated and stained with different cell surface marker antibodies: monoclonal antibodies against CD3 (clone KT3), CD4 (RM4-5), CD8 (53-6.7), B220 (RA3-6B2), CD11b (M1/70), CD11c (HL3), GR1, and TERT were obtained from BD Biosciences PharMingen or eBioscience. The F4/80 antibody was from Serotec. Fluorescence was quantified on a FACSCalibur.

Myr-PKB Transfection and GFP-FOXO Translocation

Cells were plated at $14 \times 10^3/cm^2$, and 24 h later were transfected with 0.1 $\mu g/cm^2$ pcDNA3-GFP-FOXO1 and/or pcDNA3-Myr-PKB expression plasmids using JetPEI (Brunschwig Chemie) following the manufacturer's protocol. The following day, cells were exposed to PI3K inhibitors (LY294002 at 25 μmol/L; wortmannin at 500 nmol/L; NVP-BAG956, NVP-BBD130, NVP-BEZ235, and PI103 at 1 μmol/L) or rapamycin (100 nmol/L) for 3 h. HEK293 cells were starved overnight in serum-free DMEM before treatment with the inhibitors.

For immunofluorescence, cells plated on glass coverslips ($21 \times 10^3/cm^2$) were fixed in PBS with 4% paraformaldehyde before nuclei were stained with Hoechst 33342. Coverslips were mounted on microscopy slides in Mowiol (Clariant GMbH). Images were acquired with OpenLab software (Improvision) on an Axiovert 200 M microscope (Zeiss) with a Plan-Achromat 63×/1.4 and an Orca ER II camera (Hamamatsu).

Disclosure of Potential Conflicts of Interest

No potential conflicts of interest were disclosed.

Acknowledgments

We thank Poppy Fotiadou for the critical reading of the manuscript; Mathias M. Hauri-Hohl for help with fluorescence-activated cell sorting analysis; Priska Reinhard for excellent technical assistance; Reinhard Dummer for inspiring discussions; Reinhard Dummer, Isaiah Fidler, Silvio Hemmi, Meenhard Herlyn, Adrian Ochsenbein, and Giulio Spagnoli for the supply of cell lines; Samuel Arnal for help with the *in vivo* experiment; Natasha Cmiljanovic for the synthesis of ZSTK474; and Karen C. Arden for the GFP-FOXO1 plasmid.

References

1. Vogelstein B, Kinzler KW. Cancer genes and the pathways they control. Nat Med 2004;10:789–99.

2. Vivanco I, Sawyers CL. The phosphatidylinositol 3-Kinase AKT pathway in human cancer. Nat Rev Cancer 2002;2:489–501.

3. Wymann MP, Marone R. Phosphoinositide 3-kinase in disease: timing, location, and scaffolding. Curr Opin Cell Biol 2005;17:141–9.

4. Engelman JA, Luo J, Cantley LC. The evolution of phosphatidylinositol 3-kinases as regulators of growth and metabolism. Nat Rev Genet 2006;7: 606–19.

5. Raftopoulou M, Hall A. Cell migration: Rho GTPases lead the way. Dev Biol 2004;265:23–32.

6. Bhaskar PT, Hay N. The two TORCs and Akt. Dev Cell 2007;12:487–502.

7. Samuels Y, Ericson K. Oncogenic PI3K and its role in cancer. Curr Opin Oncol 2006;18:77–82.

8. Omholt K, Krockel D, Ringborg U, Hansson J. Mutations of PIK3CA are rare in cutaneous melanoma. Melanoma Res 2006;16:197–200.

9. Curtin JA, Stark MS, Pinkel D, Hayward NK, Bastian BC. PI3-kinase subunits are infrequent somatic targets in melanoma. J Invest Dermatol 2006;126: 1660–3.

10. Stark M, Hayward N. Genome-wide loss of heterozygosity and copy number analysis in melanoma using high-density single-nucleotide polymorphism arrays. Cancer Res 2007;67:2632–42.

11. Guldberg P, thor Straten P, Ahrenkiel V, Seremet T, Kirkin AF, Zeuthen J. Somatic mutation of the Peutz-Jeghers syndrome gene, LKB1/STK11, in malignant melanoma. Oncogene 1999;18:1777–80.

12. Meier F, Busch S, Lasithiotakis K, et al. Combined targeting of MAPK and AKT signalling pathways is a promising strategy for melanoma treatment. Br J Dermatol 2007;.

13. Eisen T, Ahmad T, Flaherty KT, et al. Sorafenib in advanced melanoma: a Phase II randomised discontinuation trial analysis. Br J Cancer 2006;95: 581–6.

14. Ratain MJ, Eisen T, Stadler WM, et al. Phase II placebo-controlled randomized discontinuation trial of sorafenib in patients with metastatic renal cell carcinoma. J Clin Oncol 2006;24:2505–12.

15. Margolin K, Longmate J, Baratta T, et al. CCI-779 in metastatic melanoma: a phase II trial of the California Cancer Consortium. Cancer 2005;104: 1045–8.

16. Hu L, Zaloudek C, Mills GB, Gray J, Jaffe RB. *In vivo* and *in vitro* ovarian carcinoma growth inhibition by a phosphatidylinositol 3-kinase inhibitor (LY294002). Clin Cancer Res 2000;6:880–6.

17. Wymann MP, Zvelebil M, Laffargue M. Phosphoinositide 3-kinase signalling—which way to target? Trends Pharmacol Sci 2003;24:366–76.

18. Liu Y, Jiang N, Wu J, Dai W, Rosenblum JS. Polo-like kinases inhibited by wortmannin. Labeling site and downstream effects. J Biol Chem 2007;282: 2505–11.

19. Fan QW, Knight ZA, Goldenberg DD, et al. A dual PI3 kinase/mTOR inhibitor reveals emergent efficacy in glioma. Cancer Cell 2006;9:341–9.

20. Raynaud FI, Eccles S, Clarke PA, et al. Pharmacologic characterization of a potent inhibitor of class I phosphatidylinositide 3-kinases. Cancer Res 2007;67: 5840–50.

21. Chen JS, Zhou LJ, Entin-Meer M, et al. Characterization of structurally distinct, isoform-selective phosphoinositide 3′-kinase inhibitors in combination with radiation in the treatment of glioblastoma. Mol Cancer Ther 2008;7: 841–50.

22. Yaguchi S, Fukui Y, Koshimizu I, et al. Antitumor activity of ZSTK474, a new phosphatidylinositol 3-kinase inhibitor. J Natl Cancer Inst 2006;98: 545–56.

23. Kong D, Yamori T. ZSTK474 is an ATP-competitive inhibitor of class I phosphatidylinositol 3 kinase isoforms. Cancer Sci 2007;98:1638–42.

24. Casagrande F, Bacqueville D, Pillaire MJ, et al. G1 phase arrest by the phosphatidylinositol 3-kinase inhibitor LY 294002 is correlated to up-regulation of p27Kip1 and inhibition of G1 CDKs in choroidal melanoma cells. FEBS Lett 1998;422:385–90.

25. Blanco-Aparicio C, Pequeno B, Moneo V, et al. Inhibition of phosphatidylinositol-3-kinase synergizes with gemcitabine in low-passage tumor cell lines correlating with Bax translocation to the mitochondria. Anticancer Drugs 2005;16: 977–87.

26. Smalley KS, Haass NK, Brafford PA, Lioni M, Flaherty KT, Herlyn M. Multiple signaling pathways must be targeted to overcome drug resistance in cell lines derived from melanoma metastases. Mol Cancer Ther 2006;5: 1136–44.

27. Bedogni B, Welford SM, Kwan AC, Ranger-Moore J, Saboda K, Powell MB. Inhibition of phosphatidylinositol-3-kinase and mitogen-activated protein kinase kinase 1/2 prevents melanoma development and promotes melanoma regression in the transgenic TPRas mouse model. Mol Cancer Ther 2006;5: 3071–7.

28. Maira SM, Stauffer F, Brueggen J, et al. Identification and characterization of NVP-BEZ235, a new orally available dual phosphatidylinositol 3-kinase/mammalian target of rapamycin inhibitor with potent *in vivo* antitumor activity. Mol Cancer Ther 2008;.

29. Stauffer F, Maira SM, Furet P, Garcia-Echeverria C. Imidazo[4,5-c]quinoline as inhibitors of the PI3K/PKB-pathway. Bioorg Med Chem Lett 2007;.

30. Lin J, Adam RM, Santiestevan E, Freeman MR. The phosphatidylinositol 3′-kinase pathway is a dominant growth factor-activated cell survival pathway in LNCaP human prostate carcinoma cells. Cancer Res 1999;59:2891–7.

31. Wen Y, Hu MC, Makino K, et al. HER-2/neu promotes androgen-independent survival and growth of prostate cancer cells through the Akt pathway. Cancer Res 2000;60:6841–5.

32. Carson JP, Kulik G, Weber MJ. Antiapoptotic signaling in LNCaP prostate cancer cells: a survival signaling pathway independent of phosphatidylinositol 3′-kinase and Akt/protein kinase B. Cancer Res 1999;59:1449–53.

33. Andjelkovic M, Alessi DR, Meier R, et al. Role of translocation in the activation and function of protein kinase B. J Biol Chem 1997;272:31515–24.

34. Huang H, Tindall DJ. Dynamic FoxO transcription factors. J Cell Sci 2007; 120:2479–87.

35. van der Horst A, Burgering BM. Stressing the role of FoxO proteins in lifespan and disease. Nat Rev Mol Cell Biol 2007;8:440–50.

36. Ruckle T, Schwarz MK, Rommel C. PI3Kγ inhibition: towards an 'aspirin of the 21st century'? Nat Rev Drug Discov 2006;5:903–18.

37. Marone R, Cmiljanovic V, Giese B, Wymann MP. Targeting phosphoinositide 3-kinase—moving towards therapy. Biochim Biophys Acta 2007;.

38. Smalley KS, Lioni M, Dalla Palma M, et al. Increased cyclin D1 expression can mediate BRAF inhibitor resistance in BRAF V600E-mutated melanomas. Mol Cancer Ther 2008;7:2876–83.

39. Hussein MR. Tumour-infiltrating lymphocytes and melanoma tumorigenesis: an insight. Br J Dermatol 2005;153:18–21.

40. Sarbassov DD, Guertin DA, Ali SM, Sabatini DM. Phosphorylation and regulation of Akt/PKB by the rictor-mTOR complex. Science 2005;307:1098–101.

41. Feng J, Park J, Cron P, Hess D, Hemmings BA. Identification of a PKB/Akt hydrophobic motif Ser-473 kinase as DNA-dependent protein kinase. J Biol Chem 2004;279:41189–96.

42. Bozulic L, Surucu B, Hynx D, Hemmings BA. PKBα/Akt1 acts downstream of DNA-PK in the DNA double-strand break response and promotes survival. Mol Cell 2008;30:203–13.

43. Anand P, Gruppuso PA. Rapamycin inhibits liver growth during refeeding in rats via control of ribosomal protein translation but not cap-dependent translation initiation. J Nutr 2006;136:27–33.

44. Hanahan D, Weinberg RA. The hallmarks of cancer. Cell 2000;100:57–70.

45. Phung TL, Ziv K, Dabydeen D, et al. Pathological angiogenesis is induced by sustained Akt signaling and inhibited by rapamycin. Cancer Cell 2006;10: 159–70.

46. Del Bufalo D, Ciuffreda L, Trisciuoglio D, et al. Antiangiogenic potential of the mammalian target of rapamycin inhibitor temsirolimus. Cancer Res 2006;66: 5549–54.

47. Skinner HD, Zheng JZ, Fang J, Agani F, Jiang BH. Vascular endothelial growth factor transcriptional activation is mediated by hypoxia-inducible factor 1α, HDM2, and p70S6K1 in response to phosphatidylinositol 3-kinase/AKT signaling. J Biol Chem 2004;279:45643–51.

48. Wang X, Yue P, Chan CB, et al. Inhibition of mammalian target of rapamycin induces phosphatidylinositol 3-kinase-dependent and Mnk-mediated eukaryotic translation initiation factor 4E phosphorylation. Mol Cell Biol 2007;27:7405–13.

49. Li W, Petrimpol M, Molle KD, Hall MN, Battegay EJ, Humar R. Hypoxia-induced endothelial proliferation requires both mTORC1 and mTORC2. Circ Res 2007;100:79–87.

50. Rolink AG, Andersson J, Melchers F. Characterization of immature B cells by a novel monoclonal antibody, by turnover and by mitogen reactivity. Eur J Immunol 1998;28:3738–48.

51. Rudin M, McSheehy PM, Allegrini PR, et al. PTK787/ZK222584, a tyrosine kinase inhibitor of vascular endothelial growth factor receptor, reduces uptake of the contrast agent GdDOTA by murine orthotopic B16/BL6 melanoma tumours and inhibits their growth *in vivo*. NMR Biomed 2005;18:308–21.

52. Sini P, Samarzija I, Baffert F, et al. Inhibition of multiple vascular endothelial growth factor receptors (VEGFR) blocks lymph node metastases but inhibition of VEGFR-2 is sufficient to sensitize tumor cells to platinum-based chemotherapeutics. Cancer Res 2008;68:1581–92.

53. Garcia-Echeverria C, Pearson MA, Marti A, et al. *In vivo* antitumor activity of NVP-AEW541—a novel, potent, and selective inhibitor of the IGF-IR kinase. Cancer Cell 2004;5:231–9.

54. Knight ZA, Gonzalez B, Feldman ME, et al. A pharmacological map of the PI3-K family defines a role for p110α in insulin signaling. Cell 2006;125:733–47.

A

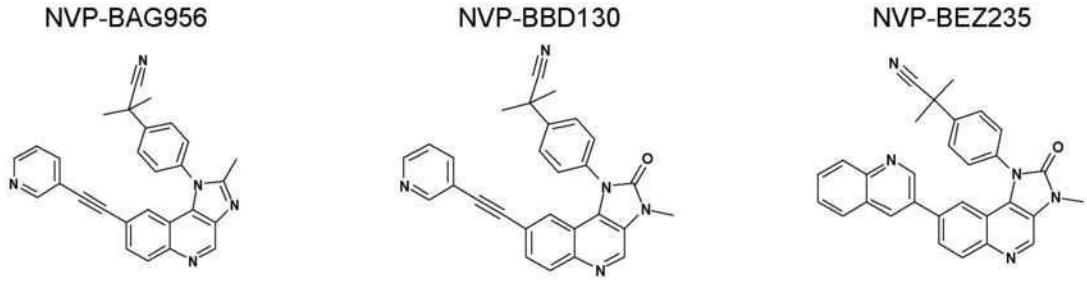
NVP-BAG956
NVP-BBD130
NVP-BEZ235

B

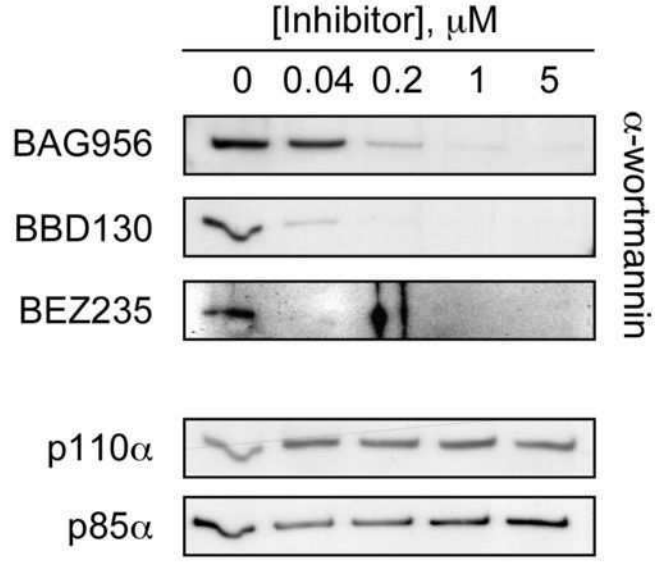
[Inhibitor], μM
0 0.04 0.2 1 5
BAG956
BBD130
BEZ235
α-wortmannin
p110α
p85α

A

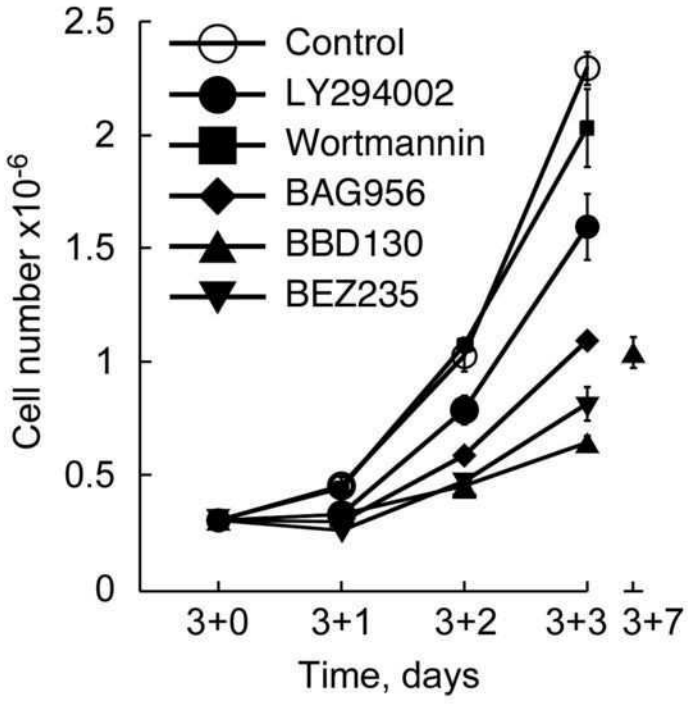
Control
LY294002
Wortmannin
BAG956
BBD130
BEZ235
Cell number x10-6
2.5
2
1.5
1
0.5
0
3+0
3+1
3+2
3+3
3+7
Time, days

B

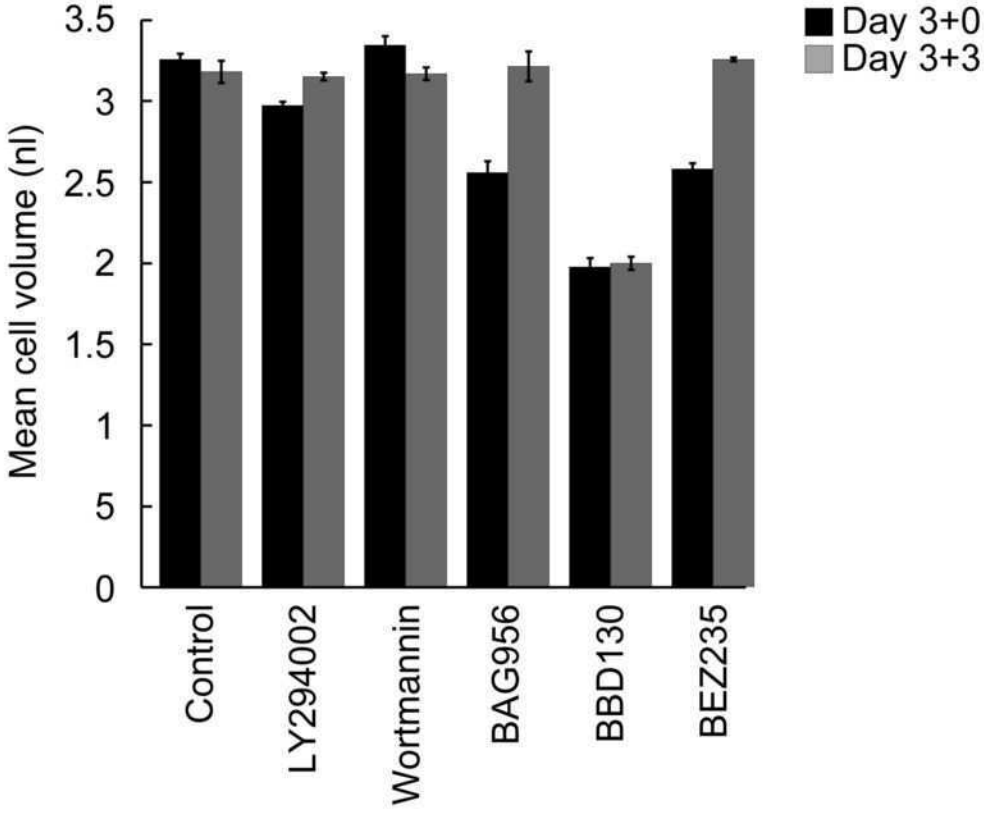
Day 3+0
Day 3+3
Mean cell volume (nl)
3.5
3
2.5
2
1.5
1
5
0
Control
LY294002
Wortmannin
BAG956
BBD130
BEZ235

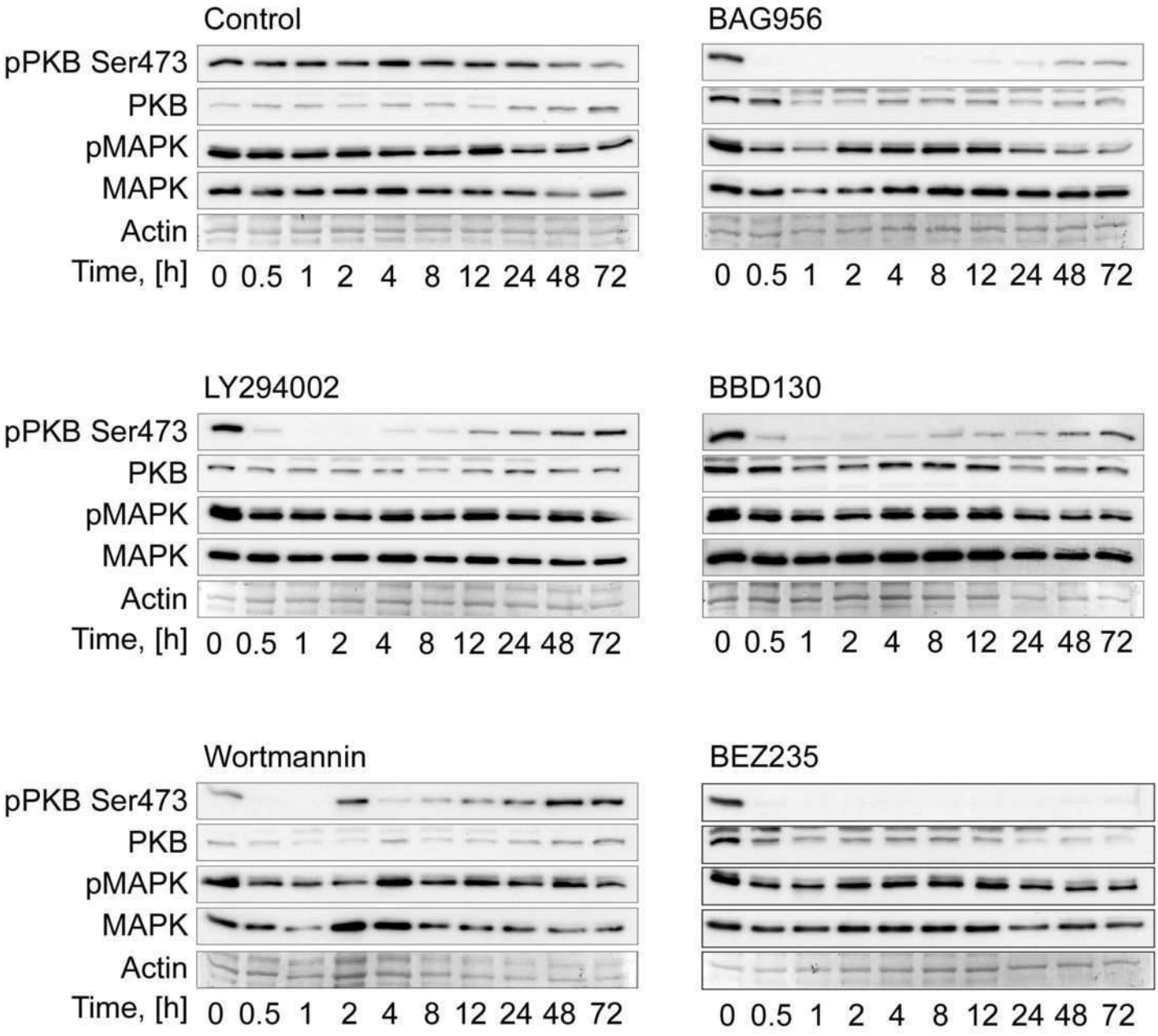
Control
pPKB Ser473
PKB
pMAPK
MAPK
Actin
Time, [h] 0 0.5 1 2 4 8 12 24 48 72
BAG956
0 0.5 1 2 4 8 12 24 48 72
LY294002
pPKB Ser473
PKB
pMAPK
MAPK
Actin
Time, [h] 0 0.5 1 2 4 8 12 24 48 72
BBD130
0 0.5 1 2 4 8 12 24 48 72
Wortmannin
pPKB Ser473
PKB
pMAPK
MAPK
Actin
Time, [h] 0 0.5 1 2 4 8 12 24 48 72
BEZ235
0 0.5 1 2 4 8 12 24 48 72

A

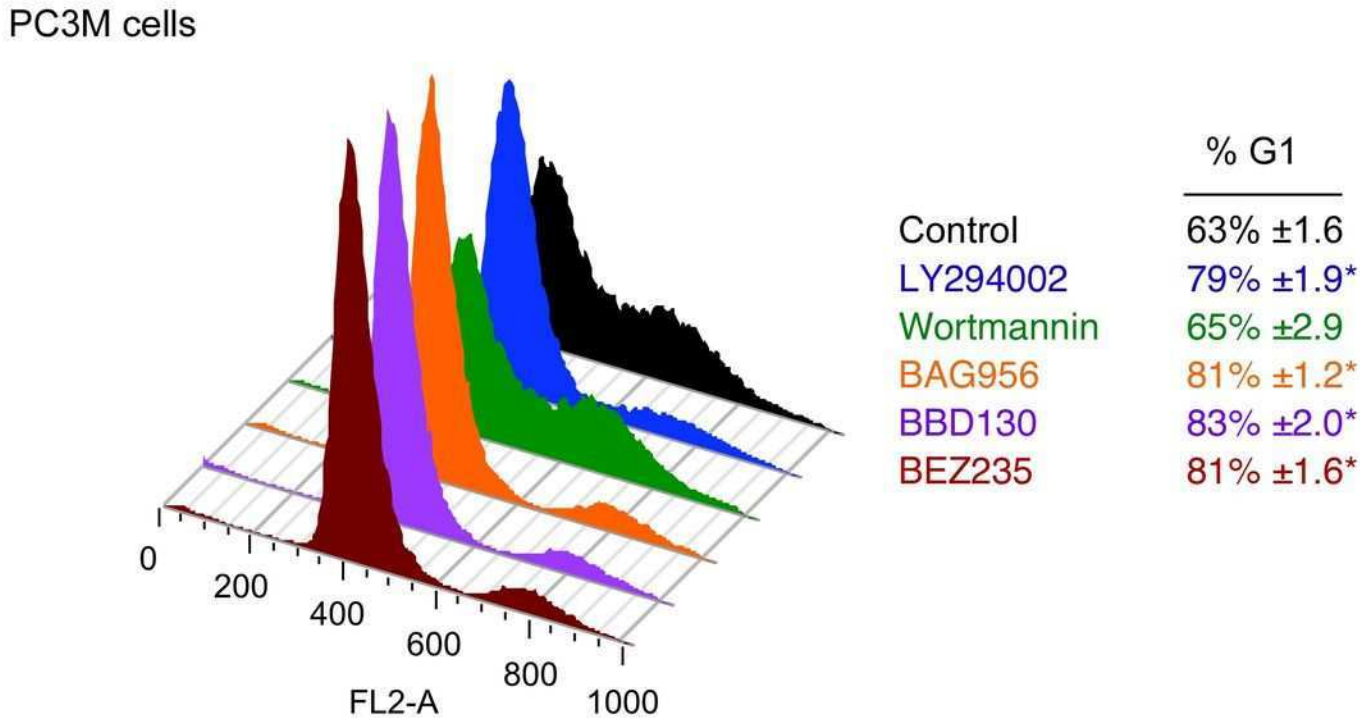
PC3M cells
0
200
400
600
800
1000
FL2-A
% G1
Control 63% ±1.6
LY294002 79% ±1.9*
Wortmannin 65% ±2.9
BAG956 81% ±1.2*
BBD130 83% ±2.0*
BEZ235 81% ±1.6*

B

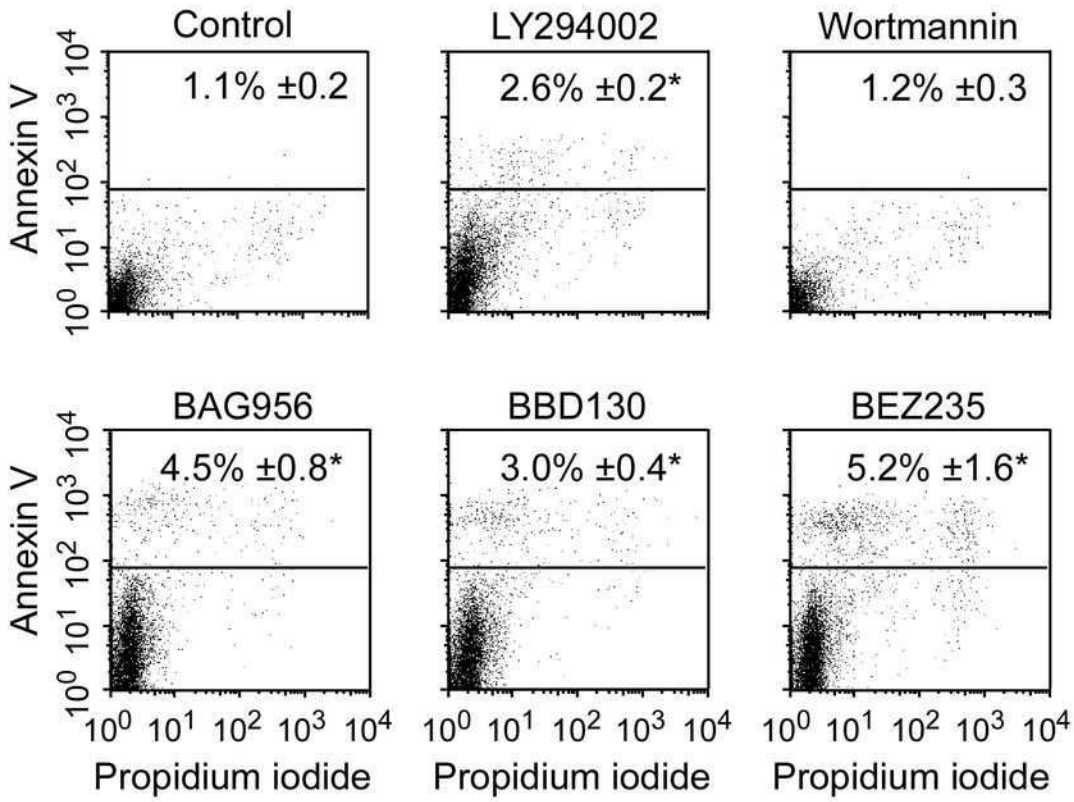
Control
1.1% ±0.2
LY294002
2.6% ±0.2*
Wortmannin
1.2% ±0.3
BAG956
4.5% ±0.8*
BBD130
3.0% ±0.4*
BEZ235
5.2% ±1.6*
Annexin V
Propidium iodide
10^0 10^1 10^2 10^3 10^4

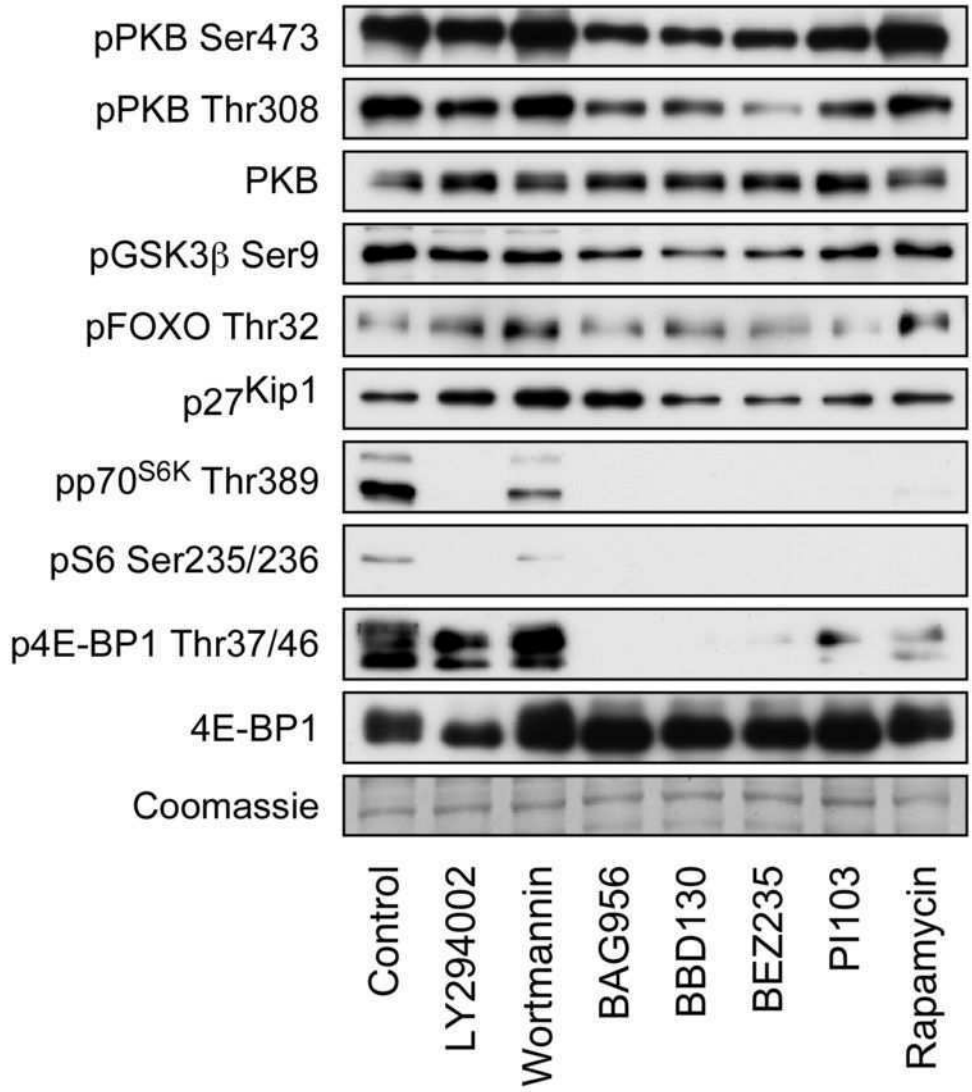
pPKB Ser473
pPKB Thr308
PKB
pGSK3β Ser9
pFOXO Thr32
p27Kip1
pp70S6K Thr389
pS6 Ser235/236
p4E-BP1 Thr37/46
4E-BP1
Coomassie
Control
LY294002
Wortmannin
BAG956
BBD130
BEZ235
PI103
Rapamycin

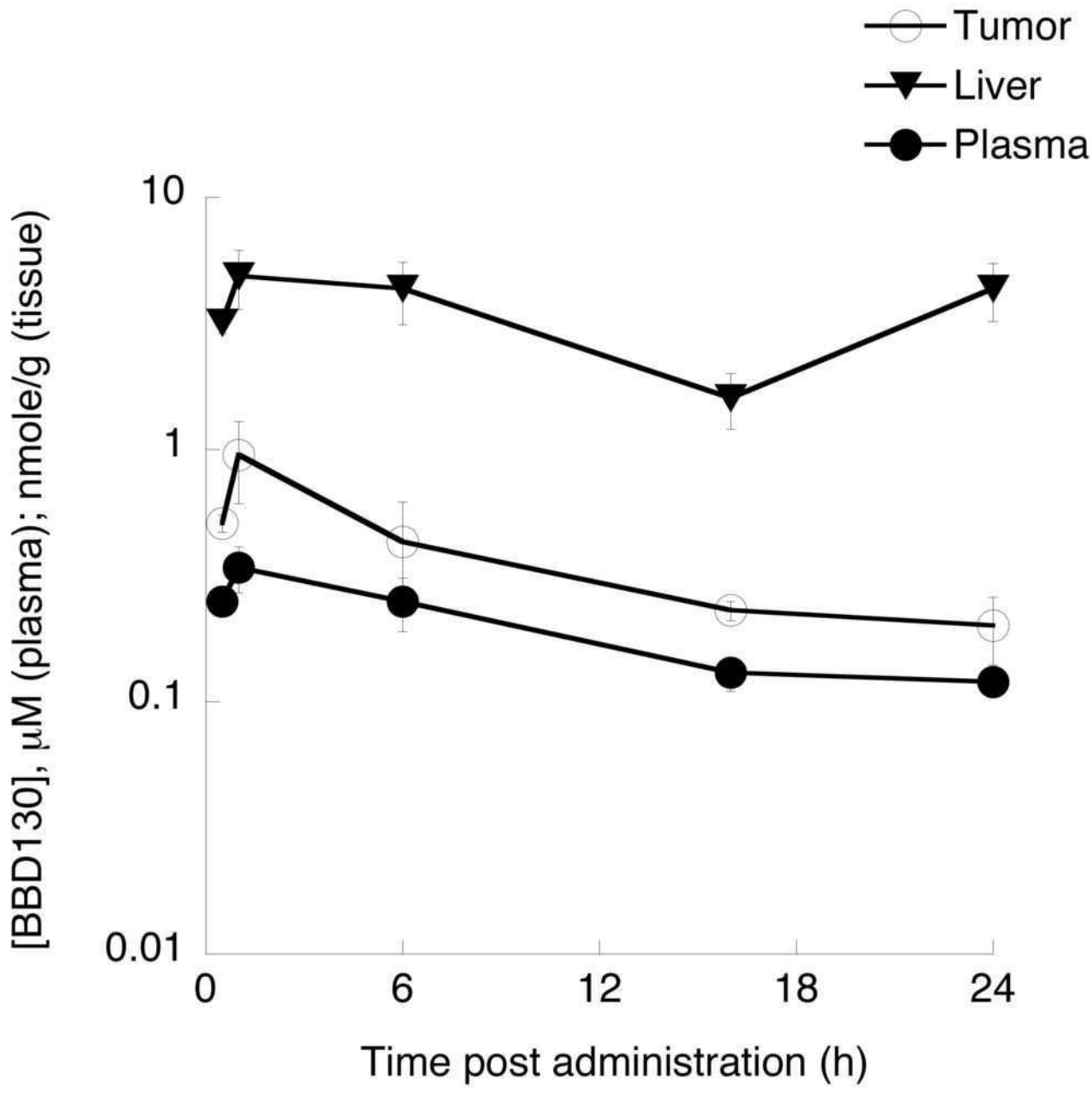
Tumor
Liver
Plasma
10
1
0.1
0.01
[BBD130], μM (plasma); nmole/g (tissue)
0
6
12
18
24
Time post administration (h)

Supplementary Information for

Targeting Melanoma with Dual PI3K/mTOR Inhibitors

Romina Marone[1], Dominik Erhart[1], Thomas Bohnacker[1], Christian Schnell[2], Vladimir Cmiljanovic[3], Frédéric Stauffer[2], Carlos Garcia-Echeverria[2], Bernd Giese[3], Sauveur-Michel Maira[2], Matthias P. Wymann[1]

[1]Inst. Biochemistry and Genetics, Dept. for Biomedicine, Mattenstrasse 28, University of Basel, CH-4058 Basel, Switzerland; [2]Novartis Institutes for Biomedical Research, Oncology Disease Area, CH-4002 Basel, Switzerland; [3]Dept. of Chemistry, University of Basel, CH-4058 Basel, Switzerland.

To whom correspondence should be addressed:

Matthias P. Wymann

Inst. Biochemistry and Genetics

Dept. of Biomedicine

Mattenstrasse 28

CH-4058 Basel, Switzerland

Tel. +41 61 695 3046; Fax. +41 61 267 3566; Matthias.Wymann@UniBas.CH

Supplementary Experimental Procedures

Wortmannin-competition assay

Recombinant p110α/p85α protein complex (Millipore) was pre-incubated with the indicated concentrations of NVP-BBD130, NVP-BAG956 or NVP-BEZ235 at 37°C for 30 min., before the samples were transferred to ice and wortmannin (200 nM) was added for 15 min. Protein samples (0.13 µg / lane) were subjected to SDS-PAGE and blotted onto a PVDF membrane. Immunological detection of wortmannin covalently attached to p110α was achieved using polyclonal rabbit α-wortmannin antibodies (1). Loading controls for p110α and p85α were performed using monoclonal anti-p110α (kindly obtained from A. Klippel) and polyclonal anti-p85a antibodies (1).

Supplementary Figure Legends

Figure S1.

A: Chemical structures of NVP-BAG956, NVP-BBD130 and NVP-BEZ235.

B: Wortmannin competition assay.

Covalent binding of wortmannin to PI3Kα (p85α/p110α complex) was prevented by pre-incubation of recombinant PI3Kα complex with the depicted PI3K inhibitors. The PI3K complex was incubated with increasing concentrations of NVP-BAG956, NVP-BBD130 or NVP-BEZ235, before wortmannin was added, and samples were subsequently subjected to SDS-PAGE and immunodetection of protein-bound wortmannin, p110α and p85α.

Figure S2. A and B: A2058 cell were treated for 3 days with PI3K inhibitors. Cells were subsequently trypsinized, washed once with PBS and replated at the same concentration. Cell number and cell volume were measured for up to 7 days (for NVP-BBD130 treated cells) in the absence of PI3K inhibitors. Data are means of triplicates ± SEM.

Figure S3. Changes in the levels of phosphorylated PKB and MAPK in A2058 cells treated with PI3K inhibitors.

Cells were treated with different PI3K inhibitors and total cell lysates were prepared at different time intervals. Levels of phosphorylated and total PKB (upper band seen in some panels is a non-specific interaction) and MAPK were detected by western blotting. Coomassie blue-stained actin served as loading control.

Figure S4. Effect of PI3K inhibition on cell cycle profile and apoptosis.

A: Determination of cell cycle profile of the prostate cancer cell line PC3M. The cells were exposed to one dose of PI3K inhibitors for three days. Cell cycle profile was evaluated by FACS. *$p<0.002$

B: Evaluation of apoptosis in A2058 cells upon PI3K inhibition. A2058 melanoma cells were treated for 3 days with PI3K inhibitors. Annexin V positive cells were visualized by FACS. *$p<0.002$

Figure S5. Effect of expression of Myr-PKB (constitutively active PKB/Akt) on serum-deprived and inhibitor-treated HEK293 cells. HEK293 cells expressing Myr-PKB were exposed for 2 hours to the indicated PI3K inhibitors and rapamycin. Phosphoproteins in total cell lysates were detected by western blotting using the antibodies described in the main text (see Experimental Procedures).

Figure S6. Pharmacokinetic/pharmacodynamic relationship for BBD130. Mice bearing a PC3M tumor were treated orally once with a dose of 50 mg/kg BBD130. The animals were then sacrificed after 0.5, 1, 6, 16 and 24 hours after treatment and tumor, liver and plasma were collected (n=4). The concentration of the inhibitor in these tissues was quantified using a reverse-phase high performance liquid chromatography/UV (for a detailed protocol see Maira et al. (2)).

Table S1: PTEN, BRaf, NRas and p53 status in melanoma cells.

Protein levels / Mutation	PTEN	BRaf	NRas	p53
A2058	- mut	V600E	wt	++ V274F
A375	+ wt	V600E	wt	+ wt
B16F1	+	wt		(+)
B16F10	+	wt	wt	(+) wt
C32	- mut	V600E	wt	+++ wt
Hs294T	-			++
Malme	++ wt	V600E	wt	(+) wt
Malme3M	+ wt	wt		+
SKMel2	+ wt	wt	Q61R	+++ G245S
SKMel23	- mut	wt	wt	+
WM35	(+)	V600E	wt	+
1205lu	-	V600E	wt	+
Melanocytes	++++ wt	wt	wt	(+) wt

Status of signaling proteins in human melanocytes, and human and mouse melanoma cells used here are shown. PTEN protein expression levels and mutations in PTEN, BRaf, NRas and p53 are depicted. Total cell lysates were analyzed by immuno-blotting for PTEN and p53. Mutations in PTEN, BRaf, NRas and p53 were identified earlier (public data base of the Sanger Institute; for B16F1 and F10 see (3); for SKMel23 and Malme see (4, 5); for WM35 and 1205lu see (6)). mut = mutated; wt = wild type.

Table S2: PI3K inhibitor action on melanoma cell proliferation and apoptosis.

A) Cells arrested in G1, % of total cell number

	Control	LY294002	Wortmannin	BAG956	BBD130	BEZ235
A375	60±4.0	71±6.4	56±2.4	73±2.6*	75±2.5*	71±4.5
B16BL6	66±1.5	74±0.8*	64±1.9	73±0.5*	75±0.8*	76±1.0*
C32	45±4.4	45±1.1	40±2.2	45±1.3	44±1.3	39±2.7
SKMel23	56±2.1	58±2.5	58±2.0	80±2.1*	77±3.1*	80±5.5*

B) Annexin V positive cells, % of total cell number

	Control	LY294002	Wortmannin	BAG956	BBD130	BEZ235
A375	0.4±0.1	1.6±0.2	0.5±0.3	0.4±0.1	0.4±0.1	0.4±0.01
B16BL6	1.3±0.3	7.1±1.3*	1.5±0.3	3.1±0.9	4.4±1.1*	6.6±0.04*
C32	0.4±0.1	0.9±0.4	0.7±0.4	1.3±0.5	2.2±0.7	2.9±0.1*
SKMel23	1.1±0.2	1.8±0.4	0.9±0.2	4.4±0.9*	4.5±0.6*	8.0±2.2*

Melanoma cells were exposed to a single dose of the indicated PI3K inhibitor for 3 days. The cells were trypsinized, and stained with propidium iodide for cell cycle analysis (A) or with annexin V and propidium iodide for apoptosis measurement (B). The data were acquired on a FACS Calibur. The results are presented as mean ± SEM, $n>3$ (difference versus untreated control: *: $p<0.05$).

Table S3: Effects of PI3K inhibition on mouse liver enzymes and proteins.

	Healthy control	Vehicle control	BBD130 40mg/kg	BBD130 2x20mg/kg	PI103 10mg/kg
ASAT (U/l)	56.7±8.2	328.4±83.4	625.5±154.7	313.7±64.9	329.7±148.8
ALAT (U/l)	22.0±2.89	35.6±8.6	198.2±58.1*	137.7±29.6*	62.0±18.2
GGT (U/l)	1.0±0	6.4±1.5	6.0±1.0	4.5±1.3	5.5±2.7
LDH (U/l)	229±11.1	2392±449.2	2137±287.9	1310±233.82	4819±3205.2
CPK (U/l)	99.7±27.4	328.2±189.6	367.7±163.7	395.7±137.4	121.7±21.4
Cholesterol (mmol/l)	1.72±0.23	2.03±0.24	3.22±0.45	3.85±1.0*	1.82±0.13
HDL (mmol/l)	1.60±0.26	1.44±0.14	1.68±0.28	1.55±0.31	1.09±0.11
Albumin (g/l)	35.57±0.75	32.90±2.1	36.35±3.3	33.10±1.5	37.23±1.97
Total protein (g/l)	51.20±0.32	45.68±3.2	49.55±5.3	49.13±2.7	48.87±3.96

Mouse blood was taken from the *vena cava*, and serum was prepared. Diagnostic (liver) markers present in serum were analyzed according to the standard hospital serological protocols (kindly processed at the University Children's Hospital Basel, UKBB). Data are presented as mean ± SEM, n>4 (*: $p<0.05$ versus vehicle control group).

Table S4: Effects of PI3K inhibition on the frequency of immune cells in the spleen and bone marrow.

A) Immune cells in the spleen

	Healthy control	Vehicle control	BBD130 40mg/kg	BBD130 2x20mg/kg	PI103 10mg/kg
CD3	23.9±5.0	12.5±4.9	7.3±4.4	10.0±2.6	16.8±1.1
CD4	16.5±3.8	7.5±3.7	3.9±2.5	5.7±1.7	10.7±0.5
CD8	5.8±0.8	4.0±1.3	2.7±1.8	3.6±1.0	4.7±0.2
B220	53.9±4.3	34.1±8.9	19.5±6.2	25.4±7.7	44.3±11.3
NK 1.1	3.1±1.5	2.4±0.7	1.5±0.5	2.0±0.6	3.6±0.7
F4/80	8.9±1.7	52.0±47.4	70.6±46.8	28.4±16.8	38.5±11.6
CD11b	4.4±0.9	4.9±0.6	4.0±1.6	3.5±1.5	7.0±0.8*
Gr1	1.3±0.7	1.7±0.5	1.5±0.8	1.0±0.7	2.5±0.3

B) Immune cells in bone marrow

	Healthy control	Vehicle control	BBD130 40mg/kg	BBD130 2x20mg/kg	PI103 10mg/kg
B220	24.8±0.3	10.6±11.2	7.9±2.3	11.7±7.9	17.5±3.8
Gr1	29.9±1.7	22.2±5.4	30.4±9.3	26.7±6.6	33.5±4.3*
F4/80	44.6±5.4	65.0±9.9	56.3±5.1	53.6±1.8	53.6±3.5
TER119	41.2±2.0	62.7±14.0	55.3±12.2	56.8±12.6	45.3±5.8

Spleens and femurs of mice treated as indicated were collected at the end of the experiment (see Fig. 3), and cell suspensions were prepared. The cells were incubated with antibodies against different cell type-specific markers. Relative cell numbers were determined on a FACS Calibur. The data are expressed in million cells per spleen or bone marrow and are mean of triplicates ± SEM (*: $p<0.05$ versus vehicle control group).

Supplementary References:

1. Wymann MP, Bulgarelli-Leva G, Zvelebil MJ et al. Wortmannin inactivates phosphoinositide 3-kinase by covalent modification of Lys-802, a residue involved in the phosphate transfer reaction. Mol Cell Biol 1996;16:1722-33.
2. Maira SM, Stauffer F, Brueggen J et al. Identification and characterization of NVP-BEZ235, a new orally available dual phosphatidylinositol 3-kinase/mammalian target of rapamycin inhibitor with potent in vivo antitumor activity. Mol Cancer Ther 2008
3. Melnikova VO, Bolshakov SV, Walker C, Ananthaswamy HN. Genomic alterations in spontaneous and carcinogen-induced murine melanoma cell lines. Oncogene 2004;23:2347-56.
4. Tsao H, Zhang X, Fowlkes K, Haluska FG. Relative reciprocity of NRAS and PTEN/MMAC1 alterations in cutaneous melanoma cell lines. Cancer Res 2000;60:1800-4.
5. Tsao H, Goel V, Wu H, Yang G, Haluska FG. Genetic interaction between NRAS and BRAF mutations and PTEN/MMAC1 inactivation in melanoma. J Invest Dermatol 2004;122:337-41.
6. Smalley KS, Contractor R, Haass NK et al. Ki67 expression levels are a better marker of reduced melanoma growth following MEK inhibitor treatment than phospho-ERK levels. Br J Cancer 2007;96:445-9.

European Journal of Pharmaceutical Sciences 40 (2010) 143–147

Contents lists available at ScienceDirect

European Journal of Pharmaceutical Sciences

journal homepage: www.elsevier.com/locate/ejps

(*E*,*Z*)-3-(3′,5′-Dimethoxy-4′-hydroxy-benzylidene)-2-indolinone blocks mast cell degranulation

S. Kiefer[a], A.C. Mertz[b], A. Koryakina[a], M. Hamburger[a,*], P. Küenzi[a]

[a] *Institute of Pharmaceutical Biology, University of Basel, Klingelbergstrasse 50, 4056 Basel, Switzerland*
[b] *Institute of Biochemistry and Genetics, Department of Biomedicine, University of Basel, Mattenstrasse 28, 4058 Basel, Switzerland*

ARTICLE INFO

Article history:
Received 15 January 2010
Accepted 20 March 2010
Available online 27 March 2010

Keywords:
Isatis tinctoria
Woad
Degranulation
Granule exocitosis
Indolinone
Mast cells

ABSTRACT

(*E*,*Z*)-3-(3′,5′-Dimethoxy-4′-hydroxy-benzylidene)-2-indolinone (indolinone) is an alkaloid that has been identified as a pharmacologically active compound in extracts of the traditional anti-inflammatory herb *Isatis tinctoria*. Indolinone has been shown to inhibit compound 48/80-induced mast cell degranulation in vitro. Application of indolinone to bone marrow derived mast cells showed that it was uniformly distributed in the cytoplasm and that cellular uptake was terminated within minutes. Pre-treatment of IgE-sensitized mast cells with 100 nM indolinone rendered them insensitive against FcεRI-receptor dependent degranulation. However, upstream signalling induced by antigen such as activation of PI3-K and MAPK remained unaffected. We conclude that indolinone blocks mast cell degranulation at the level of granule exocitosis with an IC_{50} of 54 nm.

1. Introduction

Isatis tinctoria (woad) is an ancient European dye and medicinal plant. It has traditionally been used as a source of indigo for blue dye and as anti-inflammatory medicine (Danz, 2000). In China, the closely related *Isatis indigotica* is monographed in the Chinese Pharmacopoeia where it is indicated as a treatment for inflammation. Natural indigo, obtained by processing of various indigo plants, is used in traditional Chinese medicine to treat inflamed skin, intestines or mucosa (Stöger, 1999–2009). We confirmed the anti-inflammatory and anti-allergic potential of lipophilic *I. tinctoria* leaf extracts some years ago in a pharmacological profiling involving some 20 clinically relevant targets (Danz, 2000; Hamburger, 2002), and later in several in vivo models for inflammation and allergy, and in a clinical pilot study for topical application (Heinemann et al., 2004; Recio et al., 2006a,b).

Several pharmacologically active constituents of woad have been identified, such as tryptanthrin, indirubin, α-linoleic acid, and (*E*,*Z*)-3-(3′,5′-dimethoxy-4′-hydroxy-benzylidene)-2-indolinone (indolinone). Tryptanthrin is a potent inhibitor of COX-2 (Danz et al., 2001) and 5-LOX (Oberthur et al., 2005), and of nitric oxide (NO) production catalyzed by inducible NO synthase (iNOS) (Ishihara et al., 2000). Indirubin is used in Chinese medicine as an antileukemia drug and has been shown to inhibit cyclin-dependent-kinase 2 (CDK2) (Hoessel et al., 1999). The lipid constituent α-linolenic acid inhibited 5-LOX (Oberthur et al., 2005) and seems to act as a competitor of arachidonic acid and thus reduces cellular inflammatory responses (Simopoulos, 2002). Indolinone inhibited compound 48/80-induced histamine release from rat peritoneal mast cells but not the related compound (*E*,*Z*)-3-(4′-isopropylbenzylidene)-2-indolinone (Ind7) (Ruster et al., 2004).

Indolin-2-one derivatives have been tested in disease models for multiple sclerosis (Bouerat et al., 2005), cancer (Kaur and Talele, 2008), HIV (Boechat et al., 2007), and infectious diseases (Bouchikhi et al., 2008), and an indolin-2-one derivative, sunitinib, was recently approved as tyrosine kinase inhibitor for treatment of renal cell carcinoma and imatinib-resistant gastrointestinal stromal tumours (Atkins et al., 2006). The indolin-2-one scaffold seems to exhibit some general kinase-inhibitory activity. Substituted indolin-2-ones occupy the ATP-binding site and act as ATP-mimetic inhibitors (Sun et al., 1998). This suggested that the anti-allergic effect of indolinone could be related to some kinase-inhibitory properties.

Although many cells are involved in allergy and inflammation, mast cells play an important role as initial effectors due

Abbreviations: BMMC, murine bone marrow derived mast cells; DNP, dinitrophenyl; MAPK, mitogen-activated protein kinase; ERK, extracellular-regulated kinase; PI3-K, phosphatidylinositol 3-kinase; PKB, protein kinase B; SNARE, soluble N-ethylmaleimide-sensitive-factor attachment receptor.

* Corresponding author. Tel.: +41 61 2671425; fax: +41 61 2671474.
E-mail address: matthias.hamburger@unibas.ch (M. Hamburger).

0928-0987/$ – see front matter © 2010 Elsevier B.V. All rights reserved.
doi:10.1016/j.ejps.2010.03.016

to their tissular localisation. By release of pro-inflammatory molecules, mast cells initialise processes that result in early and late phase allergic reactions. They are implicated in many diseases, such as allergy and asthma, gastrointestinal disorders, rheumatic diseases and multiple sclerosis (Hofmann and Abraham, 2009). Degranulation of mast cells requires binding of IgE antibodies to the high affinity IgE receptor (FcεRI) for activation and crosslinking of these antibodies by subsequent binding of an antigen (Rivera et al., 2008; Rivera and Olivera, 2008). The crosslinking induces intracellular signalling events that lead to activation of the protein kinase Lyn that in turn phosphorylates immunoreceptor tyrosine-based activation motifs (ITAMs) and Syk kinases. Class IA PI3-K recognise phosphorylated ITAMs as docking sites, which leads to the production of PtdIns(3,4,5)P_3 that recruits PKB (also known as Akt), leading to its activation and initiates a signalling cascade involving Bruton's tyrosine kinase (Btk) and phospholipase Cγ and the Raf-MEK-MAPK pathway. This eventually induces opening of plasma membrane calcium channels leading to degranulation (Burgoyne and Morgan, 2003). However, the FcεRI-mediated mast cell response is limited by subsequent de-phosphorylation of PtdIns(3,4,5)P_3 to PtdIns(3,4)P_2 by SH2-containing inositol 5′-phosphatase (SHIP).

Subsequent granule exocitosis occurs in a highly regulated and conserved way depending on Ca^{2+} and is related to synaptic vesicle exocytosis and most likely takes advantage of the same protein components such as SNARE's (soluble N-ethylmaleimide-sensitive-factor attachment receptors) (Burgoyne and Morgan, 2003). Anti-inflammatory, anti-allergic or immunosuppressive drugs such as corticosteroids or calcineurin-antagonists inhibit degranulation but additionally have many side-effects (Ludowyke and Lagunoff, 1985).

The aim of this study was to elucidate whether indolinone interacts with the pathways that lead to mast cell activation and degranulation, and at what level this interaction occurs.

2. Materials and methods

2.1. Chemicals and cell culture

Murine bone marrow derived mast cells (BMMCs) were cultured in Iscove's modified Dulbecco's medium (IMDM; Sigma–Aldrich, Buchs, Switzerland) supplemented with 10% heat-inactivated fetal calf serum (FCS; Amimed, Basel, Switzerland), 100 U/ml penicillin/streptomycin, and 2 mM L-glutamine (both from Invitrogen, Basel, Switzerland). Cells were grown in humified atmosphere containing 5% CO_2 and maintained with 2 ng/ml recombinant murine interleukin-3 (IL3; Pepro-Tech EC Ltd., London, UK). Chemicals used were: stem cell factor (SCF; Biosource, Invitrogen, Basel, Switzerland), adenosine (Ade; Sigma–Aldrich, Buchs, Switzerland), LY294002 (Alexis Corporation, Lausen, Switzerland), and wortmannin (Wort; Sigma–Aldrich). All solvents used were from Scharlau (Barcelona, Spain).

(*E*,*Z*)-3-(3′,5′-Dimethoxy-4′-hydroxy-benzylidene)-2-indolinone (indolinone) and (*E*,*Z*)-3-(4′-isopropylbenzylidene)-2-indolinone (Ind7) were synthesised according to a general protocol for indolinones (Sun et al., 1998). For indolinone, the ratio of slowly interconverting *E* and *Z* isomers was determined as 81:19 by HPLC (Ruster et al., 2004). Indolinone showed fluorescence when excited at 488 nm or 405 nm, with an emission maximum at 499 nm. The absorption maxima are at 256 and 380 nm.

2.2. Western blot

Immunoblot analysis was performed according to standard procedures. Equal amounts of cellular protein were separated on SDS-PAGE and transferred to a nitrocellulose membrane. Membranes were blocked and incubated overnight at 4 °C with specific primary antibody diluted in blocking buffer (5% bovine serum albumin in TBS-Tween): anti-phospho-PKB (Thr308) 1:1000; anti-phospho-ERK1/2 (Thr202/Tyr204) 1:1000. Specific bands were tagged with HRP conjugated secondary antibodies (Cell Signaling Technology, Beverly, MA) and detected using enhanced chemiluminescence (ECL Plus System, GE Healthcare, Little Chalfont, UK).

2.3. Degranulation assays

Release of histamine-containing granules was quantified by the determination of β-hexosaminidase in cell supernatants as described (Laffargue et al., 2002). Alternatively, Annexin-V staining of exposed membrane phosphatidylserine was carried out using the Annexin-V assay kit (Roche Diagnostics, Rotkreuz, Switzerland) following the manufacturer's protocol. The cells were then left to adhere to glass coverslips, fixed and assayed as described in Section 2.4.

2.4. Fluorescence microscopy

BMMC cells were suspended in PBS and left to adhere to glass coverslips and fixed in 4% formaldehyde in PBS for a minimum of 15 min at 4 °C. Nuclei were stained with DRAQ5 (Alexis Corporation, Lausen, Switzerland) according to the manufacturer's protocol. Cells plated on coverslips were mounted on glass slides with Fluorescent Mounting Medium (DakoCytomation, Glostrup, Denmark) and visualised by confocal microscopy (Leica DM RXE scanning confocal microscope) using Leica confocal software, version 2.5 (Leica Microsystems, Heidelberg, Germany).

2.5. Kinase assay

Appropriate concentrations of PI3-K isoforms p110 α, β, γ GST, γ tr, and δ (fused to interSH2 domains, a kind gift from Novartis, Basel, Switzerland) were mixed with 10 μg/ml L-α-phosphatidylinositol (Sigma–Aldrich, Buchs, Switzerland) dissolved in 0.3% octylglucoside kinase buffer (10 mM Tris–HCl, 3 mM $MgCl_2$, 50 mM NaCl, 0.8 mM CHAPS, 1 mM DTT). After 5 min pre-treatment with indolinone or DMSO, 2 μM ATP (Roche, Basel, Switzerland) dissolved in kinase buffer were added to start the reaction. Reactions were incubated for 30–90 min, depending on the kinase isoform. Kinase Glo (Promega, Madison, WI) was added to each well to start the luciferase reaction. After 15 min incubation at room temperature, plates (white 96 well luciferase plates (Berthold, Bad Wildbad, Germany)) were read out in a luminometer (Centro LB 960, Berthold) with an integration time of 0.5 s. Samples were run in duplicate.

3. Results

3.1. Localisation of indolinone in BMMC

Due to the fluorescent properties of indolinone (A), we were able to visualise high concentrations (≥50 μM) to directly determine its localisation in cells and monitor cellular uptake by flow cytometry. Analysis of indolinone-stained cells (50 μM) by confocal microscopy (Fig. 1B) showed equal distribution throughout the cytoplasm, but no staining of the nucleus, suggesting discrete

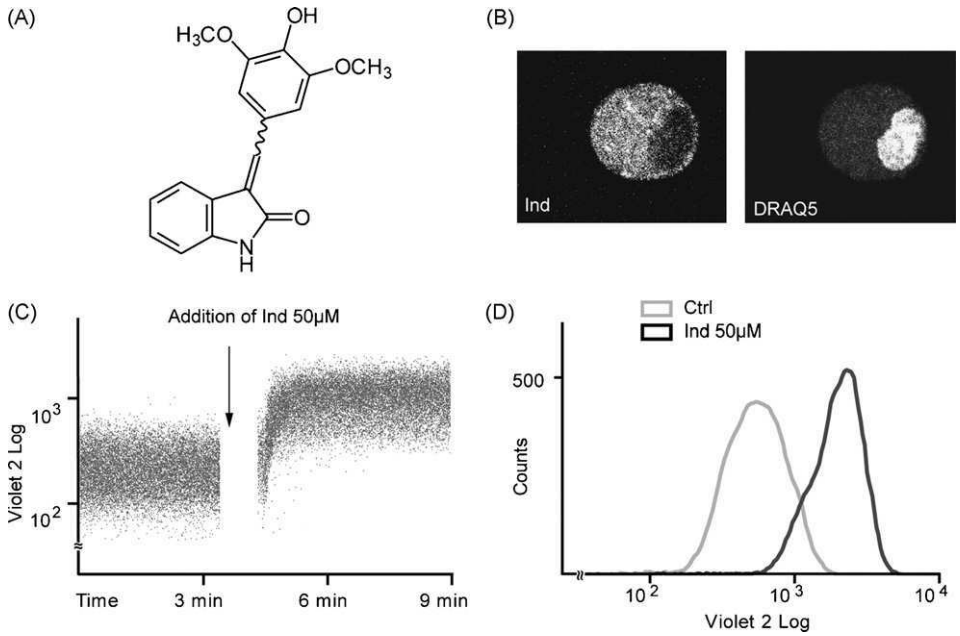

Fig. 1. Chemical structure of indolinone and its localisation in BMMCs. (A) Structure of (*E,Z*)-3-(3′,5′-dimethoxy-4′-hydroxy-benzylidene)-2-indolinone (indolinone). (B–D) Due to the fluorescent properties of indolinone itself, it was possible to monitor its appearance and localisation in the cell. (B) BMMCs were fixed, stained with 50 μM indolinone and DRAQ5 and mounted for fluorescence microscopy. The upper panel illustrates localisation of indolinone in the cell, the lower panel shows DRAQ5 staining of the nucleus. (C + D) Flow cytometry analysis of BMMCs. (C) Administration of 50 μM indolinone during ongoing measurement. (D) Fluorescence of BMMC before and after addition of 50 μM indolinone (Ind).

binding to residing proteins. Administration of indolinone during flow cytometry measurement produced instantaneous increase in cytoplasmatic fluorescence. After less than 3 min no further increase was detected and fluorescence persisted for the duration of the measurement (15 min) (Fig. 1C and 1D). Repeated washes and prolonged incubation in indolinone-free media for up to 2 h before measurement did apparently not reduce the intracellular concentration (not shown). Thus, indolinone was immediately taken up into the cells and retained in the cytosol. Unfortunately, concentrations smaller than 50 μM could not be detected by immunofluorescence microscopy or FACS analysis.

3.2. Inhibition of degranulation in murine bone marrow derived mast cells

Indolinone had been previously shown to inhibit compound 48/80-induced histamine release in rat peritoneal mast cells (Ruster et al., 2004). We reconfirmed this effect in antigen-stimulated degranulation of murine bone marrow derived mast cells (BMMCs), to demonstrate that this effect was neither species-dependent nor assay-specific. BMMCs were sensitized overnight with IgE directed against dinitrophenol-modified human serum albumin (DNP-HSA) (100 ng/ml), and indolinone at indicated concentrations was added 30 min prior to antigen-challenge where applicable. Degranulation was simultaneously induced with the experimental allergen DNP-albumin (10 ng/ml). Mast cell granule release was assessed by the activity of β-hexosaminidase, a marker enzyme for histamine-containing granules. At concentrations ≥50 nM, indolinone efficiently reduced the amount of released β-hexosaminidase to control levels (Fig. 2).

3.3. No inhibition of PI3-Ks and ERK1/2 by indolinone

The activity of all PI3-Ks class IA and IB isoforms (α, β, γ, δ) that are responsible for the generation of PtdIns(3,4,5)P_3, was tested in an in vitro assay after addition of different concentrations of indolinone. The γ isoform was tested in two different ways, as the complete GST tagged enzyme and as a truncated form with 144 amino acids less. Indolinone inhibited all PI3-K isoforms to some extent (Fig. 3A). When incubated with 50 μM indolinone, the α and the δ isoform were inhibited to less than 50%, whereas the other isoforms still showed activities over 60%. Since degranulation in BMMC is predominantly induced by PI3-Kγ, we concluded that indolinone-induced inhibition of degranulation is independent of PI3-Ks.

This assumption was further supported by Western blot analysis showing inhibition of PKB phosphorylation upon antigen-challenge at concentrations higher than 1 μM indolinone (Fig. 3B). In contrast, phosphorylation of ERK1/2 was only blocked at concentrations of 50 μM.

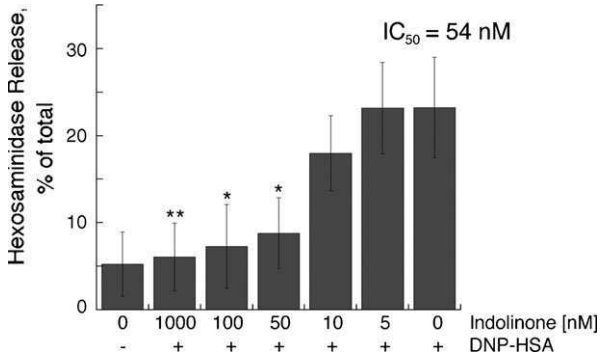

Fig. 2. Mast cell degranulation by IgE/antigen stimulation is blocked by indolinone. Granule release was followed by hexosaminidase activity in BMMCs previously incubated with saturating levels of IgE overnight, and subsequently challenged with 10 ng/ml DNP-HSA before hexosaminidase was assessed in the cell supernatant. Indolinone was added to the cells 30 min before challenge where indicated. Ctrl—4.17% ± 3.15%; 1 μM—4.90% ± 7.95%; 100 nM—6.08% ± 5.81%; 50 nM—7.97% ± 5.64%; 10 nM—14.51% ± 5.87%; 5 nM—24.12% ± 4.97%; no indolinone—23.23% ± 5.77%.

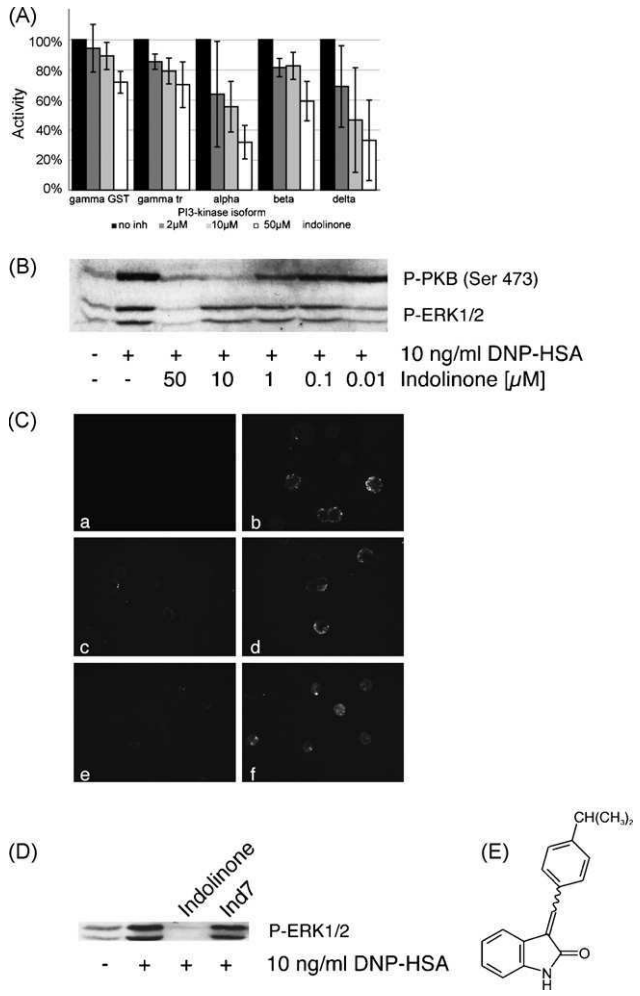

Fig. 3. Indolinone blocks degranulation at the level of granule release. (A) PI3-Ks were co-incubated with ATP and indolinone at indicated concentrations or with DMSO as a control. Kinase activity was determined as consumption of ATP, and residual ATP was measured by luciferase reaction. Samples were measured as duplicates in three independent experiments. The kinase activity of the control was defined as 100%. (B) Western blot analysis of BMMC cells (0.5×10^6) previously incubated with saturating levels of IgE. The cells were starved in 2% serum for 4 h, pre-treated with indolinone or DMSO for 30 min as indicated, and then challenged with 10 ng/ml DNP-HSA for 2 min. Untreated cells were used as control. Shown are typical results from three independent experiments. (C) Mast cells were sensitized with IgE overnight and challenged with 10 ng/ml DNP-HSA (b–f). The following substances were added to the cells 30 min before challenge: (a + b) DMSO; (c) 100 nM indolinone; (d) 100 nM Ind7; (e) 1 μM indolinone; (f) 1 μM Ind7. Cells were fixed with 4% p-formaldehyde and stained with Annexin-V-FITC and analysed by immunofluorescence. Shown is a typical experiment. (D) Western blot analysis of BMMC cells (0.5×10^6) previously incubated with saturating levels of IgE. The cells were starved in 2% serum for 4 h, pre-treated with 50 μM indolinone, Ind7 or DMSO for 30 min as indicated, and then challenged with 10 ng/ml DNP-HSA for 2 min. (E) Chemical structure of Ind7 ((*E*,*Z*)-3-(4′-isopropylbenzylidene)-2-indolinone).

Granule exocitosis was efficiently blocked at concentrations as low as 1 μM (Fig. 3C), as was already suggested by the β-hexosaminidase-release assay (Fig. 2). However, the indolinone derivative Ind7 (Fig. 3E) (Ruster et al., 2004) was completely ineffective at any of the concentrations tested. This finding was confirmed by Western blot analysis of IgE-sensitized BMMCs that were challenged with antigen for 2 min in absence or presence of 50 μM indolinone or Ind7 (Fig. 3D).

4. Discussion

The only drugs in clinical use that directly inhibit mast cell degranulation are disodium cromoglycate and its derivative nedocromil (Corin, 2000). Cromoglycate was developed from khellin, a furanochromone from the anti-allergic plant *Ammi visnaga*. It is a mast cell stabilising agent that has been shown to block ion-channels. However, cromoglycate likely has additional effects and its mode of action is still not very clear despite decades of clinical use (Kay et al., 1987). Various other agents have been used as experimental inhibitors of degranulation (Ludowyke and Lagunoff, 1985) but were not suitable as drugs. The most recent approaches include Syk kinase inhibitors (Masuda and Schmitz, 2008; Matsubara et al., 2006) and anti-IgE antibodies. One such anti-IgE antibody, omalizumab (Xolair), has recently reached the market (Chang and Shiung, 2006; Gomez et al., 2007).

Extracts of *I. tinctoria* have traditionally been used in the treatment of anti-inflammatory complaints. Previous studies assigned specific facets of the in vitro pharmacological spectrum of the extract to specific compounds (Danz et al., 2001; Oberthur et al., 2005) in this complex multi-component mixture. In the model of compound 48/80-stimulated mast cell degranulation, indolinone was significantly more potent than disodium cromoglycate (IC_{50} of 15 μM (0.0045 μg/ml) vs 1.5 mM). In an earlier study *Isatis* extract had an IC_{50} of 2.3 μg/ml in this assay (Hamburger, 2002). Given that indolinone is a minor constituent in the extract (typical concentrations of 0.04%) (Mohn et al., 2007), it is likely that other components of the extract contribute to its mast cell stabilising activity.

Indolinone fulfils Lipinski's Rule of Five (Lipinski et al., 2001) and, hence, possesses drug-like properties. The compound has a calculated distribution coefficient (clogD) of 2.28 at pH 7, and a polar surface area (PSA) of 67.8 Å^2. These physico-chemical properties explain its rapid cellular uptake and distribution in the cytoplasm and, hence, its persistence within the cell and prolonged inhibitory activity.

In this study we have shown that indolinone blocks antigen-induced mast cell degranulation with an IC_{50} of 54 nM that does not involve inhibition of kinases directly downstream of FcεRI. It does, however, interrupt granule exocytosis by an yet unknown mechanism, possibly by binding to proteins on the surface of granules such as SNARE that play a vital role in regulated exocytosis in mast cells (Puri et al., 2003). Within a series of structurally related benzylidene-2-indolinones (Ruster et al., 2004), inhibition of mast cell degranulation was only observed with indolinone with no apparent toxicity, as BMMCs and other primary cell lines such as lymph node cells remained unaffected by treatment with ≥50 μM indolinone for more than a week.

The apparent selectivity of the compound, its potency and favourable physico-chemical properties render this molecule as an interesting lead structure for development of new anti-allergic agents.

Acknowledgment

Financial support from the Swiss National Science Foundation (Project 205321-116157/1) is gratefully acknowledged.

References

Atkins, M., Jones, C.A., Kirkpatrick, P., 2006. Sunitinib maleate. Nat. Rev. Drug Discov. 5, 279–280.

Boechat, N., Kover, W.B., Bongertz, V., Bastos, M.M., Romeiro, N.C., Azevedo, M.L., Wollinger, W., 2007. Design, synthesis and pharmacological evaluation of HIV-1 reverse transcriptase inhibition of new indolin-2-ones. Med. Chem. 3, 533–542.

Bouchikhi, F., Rossignol, E., Sancelme, M., Aboab, B., Anizon, F., Fabbro, D., Prudhomme, M., Moreau, P., 2008. Synthesis and biological evaluation of diversely substituted indolin-2-ones. Eur. J. Med. Chem. 43, 2316–2322.

Bouerat, L., Fensholdt, J., Liang, X., Havez, S., Nielsen, S.F., Hansen, J.R., Bolvig, S., Andersson, C., 2005. Indolin-2-ones with high in vivo efficacy in a model for multiple sclerosis. J. Med. Chem. 48, 5412–5414.

Burgoyne, R.D., Morgan, A., 2003. Secretory granule exocitosis. Physiol. Rev. 83, 581–632.

Chang, T.W., Shiung, Y.Y., 2006. Anti-IgE as a mast cell-stabilizing therapeutic agent. J. Allergy Clin. Immunol. 117, 1203–1212, quiz 1213.

Corin, R.E., 2000. Nedocromil sodium: a review of the evidence for a dual mechanism of action. Clin. Exp. Allergy 30, 461–468.

Danz, H., 2000. Untersuchungen zur antiinflammatorischen Wirkung und zur Analytik von Tryptantrin in *Isatis tinctoria* L. Dr. rer. nat. Thesis. Biologisch-Pharmazeutische Fakultät, Friedrich-Schiller University, Jena.

Danz, H., Stoyanova, S., Wippich, P., Brattstrom, A., Hamburger, M., 2001. Identification and isolation of the cyclooxygenase-2 inhibitory principle in *Isatis tinctoria*. Planta Med. 67, 411–416.

Gomez, G., Jogie-Brahim, S., Shima, M., Schwartz, L.B., 2007. Omalizumab reverses the phenotypic and functional effects of IgE-enhanced Fc epsilonRI on human skin mast cells. J. Immunol. 179, 1353–1361.

Hamburger, M., 2002. *Isatis tinctoria*—from the rediscovery of an ancient medicinal plant towards a novel anti-inflammatory phytopharmaceutical. Phytochem. Rev. 1, 333–344.

Heinemann, C., Schliemann-Willers, S., Oberthur, C., Hamburger, M., Elsner, P., 2004. Prevention of experimentally induced irritant contact dermatitis by extracts of *Isatis tinctoria* compared to pure tryptanthrin and its impact on UVB-induced erythema. Planta Med. 70, 385–390.

Hoessel, R., Leclerc, S., Endicott, J.A., Nobel, M.E., Lawrie, A., Tunnah, P., Leost, M., Damiens, E., Marie, D., Marko, D., Niederberger, E., Tang, W., Eisenbrand, G., Meijer, L., 1999. Indirubin, the active constituent of a Chinese antileukaemia medicine, inhibits cyclin-dependent kinases. Nat. Cell Biol. 1, 60–67.

Hofmann, A.M., Abraham, S.N., 2009. New roles for mast cells in modulating allergic reactions and immunity against pathogens. Curr. Opin. Immunol. 21, 679–686.

Ishihara, T., Kohno, K., Ushio, S., Iwaki, K., Ikeda, M., Kurimoto, M., 2000. Tryptanthrin inhibits nitric oxide and prostaglandin E(2) synthesis by murine macrophages. Eur. J. Pharmacol. 407, 197–204.

Kaur, K., Talele, T.T., 2008. 3D QSAR studies of 1,3,4-benzotriazepine derivatives as CCK(2) receptor antagonists. J. Mol. Graph Model. 27, 409–420.

Kay, A.B., Walsh, G.M., Moqbel, R., MacDonald, A.J., Nagakura, T., Carroll, M.P., Richerson, H.B., 1987. Disodium cromoglycate inhibits activation of human inflammatory cells in vitro. J. Allergy Clin. Immunol. 80, 1–8.

Laffargue, M., Calvez, R., Finan, P., Trifilieff, A., Barbier, M., Altruda, F., Hirsch, E., Wymann, M.P., 2002. Phosphoinositide 3-kinase gamma is an essential amplifier of mast cell function. Immunity 16, 441–451.

Lipinski, C.A., Lombardo, F., Daminy, B.W., Feeney, P.J., 2001. Experimental and computational approchaches to estimate solubility and permeability in drug discovery and development settings. Adv. Drug Deliv. Rev. 46, 3–26.

Ludowyke, R., Lagunoff, D., 1985. Drug inhibition of mast cell secretion. Prog. Drug Res. 29, 277–301.

Masuda, E.S., Schmitz, J., 2008. Syk inhibitors as treatment for allergic rhinitis. Pulm. Pharmacol. Ther. 21, 461–467.

Matsubara, S., Li, G., Takeda, K., Loader, J.E., Pine, P., Masuda, E.S., Miyahara, N., Miyahara, S., Lucas, J.J., Dakhama, A., Gelfand, E.W., 2006. Inhibition of spleen tyrosine kinase prevents mast cell activation and airway hyperresponsiveness. Am. J. Respir. Crit. Care Med. 173, 56–63.

Mohn, T., Potterat, O., Hamburger, M., 2007. Quantification of active principles and pigments in leaf extracts of *Isatis tinctoria* by HPLC/UV/MS. Planta Med. 73, 151–156.

Oberthur, C., Jaggi, R., Hamburger, M., 2005. HPLC based activity profiling for 5-lipoxygenase inhibitory activity in *Isatis tinctoria* leaf extracts. Fitoterapia 76, 324–332.

Puri, N., Kruhlak, M.J., Whiteheart, S.W., Roche, P.A., 2003. Mast cell degranulation requires N-ethylmaleimide-sensitive factor-mediated SNARE disassembly. J. Immunol. 171, 5345–5352.

Recio, M.C., Cerda-Nicolas, M., Hamburger, M., Rios, J.L., 2006a. Anti-arthritic activity of a lipophilic woad (*Isatis tinctoria*) extract. Planta Med. 72, 715–720.

Recio, M.C., Cerda-Nicolas, M., Potterat, O., Hamburger, M., Rios, J.L., 2006b. Anti-inflammatory and antiallergic activity in vivo of lipophilic *Isatis tinctoria* extracts and tryptanthrin. Planta Med. 72, 539–546.

Rivera, J., Fierro, N.A., Olivera, A., Suzuki, R., 2008. New insights on mast cell activation via the high affinity receptor for IgE. Adv. Immunol. 98, 85–120.

Rivera, J., Olivera, A., 2008. A current understanding of Fc epsilon RI-dependent mast cell activation. Curr. Allergy Asthma Rep. 8, 14–20.

Ruster, G.U., Hoffmann, B., Hamburger, M., 2004. Inhibitory activity of indolin-2-one derivatives on compound 48/80-induced histamine release from mast cells. Pharmazie 59, 236–237.

Simopoulos, A.P., 2002. Omega-3 fatty acids in inflammation and autoimmune diseases. J. Am. Coll. Nutr. 21, 495–505.

Stöger, E., 2009. Arzneibuch der chinesischen Medizin, 2nd edition. Deutscher Apotheker-Verlag, Stuttgart.

Sun, L., Tran, N., Tang, F., App, H., Hirth, P., McMahon, G., Tang, C., 1998. Synthesis and biological evaluations of 3-substituted indolin-2-ones: a novel class of tyrosine kinase inhibitors that exhibit selectivity toward particular receptor tyrosine kinases. J. Med. Chem. 41, 2588–2603.

Journal of Pharmaceutical and Biomedical Analysis xxx (2010) xxx–xxx

Contents lists available at ScienceDirect

Journal of Pharmaceutical and Biomedical Analysis

journal homepage: www.elsevier.com/locate/jpba

Separation and detection of all phosphoinositide isomers by ESI-MS

Sabine Kiefer[a], Johannes Rogger[a], Anna Melone[b], Ann C. Mertz[b], Anna Koryakina[a], Matthias Hamburger[a], Peter Küenzi[a,*]

[a] Institute of Pharmaceutical Biology, University of Basel, Klingelbergstrasse 50, 4056 Basel, Switzerland
[b] Institute of Biochemistry and Genetics, Department of Biomedicine, University of Basel, Mattenstrasse 28, 4058 Basel, Switzerland

ARTICLE INFO

Article history:
Received 10 December 2009
Received in revised form 22 March 2010
Accepted 23 March 2010
Available online xxx

Keywords:
Phosphoinositides
Phosphatidylinositol 3,4,5 triphosphate
LC–MS
ESI
Reversed phase ion-pair chromatography

ABSTRACT

Phosphoinositides (PIs) play fundamental roles as signalling molecules in numerous cellular processes. Direct analysis of PIs is typically accomplished by metabolic labelling with ^{3}H-inositol or inorganic ^{32}P followed by deacylation, ion-exchange chromatography and flow scintillation detection. This analysis is laborious, time-consuming, and involves massive amounts of radioactivity. To overcome these limitations we established a robust, non-radioactive LC–ESI–MS assay for the separation and analysis of deacylated PIs that allows discrimination of all isomers without the need for radioactive labelling. We applied the method to various cell types to study the PI levels upon specific stimulation.

1. Introduction

The inositol containing glycerophospholipids, collectively known as phosphoinositides (PIs), play a fundamental role in diverse cellular functions such as cell growth and differentiation, motility, calcium mobilisation and oncogenesis [1,2]. The family of the phosphoinositides consists of the non-phosphorylated precursor phosphatidylinositol (PtdIns) and seven derivatives with different phosphorylation patterns on the myo-inositol ring, where the 3-, 4- and 5-positions can be phosphorylated by specific kinases (Fig. 1A).

PIs derived from PtdIns and its phosphorylation products phosphatidylinositol-4-phosphate (PtdIns4*P*) and phospha tidylinositol-4,5-bisphosphate (PtdIns(4,5)P_2) form the so called canonical pathway [3] and are believed to be kept at constant levels at the plasma membrane. The other PIs are considered to be low-abundant signalling molecules that transiently appear upon stimulation. Stimulation with growth factors or insulin leads to increased PtdIns(3,4,5)P_3 levels, which in turn produces specific cellular responses. The bisphosphorylated PIs containing PtdIns(3,4)P_2, PtdIns(4,5)P_2, and PtdIns(3,5)P_2 moieties play distinct roles in signal prolongation after PtdIns(3,4,5)P_3 inducing stimuli, regulation of the actin cytoskeleton and vesicle transport, respectively [4–8]. PIs containing phosphoinositide monophosphates were long thought to be mere intermediates in the pathway but are now recognised to possess specific functions by themselves in protein sorting, vesicular trafficking and in osmotic stress response [9–12].

Analysis of PIs has been achieved in several ways. Most frequently, metabolic radioisotope labelling with inorganic ^{32}P or ^{3}H-inositol, lipid extraction, hydrolysis followed by chromatographic separation and radiographic analysis of phosphoinositides has been used [13–15]. Metabolic labelling involves very high doses of radioactivity (GBq), long labelling times and only detects the turnover of PIs, whereas dormant pools of PIs remain unlabelled. More recent approaches include fluorescent-labelled binding proteins for specific PIs, and antibodies directed against PIs [16,17]. However, differentiation of all the mono- and bisphosphorylated positional isomer PIs, has not been achieved yet.

Two fundamentally different approaches have been pursued in PI analysis: (i) a comprehensive profiling of intact PIs [18–21] and (ii) head group analysis after cleavage of the lipid moieties [22,23]. The first approach used in lipidomics leads to a highly complex picture due to a plethora of closely related molecules that only vary in their lipid moieties. This approach including quantification has been successfully applied to cells producing phophoinositides with limited complexity in their lipid residues, such as platelets [24–26]. Even though the analysis of intact PIs would be the preferred approach, it is currently unsuitable for most cells due to the overwhelming complexity of their PI patterns. Therefore, separation and detection of the head groups following deacylation (Fig. 1B) is a more suitable approach if the focus lies on the detec-

* Corresponding author. Present address: CSL Behring, Wankdorfstrasse 10, 3022 Bern, Switzerland. Tel.: +41 31 344 40 48.
E-mail addresses: peter.kueenzi@cslbehring.com, peter.kueenzi@unibas.ch (P. Küenzi).

0731-7085/$ – see front matter © 2010 Elsevier B.V. All rights reserved.
doi:10.1016/j.jpba.2010.03.029

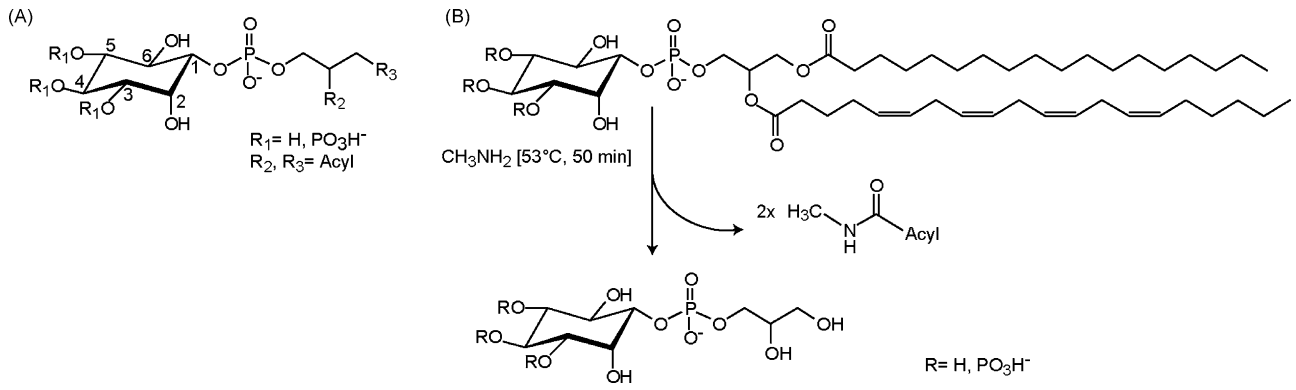

Fig. 1. (A) Structure of a typical PtdIns, sn-1-stearoyl-2-arachidonyl-phosphatidylinositol and the performed deacylation step, resulting in cleavage of the lipid moiety. (B) Structure of phosphatidylinositol-3,4,5-trisphosphate (PtdInsP_3); numbering of the myo-inositol ring is indicated.

tion of the change in phosphorylation pattern that exerts the major influence on the subsequently elicited signalling. Given the low abundance of certain PIs, even the analysis of deacylated lipids is highly challenging.

As alternatives to radioisotope labelling, analysis by mass spectrometry [27], suppressed conductivity detection [28] and evaporative light scattering detection (ELSD) [29] have been used. Unfortunately, none of these allowed a discrimination of all isomers. An LC–ESI–MS method for separation of deacylated PtdInsP_2 isomers has been recently published [14]. However, chromatography suffered from poor peak shape and co-elution of PtdIns(3,5)P_2 and PtdIns(3,4,5)P_3.

Since the PtdIns moieties of PIs can be interconverted by specific kinases and phosphatases, inhibition, stimulation, modification, or deletion of one of these enzymes may have profound implications on the biological response. Therefore, separation and simultaneous detection of all headgroups of PIs is of major importance for a better understanding of their biological roles, and a robust and sensitive method is of general interest to researchers involved in cell signalling.

2. Experimental

2.1. LC–MS instrumentation

HPLC separation was carried out on a series 1100 system equipped with degasser, binary high pressure mixing pump, and column thermostat (Agilent Technologies). A liquid handler 215 (Gilson) was used as autosampler. The HPLC was coupled to an Esquire 3000 ion trap mass spectrometer equipped with an electrospray (ESI) interface (Bruker Daltonics). Data acquisition and processing was performed using HyStar 3.0 software from Bruker Daltonics.

2.2. LC–MS method

2.2.1. Ion-pair chromatography

N,N-dimethylhexylamine (DMHA; Acros, Thermo Fisher) was used as ion-pair reagent. Mobile phase A consisted of water containing 5 mM DMHA and 4 mM glacial acetic acid (Sigma–Aldrich) and mobile phase B of acetonitrile or methanol with 5 mM DMHA and 4 mM glacial acetic acid. All solvents were from Scharlau (Scharlau, Barcelona, Spain).

2.2.2. Columns

Various columns were tested for suitability in phosphoinositide analysis, including Atlantis C18 (150 mm × 4.6 mm, 5 μm) and T3 (150 mm × 3.5 mm, 3 μm; Waters, Baden, Switzerland), Nucleosil C100 (250 mm × 4.6 mm, 5 μm; Macherey-Nagel, Düren, Germany), liChrospher diol (125mm × 4.0 mm, 5 μm; Merck, Darmstadt, Germany) and Aqua C18 (250 mm × 4.6 mm, 5 μm and 75 mm × 2.0 mm, 3 μm; Phenomenex, Torrance, CA).

2.2.3. Separation of phosphoinositides

2.2.3.1. Method 1. Separation of deacylated PIs with different numbers of phosphorylations; PtdIns, PtdIns*P*, PtdInsP_2 and PtdInsP_3, was achieved by ion-pair chromatography on a Aqua C18 column (3 μm, 125 Å, 75 mm × 2.0 mm). A gradient from mobile phase B (acetonitrile) 0.1 to 50% in 25 min and a wash step (50% B to 100% B in 3 min, 100% B for 12 min, 100% B to 0.1% B in 5 min, 0.1% B for 5 min) was applied.

2.2.3.2. Method 2. Separation of deacylated PIs with different numbers of phosphorylation plus additional separation of phosphoinositides bisphosphate isomers PtdIns(4,5)P_2, PtdIns(3,5)P_2, PtdIns(3,4)P_2, was achieved by ion-pair chromatography on an Aqua C18 column (125 Å, 250 mm × 4.6 mm, 5 μm). A gradient from mobile phase B (acetonitrile) 15 to 35% in 40 min followed by a wash sequence (35% B to 100% B in 2 min, 100% B for 15 min, 100% B to 15% B in 3 min, 15% B for 5 min) was applied.

2.2.3.3. Method 3. Separation of PtdIns(3)*P*, PtdIns(4)*P* and PtdIns(5)*P*, additionally to separation of all other PIs, was performed with methanol as mobile phase B and a gradient from 15 to 50% in 60 min, followed by a wash step (50% B to 100% B in 2 min, 100% B for 15 min, 100% B to 15% B in 3 min, 15% B for 5 min).

2.3. Mass spectrometry

Negative ion LC–MS spectra on the ion trap instrument were recorded after optimization of settings, under ion charge control conditions (ICC 20000) at a scan speed of 13,000 *m*/*z*/s, using a gauss filter width of 0.2 *m*/*z*. Nitrogen was used as a drying gas at a flow rate of 10 l/min and as a nebulizing gas at a pressure of 30 psi. The nebulizer temperature was set to 300 °C. Spectra were recorded in the range of *m*/*z* 200–600 in negative mode. Capillary voltage was at 4500 V, endplate offset at −500 V, capillary end voltage at −115.0 V, skimmer voltage −40.0 V and trap drive at 53.4.

2.4. Flow scintillation analysis

Levels of radioactively labelled intracellular phosphatidylinositides were determined essentially as described [30]. Briefly, 4 million cells were incubated with 500 μCi $^{32}P_i$ for 60 min at 37 °C. After removal of non-incorporated $^{32}P_i$, cells were extracted as described below. The column effluent was splitted and exam-

Please cite this article in press as: S. Kiefer, et al., Separation and detection of all phosphoinositide isomers by ESI-MS, J. Pharm. Biomed. Anal. (2010), doi:10.1016/j.jpba.2010.03.029

ined online with a FLO-ONE A500 β-detector (Packard–Perkin Elmer).

2.5. Chemicals and cell culture

Murine bone marrow cells were cultured in Iscove's Modified Dulbecco's medium (IMDM; Sigma–Aldrich) supplemented with 10% heat-inactivated fetal calf serum (FCS; Amimed, Basel, Switzerland), 100 U/ml penicillin/streptomycin and 2 mM L-glutamine (both from Invitrogen, Basel, Switzerland). Cells were grown in humified atmosphere containing 5% CO_2 and maintained with 2 ng/ml recombinant murine interleukin-3 (IL3; PeproTech EC Ltd., London, UK).

Human embryonic kidney cells HEK 293 were cultured in Dulbecco's Modified Eagle's Medium (DMEM; Sigma–Aldrich) supplemented with 10% FCS, 100 U/ml penicillin/streptomycin and 2 mM L-glutamine. Cells were transfected with jetPEI cationic polymer transfection reagent (Polyplus-Transfection, Illkirch, France) according to the manufacturers' instructions. Twenty-four hour before transfection, cells were plated at 10^6 cells/25 cm^2 flask, then transfected with 2.6 μg GST-Vps34 and 0.4 μg Myc-S6K. Thirty hour after transfection, cells were starved over night and experiments were performed the following day.

Platelets were isolated from blood of healthy donors. Blood samples were mixed with acid citrate dextrose ACD (10.1 mM glucose, 30 μM citric acid, pH 6.5 in 0.9% NaCl, all from Sigma–Aldrich) and centrifuged for 5 min at 1000 × *g* [31]. Platelet rich plasma was collected and washed in PBS.

Chemicals used for experiments were: adenosine (Ade), N-formyl-Met-Leu-Phe (fMLP), wortmannin (wort) (all from Sigma–Aldrich).

Phosphoinositide standards used were: Phosphoinositides sodium salt from bovine brain (Sigma–Aldrich), PtdIns(3,4)P_2, PtdIns(3,5)P_2 and PtdIns(3,4,5)P_2 as 1,2-dioctanoyl-sn-glycero-3-phosphoinositolphosphates ammonium salt and PtdIns3*P* and PtdIns5*P* as 1-heptadecanoyl-2-(5Z,8Z,11Z,14Z-eicosatetraenoyl)-sn-glycero-3-phosphoinositolphosphates ammonium salt from Avanti Polar Lipids (Avanti Polar Lipids, Alabaster, AL).

2.6. Extraction, deacylation and sample preparation

Extraction of PIs was adapted from Ogiso et al. [27], who described a modified acidic Bligh-Dyer extraction [32] with addition of NaCl to the aqueous phase to help reducing loss of PIs. Briefly, ca. 10^6 cells were extracted with 2 ml methanol, 2 ml 1 M HCl, 0.15 ml 2 M NaCl and 2 ml chloroform (solvents from Scharlau, other reagents from Sigma–Aldrich). Methanol was supplemented with PhosSTOP (Roche, Basel, Switzerland), 1 mM NaF, 3 mM BHT and 0.5 mM phosphatidic acid (all from Sigma–Aldrich). The two phases were mixed well and centrifuged shortly for separation. The lower organic phase was removed, evaporated by nitrogen stream and transferred to deacylation. Dried samples were incubated with methylamine solution in water/methanol/n-butanol (43:46:11) at 53 °C for 50 min, all solvent was evaporated under vacuum, and then extracted with a mixture of n-butanol/petrol ether 40–60°/ethyl formiate (20:4:1) and water [33]. The water-phase was dried in vacuum and the samples were dissolved in 40 μl of solvent A for LC–MS analysis.

3. Results and discussion

3.1. Separation of phosphoinositides in order of increasing phosphorylation

Separation of anionic or phosphorylated compounds is typically achieved by ion-exchange chromatography. However, typical ion-pairing reagents are not volatile and, hence, not compatible with LC–MS. We tested several volatile and MS-compatible ion-pairing reagents, such as formic acid, ammonium formiate and N,N-dimethyl-hexylamine (DMHA) and applied them on various columns (Nucleosil C100, LiChrospher Diol and Phenomenex Aqua C18). The only acceptable separation of a phosphoinositide reference mixture was achieved on a short (75 mm) Phenomenex Aqua C18 column with the addition of DMHA. Subsequently, we tested different gradient profiles, column temperatures, pH and concentrations of DMHA to optimize separation. Column temperature had a slight impact, and the best separation was obtained at 15 °C. In contrast, pH of the mobile phase was critical. Best results were obtained around pH 7, while lower pH values lead to peak tailing and split peaks and higher pH resulted in shorter retention times. Increase of DMHA concentration from 5 to 10 mM and 20 mM did not enhance the quality of the separation. A water-acetonitrile gradient was applied and the final gradient program was 0.1–50% ACN (containing 5 mM DMHA) in 25 min, leading to the separation of a PI standard mixture shown in Fig. 2A. Peaks shown resulted from 0.1 μg of deacylated PtdIns(3,4,5)P_3 standard mixed with 4 μg of deacylated phosphoinositde extract (mixture of PtdIns, PtdIns4*P* and PtdIns(4,5)P_2).

Separation of a mixture of PIs standards was also achieved under isocratic conditions (27% ACN and 73% water) but separation of biological samples, however, could not be achieved under these conditions, probably due to interference with the biological matrix.

To test the applicability of our method to biological samples, we analysed mast cell extracts. Mast cells are known to produce large amounts of PtdIns(3,4,5)P_3 upon activation that can be provoked *in vitro* by stimulation with adenosine [30]. Murine bone marrow derived mast cells (BMMCs) were stimulated with 5 μM adenosine for 30 s, the lipids were extracted, deacylated and analysed with method 1. Our method clearly succeeded in reproducing the increased amounts of PtdIns(3,4,5)P_3 upon stimulation of mast cells with adenosine, whereas peaks of PtdIns and PtdIns*P* remained constant (Fig. 2B and C).

3.2. Positional isomer separation of phosphatidylinositol bisphosphates

To achieve separation of PtdInsP_2 positional isomers various columns were tested, including Nucleosil C100, Atlantis C18, Atlantis T3 and Phenomenex Aqua C18. The separation was only achieved on a Phenomenex Aqua column (column length 250 mm) and a water–acetonitrile gradient (containing 5 mM DMHA as ion-pair reagent) (method 2). A mixture of standards of all PtdInsP_2 isomers was separated in the elution order of PtdIns(3,4)P_2, PtdIns(4,5)P_2 and PtdIns(3,5)P_2 (Fig. 3A and B). Peaks shown resulted from 0.1 μg of deacylated PtdIns(3,5)P_2 and PtdIns(3,4)P_2 standard mixed with 4 μg of deacylated phosphoinositde extract (mixture of PtdIns, PtdIns4*P* and PtdIns(4,5)P_2). Several other solvent mixtures and addition of modifiers were tested. A separation with a different elution order (PtdIns(3,4)P_2, PtdIns(3,5)P_2 and PtdIns(4,5)P_2) was obtained with a water–methanol gradient (containing 5 mM DMHA) (method 3) (Fig. 3C and D).

Vps34 transfected HEK 293 cells under hyperosmolar stress were used as a model to test the analysis of PtdIns(3,5)P_2 from biological samples. The PI3-kinase Vps34 is known to stimulate osmotic stress related production of PtdIns(3,5)P_2 in yeast [22,28]. HEK Vps34 were incubated for 10 min in a medium supplemented with 1 M NaCl solution to induce stimulation of Vps34, and generation of PtdIns3*P* leading to production of PtdIns(3,5)P_2. As can be seen in Fig. 4A and B, the transfection with Vps34 already induced some production of PtdIns(3,5)P_2, which was then further increased upon NaCl hyperosmotic stimulation.

Please cite this article in press as: S. Kiefer, et al., Separation and detection of all phosphoinositide isomers by ESI-MS, J. Pharm. Biomed. Anal. (2010), doi:10.1016/j.jpba.2010.03.029

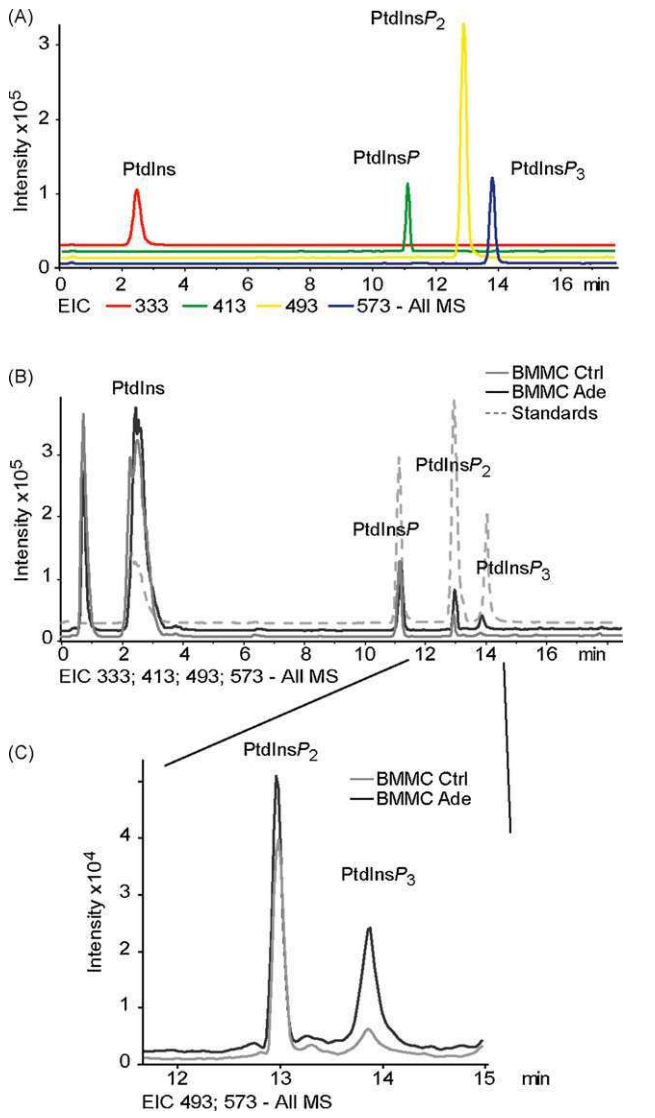

Fig. 2. (A) Extracted ion chromatogram (EIC) of deacylated phosphoinositide standards (PtdIns, PtdIns*P*, PtdInsP_2 and PtdInsP_3) mixture. (B) EIC of cell samples from 4 mio BMMC and standards. Cells were stimulated with adenosine (Ade) 5 μM for 30 s to induce production of PtdInsP_3. (C) Peaks of PtdInsP_2 and PtdInsP_3 from control cells in relation to stimulated cells, levels of PtdInsP_3 increased after stimulation with adenosine. Column: Phenomenex Aqua C18 (75 mm × 2 mm, 3 μm). Solvent A: H_2O (+5 mM DMHA), solvent B: acetonitrile (+5 mM DMHA). Gradient: 0.1% B to 50% B in 25 min.

Analysis of PtdIns(3,4)P_2 in biological samples was tested with human blood platelets. In comparison to many other cell models, platelets produce PtdIns(3,4)P_2 in relatively large amounts upon activation. PtdIns(3,4,5)P_3 is degraded to PtdIns(3,4)P_2 by the 5-phosphatase SHIP1 [34]. PtdIns(3,4)P_2 is responsible for the persistence of the signal induced by PtdIns(3,4,5)P_3 [8,35]. For detection of PtdIns(3,4)P_2, platelets were stimulated for 90 s with fMLP. This resulted in elevated amounts of PtdIns(3,4)P_2 which were not present in control cells (Fig. 4C and D).

3.3. Positional isomer separation of phosphatidylinositol monophosphates

Separation of the mono-phosphorylated isomers was only achieved with methanol–water mixtures as mobile phase (Fig. 5A and B), whereas the use of acetonitrile resulted in co-elution of PtdIns3*P* and PtdIns5*P*.

The method was applied to Vps34 transfected HEK cells as model. Vps34 is stimulated by amino acid addition through a yet unknown mechanism [36]. Starvation and subsequent amino acid supplementation stimulates Vps34 and induces the generation of PtdIns3*P* [37,38]. Thus, HEK Vps34 cells were serum and amino acid starved for 12 and 2 h, respectively. By addition of serum and amino acids, cells were stimulated for 30 min prior to extraction of lipids, deacylation and analysis. The stimulation with serum and amino acids induced production of PtdIns3*P*, which, in contrast, was inhibited by incubation with the PI3-kinase inhibitor wortmannin 15 min prior to and during stimulation with amino acids and serum (Fig. 5C and D).

3.4. Comparison with radiolabelling method

For comparison with the standard detection method of scintillation analysis, we applied radiolabelled samples to the newly developed HPLC method combined with subsequent scintillation analysis. This also gave a reconfirmation of the peaks measured with MS. The large loop size of 1 ml within the flow scintillation analyser and a flow rate of only 0.5 ml/min resulted in very broad and asymmetric peaks. Nevertheless, peaks of the major PIs could be detected (Fig. 6A and B). A radioactive labelled cell sample showed all major PI peaks (Fig. 6C) at the same retention times as when detected with MS. So did a radioactive labelled standard of PtdIns3*P* (Fig. 6C) that was clearly different to the retention time of the cellular PtdIns4*P* peak.

3.5. Discussion

The separation of PIs differing in number of phosphorylations was successfully achieved with method 1 and applied to analysis of phosphoinositides in cell samples. For analysis of PtdIns(3,4,5)P_3 this method offers a good alternative to the assay involving radiolabelling and anion-exchange HPLC. The short analysis time facilitates handling of large sample numbers.

Separation of isomers was achieved on the same column type, but of longer size and hence increased separation capacity (method 2). This assay offers new perspectives for research on phosphoinositide signalling. The low-abundant PtdInsP_2 isomers can now be separated and analysed without the need for radioactive labelling.

Replacing acetonitrile by methanol enabled the separation of PtdIns3*P*, PtdIns4*P* and PtdIns5*P* (method 3). This isomer separation has not been possible before. Also the PtdInsP_2 isomers could be separated with method 3, albeit in a different elution order when compared to method 2. This hampered a complete separation of the highly abundant PtdIns(4,5)P_2 from the trace isomer PtdIns(3,5)P_2. Therefore, analysis of the biologically important PtdIns(3,5)P_2 should be performed with method 2.

Separation of PtdInsP_2 isomers has been shown before on a cyclodextrin column [14], but co-eluting peaks of PtdIns(3,4,5)P_3 and PtdIns(3,5)P_2 limited the usefulness of the method. Also, separation of PtdIns*P* isomers was neither shown nor discussed in that publication. Compared to a cyclodextrin column the polar endcapped RP-column used here exhibits a more predictable chromatographic behaviour, offers more options for method refinement, and is widely applicable. Furthermore, robustness of the column and reproducibility and stability of separations are very high.

The methods presented here were successfully applied to relevant biological samples. The extraction procedure of PIs remains a major concern. As extensively discussed by Ogiso et al. [27], recovery rates of PIs are generally poor and decrease with increasing phosphorylation. Due to the amphiphilic properties these lipids are difficult to extract. The ionic headgroup adsorbs easily to glass surfaces, whereas the lipid moiety adsorbs to plastic. However,

Please cite this article in press as: S. Kiefer, et al., Separation and detection of all phosphoinositide isomers by ESI-MS, J. Pharm. Biomed. Anal. (2010), doi:10.1016/j.jpba.2010.03.029

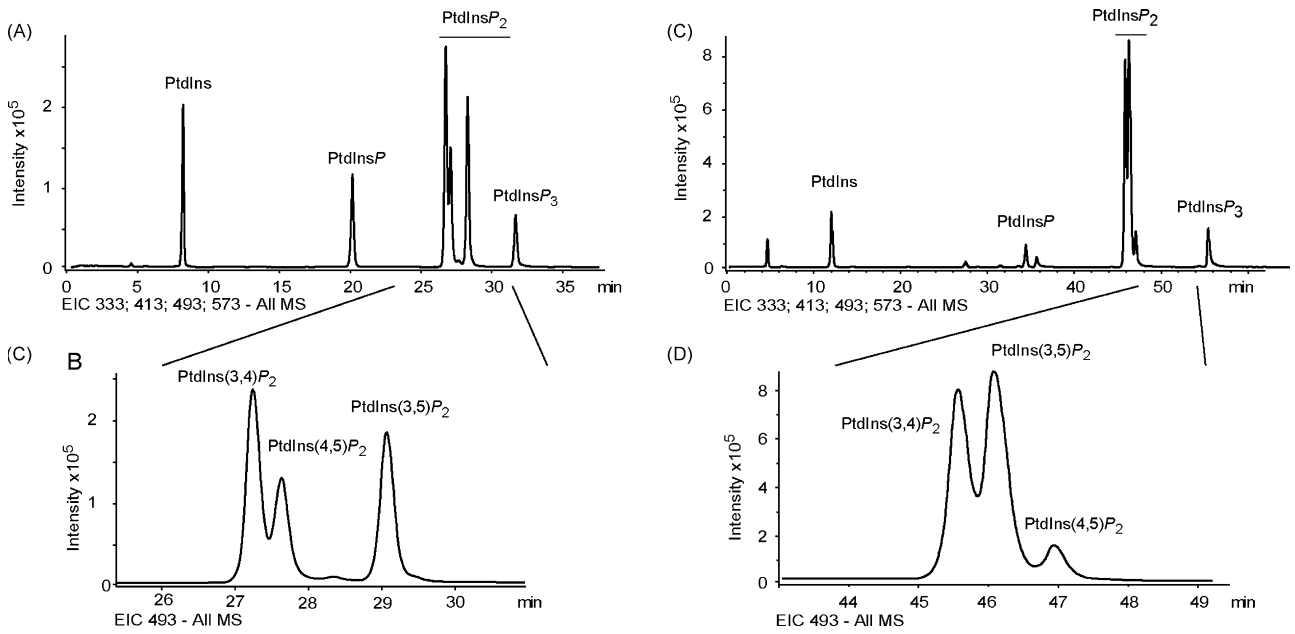

Fig. 3. (A and B) Separation of a standard mixture of PIs containing all PtdInsP_2 regioisomers. (B) Elution of the isomers of PtdInsP_2 in following order: PtdIns(3,4)P_2, PtdIns(4,5)P_2 and PtdIns(3,5)P_2. Column: Phenomenex Aqua C18 (250 mm × 4.6 mm, 5 μm). A: H_2O (+5 mM DMHA), B: acetonitrile (+5 mM DMHA). Gradient: 15% B to 35% B in 40 min. (C and D) Separation of a standard mixture of PIs containing all PtdInsP_2 regioisomers. (D) Separation of PtdInsP_2 isomers in sequence of PtdIns(3,4)P_2, PtdIns(3,5)P_2 and PtdIns(4,5)P_2. Column: Phenomenex Aqua C18 (250 mm × 4.6 mm, 5 μm). A: Methanol (+5 mM DMHA), B: acetonitrile (+5 mM DMHA). Gradient: 15% B to 50% B in 60 min.

measures can be taken to reduce loss of analytes, such as use of silanized glassware to prevent adsorption at glass surfaces [26], and lipid pre-treatment of plastic surfaces with lipids as adsorption protectants. We used plastic tubes, added lipids as adsorption protectants, and phosphatase inhibitors to prevent hydrolysis. These combined measures noticably increased extraction yields. However, further optimization is needed towards a robust and fully validated quantitative analysis of PI headgroups. This could be achieved by spiking with suitable internal standards at the beginning of the extraction procedure which ideally should be a PI with a stable-isotope labelled headgroup. However, such standards are not commercially available. An issue is the efficiency of extraction of phospholipids with different degrees of phosphorylation. There are clear indications that replacing the widely used extraction with chloroform/methanol by butanol increases the yield of highly phosphorylated PtdIns isoforms ([26], Traynor-Kaplan and

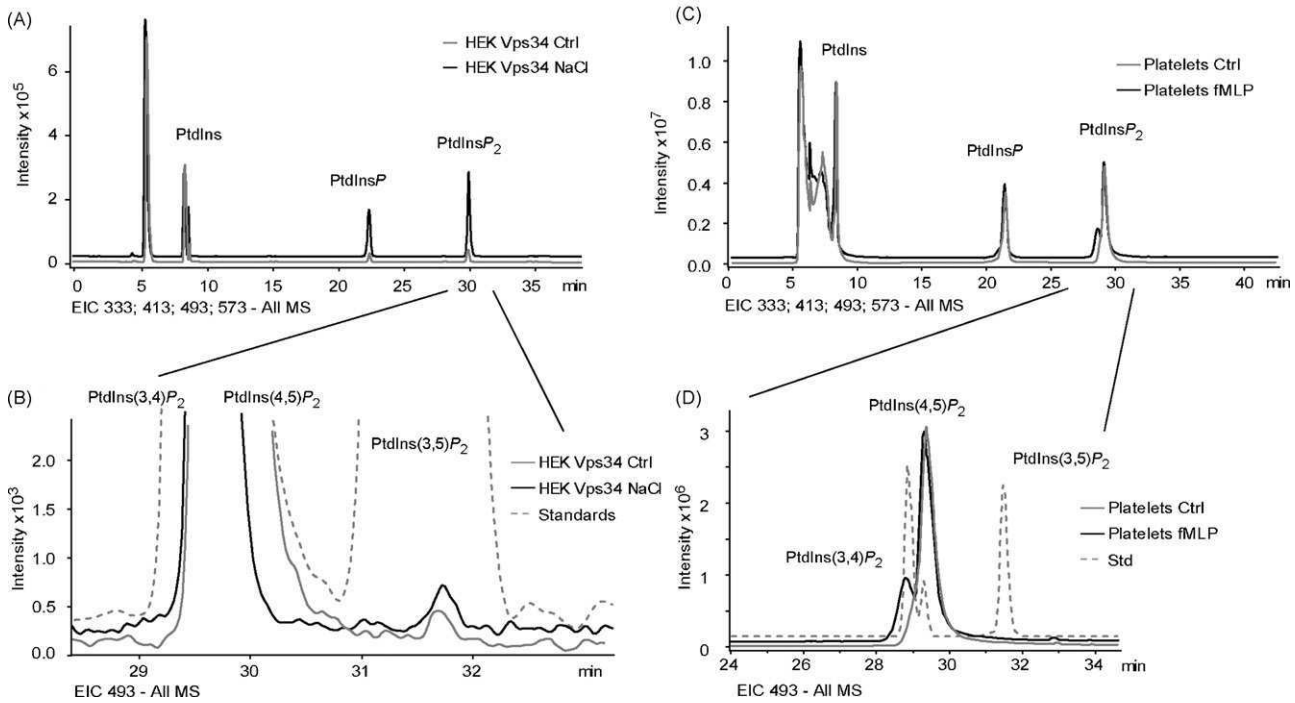

Fig. 4. Analysis of phosphoinositide cell samples. (A and B) Extracted ion chromatograms (EIC) of HEK Vps34 cell samples showed increased amounts of PtdIns(3,5)P_2, that were further increased by stimulation with 1 M NaCl for 10 min. (C and D) EIC of lipids extracted from platelets, control sample and stimulated with fMLP for 1 min. Stimulation induced generation of PtdIns(3,4)P_2 that was not present in the control sample. Column: Phenomenex Aqua C18 (250 mm × 4.6 mm, 5 μm). A: H_2O (+5 mM DMHA), B: acetonitrile (+5 mM DMHA). Gradient: 15% B to 35% B in 40 min.

Please cite this article in press as: S. Kiefer, et al., Separation and detection of all phosphoinositide isomers by ESI-MS, J. Pharm. Biomed. Anal. (2010), doi:10.1016/j.jpba.2010.03.029

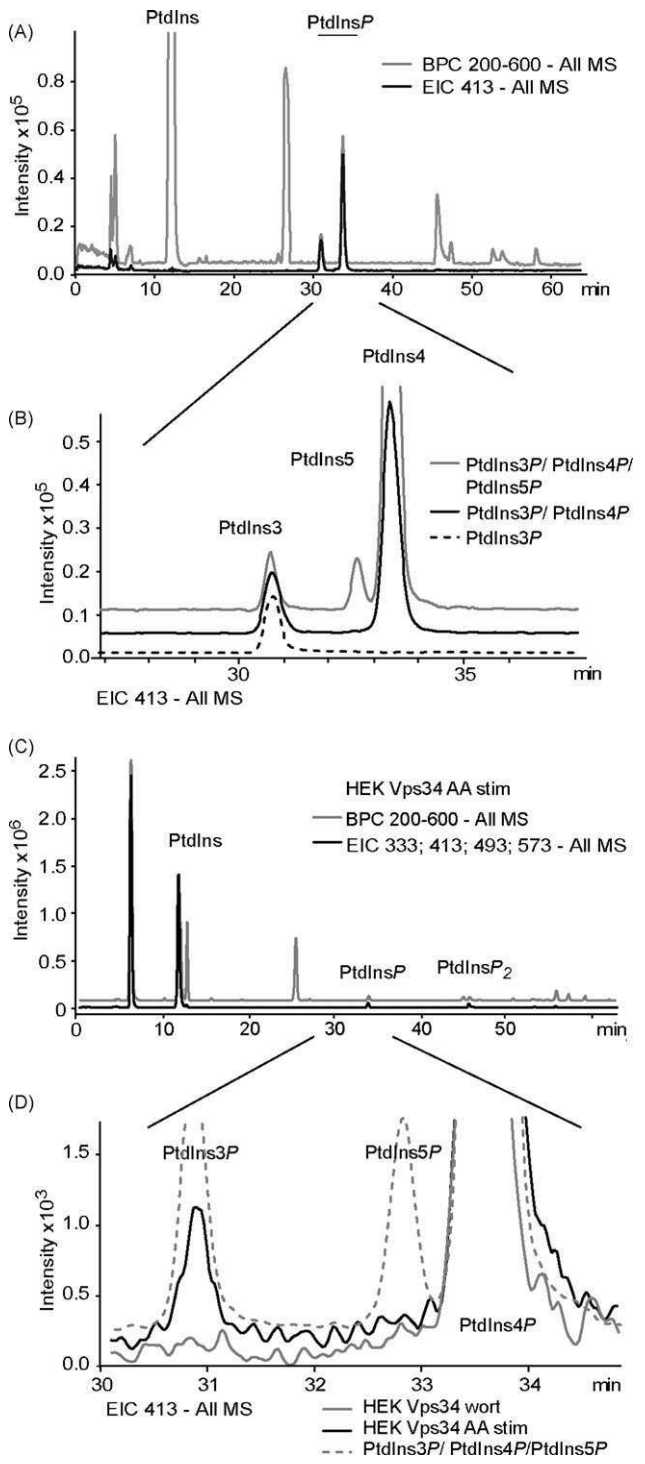

Fig. 5. (A and B) Extracted ion chromatogram (EIC) and base peak chromatogram (BPC) of mixed standards of phosphoinositide monophosphates separated according to method 3. Separation of PtdIns3*P*, PtdIns4*P* and PtdIns5*P* was achieved. (C) BPC and EIC of a HEK Vps34 cell sample. (D) EIC of HEK Vps34 cell samples that were amino acid stimulated and incubated with wortmannin 15 min prior to and during amino acid stimulation. The increase in PtdIns3*P* following amino acid starvation and subsequent stimulation was blocked by addition of wortmannin. Column: Phenomenex Aqua C18 (250 mm × 4.6 mm, 5 μm). A: H_2O (+5 mM DMHA), B: methanol (+5 mM DMHA). Gradient: 15% B to 50% B in 60 min.

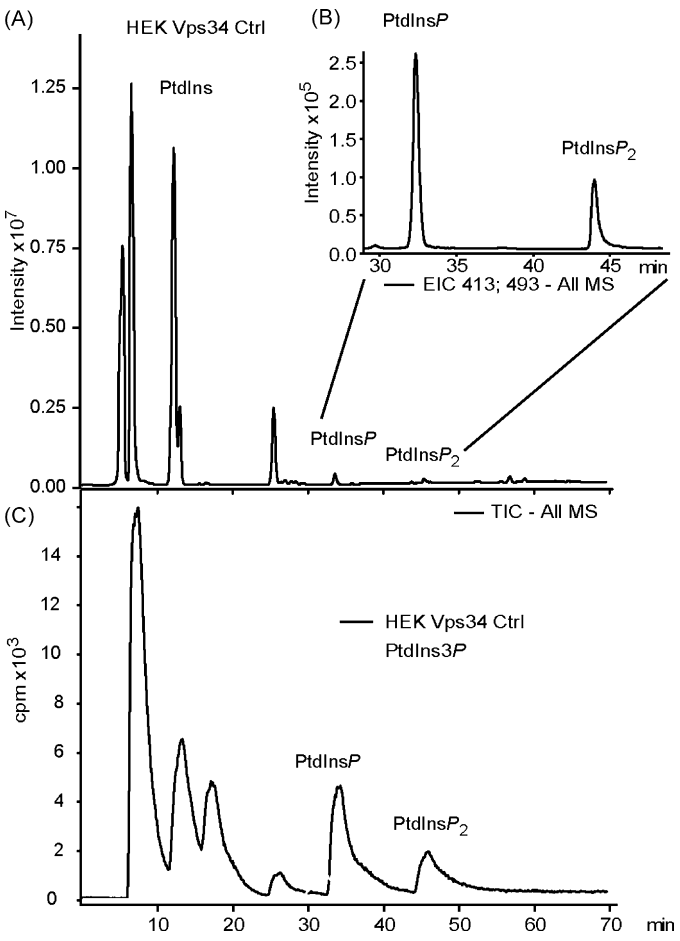

Fig. 6. (A and B) Total ion chromatogram (TIC) and extracted ion chromatogram (EIC) of a HEK Vps34 control cell sample separated according to method 3. (C) Chromatogram of parallel online flow scintillation analysis of the same HEK Vps34 cell sample and a standard of PtdIns3*P*. Column: Phenomenex Aqua C18 (250 mm × 4.6 mm, 5 μm). A: Methanol (+5 mM DMHA), B: acetonitrile (+5 mM DMHA). Gradient: 15% B to 50% B in 60 min.

Küenzi, unpublished data). Thus, a semi-quantitative analysis that compares peak intensities of highly variable (e.g. PtdIns(3,4,5)P_3) and basically unvaried (e.g. PtdIns(4,5)P_2) headgroups is currently the most suitable approach.

The direct parallel analysis with online flow scintillation and mass spectrometry showed the comparability of the two methods. The LC–MS assay presented here offers a superior approach for analysis of intracellular PI levels including differentiation of the biologically relevant PtdIns*P* and PtdInsP_2 isomers.

Further development of the method can be envisaged by a translation to UPLC, thereby taking advantage of shorter analyses and equal or superior chromatographic resolution. There is a general need for further improvement of sample workup in PI analysis, as isolation and deacylation of the PtdIns is time-consuming and difficult. Also, the issue of possible discriminatory extraction of certain PtdIns needs further investigation. Nevertheless, the LC–MS methods presented here enable simultaneous analysis of all currently known deacylated PtdIns and thus are a useful tool for cell signalling studies.

References

[1] L.C. Skwarek, G.L. Boulianne, Great expectations for PIP: phosphoinositides as regulators of signaling during development and disease, Dev. Cell 16 (2009) 12–20.
[2] M.P. Wymann, R. Schneiter, Lipid signalling in disease, Nat. Rev. Mol. Cell Biol. 9 (2008) 162–176.

Please cite this article in press as: S. Kiefer, et al., Separation and detection of all phosphoinositide isomers by ESI-MS, J. Pharm. Biomed. Anal. (2010), doi:10.1016/j.jpba.2010.03.029

[3] B. Payrastre, K. Missy, S. Giuriato, S. Bodin, M. Plantavid, M. Gratacap, Phosphoinositides: key players in cell signalling, in time and space, Cell. Signal. 13 (2001) 377–387.
[4] I.H. Batty, J. van der Kaay, A. Gray, J.F. Telfer, M.J. Dixon, C.P. Downes, The control of phosphatidylinositol 3,4-bisphosphate concentrations by activation of the Src homology 2 domain containing inositol polyphosphate 5-phosphatase 2, SHIP2, Biochem. J. 407 (2007) 255–266.
[5] M.J. Clague, S. Urbe, J. de Lartigue, Phosphoinositides and the endocytic pathway, Exp. Cell Res. 315 (2008) 1627–1631.
[6] D. Manna, A. Albanese, W.S. Park, W. Cho, Mechanistic basis of differential cellular responses of phosphatidylinositol 3,4-bisphosphate and phosphatidylinositol 3,4,5-trisphosphate-binding pleckstrin homology domains, J. Biol. Chem. 282 (2007) 32093–32105.
[7] R.H. Michell, V.L. Heath, M.A. Lemmon, S.K. Dove, Phosphatidylinositol 3,5-bisphosphate: metabolism and cellular functions, Trends Biochem. Sci. 31 (2006) 52–63.
[8] G. Di Paolo, P. De Camilli, Phosphoinositides in cell regulation and membrane dynamics, Nature 443 (2006) 651–657.
[9] J.B. Morris, K.A. Hinchliffe, A. Ciruela, A.J. Letcher, R.F. Irvine, Thrombin stimulation of platelets causes an increase in phosphatidylinositol 5-phosphate revealed by mass assay, FEBS Lett. 475 (2000) 57–60.
[10] C. Pendaries, H. Tronchere, C. Racaud-Sultan, F. Gaits-Iacovoni, S. Coronas, S. Manenti, M.P. Gratacap, M. Plantavid, B. Payrastre, Emerging roles of phosphatidylinositol monophosphates in cellular signaling and trafficking, Adv. Enzyme Regul. 45 (2005) 201–214.
[11] D. Sbrissa, O.C. Ikonomov, R. Deeb, A. Shisheva, Phosphatidylinositol 5-phosphate biosynthesis is linked to PIKfyve and is involved in osmotic response pathway in mammalian cells, J. Biol. Chem. 277 (2002) 47276–47284.
[12] A.E. Wurmser, J.D. Gary, S.D. Emr, Phosphoinositide 3-kinases and their FYVE domain-containing effectors as regulators of vacuolar/lysosomal membrane trafficking pathways, J. Biol. Chem. 274 (1999) 9129–9132.
[13] H. Guillou, L.R. Stephens, P.T. Hawkins, Quantitative measurement of phosphatidylinositol 3,4,5-trisphosphate, Methods Enzymol. 434 (2007) 117–130.
[14] P.T. Ivanova, S.B. Milne, M.O. Byrne, Y. Xiang, H.A. Brown, Glycerophospholipid identification and quantitation by electrospray ionization mass spectrometry, Methods Enzymol. 432 (2007) 21–57.
[15] K.R. Auger, L.A. Serunian, S.P. Soltoff, P. Libby, L.C. Cantley, PDGF-dependent tyrosine phosphorylation stimulates production of novel polyphosphoinositides in intact cells, Cell 57 (1989) 167–175.
[16] H. Hama, J. Torabinejad, G.D. Prestwich, D.B. DeWald, Measurement and immunofluorescence of cellular phosphoinositides, Methods Mol. Biol. 284 (2004) 243–258.
[17] T.E. Rusten, H. Stenmark, Analyzing phosphoinositides and their interacting proteins, Nat. Methods 3 (2006) 251–258.
[18] S.B. Milne, P.T. Ivanova, D. DeCamp, R.C. Hsueh, H.A. Brown, A targeted mass spectrometric analysis of phosphatidylinositol phosphate species, J. Lipid Res. 46 (2005) 1796–1802.
[19] M. Pulfer, R.C. Murphy, Electrospray mass spectrometry of phospholipids, Mass Spectrom. Rev. 22 (2003) 332–364.
[20] M.R. Wenk, L. Lucast, G. Di Paolo, A.J. Romanelli, S.F. Suchy, R.L. Nussbaum, G.W. Cline, G.I. Shulman, W. McMurray, P. De Camilli, Phosphoinositide profiling in complex lipid mixtures using electrospray ionization mass spectrometry, Nat. Biotechnol. 21 (2003) 813–817.
[21] A.D. Postle, D.C. Wilton, A.N. Hunt, G.S. Attard, Probing phospholipid dynamics by electrospray ionisation mass spectrometry, Prog. Lipid Res. 46 (2007) 200–224.
[22] S.K. Dove, F.T. Cooke, M.R. Douglas, L.G. Sayers, P.J. Parker, R.H. Michell, Osmotic stress activates phosphatidylinositol-3,5-bisphosphate synthesis, Nature 390 (1997) 187–192.
[23] M. Laffargue, J.M. Ragab-Thomas, A. Ragab, J. Tuech, K. Missy, L. Monnereau, U. Blank, M. Plantavid, B. Payrastre, P. Raynal, H. Chap, Phosphoinositide 3-kinase and integrin signalling are involved in activation of bruton tyrosine kinase in thrombin-stimulated platelets, FEBS Lett. 443 (1999) 66–70.
[24] R.D. Byrne, M. Garnier-Lhomme, K. Han, M. Dowicki, N. Michael, N. Totty, V. Zhendre, A. Cho, T.R. Pettitt, M.J. Wakelam, D.L. Poccia, B. Larijani, PLCgamma is enriched on poly-phosphoinositide-rich vesicles to control nuclear envelope assembly, Cell Signal. 19 (2007) 913–922.
[25] M. Garnier-Lhomme, R.D. Byrne, T.M.C. Hobday, S. Gschmeissner, R. Woscholski, D.L. Poccia, E.J. Dufourc, B. Larijani, Nuclear envelope remnants: fluid membanes enriched in STEROLS and ploy phosphoinositides, PLOS One 4 (2009) 1–11.
[26] T.R. Pettitt, S.K. Dove, A. Lubben, S.D. Calaminus, M.J. Wakelam, Analysis of intact phosphoinositides in biological samples, J. Lipid Res. 47 (2006) 1588–1596.
[27] H. Ogiso, R. Taguchi, Reversed-phase LC/MS method for polyphosphoinositide analyses: changes in molecular species levels during epidermal growth factor activation in A431 cells, Anal. Chem. 80 (2008) 9226–9232.
[28] C. Nasuhoglu, S. Feng, J. Mao, M. Yamamoto, H.L. Yin, S. Earnest, B. Barylko, J.P. Albanesi, D.W. Hilgemann, Nonradioactive analysis of phosphatidylinositides and other anionic phospholipids by anion-exchange high-performance liquid chromatography with suppressed conductivity detection, Anal. Biochem. 301 (2002) 243–254.
[29] T. Gunnarsson, L. Ekblad, A. Karlsson, P. Michelsen, G. Odham, B. Jergil, Separation of polyphosphoinositides using normal-phase high-performance liquid chromatography and evaporative light scattering detection or electrospray mass spectrometry, Anal. Biochem. 254 (1997) 293–296.
[30] M. Laffargue, R. Calvez, P. Finan, A. Trifilieff, M. Barbier, F. Altruda, E. Hirsch, M.P. Wymann, Phosphoinositide 3-kinase gamma is an essential amplifier of mast cell function, Immunity 16 (2002) 441–451.
[31] B. Dewald, M. Baggiolini, Platelet-activating factor as a stimulus of exocytosis in human neutrophils, Biochim. Biophys. Acta 888 (1986) 42–48.
[32] E.G. Bligh, W.J. Dyer, A rapid method of total lipid extraction and purification, Can. J. Biochem. Physiol. 37 (1959) 911–917.
[33] N.G. Clarke, R.M. Dawson, Alkaline O leads to N-transacylation. A new method for the quantitative deacylation of phospholipids, Biochem. J. 195 (1981) 301–306.
[34] M.P. Gratacap, S. Severin, G. Chicanne, M. Plantavid, B. Payrastre, Different roles of SHIP1 according to the cell context: the example of blood platelets, Adv. Enzyme Regul. 48 (2008) 240–252.
[35] A. Sorisky, W.G. King, S.E. Rittenhouse, Accumulation of PtdIns(3,4)P2 and PtdIns(3,4,5)P3 in thrombin-stimulated platelets. Different sensitivities to $Ca2^{+}$ or functional integrin, Biochem. J. 286 (Pt 2) (1992) 581–584.
[36] P. Gulati, G. Thomas, Nutrient sensing in the mTOR/S6K1 signalling pathway, Biochem. Soc. Trans. 35 (2007) 236–238.
[37] T. Nobukuni, M. Joaquin, M. Roccio, S.G. Dann, S.Y. Kim, P. Gulati, M.P. Byfield, J.M. Backer, F. Natt, J.L. Bos, F.J. Zwartkruis, G. Thomas, Amino acids mediate mTOR/raptor signaling through activation of class 3 phosphatidylinositol 3OH-kinase, Proc. Natl. Acad. Sci. U.S.A. 102 (2005) 14238–14243.
[38] M.P. Byfield, J.T. Murray, J.M. Backer, hVps34 is a nutrient-regulated lipid kinase required for activation of p70 S6 kinase, J. Biol. Chem. 280 (2005) 33076–33082.

Please cite this article in press as: S. Kiefer, et al., Separation and detection of all phosphoinositide isomers by ESI-MS, J. Pharm. Biomed. Anal. (2010), doi:10.1016/j.jpba.2010.03.029

creative commons

Namensnennung-Keine kommerzielle Nutzung-Keine Bearbeitung 2.5 Schweiz

---

Sie dürfen:

das Werk vervielfältigen, verbreiten und öffentlich zugänglich machen

Zu den folgenden Bedingungen:

Namensnennung. Sie müssen den Namen des Autors/Rechteinhabers in der von ihm festgelegten Weise nennen (wodurch aber nicht der Eindruck entstehen darf, Sie oder die Nutzung des Werkes durch Sie würden entlohnt).

Keine kommerzielle Nutzung. Dieses Werk darf nicht für kommerzielle Zwecke verwendet werden.

Keine Bearbeitung. Dieses Werk darf nicht bearbeitet oder in anderer Weise verändert werden.

- Im Falle einer Verbreitung müssen Sie anderen die Lizenzbedingungen, unter welche dieses Werk fällt, mitteilen. Am Einfachsten ist es, einen Link auf diese Seite einzubinden.
- Jede der vorgenannten Bedingungen kann aufgehoben werden, sofern Sie die Einwilligung des Rechteinhabers dazu erhalten.
- Diese Lizenz lässt die Urheberpersönlichkeitsrechte unberührt.

Quelle: http://creativecommons.org/licenses/by-nc-nd/2.5/ch/ Datum: 3.4.2009